GOLD IN THE NORTHERN YELLOWKNIFE GREENSTONE BELT, CANADA AND Pb-Zn-Cu IN THE MVT DEPOSITS OF S.E. MISSOURI: GEOCHEMICAL STUDIES AND NUMERICAL MODELS

A Thesis
presented to
the Faculty of the Graduate School
University of Missouri-Columbia

In Partial Fulfillment
of the Requirements for the Degree
Master of Science

by
LAURA ELIZABETH PERRY

Dr. Kevin L. Shelton, Thesis Advisor

July 2016

The undersigned, appointed by the Dean of the Graduate School, have examined the thesis entitled:

GOLD IN THE NORTHERN YELLOWKNIFE GREENSTONE BELT, CANADA AND Pb-Zn-Cu IN THE MVT DEPOSITS OF S.E. MISSOURI: GEOCHEMICAL STUDIES AND NUMERICAL MODELS

presented by Laura E. Perry
a candidate for the degree of Master of Science
and hereby certify that in their opinion it is worthy of acceptance.

_____

Dr. Kevin L. Shelton

_____

Dr. Martin S. Appold

_____

Dr. Tommi A. White

ACKNOWLEDGEMENTS

I would like to thank my thesis advisor, Professor Kevin L. Shelton, for his patience and incredible guidance during the writing process of this thesis. I thank him for tailoring my thesis projects to accommodate my interests perfectly, for continuously challenging me, and for teaching me more than I ever expected to learn during my time as a Master's student.

Great thanks also go to the remaining members of my thesis committee, Professors Martin Appold and Tommi White, for their expertise and advice during the construction of this thesis. I greatly appreciate the assistance provided by Professor Eric Sandvol while I learned the nuances of operating MATLAB, the extra instruction from Professor Martin Appold in using Geochemist's Workbench, and the numerous letters of recommendation provided by Professor Miriam Barquero-Molina. I would also like to offer many thanks to Professor Jim Schiffbauer for his many contributions to the graphics and conceptual models that have been used during the research and presentations of Prof. Shelton and I.

I am grateful for the financial support provided to me by the donors of the Hugh McKinstry Fund, administered by the Society of Economic Geologists Student Grant Committee, and the donors of the Midas Ore Research Fund of the University of Missouri's Geological Sciences department. I also thank the Geological Sciences department for the teaching assistantship that I enjoyed for two years.

Finally, I express my deepest thanks for the love and unwavering support from my family and friends during the last two challenging and rewarding years.

TABLE OF CONTENTS

LIST OF ILLUSTRATIONS

Figure Page

LIST OF TABLES

CHAPTER I: INTRODUCTION

This thesis employs various numerical and geochemical techniques to investigate the major controlling factors and depositional processes responsible for ore formation in two types of ore deposits in study areas in North America: (1) the Discovery-Ormsby and Clan Lake gold-bearing areas of the Yellowknife Greenstone Belt, Northwest Territories, Canada and (2) the southeastern Missouri Pb-Zn-Cu ore district.

Numerical analysis of alteration geochemistry of metavolcanic rocks in the Discovery-Ormsby and Clan Lake areas of the Yellowknife Greenstone Belt (Chapter 2)

Discovery-Ormsby and Clan Lake are areas of active gold exploration in the northern end of the Yellowknife Greenstone Belt, Northwest Territories, Canada. Gold occurs principally within extensively silicified and sulfidized metavolcanic rocks of the Archean Banting Group. Recent geochemical studies of each area (Hansen, 2013) have identified spatial correlations between gold enrichment and the $\delta^{18}O$ values of quartz veins and wall rocks, which likely define zones of auriferous hydrothermal fluid introduction. However, plots of gold concentration versus various chemical elements do not show an obvious host lithology control on gold deposition, nor do they show anticipated correlations between gold and elements associated with common types of alteration that are observed (i.e. silicification, sulfidation, and potassic alteration).

Chapter 2 further investigates the factors controlling alteration and gold deposition in the Discovery-Ormsby and Clan Lake areas using 3-D modeling to evaluate the spatial distribution of the intensity of potassic alteration by reconstructing the

chemistries of altered metavolcanic host rocks (i.e. molar ratios among K, Na, Ca, and Al) according to mineral phases associated commonly with potassic alteration. These models will help to address several questions regarding ore formation and exploration strategies in the northern YGB: Can these numerical techniques be applied successfully to metavolcanic rocks? Is potassic alteration related spatially to gold distribution? If so, does the spatial distribution of wall rock alteration indicate contemporaneous potassic alteration and gold deposition, or does it instead suggest a post-gold hydrothermal event during which potassic alteration overprinted previous alteration patterns and remobilized gold? It is hoped that this chapter will demonstrate that modeling host rock alteration chemistries may be a useful tool in developing exploration strategies for metavolcanic-hosted gold deposits in the northern YGB.

Geochemical studies and reaction path modeling of MVT ores in the southeastern Missouri Pb-Zn-Cu ore field, U.S.A. (Chapters 3 and 4)

The Bonneterre Dolomite (Cambrian) hosts world-class, Pb-Zn-Cu Mississippi Valley-type (MVT) deposits of the Viburnum Trend district in southeast Missouri. Sulfide ore mineralization in the district is generally lead-dominant (Pb:Zn > 5) and occurs almost exclusively in the middle to upper portion of the Bonneterre Dolomite. Below the main Pb-Zn mining horizon of the Viburnum Trend, near the base of the Bonneterre Dolomite and in the upper portion of the underlying Lamotte Sandstone, unusually Cu-(Ni-Co)-Zn-rich ores (Zn:Pb > 2 and Cu up to 8 wt. %) have recently been identified and exploited (Cavender, 2015; Cavender et al., 2016).

Epigenetic dolomite cement associated with the atypical lower section ores in the Viburnum Trend exhibit cathodoluminescent (CL) patterns that are distinct from the pervasive CL cement stratigraphy observed in the upper Bonneterre Dolomite throughout southern Missouri and northern Arkansas, indicating the presence of multiple, chemically distinct fluids. Pronounced vertical zoning of Ni-Co-, Cu-, Zn-, and Pb-rich mineralization with increasing distance above the Lamotte Sandstone and sporadic variation in $\delta^{34}S$ values of sulfides (from -5 toward +17‰ VCDT, Cavender, 2015) have been interpreted to indicate that metal-specific mineralizing fluids utilized multiple sulfide sources and entered the system along multiple, fault-related flow paths (Cavender et al., 2016; Shelton et al., 2016).

In chapter 3, CL and stable isotope studies of dolomite cements are expanded to ore deposits in several other mining districts throughout southeast Missouri in order to document the continuity/variability in CL cement stratigraphy and isotopic compositions on a broader scale. These studies aim to address the following questions: How do the CL patterns and stable isotope compositions of dolomite cements vary spatially in southeast Missouri? Do they suggest that ore deposition in the district was the product of a single, chemically evolving fluid from a regional flow system, or do they reflect the presence of multiple mineralizing fluids, possibly flowing along regional- and local-scale fault/fracture systems? What does this suggest about the influence of localized, potentially fault-related fluids on mineralization within the Viburnum Trend and elsewhere in southeast Missouri?

In chapter 4, reaction path modeling is used to investigate potential depositional processes responsible for atypical, Cu-(Ni-Co)-Zn-rich ores in the lower Bonneterre

Dolomite in Viburnum Trend. By attempting to reproduce the observed lower ore zone (LOZ) mineralization with reaction path modeling, we hope to address the following questions: What depositional mechanisms are capable of producing the relative proportions and paragenetic sequences of sulfides that are observed in LOZ ores? Does this mineralization require the mixing of multiple, distinct fluids or might they have resulted from the chemical evolution of a single fluid along different flow paths? How can reaction path modeling help to develop a conceptual model for LOZ ore formation?

CHAPTER II: NUMERICAL ANALYSIS OF ALTERATION GEOCHEMISTRY OF GOLD-HOSTING METAVOLANIC ROCKS IN THE DISCOVERY-ORMSBY AND CLAN LAKE AREAS OF THE YELLOWKNIFE GREENSTONE BELT, NORTHWEST TERRITORIES, CANADA

ABSTRACT

Discovery-Ormsby and Clan Lake are areas of active gold exploration in the north end of the Yellowknife Greenstone Belt, Northwest Territories, Canada. Gold occurs principally within extensively silicified and sulfidized metavolcanic rocks of the Archean Banting Group (2.69-2.66 Ga). Recent geochemical studies on each of the areas (Hansen, 2013) determined that mineralization in the mafic metavolcanic rocks of the Discovery-Ormsby area resulted dominantly from metasedimentary-derived fluids, whereas mineralization in the intermediate-felsic metavolcanic complex at Clan Lake utilized metasedimentary- and metavolcanic-derived fluids. Plots of gold concentration versus various elements do not show an obvious host lithology control on gold deposition, nor do they show anticipated correlations between gold and elements associated with common types of alteration that are observed, such as silicification, sulfidation, and potassic alteration.

In order to further investigate the factors controlling alteration and gold deposition in the Discovery-Ormsby and Clan Lake areas, the present study modeled the spatial distribution of the intensity of potassic alteration (which is observed to be associated with gold in each study area) in three dimensions by reconstructing the chemistries of altered metavolcanic rocks (i.e. molar ratios among K, Na, Ca, and Al)

according to mineral phases associated commonly with potassic alteration. Numerical analysis was performed using whole-rock geochemical data provided by Tyhee Gold Corporation and 3-D models were constructed using MATLAB®.

Due to limited lithogeochemical data for the Discovery-Ormsby area, the spatial relationship between gold distribution and the intensity of potassic alteration is unclear in 3-D models. Additional data for modeling may help to determine if potassic alteration was a controlling factor on gold distribution in the Ormsby area, or if gold deposition was more dependent on physical properties (i.e. porosity and permeability) of the extensively silicified and sulfidized metavolcanic host rocks.

Models of potassic alteration at Clan Lake show that the relationship between high gold anomalies and the intensity of alteration varies spatially. In the southwestern corner of the area, gold enrichment is associated with rocks that have undergone relatively moderate degrees of potassic alteration. This area in Clan Lake is associated with high $\delta^{18}O$ values of quartz veins and wall rocks (Hansen, 2013) and may reflect a zone of enhanced porosity and permeability for hydrothermal fluids.

A linear, south-dipping zone of moderate to strong potassic alteration occurs in the central portion of the Clan Lake area that is likely coincident with inferred faults in the area. In this zone, gold is hosted in rocks that have been subjected to only weak potassic alteration. Although these gold-rich areas are hosted in weakly altered rocks, they are frequently adjacent to patches of strongly altered wall rock. This may reflect an area of dominantly quartz vein-hosted gold that was associated with fault-related hydrothermal fluid flow. Gold-bearing hydrothermal fluids may have utilized local faults, along which wall rocks experienced potassic alteration and gold was deposited

dominantly in quartz veins; alternatively, the distribution of potassic alteration that is observed in the area may have developed after gold mineralization, potentially overprinting preexisting alteration patterns and remobilizing gold locally.

INTRODUCTION

The Slave Province of northern Canada has produced approximately 16 M ozt of gold, mined primarily from the world-class Yellowknife Greenstone Belt (YGB) of the Northwest Territories (Fig. 2.1) (Goldfarb et al., 2001; Bullen and Robb, 2006; Goodwin et al., 2006). The Discovery-Ormsby area is known for the former Discovery Mine that produced approximately 1 M ozt gold from one M tonnes of ore, mined from quartz veins hosted in metasedimentary rocks, but is currently estimated to include approximately 1.2 M ozt gold in the nearby mafic metavolcanic Ormsby Member of the Giauque Lake Formation (Padgham, 1992; Bullen and Robb, 2006; Pratico, 2009a). Intermediate-felsic metavolcanic rocks of the Clan Lake area to the southwest of Discovery-Ormsby are estimated to contain approximately 350,000 ozt gold (Pratico, 2009a).

Recent geochemical studies of gold deposits in the Ormsby and Clan Lake areas (Hansen, 2013) have identified a positive correlation between the spatial distribution of gold enrichment and elevated $\delta^{18}O$ values of quartz veins and wall rocks, which appear to define large zones of hydrothermal fluid movement and may indicate a potential vector for future exploration efforts. However, whole-rock geochemical analysis of the metavolcanic rocks from these areas does not show anticipated correlations between gold concentrations and elements associated with the types of alteration that are observed frequently with gold (i.e. silicification, sulfidation, and potassic alteration) and does not indicate an obvious preferred wall rock lithology for gold deposition (Hansen, 2013).

Using the same lithogeochemical data from the Discovery-Ormsby and Clan Lake areas, the present study models the spatial distribution of hydrothermal alteration using numerical methods to recast relative elemental concentrations (specifically K, Na, Ca, and Al) in terms of mineral assemblages associated with potassic alteration. By observing the relationship between the spatial distribution of gold enrichment and the intensity of potassic alteration, this study aims to address the following questions:

1. Is there a spatial relationship between gold enrichment and potassic alteration that can be identified using 3-D modeling? Is there a spatial relationship between potassic alteration and the $\delta^{18}O$ values of quartz veins and wall rocks (Hansen, 2013)?
2. What is the relative timing of gold mineralization and potassic alteration in each area?
3. Was potassic alteration of wall rocks an important control on the spatial distribution of gold in the northern YGB, or were gold deposition and potassic alteration the results of separate hydrothermal events?
4. Can the numerical techniques used to quantify hydrothermal alteration in the current study be applied as an exploration tool for gold deposits in the northern YGB?

Exploration History

Archean terranes in Canada are estimated to contain ~ 8125 t of gold, a majority of which is found in hydrothermal gold deposits in the Slave and Superior provinces (Robert and Poulsen, 1997). The Slave province has produced ~ 16 M ozt of gold, primarily from the world-class Yellowknife Greenstone Belt (YGB) of the Northwest

Territories (Fig. 2.1) (Goldfarb et al., 2001; Bullen and Robb, 2006; Goodwin et al., 2006). Historically, the Giant and Con Mines of the southern YGB have produced most of this gold (7.0 and 5.5 M ozt, respectively) from metavolcanic host rock. Tyhee Gold Corp. has recent exploration efforts in other promising areas in the northern end of the YGB, including the Discovery-Ormsby and Clan Lake areas.

The Discovery-Ormsby area (Fig. 2.1) is known for its former gold production from the Discovery Mine from 1950 to 1968. The Discovery Mine produced approximately 1 M ozt gold from 1 M tonnes of ore from quartz veins hosted by metasedimentary rocks of the Archean Burwash Formation (Padgham, 1992; Bullen and Robb, 2006; Pratico, 2009a). Current mining plans for the Discovery-Ormsby area, however, are focusing on gold ore hosted within mafic metavolcanic rocks of the Ormsby Member of the Giauque Lake Formation of the Archean Banting Group. Resource estimations for the Ormsby zone are an approximate 10.9 M tonnes of ore (3.0 M t measured, 7.9 M t indicated), containing 1.2 M ozt gold with an average gold grade of 3.42 g/t (0.11 toz/t) (Pratico, 2009a).

The Clan Lake area is located 38 km south-southwest of the Discovery-Ormsby area (Fig. 2.1). Mining first began in the mid-1960s with a reported gold grade of 14.5 g/t (0.47 toz/t). The area has since been acquired by Tyhee Gold Corp and resource estimations for the Main Zone are approximately 350,000 ozt gold in intermediate to felsic metavolcanic host rocks with an average gold grade of 3.64 g/t (0.12 toz/t) (Pratico, 2009a).

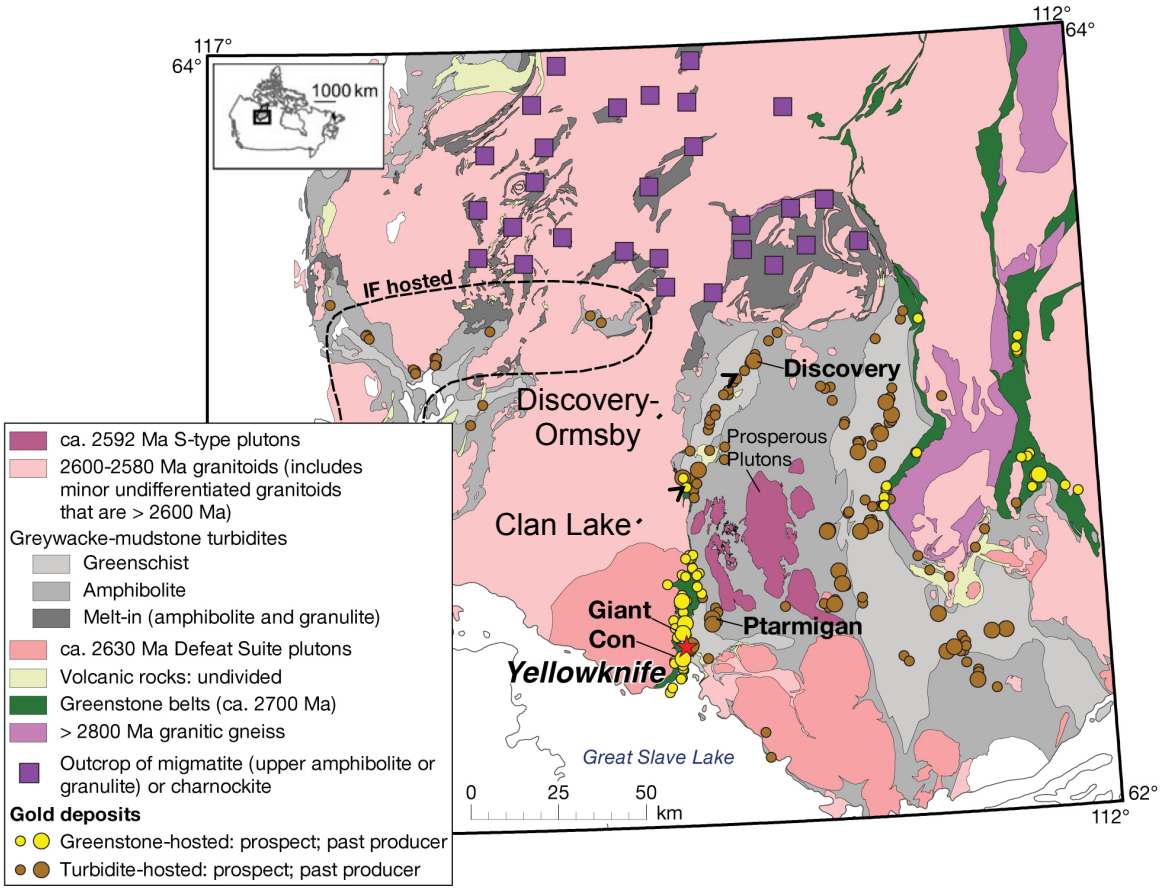

Figure 2.1. Geological map of the Slave Province of western Canada and major gold deposits of the Yellowknife Greenstone Belt (YGB) (after Ootes et al., 2011). Black arrows indicate the locations of the two study areas, Discovery-Ormsby and Clan Lake.

Geological Setting

The Archean Slave Craton is a well-exposed portion of the northwestern Canadian Shield (Stern and Bleeker, 1998; Bleeker et al., 1999; Bowring and Williams, 1999). Compared to other Archean cratons, it has an unusually high proportion of metasedimentary rocks relative to metavolcanic rocks (Helmstaedt and Padgham, 1986; Padgham and Fyson, 1992; Isachsen and Bowring, 1994; Ferguson et al., 2005). Basement rocks of this craton range in age from > 2.8 to ~ 4.0 Ga (Bleeker et al., 1999, 2000; Bowring and Williams, 1999; Sircombe et al., 2001; Ketchum et al., 2004). Rocks of the Central Slave Basement are poly-metamorphosed gneisses that reached upper greenschist-amphibolite grade with local migmatization, ranging from tonalite to granodiorite in composition (Henderson, 1985; Helmstaedt and Padgham, 1986; Bowring et al., 1989; Isachesen and Bowring, 1994; Stern and Bleeker, 1998; Bowring and Williams, 1999; Cousens et al., 2002). The Central Slave Cover Sequence unconformably overlies rocks of the Central Slave Basement rocks (Fig. 2.2) and contains quartzite, chert-magnetite iron formations, and felsic to intermediate metavolcanic rocks (Covello et al., 1988; Roscoe et al., 1989; Bleeker et al., 1999, 2000; Cousens et al., 2002; Bleeker and Hall, 2007).

Unconformably overlying rocks of the basement and cover sequence is the metamorphosed Yellowknife Supergroup, which is comprised of the Kam, Banting, and Duncan Groups (Henderson, 1985; Bleeker et al., 1999) (Fig. 2.2). The following lithological descriptions refer to original lithologies prior to metamorphism. The Kam Group (2.73-2.70 Ga) is characterized by widespread (≥ 100,000 km^2) mafic pillows and flows interbedded with volcaniclastic to quartz-feldspathic sandstones (Henderson, 1985;

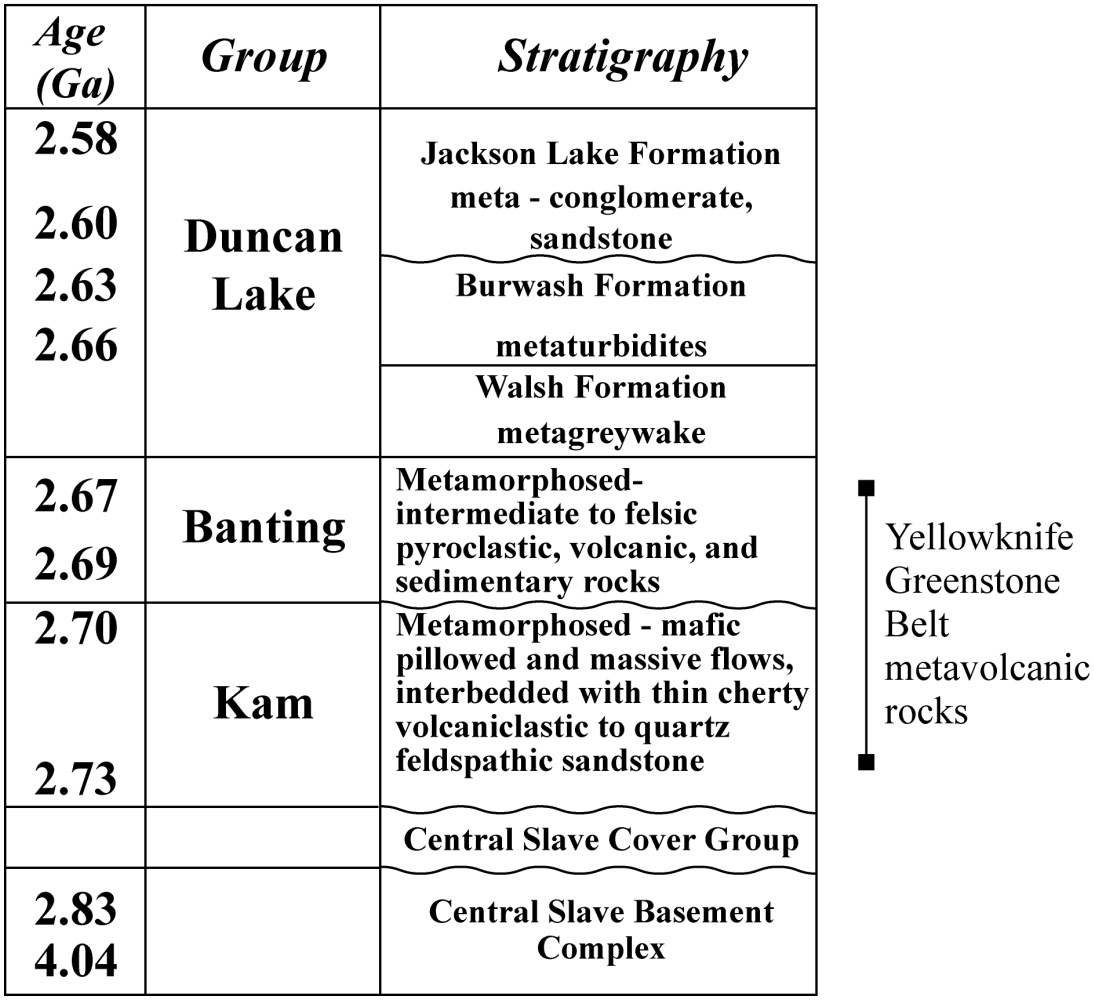

Figure 2.2. Simplified stratigraphic column of basement and supracrustal rocks of the YGB (after Whitty, 2007; Hansen, 2013). The current study focuses on gold deposits hosted within the metamorphosed volcanic rocks of the Archean Banting Group.

Helmstaedt and Padgham, 1986; Goodwin, 1988; Cousens et al., 2002; Ernst and Buchan, 2004). Unconformably overlying the Kam Group is the Banting Group (2.69-2.66 Ga), consisting of intermediate to felsic, pyroclastic volcanic rocks intercalated with tholeiitic to calc-alkaline basaltic rocks and volcanogenic sedimentary rocks that (Helmstaedt and Padgham, 1986; Goodwin, 1988; Bleeker and Hall, 2007; Pratico, 2009a). Conformably overlying the Banting Group is the Duncan Lake Group, the youngest rocks of the Yellowknife Supergroup (Henderson, 1972; Helmstaedt and Padgham, 1986; Ferguson et al., 2005; Martel and Lin, 2006). The Duncan Lake Group is subdivided into the Walsh, Burwash, and Jackson Lake formations.

The Yellowknife Supergroup is intruded by numerous, metaluminous to peraluminous, post-Burwash Formation plutons (from 2.63 to 2.59 Ga) and is crosscut by numerous Proterozoic (circa 2.2 Ga) diabase dikes and faults (Boyle, 1961; Green et al., 1968; Henderson, 1985; LeCheminant and Heaman, 1989; van Breemen et al., 1992; LeCheminant et al., 1997). Deformation within metasedimentary rocks consists of complex folding and faulting with the highest degree of shear deformation typically concentrated along zones of rock competency contrast (Boyle, 1961). Peak regional metamorphism and deformation coincided with peak magmatism (Thompson, 1989; van Breemen et al., 1992; Davis and Bleeker, 1999) and reached upper greenschist to amphibolite grade (Henderson, 1985; Helmstaedt and Padgham, 1986; Isachsen and Bowring, 1994). The transition zone between these facies may be used as a rough guide to gold deposit types in the YGB. Gold deposits within the amphibolite grade rocks are typically auriferous quartz veins hosted in metasedimentary rocks, whereas gold deposits

in the upper greenschist facies may be hosted by wall rocks (refractory sulfide-associated ores) in addition to gold-bearing quartz veins (Hansen, 2013).

Gold in the Yellowknife Greenstone Belt

In its simplest forms, economic gold mineralization requires gold-bearing source rocks, fluid(s) that are capable of transporting gold, structural conduits for focusing fluid flow, and, for refractory ores, highly reactive host rock(s). Previous studies of the southern YGB have suggested that the involvement of both metasedimentary and metavolcanic fluid reservoirs may be a necessary condition to form large gold deposits, especially wall rock-hosted ores (van Hees et al., 1999, 2006; Hansen, 2013). The influence of both metasedimentary and metavolcanic fluid reservoirs may account for substantial economic gold mineralization within smaller greenstone belts that have limited volumes of metavolcanic host rocks (Shelton et al., 2004). One scenario suggested that a shallow, eastward-dipping portion of the Yellowknife River Fault Zone (YRFZ) permitted auriferous metasedimentary-involved fluids of the Banting Group to gain access to shear zones within highly reactive metavolcanic rocks of the Kam Group (van Hees et al., 1999, 2006; Martel and Lin, 2006).

Within the YGB, economic wall-rock-hosted gold mineralization appears to favor highly reactive host rocks near the metamorphic greenschist-amphibolite facies transition. Anomalously iron-rich metavolcanic rocks, such as those of the Discovery-Ormsby area, lie along this facies transition and are an obvious potential host rock for refractory gold (sulfide-hosted ores). The ore-hosting potential of the intermediate-felsic host rocks of the Clan Lake area is not as obvious due to their lower iron contents. Numerical analysis of geochemical data for metavolcanic rocks of the Discovery-Ormsby and Clan Lake

areas employed in the present study aims to investigate (a) the control that host rock lithology and alteration may have on gold mineralization, and (b) whether or not the ores in both areas are related to similar hydrothermal systems or (c) if they instead represent chemically distinct hydrothermal systems.

Discovery-Ormsby Area

The Discovery-Ormsby area lies approximately 90 km north of Yellowknife and contains two narrow (~225 m wide), elongate (~1400 m long) metamorphosed mafic bodies of rock in the Giauque Lake Formation: the Discovery Member at the northern end, and the Ormsby Member at the southern end (Fig. 2.3). These mafic rocks are surrounded by voluminous, more ductile metasedimentary rocks of the Burwash Formation. The mafic rocks in this area have been described as metabasalts or amphibolites (e.g. Whitty, 2007; Pratico, 2009a) and have been correlated to the Archean Banting Group via U-Pb geochronology (2661 ± 5 Ma; Whitty, 2007). Major prograde metamorphic minerals are almandine garnet, biotite, quartz, plagioclase and amphiboles, produced at metamorphic conditions near the upper greenschist-amphibolite grade transition (Whitty, 2007; Pratico, 2009a). Retrograde metamorphism dominates host rock mineralogy, however, and is marked by chlorite intergrown with biotite, sericite, and carbonate (Hansen, 2013).

The rheological contrast between the more competent metavolcanic rocks of the Discovery-Ormsby area and the surrounding less competent metasedimentary rocks of the Burwash Formation is a typically fertile area for the development of orogenic gold deposits in many greenstone belts (Groves et al., 2000). Focusing of hydrothermal fluid flow and resultant gold deposition may have been facilitated by a linear zone of higher

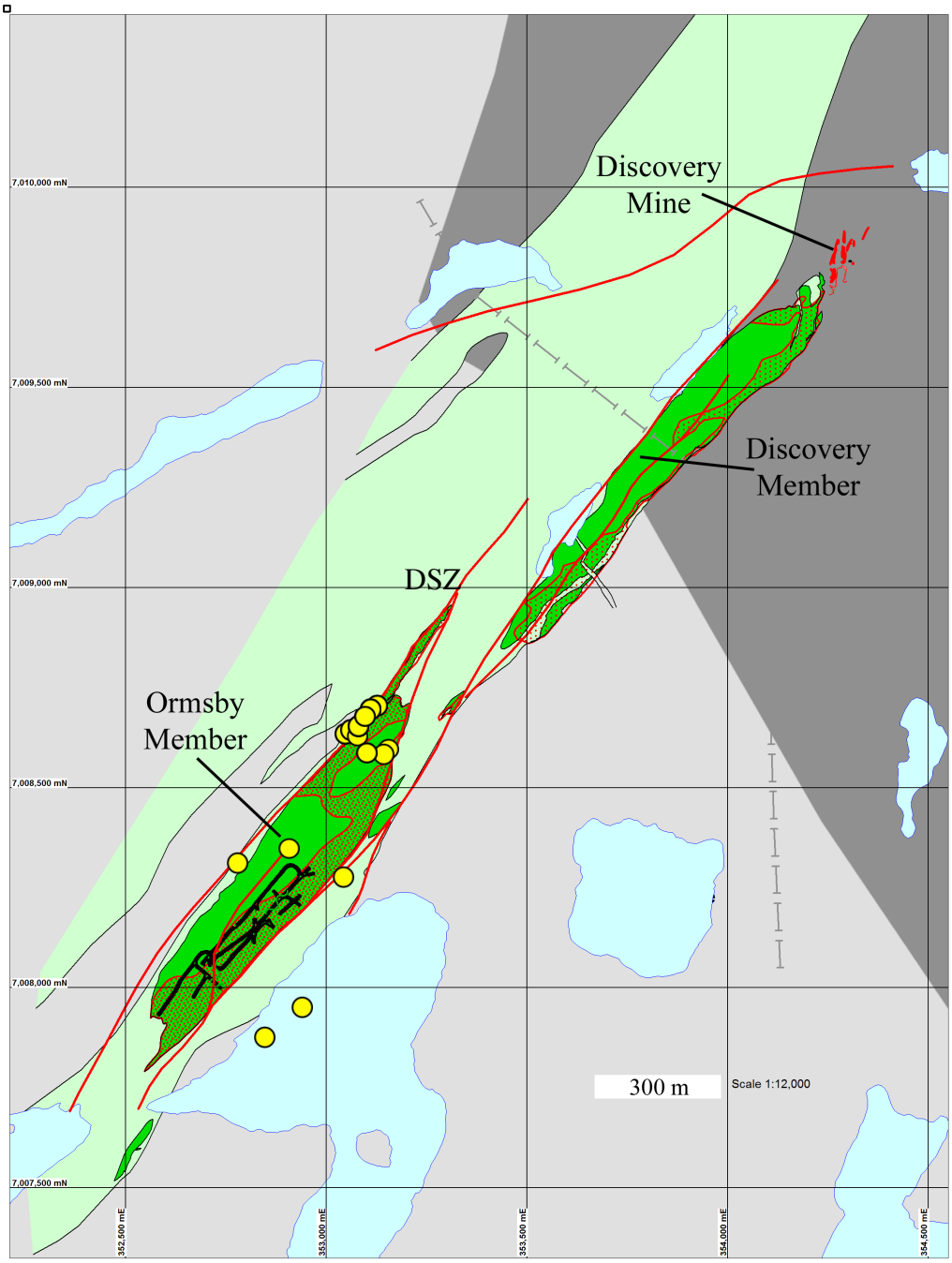

Figure 2.3. Generalized geological map of the Discovery-Ormsby area (after Pratico, 2009b). Gray areas represent metasedimentary rocks of the Burwash Formation; dark gray indicates medium metamorphic grade whereas light gray indicates low metamorphic grade. Green areas represent mafic metavolcanic rocks of the Giauque Formation. Irregular red lines in the Discovery Mine indicate quartz veins. Cross-hatched pattern represents gossan. Longer red lines represent faults, including the left-lateral Discovery Shear Zone (DSZ) (Stubley, 1997). Yellow circles indicate localities of samples used for numerical analysis in the current study; note that these localities are in the Ormsby Member only.

strain, named the Discovery shear zone, that is interpreted by Tyhee Gold Corporation to lie at the immediate western margin of the metavolcanic members (Pratico, 2009a). Deformation fabrics documented by Hansen (2013) indicate that retrograde metamorphism took place after shear deformation in the area.

Gold in the Discovery-Ormsby area

The Ormsby orebody is a silicified, sulfidized, structurally deformed mafic body (Pratico, 2009a). Gold mineralization occurs as native gold in highly silicified and sulfidized wall rocks and is associated with pyrrhotite in quartz veins and altered wall rock. Arsenopyrite is the earliest sulfide present and pre-dates gold deposition and shear deformation (Fig. 2.4) (Hansen, 2013). Within the metavolcanic host rock, early arsenopyrite that has been fractured is filled typically by pyrrhotite ± gold and more rarely base-metal sulfides (chalcopyrite, galena, and sphalerite). Less abundant pyrite is found overgrowing euhedral arsenopyrite or filling fractures in deformed arsenopyrite (Hansen, 2013).

Gold occurs both independently and intergrown with pyrrhotite in quartz veins. Clots of gold ± pyrrhotite occur in silicified wall rock, disconcordant to the deformational fabric of the rock. Gold ± pyrrhotite also appears to be associated with veins containing fragments of wall rock in which plagioclase has been altered to biotite (Hansen, 2013).

Overlapping alterations in the Discovery-Ormsby area include dominant sulfidation and silicification, potassic, and carbonate alteration. Pyrrhotite formation is pervasive in the iron-rich (up to 17.5 wt. % Fe; Hansen, 2013), highly reactive mafic metavolcanic rocks of the Discovery-Ormsby area. A felsic component in the alteration history of these mafic rocks is indicated by the presence of apatite, scheelite, and biotite

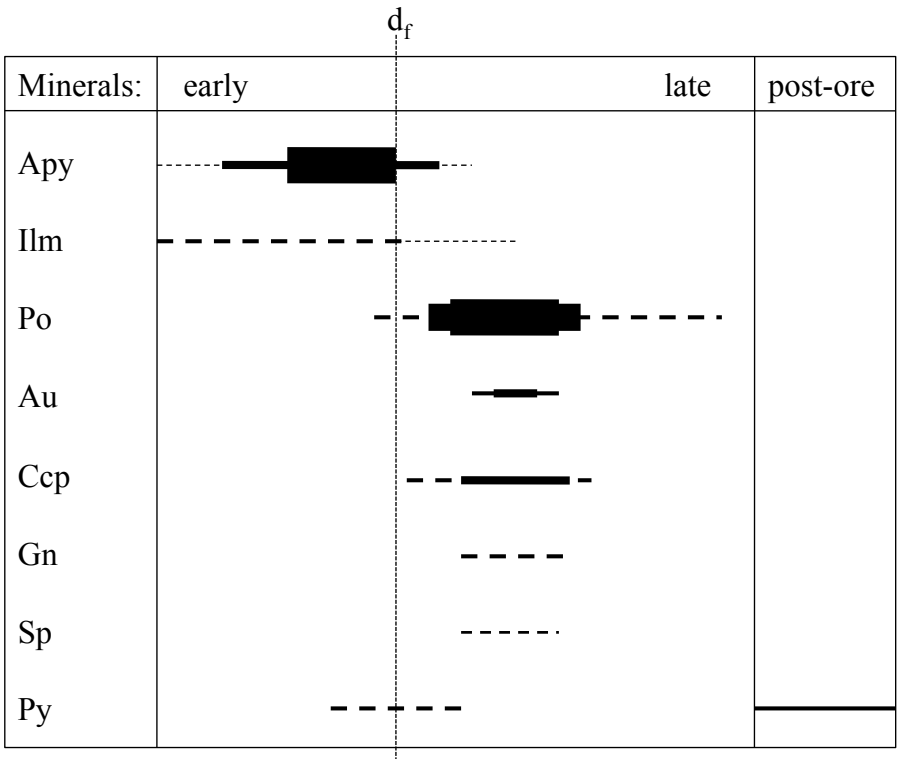

Figure 2.4. Simplified mineral paragenesis for ores in the Discovery Ormsby area (after Hansen, 2013). Abbreviations: apy = arsenopyrite; ilm = ilmenite; Au = gold; po = pyrrhotite; ccp = chalcopyrite; gn = galena; sp = sphalerite; py = pyrite; d_f = wall rock deformation fabric development.

with zircon as well as potassic alteration observed in host rocks adjacent to and within quartz veins (Hansen, 2013).

Clan Lake Area

The Clan Lake area, approximately 38 km south-southwest of the Discovery-Ormsby area (Fig. 2.1), is a larger, intermediate to felsic, metavolcanic-volcaniclastic complex (~1.5 km wide and 6.5 km long) and is surrounded by metasedimentary rocks of the Burwash Formation (Fig. 2.5). The metavolcanic rocks of the area can be categorized into four lithological units: mafic to intermediate volcanic rocks, intermediate to felsic volcanic rocks, pyroclastic rocks, and crosscutting mafic intrusions consisting of a central

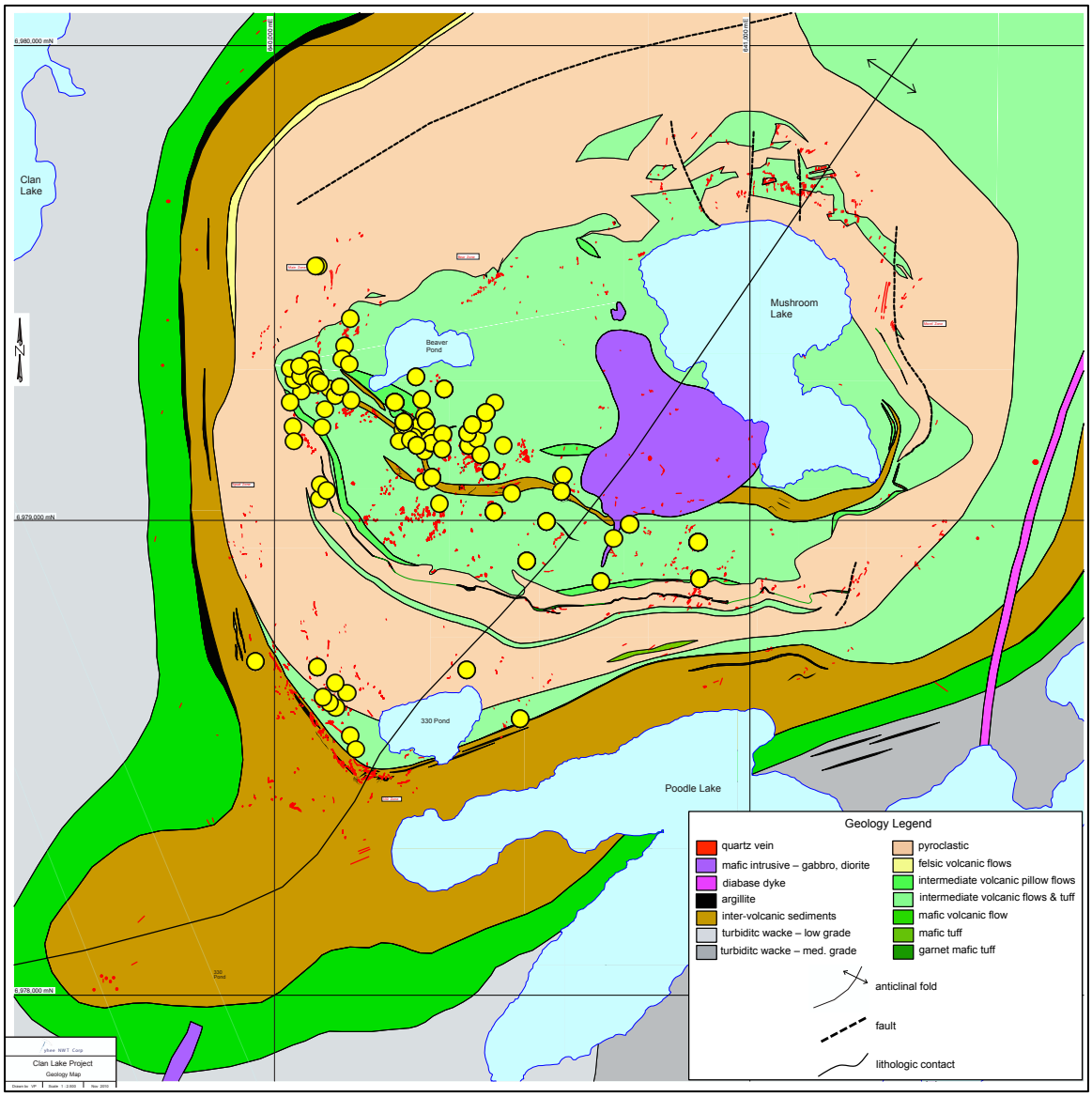

Figure 2.5. Generalized geological map of the Clan Lake area (after Pratico, 2009c). Gray areas represent metasedimentary rocks of the Burwash Formation; dark gray indicates medium metamorphic grade whereas light gray indicates low metamorphic grade. The following metavolcanic lithologies belong to the Banting Group: mafic flows (dark green), inter-volcanic sediments (brown), felsic flows (yellow), intermediate flows and tuffs (light green), pyroclastic intermediate rocks (peach), garnet-bearing mafic tuffs (medium green). Quartz veins are shown in red; dashed lines represent faults. Notice the young gabbro (purple) at the core of the complex, cross cut by a younger diabase dike (fuchsia). Yellow circles indicate localities of samples used for numerical analysis in the current study.

gabbroic body and diabase dikes (Pratico, 2009a). The first three units have been interpreted to be Banting Group age (~2.7 Ga) (Cousens et al., 2002). Metavolcanic rocks at Clan Lake have a minor mafic component but become more intermediate toward the center of the complex (Pratico, 2009a). Immobile element chemistries of the rocks at Clan Lake suggest dominantly intermediate to felsic protolith lithologies (Hansen, 2013).

A sinistral, strike-slip fault, ~1.75 km to the west of Clan Lake, is interpreted to be associated with an inferred extension of the Yellowknife River Fault Zone (Martel and Lin, 2006) and may be the major structural feature associated with deformation fabrics observed throughout Clan Lake. Major rock-forming minerals in metavolcanic units affected by deformation and metamorphism include chlorite, biotite, quartz, and hornblende with relict plagioclase. Contemporaneous deformation and metamorphism are suggested by the integration of peak metamorphic minerals (lower amphibolite grade) into shear deformational fabrics with minor retrograde overprints (Hansen, 2013).

Gold in the Clan Lake area

Most gold mineralization at Clan Lake is constrained to a 6.5 km long, 900 m wide, north-northeast striking region. Intermediate volcanic host rocks with extensive silicification, sulfidation, sericitic alteration, and potassic (biotite) alteration make up the Main Zone of Clan Lake, which is the primary drilling target in the area (Pratico, 2009a). Gold mineralization occurs as native gold, found in quartz veins and in silicified and sulfidized wall rock. Quartz veins commonly contain sulfides (chalcopyrite, galena, and sphalerite) and gangue minerals (chlorite, amphibole, biotite, and carbonates) (Hansen, 2013).

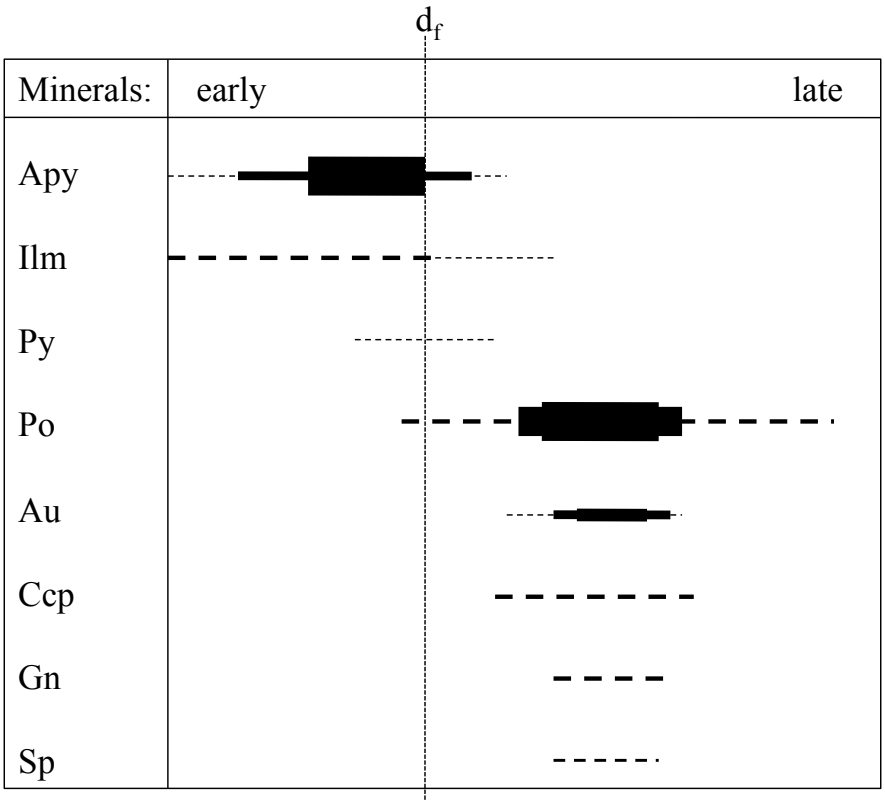

Figure 2.6. Simplified mineral paragenesis for ores in the Clan Lake area (after Hansen, 2013). Abbreviations: apy = arsenopyrite; ilm = ilmenite; Au = gold; po = pyrrhotite; ccp = chalcopyrite; gn = galena; sp = sphalerite; py = pyrite; d_f = wall rock deformation fabric development.

The Clan Lake and Discovery-Ormsby areas share similar ore mineralogies and parageneses, consisting of early arsenopyrite followed by pyrrhotite and gold (± base-metal sulfides). Arsenopyrite and a rare, early generation of pyrrhotite predate gold mineralization (Fig. 2.6). Fractures in arsenopyrite are filled frequently by gold and second generation pyrrhotite ± base-metal sulfides. In quartz veins, gold is accompanied frequently by pyrrhotite ± base-metal sulfides, or with base-metal sulfides alone. Less frequently, gold is found within wall rocks without sulfides (Hansen, 2013).

Wall-rock alteration at Clan Lake is so pervasive that it is nearly impossible in the field to locate a recognizable edge to the alteration zone (as a result of several

overprinting events) in order to define the size of the hydrothermal system. Host rocks are extensively silicified and display sericitic alteration and irregular patchy potassic alteration (Pratico, 2009a). Although host rocks at Clan Lake contain less iron (≤ 6.5 wt. % Fe) than the mafic rocks in the Discovery Ormsby area (up to 17.5 wt. % Fe), gold mineralization appears to be associated closely with sulfidation. Hansen (2013) determined that iron-liberating fluid-rock reactions (e.g. the conversion of ilmenite to titanite during the formation of pyrrhotite) must have been efficient in order to achieve sulfidation with the low iron content observed in gold-bearing host rocks at Clan Lake.

The association between gold and potassic alteration that is observed commonly in both the Discovery-Ormsby and Clan Lake areas (Pratico, 2009; Hansen, 2013) likely reflects a chemical influence on hydrothermal fluids from the voluminous granitic rocks in the Slave Province (see Appendix 1), most of which are thought to have been emplaced during peak regional metamorphism (Thompson, 1989; van Breemen et al., 1992; Davis and Bleeker, 1999).

Previous Studies of Discovery-Ormsby and Clan Lake

The following section will discuss the geochemical investigations of gold mineralization in the Discovery-Ormsby and Clan Lake areas by Hansen (2013), the results of which prompted the present study.

Oxygen Isotope Studies

Oxygen isotope studies of host rocks and quartz veins of the Discovery-Ormsby and Clan Lake areas in the southern YGB were employed by Hansen (2013) in order to assess fluid source(s) and to determine possible fluid pathways and the degree of water-rock interaction along flow paths. Nineteen samples (11 quartz veins; 8 wall rocks) from

the Discovery-Ormsby area and thirty-five samples (20 quartz veins; 15 wall rocks) from the Clan Lake area were analyzed.

Discovery-Ormsby area

Using the ranges and distribution of $\delta^{18}O$ values, quartz veins from the Discovery-Ormsby area were interpreted to reflect a dominantly metasedimentary-derived fluid, whereas those at Clan Lake reflected fluids in equilibrium with both metasedimentary and metavolcanic rock reservoirs (despite the almost exclusively metavolcanic lithology of their host rocks). 3-D block models of $\delta^{18}O_{quartz\ vein}$ and $\delta^{18}O_{whole\text{-}rock}$ values (VSMOW), constructed with the Rockworks™ software by Rockware®, were used to define fluid pathways and to evaluate water-rock reactions along these paths. The block model of $\delta^{18}O_{quartz\ vein}$ values of the Ormsby Member in the Discovery-Ormsby area shows highest $\delta^{18}O$ values to the north-northwest and lower $\delta^{18}O$ values to the south-southeast (Fig. 2.7).

Clan Lake area

At Clan Lake, block models of both $\delta^{18}O_{quartz\ vein}$ and $\delta^{18}O_{whole\text{-}rock}$ values show that values are highest at the southwestern corner of the area and form a wedge-shaped volume that narrows with increasing depth (Figs. 2.8 and 2.9). Lowest $\delta^{18}O$ values create a similar shape at the opposite (north-northeastern) corner of the model and define an apparent edge to the metasedimentary-derived fluid overprint. The results for both the Discovery-Ormbsy and Clan Lake areas (Hansen, 2013) demonstrate the utility of $\delta^{18}O$ values in determining the size of hydrothermal systems, even in a highly altered rock body (and their correlation to gold deposition, as discussed in the next section).

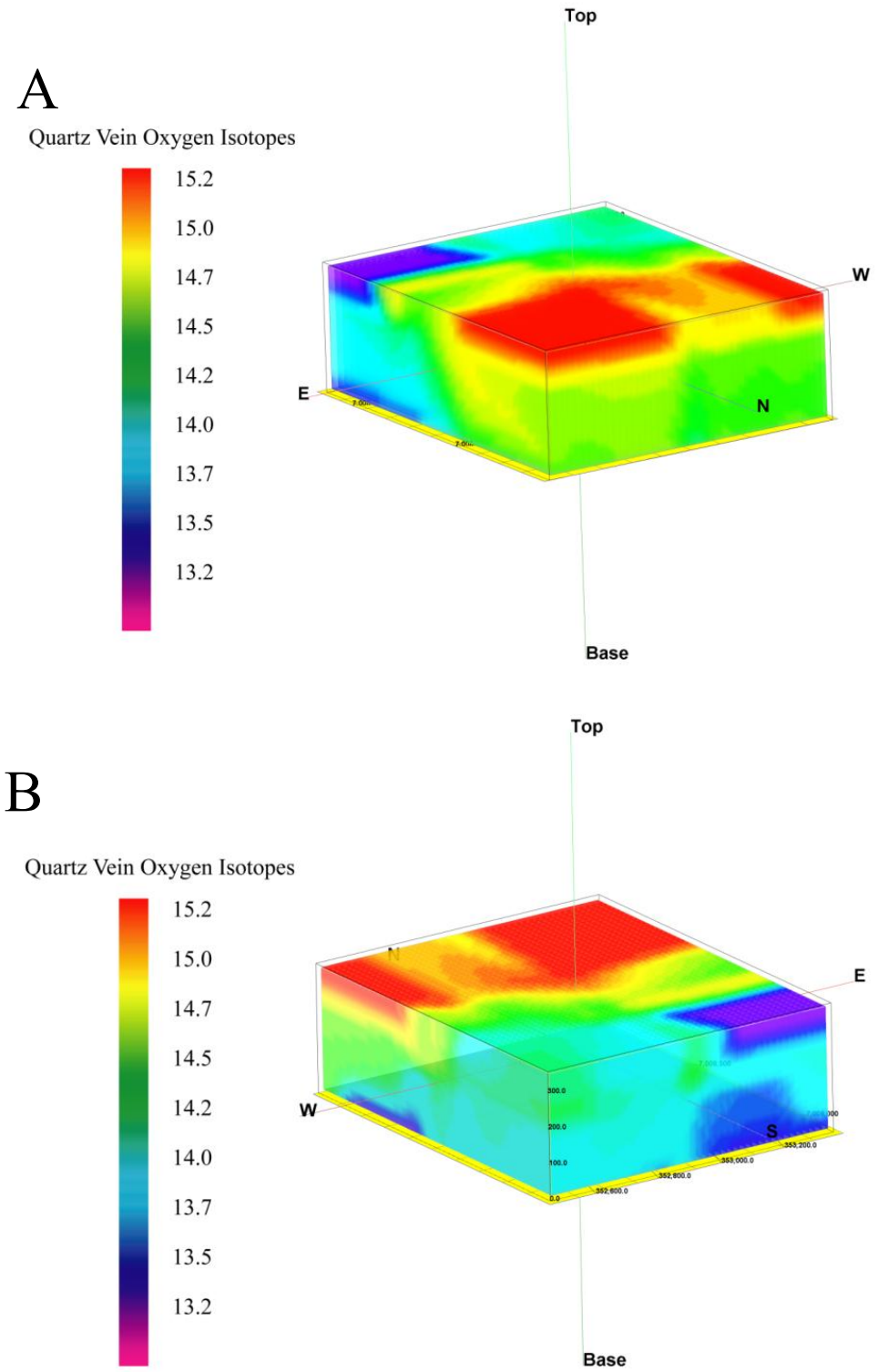

Figure 2.7. 3-D block models of $\delta^{18}O$ values (‰ VSMOW) for quartz veins from the Ormsby Member in the Discovery-Ormsby area (after Hansen, 2013). A) View from the northeast looking toward the southwest. B) View from the southwest looking toward the northeast.

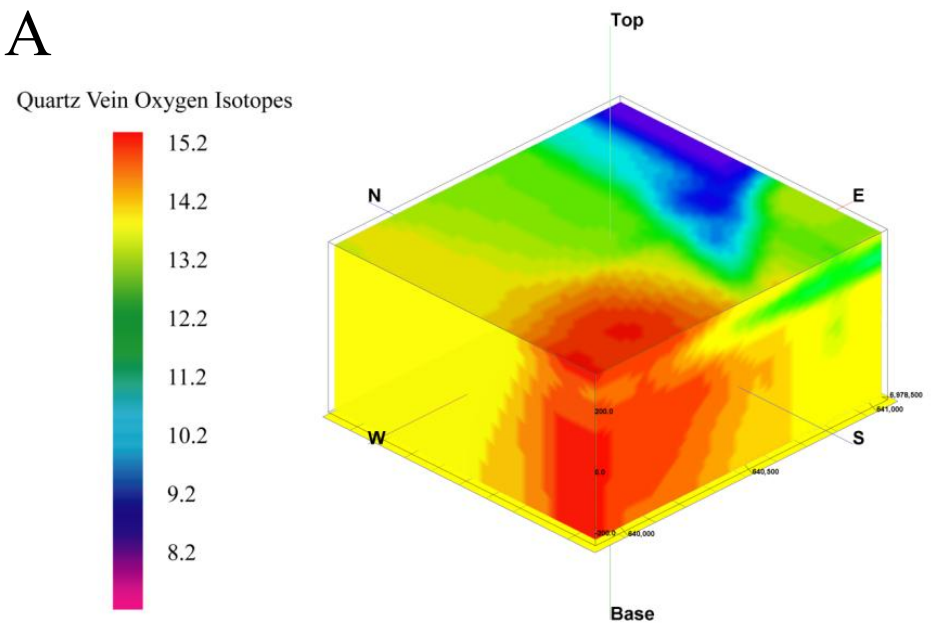

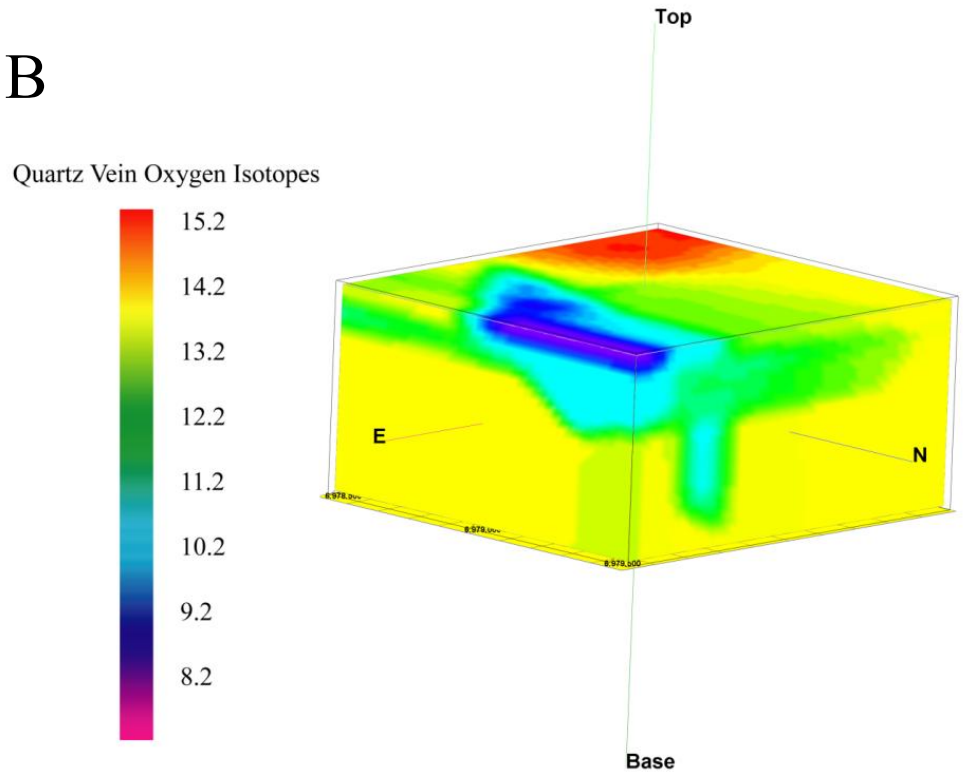

Figure 2.8. 3-D block models of $\delta^{18}O$ values (‰ VSMOW) for quartz veins from the Clan Lake area (after Hansen, 2013). A) View from the southwest looking toward the northeast. Note that highest $\delta^{18}O$ values form a wedged shape located in the southwestern corner of the block. B) View from the northeast looking toward the southwest.

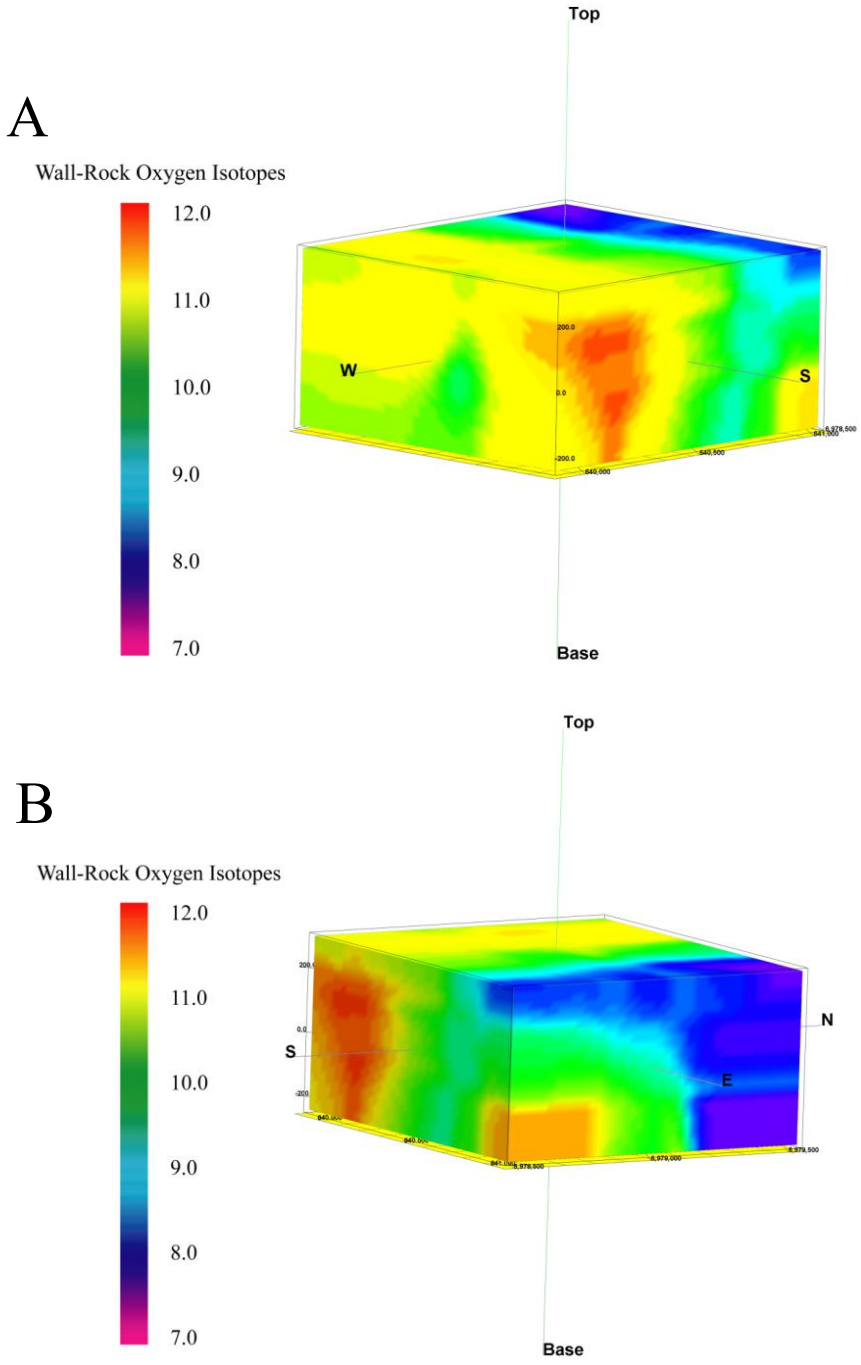

Figure 2.9. 3-D block models of $\delta^{18}O$ (‰ VSMOW) for wall rocks from the Clan Lake area (after Hansen, 2013). A) View from the southwest looking toward the northeast. B) View from the southeast looking toward the northwest.

Lithogeochemical Studies

Lithogeochemical modeling and analysis were performed by Hansen (2013) to attempt to link oxygen isotope results to host rock chemistry and gold mineralization. Tyhee Gold Corporation provided geological and geochemical data for all cores drilled to date (65 and 169 drill cores from Discovery-Ormsby and Clan Lake, respectively).

Gold distribution at Discovery-Ormsby

Hansen (2013) constructed block models of gold concentration in the same manner as the $\delta^{18}O$ models. The block model of gold concentrations in the Ormsby Member shows that high gold anomalies occur mostly in the southwestern corner of the area (Fig. 2.10). However, the 3-D model of $\delta^{18}O$ values for the same block (Fig. 2.7) shows that highest $\delta^{18}O$ values of quartz veins are in the northern portions of the Ormsby Member and that $\delta^{18}O$ values generally decrease toward the southern portion, although the total range of $\delta^{18}O_{quartz\ vein}$ values is only from 13.0 to 15.2‰ (where high gold concentrations coincide with $\delta^{18}O = \sim 13‰$, Hansen, 2013). The elevated and narrow range in $\delta^{18}O$ values of quartz veins are indicative of metasedimentary fluid that overwhelmed the entire metavolcanic Ormsby Member. This spatial relationship between $\delta^{18}O_{quartz\ vein}$ values and gold mineralization was interpreted to suggest that extensive reactions of metasedimentary-derived fluids with metavolcanic host rocks (and subsequent sulfidation and gold deposition) occurred where porosity and permeability in the host rock had been enhanced by the Discovery shear zone (Hansen, 2013).

To test the possible dependence of gold distribution on host rock chemistry, major, minor, and trace element data were plotted against one another and analyzed by Hansen (2013). However, expected correlations between gold and elements relevant

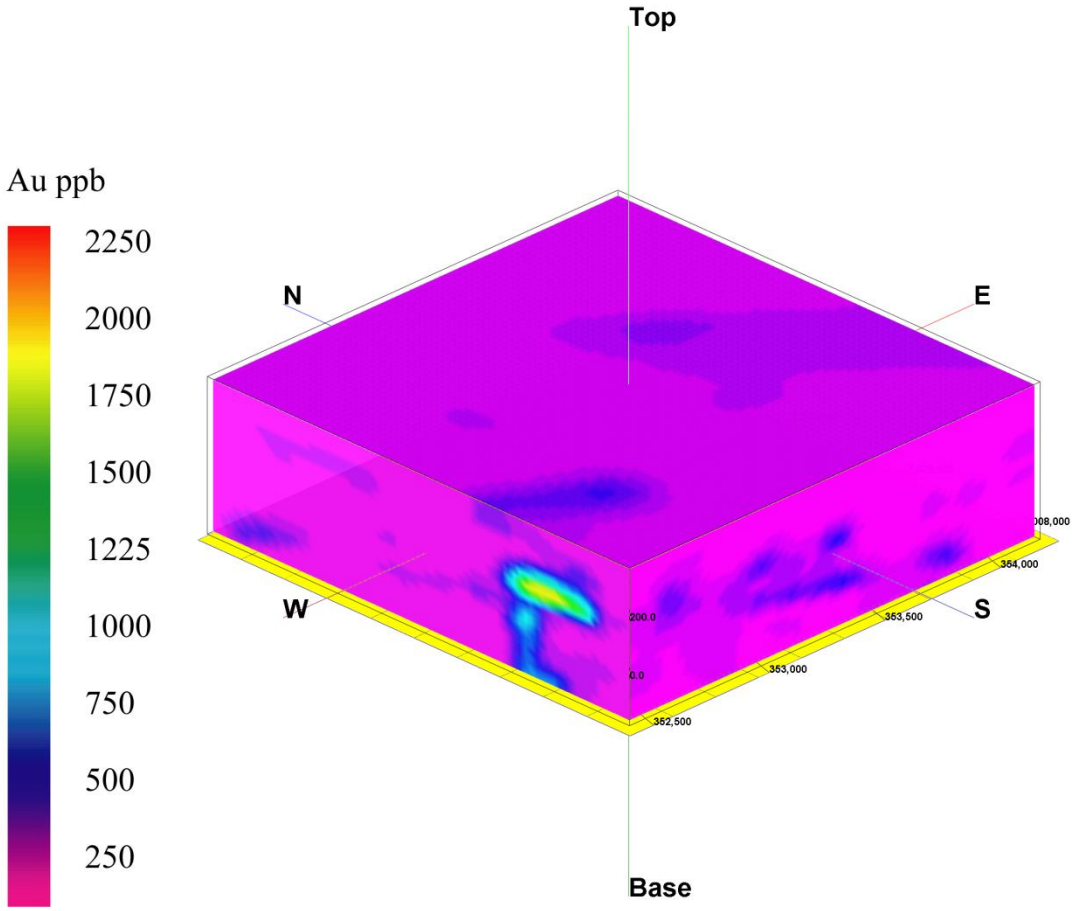

Figure 2.10. 3-D block model showing the distribution in gold concentrations (ppb) in the Ormsby Member in the Discovery-Ormsby area (after Hansen, 2013). Note the high gold anomaly in the southwestern corner of the block model.

to wall rock sulfidation (Fe and As) or to other types of alteration (e.g. Fe, K, Ca, Na involved with sericitic and potassic alteration) were not present for the Ormsby Member. This lack of anticipated correlations suggests that a factor(s) in addition to host rock chemistry influenced gold enrichment. Hansen (2013) speculated that gold deposition may have been influenced by enhanced porosity and permeability produced by structural features like faults and shear zones (i.e. the Discovery Shear Zone) that focused auriferous fluid flow to the specific portions of the metavolcanic host rocks where gold mineralization is observed.

Gold distribution at Clan Lake

Block models of gold concentrations at Clan Lake show that high gold anomalies coincide generally with elevated $\delta^{18}O$ values (Fig. 2.11). The largest volume of rock with both elevated $\delta^{18}O$ values and high gold concentrations occurs in the southwestern corner of the block model and was interpreted to represent a feeder zone for hydrothermal gold-bearing fluids derived from metasedimentary reservoirs (Hansen, 2013).

Similar to the Ormsby Member, plots between gold and various elements for Clan Lake did not produce correlations that would be associated with wall rock alteration and sulfide deposition (Fe, Ti, As, K, Ca, Na) (Hansen, 2013). Zr/Ti ratios indicated that high gold-bearing rocks did not belong exclusively to a particular lithology, and were interpreted to indicate that gold mineralization may have rather corresponded to more highly reactive metavolcanic host rock chemistries or that other factors, such as enhanced porosity and permeability, may have controlled the spatial distribution of gold.

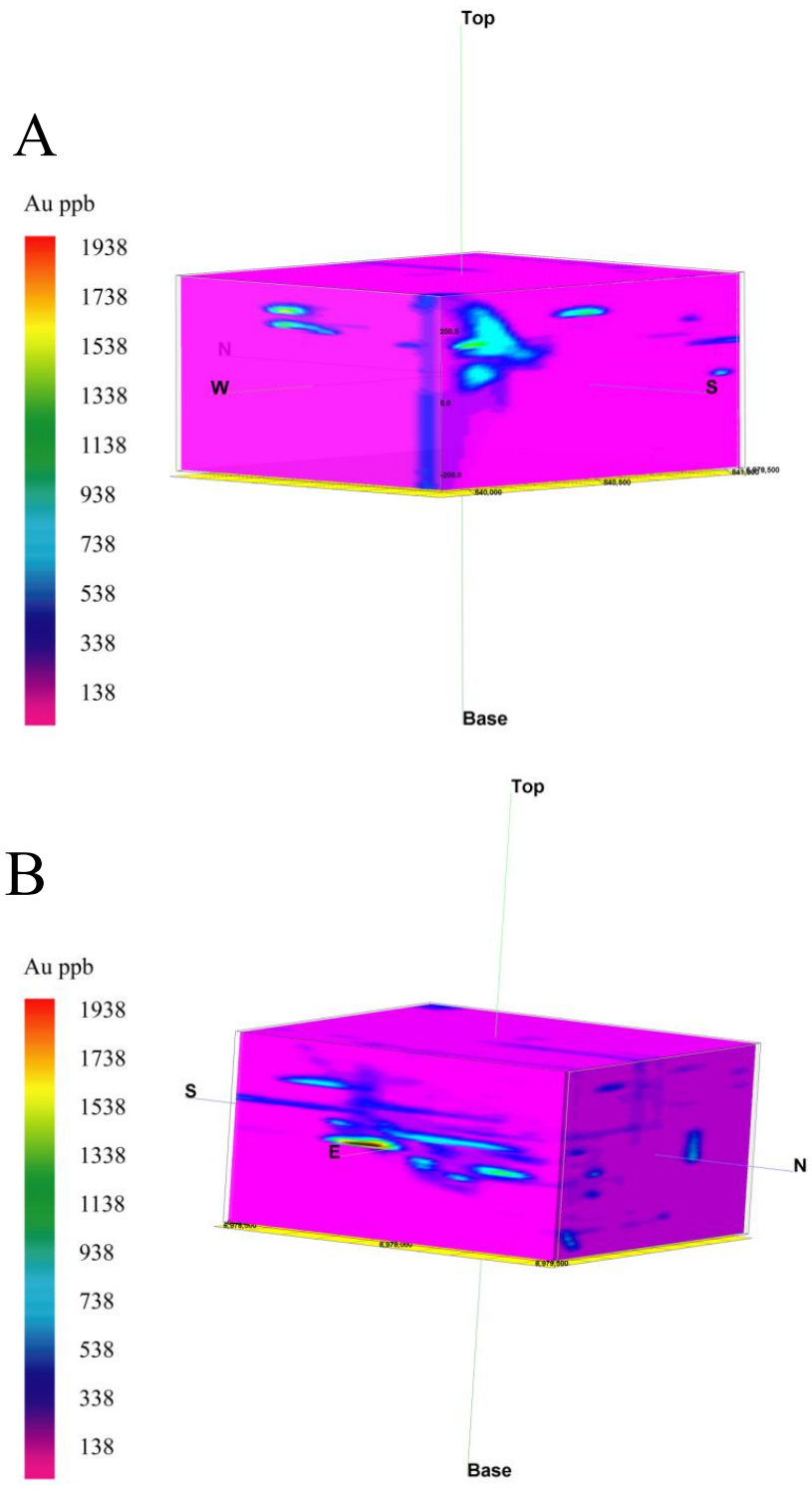

Figure 2.11. 3-D block models showing the distribution in gold concentrations (ppb) in the Clan Lake area (after Hansen, 2013). A) View from the southwest looking toward the northeast. Note the high gold anomalies in the southwestern corner and on the southern and western faces of the block model. B) View from the east looking toward the west. Note the high gold anomalies on the eastern face of the block model.

NUMERICAL ANALYSIS & DATA MODELING

Plots of elemental concentrations versus gold concentrations alone were unfortunately inconclusive in determining the influence of host rock chemistry on gold enrichment in previous research (Hansen, 2013). The present study attempts to identify spatial patterns of gold distribution and host rock chemistry in three-dimensional space using numerical methods to reconstruct elemental concentrations (specifically K, Na, Ca, and Al) in terms of mineral assemblages associated with potassic alteration. The spatial distribution of highly altered host rocks can be compared to gold enrichment in order to detect possible relationships between gold deposition and wall rock alteration reflected by current host rock chemistry.

Previous studies

Hydrothermal alteration has been quantified in the past by calculating elemental mass changes associated with K-metasomatism, based on the Pearce element ratio technique of Stanley and Madeisky (1994). Warren et al. (2007) calculated mass changes associated with hydrothermal alteration to quantify the intensity of K-metasomatism and its proximity to epithermal Au-Ag deposits in volcanic host rocks; Booden et al. (2011) applied the same technique to quantify relative K gains in metasomatism associated with epithermal Au-Ag deposits hosted in andesites and dacites in New Zealand. These studies evaluated whole-rock geochemical anomalies by calculating mass changes associated with hydrothermal alteration, comparing the compositions of altered rocks to fresh-rock equivalents, and, with the use of molar element ratios, comparing the compositions of altered rocks to the composition of hydrothermal minerals. Their results demonstrated that whole-rock geochemical techniques for evaluating K-metasomatism

are applicable to a wide range of epithermal deposits hosted by felsic, intermediate, and mafic volcanic rocks. Such techniques can be used as exploration tools by locating areas most affected by K-metasomatism, which are most likely to contain epithermal Au-Ag mineralization.

Application to the current study

Mass transfer effects associated with hydrothermal alteration will be evaluated graphically using molar element ratios calculated from whole-rock geochemical data from drill core from the Discovery-Ormsby and Clan Lake areas. This technique will be applied in order to (a) test the relationship of alteration intensity (or lack thereof) to gold concentration and (b) assess its utility as an exploration tool/ore guide in the northern YGB and in other metavolcanic-hosted gold deposits.

It is important to note that previous studies that have related mineralization to calculated intensity of hydrothermal alteration (e.g. Warren et al., 2007; Booden et al., 2011) applied to volcanic-hosted deposits, whereas gold deposits in our study areas are hosted in metamorphosed volcanic rocks. These calculations may not account for potential compositional changes in host rocks resulting from metamorphism that occurred after gold mineralization.

Methodology

All numerical analysis in this study was performed with MATLAB® by MathWorks® using the same geological and geochemical data as in Hansen (2013) provided by Tyhee Gold Corporation, who contracted Acme Analytical Laboratories, Ltd. to analyze whole-rock chemistry using fire assay and four-acid digestion followed by inductively coupled plasma atomic emission spectrometry (ICP-AES). The data set

for the Ormsby Member of the Discovery-Ormsby area came from 24 drill cores containing lithogeochemical data (representing ~2,680 individual samples) (see sample locations marked by yellow circles in Fig. 2.3). Spatial control in the Ormsby area is not optimal, as data are constrained mostly to the northeast-southwest trending zone within which most gold exploration has taken place. In contrast, the lithogeochemical data set for the Clan Lake area includes 150 drill cores (representing ~19,900 individual samples) (see sample locations marked by yellow circles in Fig. 2.5) with well-developed spatial control.

All data was filtered for analysis to omit any element concentration that was below detection level. Data points whose (2Ca + Na + K)/Al value was greater than 1.5 were omitted in an attempt to remove samples with elevated Ca concentrations resulting from carbonate alteration. Values for duplicate data points (i.e. an interval of drill core logged as having both quartz veins and metavolcanic rocks) were averaged. Additional filtering was applied to remove all core intervals logged as metasedimentary rocks or inter-volcanic sediments in order to ensure that lithologically unrelated potassium or aluminum anomalies are not included in analyses and models of metavolcanic host rocks.

Evaluating hydrothermal alteration

Assuming that Al remains immobile during metasomatic reactions (Gresens, 1967), different mineral phases associated with potassic alteration can be defined in a plot representing K concentrations relative to cumulative K, Na, and Ca concentrations (Fig. 2.12). For reference, common molar ranges for these elements in unaltered volcanic rocks are shown in Figure 2.12 (Warren et al., 2007; Booden et al., 2011). The minerals

in this diagram can be related by their respective mass changes in K, Na, and Ca during alteration, which are represented by the following equations:

(1) $NaAlSi_3O_8 + K^+ \rightarrow KAlSi_3O_8 + Na^+$,
albite K-feldspar

(2) $Na_2CaAl_4Si_8O_{24} + 2H^+ + 2K^+ \rightarrow KAlSi_3O_8 + KAl_3Si_3O_{10}(OH)_2 + SiO_2 + 2Na^+ + Ca^{2+}$,
plagioclase K-feldspar K-mica quartz

(3) $3KAlSi_3O_8 + 2H^+ \rightarrow KAl_3Si_3O_{10}(OH)_2 + 6SiO_2 + 2K^+$,
K-feldspar K-mica quartz

(4) $2KAl_3Si_3O_{10}(OH)_2 + 3H_2O + 2H^+ \rightarrow 3Al_2Si_2O_5(OH)_4 + 2K^+$
K-mica kaolinite

The slope of the line that connects a particular point on this diagram to the origin is equal to K/(2Ca + Na + K) (hereinafter referred to as "alteration index") and represents the combined effects of K, Na and Ca gains/losses associated with alteration for that point (Stanley and Madeisky, 1994; Madeisky, 1996). For example, an altered intermediate rock whose molar composition plotted at point "A" on Figure 2.12 would represent an alteration index (i.e. slope from the origin) equal to 1.0, where complete alteration to K-bearing mineral phases has occurred and all Na and Ca were lost in reaction. An altered intermediate rock at point "B" (Fig. 2.12) would have an alteration index equal to 0.25, and would represent a relative loss in Na, Ca, and K (i.e. conversion of feldspar to kaolinite or chlorite).

Modeling

Molar ratios of (2Ca + Na + K)/Al and K/Al for the Discovery-Ormsby and Clan Lake areas were first plotted onto the diagram shown in Figure 2.12 in order to confirm that the data reflect relevant alteration chemistries that warrant further study (Figs.

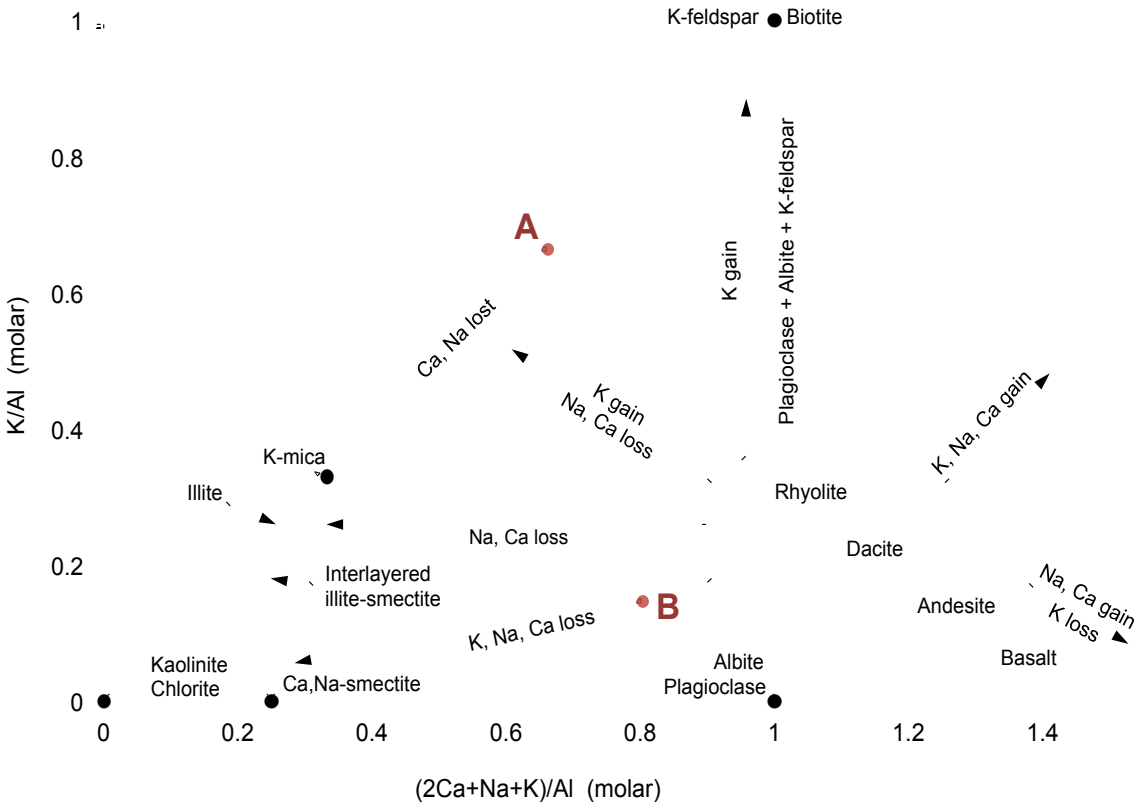

Figure 2.12. Molar ratio plot of (2Ca + Na + K)/Al versus K/Al and their relative values for typical fresh volcanic rocks (modified from Warren et al., 2007). Mass transfer reactions are indicated by arrows that point toward resultant alteration minerals. Alteration index values are assigned according to the slope of the line that connects a point to the origin; for example, point A represents an alteration index equal to 1.0, whereas point B represents an alteration index equal to 0.25 (also discussed in text).

2.13 and 2.14). Alteration index values (K/(2Ca + Na + K)) were then calculated for each study area and compiled into a three dimensional matrix according to easting, northing, and depth coordinates for each drill core. Since the data were scattered and clustered, linear interpolation was used to create a volume of data across a uniform grid. These data were then smoothed with a low-pass filter. Slices (XY, XZ, or YZ planes) through this volume permitted the alteration index calculations to be visualized at any desired coordinate in 3-D space.

Results

Diagrams and 3-D models of potassic alteration of metavolcanic rocks in the Discovery-Ormsby and Clan Lake areas are shown in Figures 2.16, 2.18, and 2.19. Additional 3-D models are included in Appendix 2 for reference. Note that some areas for which there were no data available may appear transparent in 3-D models, and should not be confused for weakly altered or unaltered rocks (which will appear as dark blue or purple areas in the models).

Discovery-Ormsby Area

The distribution of data in the molar ratio plot of (2Ca+Na+K)/Al versus K/Al in Figure 2.13 shows an encouraging trend in terms of the potential for successfully quantifying and modeling alteration. There is a clear shift to the left from values corresponding to mafic volcanic rocks, indicating a combined loss in Na and Ca, which may represent potassic metasomatism accompanied by some other type of alteration, such as chloritization, within the mafic metavolcanic host rocks of the Discovery-Ormsby area. Figure 2.15 shows that high gold anomalies appear to be associated with an

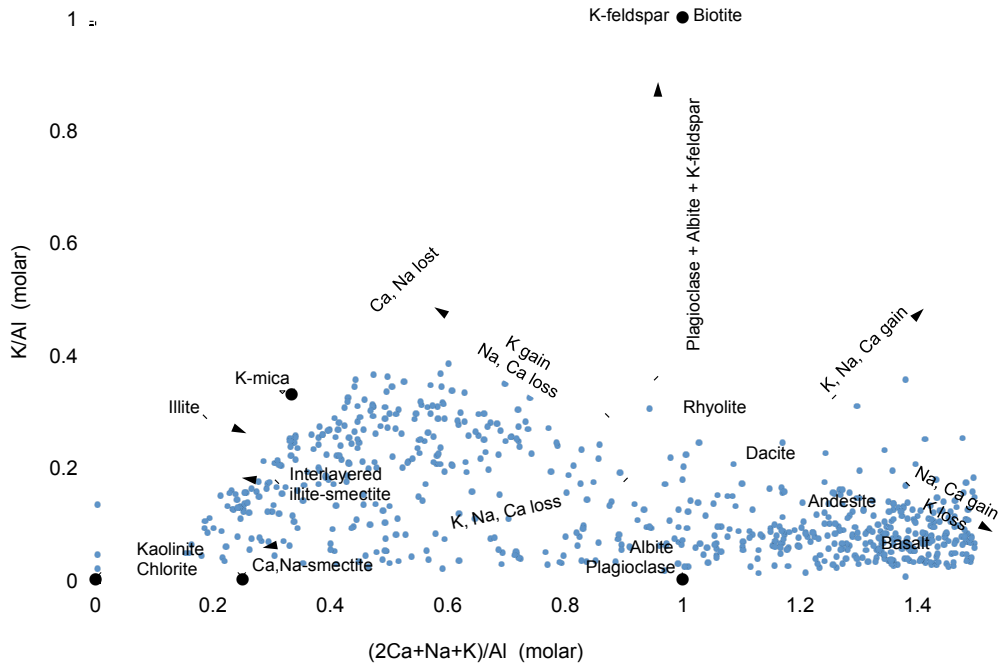

Figure 2.13. Molar ratio plot of (2Ca + Na + K)/Al versus K/Al for data from the mafic metavolcanic rocks in the Ormsby Member in the Discovery-Ormsby area.

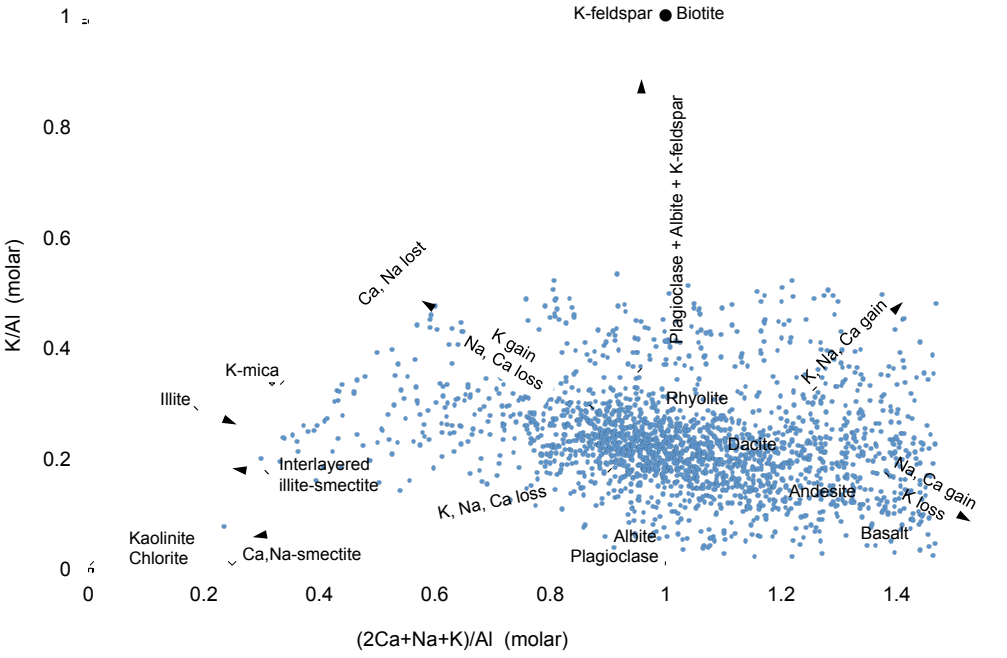

Figure 2.14. Molar ratio plot of (2Ca + Na + K)/Al versus K/Al for data from the intermediate to felsic metavolcanic rocks in the Clan Lake area. This plot only includes a selected potion of the total data in order to avoid overcrowding of data points.

alteration index of ≤ 0.15 (i.e. shallow slopes on the molar plot of K/Al versus (2Ca + Na + K)/Al in Fig. 2.13).

Although gold assays have been well documented in the Ormsby Member, less than half of the total drill core data include lithogeochemical analyses. Unfortunately, a large amount of this lithogeochemical data is for metasedimentary host rocks, particularly where drill cores are most concentrated at the northeast end of the Ormsby Member (see sample locations marked by yellow circles on Fig. 2.3). Thus, the amount of applicable data for modeling alteration chemistry in metavolcanic rocks in the Discovery-Ormsby area is limited.

3-D modeling of potassic alteration of metavolcanic rocks of the Ormsby Member (Fig. 2.16) is fairly inconclusive, largely due to limited geochemical data. The only instance of strong alteration seen in the model is in the southeast portion at elevations ≥ 150 meters (or depths ≤ ~ 160 meters), which may correspond to gold enrichment shown in Hansen's (2013) block models (Fig. 2.10). According to the model, moderate potassic alteration (alteration index ~ 0.25 to 0.30) appears to have taken place at the current surface elevation near the northwest corner of the area (Fig. 2.16a). Additional data for metavolcanic rocks with stronger spatial control are required before conclusive correlations between potassic alteration and gold enrichment can be evaluated for the Discovery-Ormsby area.

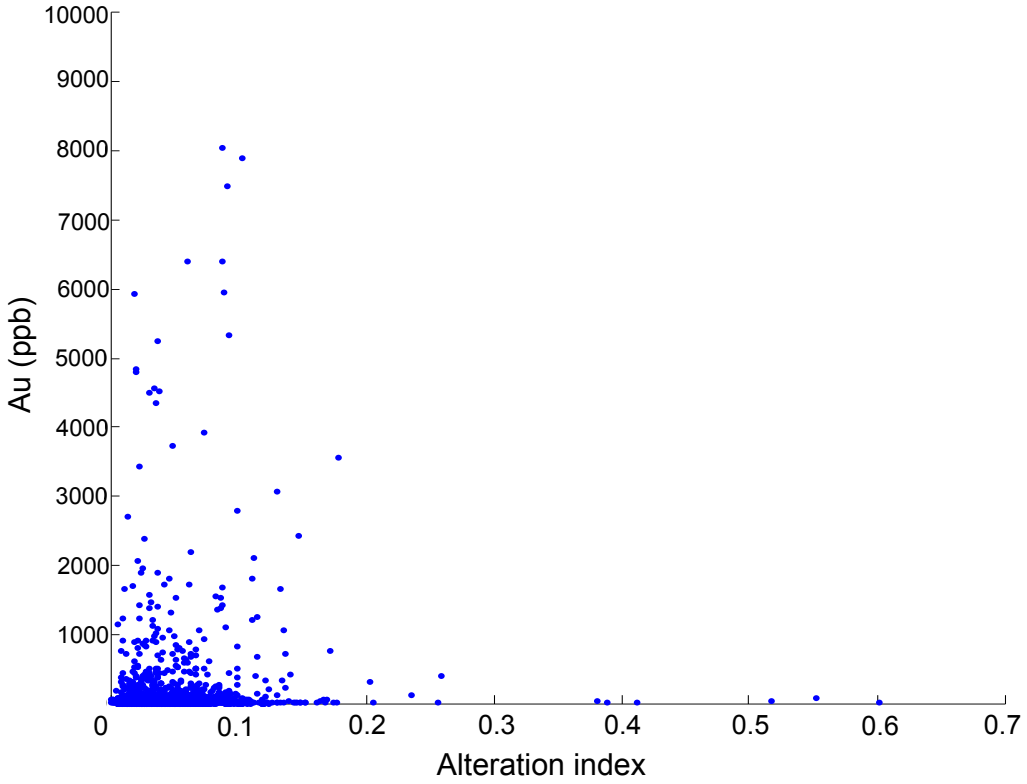

Figure 2.15. Calculated alteration index values for host rocks versus gold concentration (ppb) in the Ormsby Member in the Discovery-Ormsby area. Note that the maximum alteration index is 0.6, which represents only partial relative loss in Na and Ca (or gain in K).

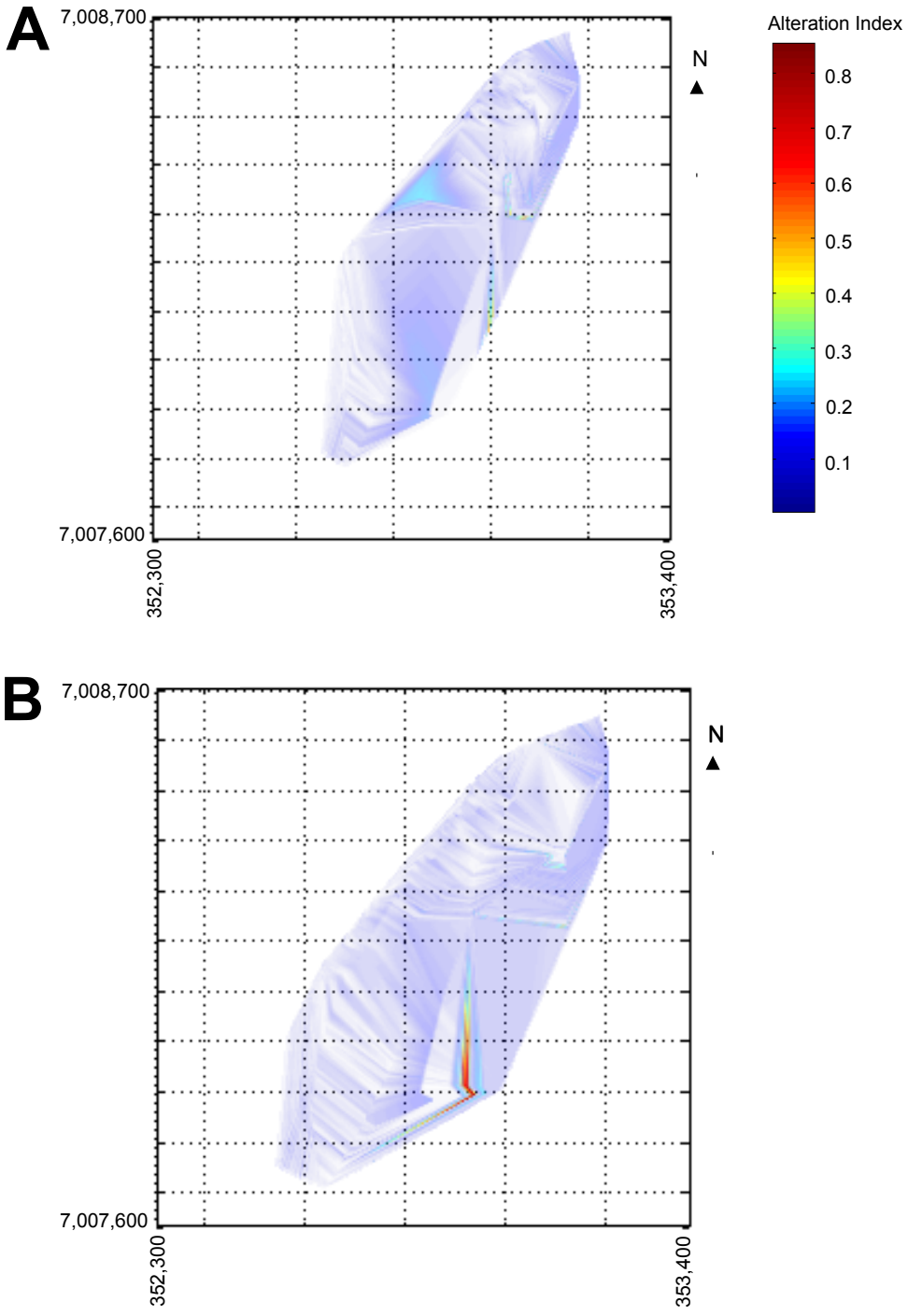

Figure 2.16. Models showing the calculated alteration index values (i.e. intensity of potassic alteration) for the mafic metavolcanic rocks in the Ormsby Member in the Discovery-Ormsby area in plan view. Model dimensions are in UTM coordinates (meters); elevations are in meters above mean sea level. A) Elevation = 250 meters a.s.l. (avg. depth = 60 m). B) Elevation = 200 meters a.s.l. (avg. depth = 110 m).

Clan Lake Area

Despite the fact that the numerical techniques employed in the present study are being applied to altered metavolcanic rocks (as opposed to altered volcanic rocks, as has been done in the past), initial calculations of alteration index values for the Clan Lake area and their associated gold concentration suggest that 3-D modeling may successfully reflect a spatial correlation between hydrothermal alteration and gold mineralization. A plot of molar (2Ca + Na + K)/Al versus K/Al for Clan Lake (Fig. 2.14) indicates that a majority of metavolcanic host rocks has been potassically altered only moderately, assuming an intermediate to felsic protolith, and that most high gold anomalies at Clan Lake correspond to an alteration index < 0.4 (Fig. 2.17).

3-D modeling reveals that strong potassic alteration of metavolcanic rocks at Clan Lake occurs as isolated, concentrated patches (which may reflect the irregular, patchy occurrence of potassic alteration documented by Pratico, 2009a), whereas weak to moderate alteration is generally more widespread (Figs. 2.18 and 2.19). In N-S transects through the eastern portion of the Clan Lake area, strong alteration appears to dip linearly to the south (Fig. 2.19a), which may be related to the south-dipping increase in $\delta^{18}O$ values with depth seen on the eastern face of $\delta^{18}O_{wall\ rock}$ block models (Hansen, 2013) (Fig. 2.9), and may reflect a local system of faults and fractures, or the northeast-southwest trending anticline in the area (Fig. 2.5).

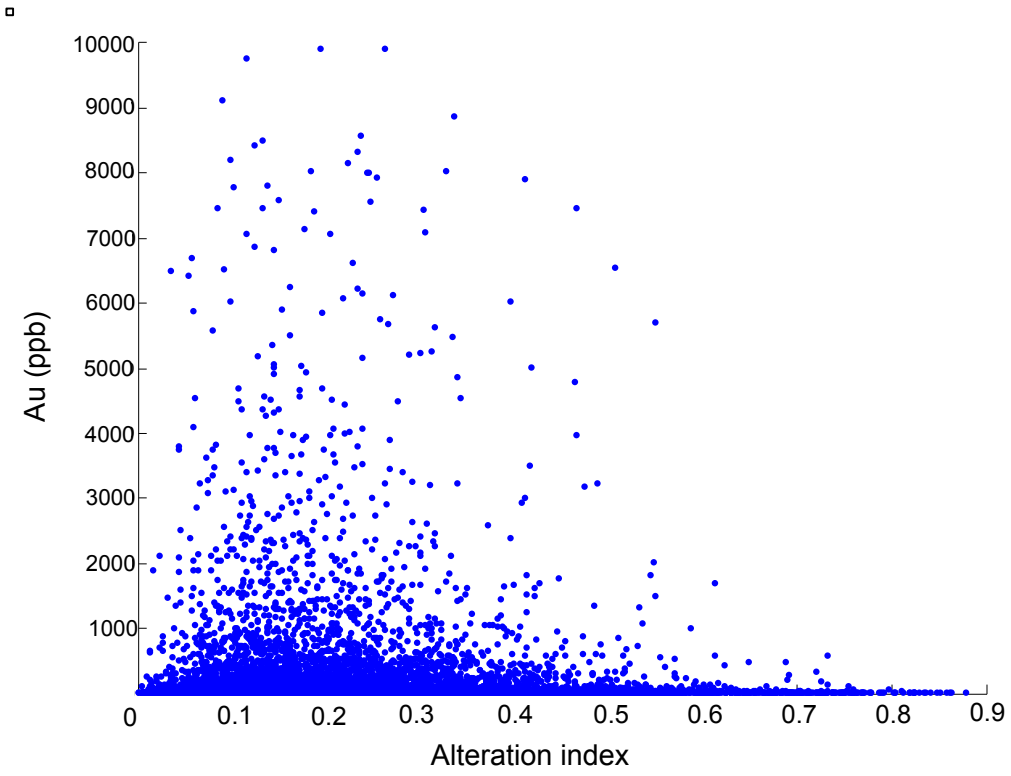

Figure 2.17. Calculated alteration index values of intermediate to felsic metavolcanic host rocks versus gold concentration in the Clan Lake area. Note that the maximum alteration index is 0.87.

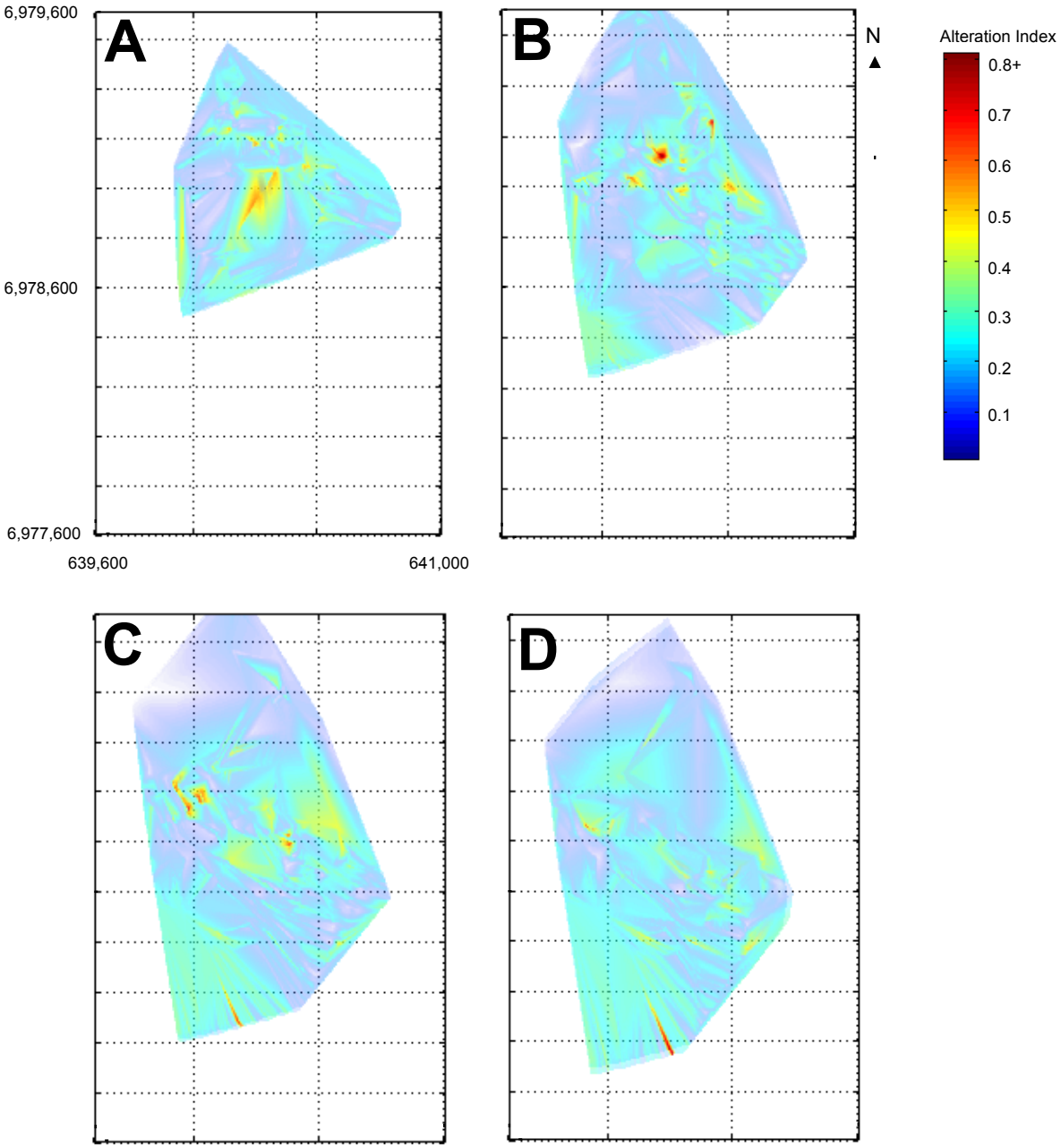

Figure 2.18. Models showing the calculated alteration index values (i.e. intensity of potassic alteration) for the intermediate to felsic metavolcanic rocks in the Clan Lake area in plan view. Model dimensions are in UTM coordinates (meters); elevations are in meters above mean sea level. A) Elevation = 250 meters a.s.l. (avg. depth = 15 m). B) Elevation = 150 meters a.s.l. (avg. depth = 115 m). C) Elevation = 50 meters a.s.l. (avg. depth = 215 m). D) Elevation = 0 meters a.s.l. (avg. depth = 265 m).

Figure 2.19. Transects showing calculated alteration index values (i.e. intensity of potassic alteration) for the intermediate to felsic metavolcanic rocks in the Clan Lake area. Model dimensions are in UTM coordinates (meters); elevations are in meters above mean sea level. A) N-S transect through the eastern portion of the area. Note the linear trend in moderately to strongly altered rocks that dips toward the south. B) N-S transect through the center of the area. Note the steeper dip in the linear trend of potassic alteration. C) N-S transect through the western portion of the area. Note that strong potassic alteration is comparatively scarce and weak to moderate potassic alteration is widespread toward the south. D) E-W transect through the northern portion of the area. E) E-W transect through the north-central portion of the area. F) E-W transect through the southern portion of the area.

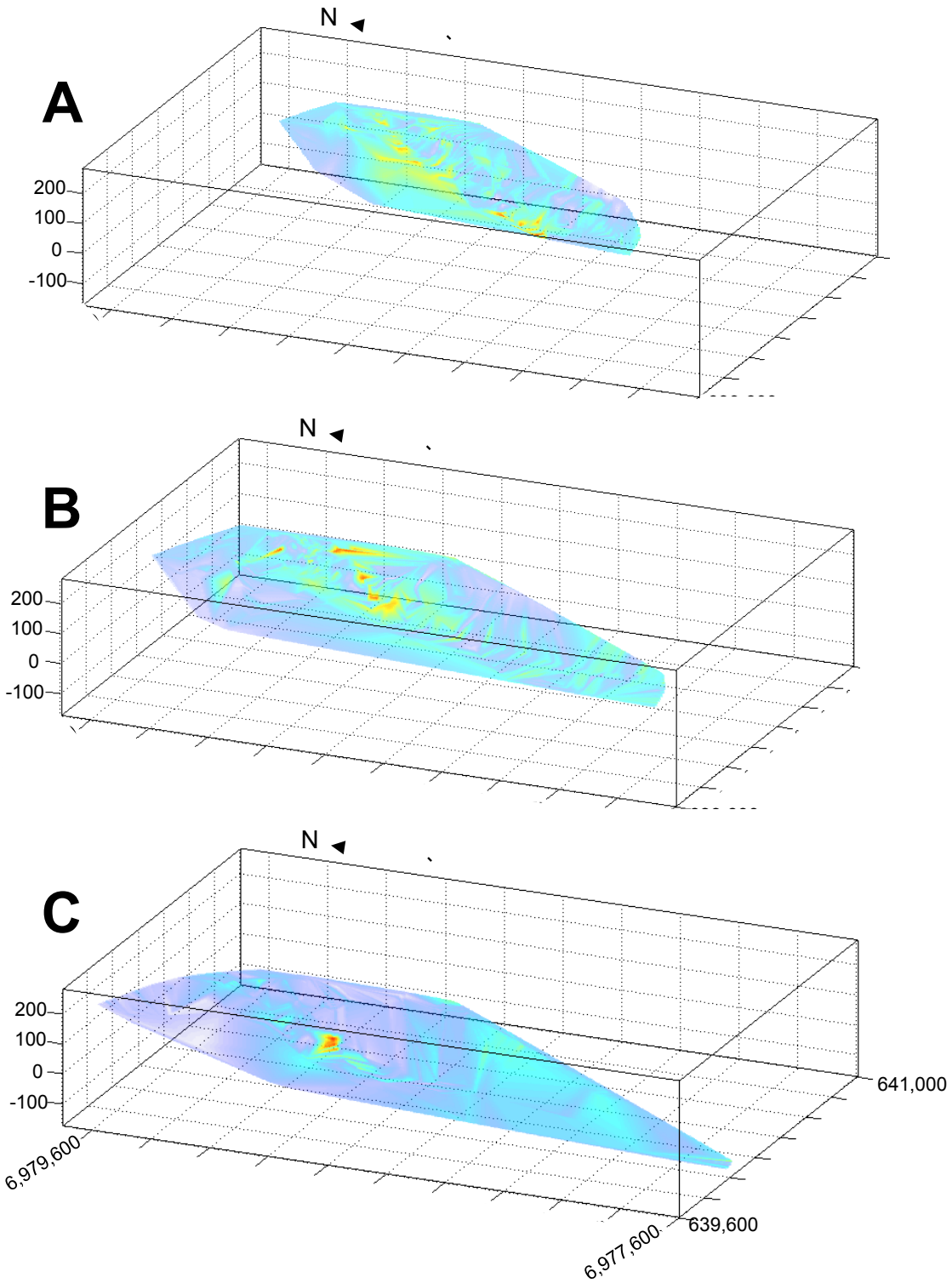
A
N
200
100
0
-100
B
N
200
100
0
-100
C
N
200
100
0
-100
6,979,600
6,977,600
639,600
641,000
0.8+
0.7
0.6
0.5
0.4
0.3
0.2
0.1
Alteration Index

Fig. 2.19 cont.

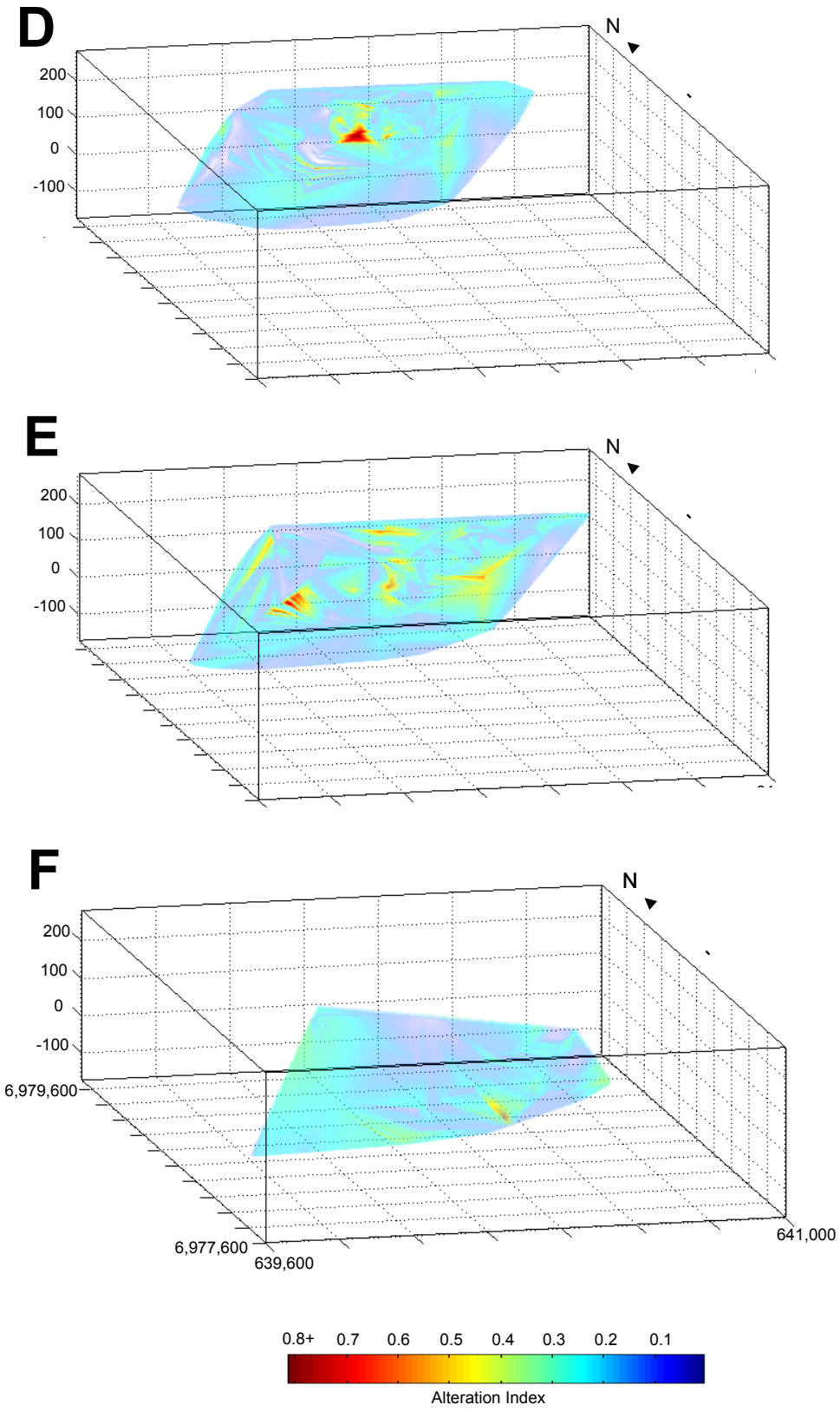
D
N
200
100
0
-100
E
N
200
100
0
-100
F
N
200
100
0
-100
6,979,600
6,977,600
639,600
641,000
0.8+ 0.7 0.6 0.5 0.4 0.3 0.2 0.1
Alteration Index

New 3-D models of gold concentrations were produced for Clan Lake using MATLAB® in order to compare the spatial distribution of alteration and gold more precisely (rather than making comparisons based solely on the block models from Hansen, 2013) (Figs. 2.20 and 2.21). In nearly all cases, areas of highest potassic alteration do not coincide with areas of gold enrichment. However, gold does appear to be associated spatially with areas that have undergone various degrees of potassic alteration. In the central and eastern portions of the area, high gold anomalies occur commonly adjacent to rocks that have experienced strong potassic alteration (alteration index ≥ 0.6). In these cases, gold enrichment is concentrated in small areas that are characterized by host rocks of low alteration or unaltered rocks. These minor occurrences of gold appear to define a northwest-southeast striking zone in which strong alteration occurs as small, concentrated patches. More frequently, gold is associated with rocks that have experienced weak to moderate potassic alteration (alteration index < 0.4), which is consistent with the trend seen in the plot of alteration index versus gold concentration (Fig. 2.17).

Moderate alteration of metavolcanic rocks at Clan Lake appears to weakly reflect the spatial distribution of $\delta^{18}O$ values of both quartz veins and wall rocks modeled by Hansen (2013). The large area of moderate potassic alteration in rocks in the southwest portion of Clan Lake, seen easily in N-S and E-W transects through alteration models (Fig. 2.19), is consistent with the wedge-like shape of highest $\delta^{18}O$ values in the southwest corner of block models (Figs. 2.8 and 2.9). Because higher $\delta^{18}O$ values in the Clan Lake block models decrease gradually to the north and east, it is difficult to discern

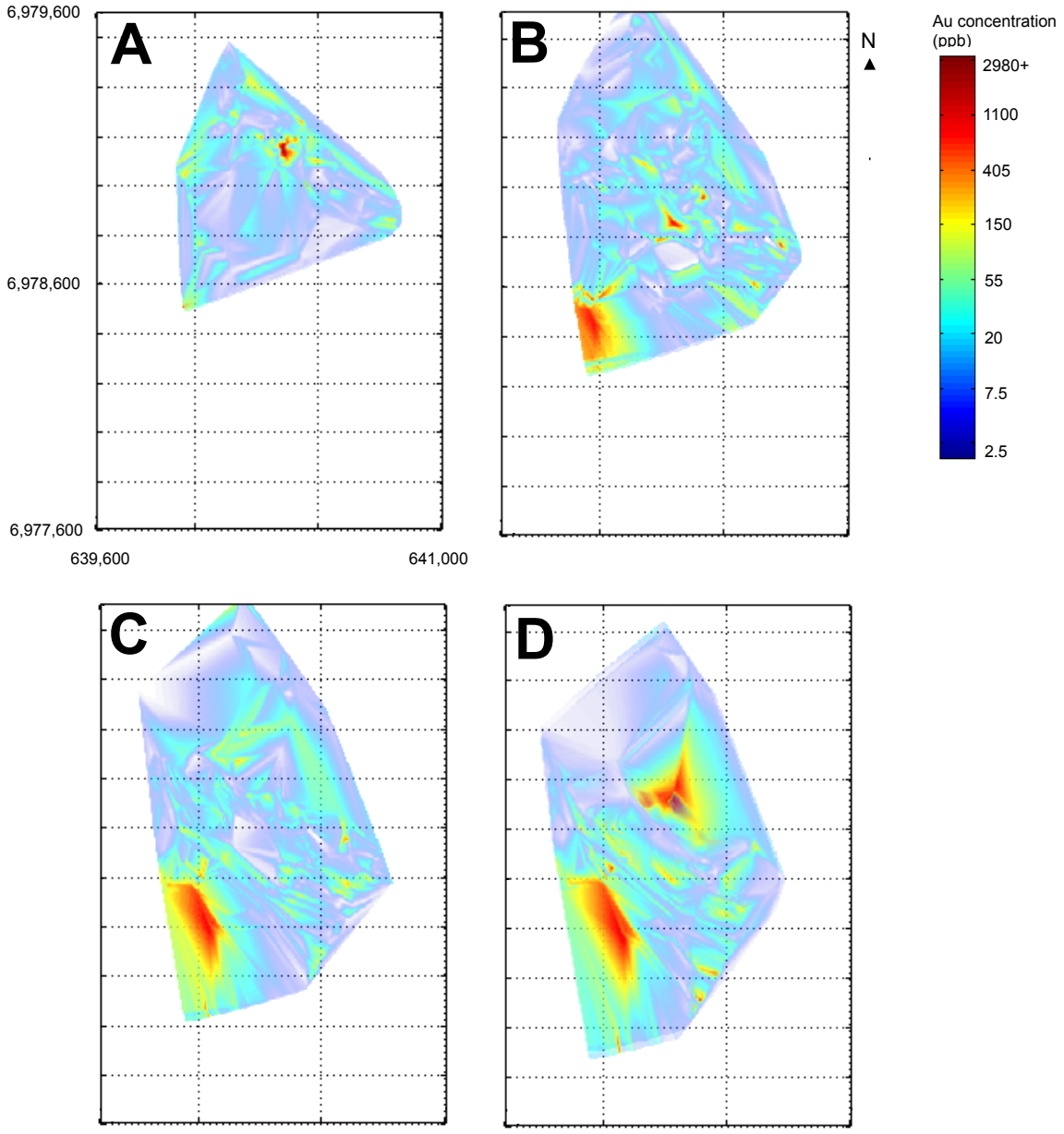

Figure 2.20. Models showing gold concentrations (ppb) from the Clan Lake area in plan view (to use for comparison to potassic alteration models shown in Fig. 2.18). Each model of gold distribution each corresponds to the elevations that were used for models in Fig. 2.18. Note the log scale used in the color bar for gold concentrations. Model dimensions are in UTM coordinates (meters); elevations are in meters above mean sea level. A) Elevation = 250 meters a.s.l. (avg. depth = 15 m). B) Elevation = 150 meters a.s.l. (avg. depth = 115 m). C) Elevation = 50 meters a.s.l. (avg. depth = 215 m). D) Elevation = 0 meters a.s.l. (avg. depth = 265 m).

Figure 2.21. Transects showing gold concentrations (ppb) from the Clan Lake area (to use for comparison to potassic alteration models shown in Fig. 2.19; also refer to the block models of Hansen, 2013 in Fig. 2.11). Transects through models of gold concentrations each correspond to the easting or northing coordinates that were used for models in Fig. 2.19. Note the log scale used in the color bar for gold concentrations. Model dimensions are in UTM coordinates (meters); elevations are in meters above mean sea level. A) N-S transect through the eastern portion of the area. Note that gold enrichment does not appear to reflect a south-dipping, linear trend as clearly as the potassic alteration transect does in Fig. 2.19a. B) N-S transect through the center of the area. C) N-S transect through the western portion of the area. Note the high gold anomaly in the south. D) E-W transect through the northern portion of the area. E) E-W transect through the north-central portion of the area. Note the absence of high gold concentrations in areas where potassic alteration appears relatively strong in Fig. 2.19e. F) E-W transect through the southern portion of the area. Note the high gold anomaly that coincides with moderately intense potassic alteration in Fig. 2.19f.

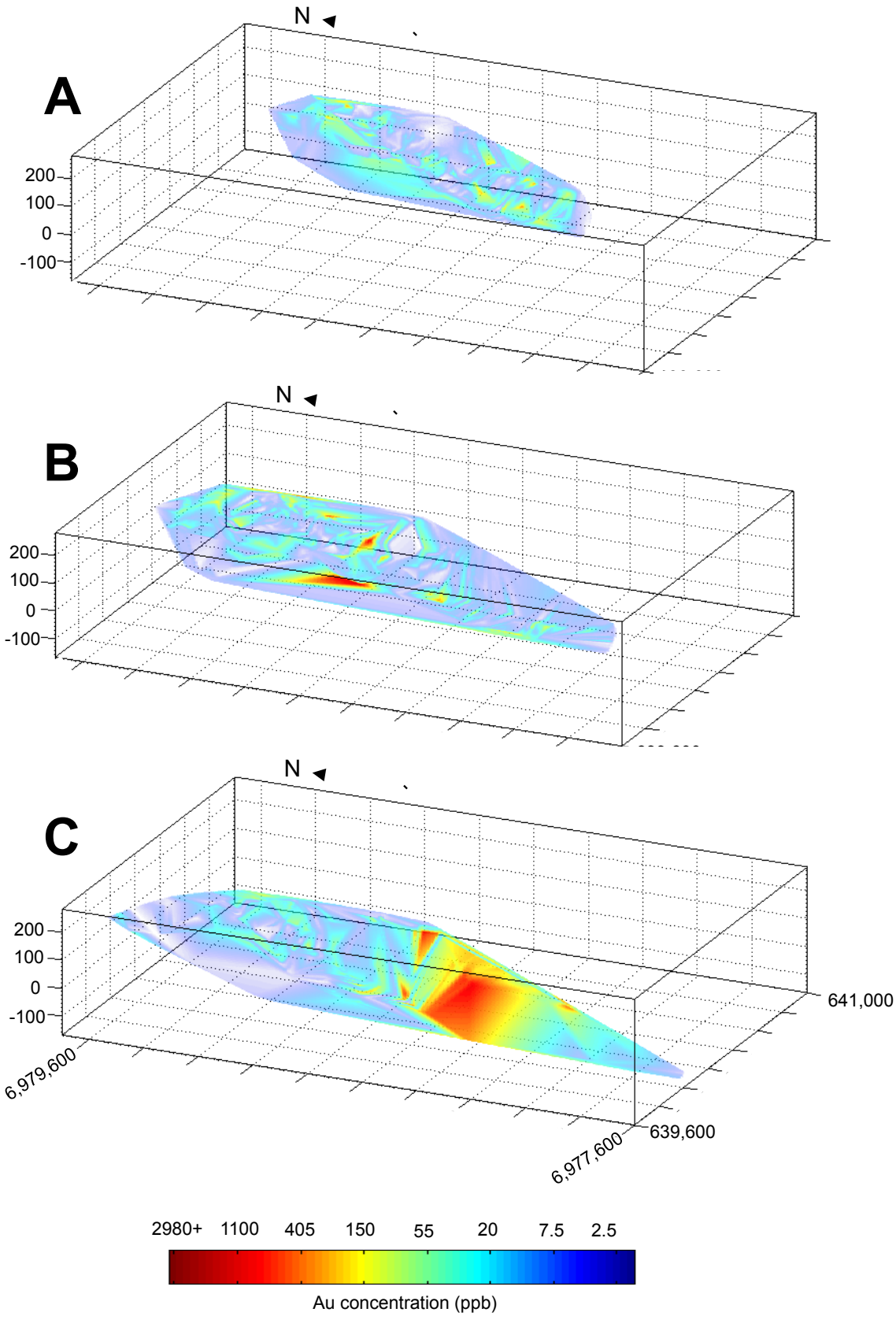
A
N
200
100
0
-100
B
N
200
100
0
-100
C
N
200
100
0
-100
6,979,600
641,000
639,600
6,977,600
2980+
1100
405
150
55
20
7.5
2.5
Au concentration (ppb)

Fig. 2.21 cont.

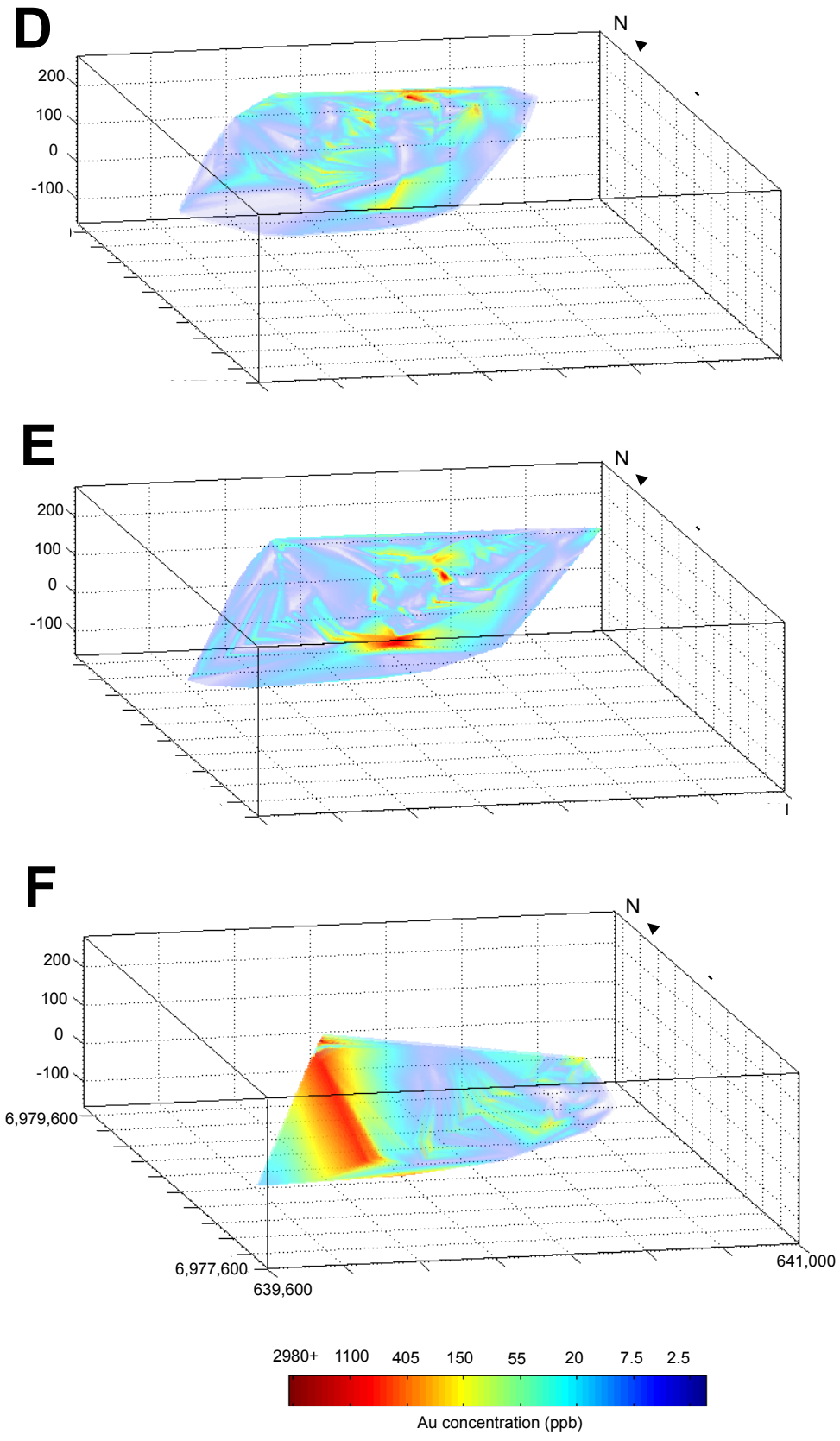
D
N
200
100
0
-100
E
N
200
100
0
-100
F
N
200
100
0
-100
6,979,600
6,977,600
639,600
641,000
2980+ 1100 405 150 55 20 7.5 2.5
Au concentration (ppb)

whether the southwest corner of Clan Lake is the only instance of correlation between the degree of potassic alteration and $\delta^{18}O$ values.

DISCUSSION

Discovery-Ormsby Area

Although potassic alteration was subordinate to the extensive silicification and sulfidation (and lesser carbonate alteration) within the mafic metavolcanic rocks at Discovery-Ormsby, its association with gold deposition justified the current study's attempt to model its spatial distribution for comparison with the distribution in gold enrichment.

Due to a limited lithogeochemical dataset, 3-D models of alteration of metavolcanic rocks of the Ormsby Member seem fairly inconclusive in terms of a spatial relationship between gold mineralization and host rock alteration. Higher gold concentrations appear to be associated with a low alteration index (≤ 0.15), which may indicate that potassic alteration had little influence on gold deposition (or could reflect higher sample density of rocks with lower alteration index values); but, the trend toward lower molar (2Ca + Na + K)/Al values seen in Figure 2.13 suggests that K-related metasomatism may have played a more important role in the history of mineralization in the Discovery-Ormsby area than the models imply.

Future 3-D modeling of alteration chemistries of metavolcanic host rocks in the Discovery-Ormsby area (provided that more whole-rock geochemical data become available) may be able to determine if potassic metasomatism was facilitated by fluid conduits associated with the Discovery Shear Zone, even if it was not the dominant type

of alteration in the area. This would lend credence to the theory that gold mineralization in the Discovery-Ormsby area required a combination of highly reactive host rocks and concentrated fluid flow through structural conduits (Hansen, 2013).

Clan Lake Area

3-D models show that the sericite and patchy potassic alteration documented by Pratico (2009a) are often adjacent to high gold anomalies at Clan Lake. Intermixed patches of strongly and weakly altered wall rocks are most common in the central portion of the Clan Lake models. The patches of more weakly altered rocks in these zones correspond frequently to high gold anomalies (e.g. Figs. 2.19b and 2.21b), which likely represent quartz vein-hosted gold deposits (as quartz veins are low in K, Na, and Ca). In many cases, the strongly altered wall rocks adjacent to these gold-hosting quartz veins do not contain significant concentrations of gold themselves. Instead, a widespread zone of moderately altered rocks, typically at the southwestern portion of the models, are associated with high gold anomalies (e.g. Figs. 2.18d and 2.20d), which likely represent occurrences of wall rock-hosted (refractory) gold.

Block models of $\delta^{18}O_{\text{quartz vein}}$ and $\delta^{18}O_{\text{wall rock}}$ values (Hansen, 2013) are broadly consistent with the spatial distribution of potassic alteration in the Clan Lake area. It is unclear how the irregular patches of strongly altered rocks in the central portion of Clan Lake are related to $\delta^{18}O$ distribution. However, alteration in the southwest corner does appear to coincide with the wedge-shaped distribution of high $\delta^{18}O$ values for both quartz veins and wall rocks in the block models. The apparent spatial uniformity in potassic alteration in the southwestern corner of Clan Lake (in contrast to the irregular, patchy distribution of potassic alteration in the central portions of the area) suggests that quartz

veins may either be comparatively scarce or may occur as smaller, disseminated veinlets and that gold is likely hosted predominantly within wall rocks in that area.

Hansen (2013) speculated that the trend of high $\delta^{18}O$ values in the southwest corner, decreasing gradually to the northeast, could be used as a tool to locate an approximate edge to the mineralizing system at Clan Lake. Considering that the uniformity of alteration in metavolcanic rocks also decreases to the northeast (e.g. Fig. 2.18b), these models may have implications about the porosity and permeability of host rocks. Perhaps enhancement of porosity and permeability was most extensive in the southwestern portion of Clan Lake. In that case, metasedimentary-derived fluids with high $\delta^{18}O$ values would most likely have been introduced to the system through this zone, overprinting metavolcanic host rocks and leading to uniformly distributed potassic alteration and sulfidation of wall rocks with gold deposition in wall rocks and small quartz veins. This may have resulted in an increased prevalence of quartz vein-hosted gold and silicification (relative to wall rock-hosted gold and sulfidation) as gold-bearing fluids moved away from their source and their influence on the $\delta^{18}O$ values of host rocks decreased gradually.

Relative timing of ore deposition and potassic alteration

Attempts to construct a genetic timeline for gold mineralization and potassic alteration are constrained by multiple observations in 3-D models: (a) the southwestern corner of the Clan Lake area is characterized by uniform distribution of potassic alteration and gold enrichment, in contrast to the presence of gold typically adjacent to patches of strong potassic alteration in the central portion of the area, (b) the strongest spatial correlation between potassic alteration and $\delta^{18}O$ values of wall rocks and quartz

veins (Hansen, 2013) occurs in the SW corner of the area (where gold mineralization is also extensive), and (c) in the central portion of the Clan Lake area, moderate to strong potassic alteration appears to define a south-dipping, roughly NNW-SSE trending linear zone (e.g. Fig. 2.19a) that may have been controlled by fault and fracture networks (see inferred faults in Fig. 2.5 and Appendix 1).

High gold anomalies nearly always occur either within broad zones of moderate potassic alteration (alteration index ~ 0.2 to 0.3) or in concentrated clusters adjacent to irregular patches of strongly altered rocks (alteration index > 0.5). However, the presence of moderate to strong potassic alteration is not invariably associated with gold enrichment, which may suggest that gold mineralization and potassic alteration represent separate hydrothermal events. The strong spatial correlation between gold enrichment, high $\delta^{18}O$ values, and moderate potassic alteration in the southwestern corner of the Clan Lake area might imply that these events overlapped in time and/or that enhanced porosity and permeability may have consistently influenced fluid movement through the history of gold deposition and wall rock alteration.

In the central portion of the Clan Lake area, the south-dipping linear zone of potassic alteration may suggest that local fault and fracture systems had a significant influence on hydrothermal fluid flow. If potassic alteration in this area post-dated gold mineralization, then this zone may represent where later hydrothermal fluids (possibly traveling along faults) remobilized gold locally into the small patches that are observed in 3-D models. Alternatively, if potassic alteration and gold deposition were contemporaneous, then fault-controlled hydrothermal fluids may have preferentially deposited gold near or within previously silicified or sulfidized rocks.

It is not clear how the irregular, patchy nature of strong potassic alteration in the central portion of Clan Lake relates to the uniform distribution of moderate potassic alteration in the southwestern corner of the area. However, the distribution of $\delta^{18}O$ values in block models could suggest that potassic alteration occurred in multiple stages, where early potassic alteration may have accompanied gold deposition, and later potassic alteration partially overprinted earlier alteration patterns and remobilized gold along fault-related flow paths.

CONCLUSIONS

Numerical analysis and 3-D models of metavolcanic host rock chemistries recast in terms of potassic alteration assemblages in the Discovery-Ormsby and Clan Lake areas have led to the following conclusions:

1. Molar ratios calculated from the mass changes in K, Na, and Ca that are associated with potassic alteration can be applied as an effective technique to quantify hydrothermal alteration in metamorphosed volcanic rocks and can be used to assess spatial relationships between potassic alteration and gold deposition. Molar plots of (2Ca + Na +K)/Al versus K/Al for mafic metavolcanic rocks in the Discovery-Ormsby area suggest that this technique may even be applicable to rocks in which potassic alteration was not the dominant type of alteration associated with gold deposition.
2. The limited lithogeochemical data that were available for the Ormsby Member did not show strong spatial correlations between potassic alteration of mafic metavolcanic host rocks and gold enrichment. If the absence of such a correlation

is valid and not merely the consequence of a limited data set, it may indicate that the spatial distribution of gold deposits may have been dependent on physical properties of host rocks, such as porosity and permeability enhanced by the Discovery Shear Zone (Fig. 2.2), in addition to host rock chemistry.

3. 3-D models of potassic alteration intensity in the Clan Lake area show an irregular, patchy distribution of strongly altered rocks in the central portion of the area, whereas the southwestern corner is characterized by a uniform, widespread zone of moderate potassic alteration that coincides with high gold anomalies and high $\delta^{18}O$ values (Hansen, 2013). The moderately altered rocks in southwestern portion of the Clan Lake area may represent a zone in which hydrothermal fluids were controlled principally by enhanced porosity and permeability in wall rocks. The linear, south-dipping trend in the strongly altered rocks in the central portion of Clan Lake may indicate that faults were also an important control on hydrothermal fluid flow.
4. The spatial distribution of potassic alteration at Clan Lake may reflect a hydrothermal event subsequent to the gold mineralizing event. The later hydrothermal fluids would have overprinted previous alteration patterns and may have remobilized gold to produce the irregular, patchy distribution of potassic alteration and gold enrichment that is observed in the central portion of 3-D models for Clan Lake.
5. Numerical analysis and 3-D modeling of potassic alteration intensity may be a useful exploration tool for gold in the northern YGB and in other volcanic- or metavolcanic-hosted gold deposits. In cases similar to the Clan Lake area, where

alteration is so extensive that a recognizable edge to the hydrothermal system is undetectable in the field, numerical models of potassic alteration may aid geologists in determining hydrothermal fluid flow patterns and identifying important controls on flow pathways, such as fault systems, that may provide insight into the location of other major gold deposits and their formation.

REFERENCES

Bleeker, W., and Hall, B., 2007, The Slave Craton: Geology and metallogenic evolution, in Goodfellow, W.D., ed., Mineral Deposits of Canada: A Synthesis of Major Deposit-Types, District Metallogeny, the Evolution of Geological Provinces, and Exploration Methods: Geological Association of Canada, Mineral Deposits Division, Special Publication, no. 5, p. 849-879.

Bleeker, W., Ketchum, J. W. F., Jackson, V.A., and Villeneuve, M.E., 1999, The Central Slave Basement Complex, Part I: Its structural topology and autochthonous cover: Canadian Journal of Earth Sciences, v. 36, p. 1083-1109.

Bleeker, W., Stern, R., and Sircombe, K., 2000, Why the Slave Province, Northwest Territories, got a little bigger: Geological Survey of Canada, Current Research 2000-C2, 9 p.

Bowring, S. A., and Williams, I. S., 1999, Priscoan (4.00-4.03 Ga) orthogneisses from northwestern Canada: Contributions to Mineralogy and Petrology, v. 134, p. 3-16.

Bowring, S. A., Williams, I. S., and Compston, W., 1989, 3.96 Ga gneisses from the Slave Province, Northwest Territories, Canada: Geology, v. 17, p. 971-975.

Boyle, R. W., 1961, The Geology, Geochemistry and Origin of the Gold Deposits of the Yellowknife District: Geological Survey of Canada, Memoir 310, 193 p.

Bullen, W., and Robb, M., 2006, Economic contribution of gold mining in the Yellowknife mining district, in Anglin, C.D., ed., Gold in the Yellowknife Greenstone Belt, Northwest Territories: Results of the EXTECH III Multidisciplinary Research Project: Geological Association of Canada, Mineral Deposits Division, Special Publication No. 3. p. 38-48.

Cousens, B., Facey, K., and Falck, H., 2002, Geochemistry of the late Archean Banting Group, Yellowknife greenstone belt, Slave Province, Canada: Simultaneous melting of upper mantle and juvenile mafic crust: Canadian Journal of Earth Sciences, v. 39, p. 1635-1656.

Covello, L., Roscoe, S. M., Donaldson, J. A., Roach, D., and Fyson, W. K., 1988, Archean quartz arenite and ultramafic rocks at Beniah Lake, Slave structural province, N.W.T.: Geological Survey of Canada, Current Research, Part C, Paper 88-1C, 10p.

Davis, W. J., and Bleeker, W., 1999, Timing of plutonism, deformation, and metamorphism in the Yellowknife Domain, Slave Province, Canada: Canadian Journal of Earth Sciences, v. 36, p. 1169-1187.

Ernst, R. E., and Buchan, K. L., 2004, Large igneous provinces (LIPs) in Canada and adjacent regions: 3 Ga to Present: Geoscience Canada, v. 31, p. 103-126.

Ferguson, M. E., Waldron, J. W. F., and Bleeker, W., 2005, The Archean deep-marine environment: Turbidite architecture of the Burwash Formation, Slave Province, Northwest Territories: Canadian Journal of Earth Sciences, v. 42, p. 935-954.

Goldfarb, R. J., Groves, D. I., and Gardoll, S., 2001, Orogenic gold and geologic time: a global synthesis: Ore Geology Reviews, v. 18, p. 1-75.

Goodwin, A. M., 1988, Geochemistry of Slave Province volcanic rocks: Yellowknife Belt, *in* Padgham, W. A., ed., Contributions to the geology of the Northwest Territories: Indian and Northern Affairs Canada, v. 3, p. 13–25.

Goodwin, A.M., Lambert, M.B., and Ujike, O., 2006, Geochemical and metallogenic relations in volcanic rocks of the southern Slave Province: implications for late Neoarchean tectonics: Canadian Journal of Earth Sciences, v. 43, p. 1835-1857.

Green, D. C., Baadsgaard, H., and Cumming, G. L., 1968, Geochronology of the Yellowknife area, Northwest Territories, Canada: Canadian Journal of Earth Sciences, v. 5, p. 725-735.

Gresens, R. L., 1967, Composition-volume relationships of metasomatism: Chemical geology, v. 2, p. 47-65.

Groves, D. I., Goldfarb, R. J., Knox-Robinson, C. M., Ojala, J., Gardoll, S., Yun, G. Y., and Holyland, P., 2000, Late-kinetmatic timing of orogenic gold deposits and significance for computer-based exploration techniques with emphasis on the Yilgarn Block, Western Australia: Ore Geology Reviews, v. 17, p. 1–38.

Helmstaedt, H., and Padgham, W. A., 1986, A new look at the stratigraphy of the Yellowknife Supergroup at Yellowknife, N.W.T.: Implications for the age of gold-bearing shear zones and Archean basin evolution: Canadian Journal of Earth Sciences, v. 23, p. 454-475.

Henderson, J. B., 1972, Sedimentology of Archean turbidites at Yellowknife, Northwest Territories: Canadian Journal of Earth Sciences, v. 9, p. 882–902.

Henderson, J. B., 1985, Geology of the Yellowknife-Hearne Lake Area, District of Mackenzie: A segment across an Archean basin: Geological Survey of Canada, Memoir, v. 414, 135 p.

Isachsen, C. E., and Bowring, S. A., 1994, Evolution of the Slave Craton: Geology, v. 22, p. 917-920.

Ketchum, J. W. F., Bleeker, W., and Stern, R. A., 2004, Evolution of an Archean basement complex and its autochthonous cover, southern Slave Province, Canada: Precambrian Research, v. 135, p. 149-176.

LeCheminant, A. N., and Heaman, L. M., 1989, Mackenzie igneous events, Canada: Middle Proterozoic magmatism associated with ocean opening: Earth and Planetary Science Letters, v. 96, p. 38–48.

LeCheminant, A. N., Buchan, K. L., van Breemen, O., and Heaman, L., 1997, Paleoproterozoic continental break-up and reassembly: Evidence from 2.19 Ga diabase dyke swarms in the Slave and Western Churchill Provinces, Canada: Geological Association of Canada, Program with Abstracts, v. 22, p. A86.

Madeisky, H. E., 1996, A lithogeochemical and radiometric study of hydrothermal alteration and metal zoning at the Cinola epithermal gold deposit, Queen Charlotte Islands, British Columbia, *in* Coyner, A. R., and Fahey, P. L., eds., Geology and Ore Deposits of the American Cordillera, v. 3, p. 1153-1185.

Martel, E., and Lin, S., 2006, Structural evolution of the Yellowknife greenstone belt, with emphasis on the Yellowknife River Fault Zone and the Jackson Lake Formation, *in* Anglin, C.D., ed., Gold in the Yellowknife Greenstone Belt, Northwest Territories: Results of the EXTECH III Multidisciplinary Research Project: Geological Association of Canada, Mineral Deposits Division, Special Publication, no. 3. p. 95-115.

Ootes, L., Morelli, R. M., Creaser, R. A., Lentz, D. R., Falck, H., and Davis, W. J., 2011, The timing of Yellowknife gold mineralization: A temporal relationship with crustal anatexis?: Economic Geology, v. 106, p. 713-720.

Padgham, W. A., 1992, Mineral deposits in the Archean Slave structural province: Lithological and tectonic setting: Precambrian Research, v. 58, p. 1-24.

Padgham, W. A., and Fyson, W. K., 1992, The Slave Province: A distinct Archean craton: Canadian Journal of Earth Sciences, v. 29, p. 2072-2086.

Pratico, V., 2009a, Report on the resource estimate of the Yellowknife gold project, Report Filing: NTS 85P/4 & 85P/5.

Pratico, V., 2009b, Geological map of the Discovery-Ormsby area: Internal Tyhee Gold Corporation Document.

Pratico, V., 2009c, Geological map of the Clan Lake area: Internal Tyhee Gold Corporation Document.

Pratico, V., 2011, Regional geology map: Internal Tyhee Gold Corporation Document.

Roscoe, S. M., Stubley, M., and Roach, D., 1989, Archean quartz arenites and pyritic paleoplacers in the Beaulieu River supracrustal belt, Slave structural province, N.W.T.: Geological Survey of Canada, Current Research, Part C, Paper 89-1C, 16 p.

Shelton, K. L., McMenamy, T. A., van Hees, E. H. P., and Falck, H., 2004, Deciphering the complex fluid history of a greenstone-hosted gold deposit: Fluid inclusion and stable isotope studies of the Giant mine, Yellowknife, Northwest Territories, Canada: Economic Geology, v. 99, p. 1643-1663.

Sircombe, K. N., Bleeker, W., and Stern, R. A., 2001, Detrital zircon geochronology and grain-size analysis of ~2800 Ma Mesoarchean proto-cratonic cover succession, Slave Province, Canada: Earth and Planetary Science Letters, v. 189, p. 207-220.

Stanley, C. R., and Madeisky, H. E., 1994, Lithogeochemical exploration for hydrothermal ore deposits using Pearce element ratio analysis: Geological Association of Canada Short Course Notes, v. 11, p. 193-212.

Stern, R. A., and Bleeker, W., 1998, Age of the world's oldest rocks refined using Canada's SHRIMP: The Acasta gneiss complex, Northwest Territories, Canada: Geoscience Canada, v. 25, p. 27-31.

Stubley, M., 1997, Geology of the Discovery Property: Unpublished company report to GMD Resource Corp. accompanying a 1:2400 scale geological map, 23 p.

Thompson, P. H., 1989, Moderate overthickening of thinned sialic crust and the origin of granitic magmatism and regional metamorphism in low-P – high-T terranes: Geology, v. 17, p. 520-523.

van Breemen, O., Davis, W. J., and King, J. E., 1992, Temporal distribution of granitoid plutonic rocks in the Archean Slave Province, northwest Canadian Shield: Canadian Journal of Earth Sciences, v. 22, p. 2186– 2199.

van Hees, E. H. P., Shelton, K. L., McMenamy, T. A., Ross, L. M. Jr., Cousens, B. L., Falck, M., Robb, M. E., and Canam, T. W., 1999, Metasedimentary influence on metavolcanic-rock-hosted greenstone gold deposits: Geochemistry of the Giant mine, Yellowknife, Northwest Territories, Canada: Geology, v. 27, p. 71–74.

van Hees, E. H., Kirkham, G. D., Sirbescu, M. L., Shelton, K. L., Hauser, R. L., and Falck, H., 2006, Large lithogeochemical alteration halos around Yellowknife gold deposits and implications for fluid pathways, *in* Anglin, C.D., ed., Gold in the Yellowknife Greenstone Belt, Northwest Territories: Results of the EXTECH III Multidisciplinary Research Project: Geological Association of Canada, Mineral Deposits Division, Special Publication, no. 3, p. 232-248.

Whitty, W., 2007, Structural and metamorphic evolution of the Ormsby Zone and relative timing of gold mineralization: A newly defined Archean orogenic gold prospect hosted on the Discovery property, Yellowknife greenstone belt, Slave Province, Canada [M.Sc. thesis]: Vancouver, University of British Columbia, 113 p.

CHAPTER III: CATHODOLUMINESCENCE (CL) PETROGRAPHY AND STABLE ISOTOPE GEOCHEMISTRY OF VARIOUS ORE DISTRICTS IN THE SOUTHEASTERN MISSOURI MVT ORE FIELD, U.S.A.

ABSTRACT

Epigenetic dolomite cements with a distinctive cathodoluminescent (CL) microstratigraphy are associated with main stage Pb-Zn sulfide mineralization hosted primarily in the middle to upper Bonneterre Dolomite of the Viburnum Trend subdistrict. The regional extent of the dolomite CL stratigraphy points to a large-scale, basin-derived fluid flow system being responsible for the district's Pb-Zn deposits. Recently discovered Cu-(Ni-Co)-Zn-rich ores above the Lamotte Sandstone-Bonneterre Dolomite contact reflect early, fault/fracture-control of ore fluids and are associated with two generations of dolomite cement whose CL patterns are distinct from and pre-date the regional dolomite cement (Cavender, 2015; Cavender et al., 2016). CL and stable isotope studies of these and other dolomite cements from subdistricts throughout southeast Missouri were undertaken to determine whether fault-related ores and their dolomite cements represent a single fluid that evolved chemically along different flow paths or instead reflect multiple, perhaps more localized fluid sources unrelated to regional fluid flow. Disparities in CL patterns of dolomite cements among ore subdistricts indicate mineralizing fluids utilized multiple, local- to regional-scale fault/fracture systems.

Variability in $\delta^{18}O$ and $\delta^{13}C$ values of these dolomite cements likely reflects fluid-rock reactions along specific flow paths. In deep ores of the Viburnum Trend, decreasing $\delta^{18}O$ values (from ~ -3 toward -8‰ VPDB) with increasing distance above the Lamotte-

Bonneterre contact reflect the progressive reaction of deeper, fault-related fluids with dolomitized host rocks formed in an isotopically distinct overlying flow system. In some subdistricts, dolomite cements with distinct CL patterns have similar $\delta^{18}O$ values (~ -8‰), regardless of stratigraphic position or host carbonate facies. They may reflect a common fluid-dominated, regional flow system in which stratigraphically separated fluids experienced more local control of their chemistry and CL behavior.

The regional dolomite CL stratigraphy within the upper Bonneterre Dolomite, and its associated ore mineralization in the Viburnum Trend, likely resulted from a large-scale fluid flow system. However, CL patterns and stable isotope compositions of dolomite cements elsewhere in southeast Missouri, especially in stratigraphically lower rocks, require the presence of multiple early, fault-related ore-fluid systems.

INTRODUCTION

The Bonneterre Dolomite (Cambrian) hosts world-class, Pb-Zn-Cu Mississippi Valley-type (MVT) deposits of the Viburnum Trend district in southeast Missouri. Sulfide ore mineralization in the district is generally lead-dominant (Pb:Zn > 5) and occurs almost exclusively in the middle to upper portion of the Bonneterre Dolomite as bedded or replacement deposits, associated typically with the reef-grainstone facies of the formation. Below the main Pb-Zn mining horizon of the Viburnum Trend, near the base of the Bonneterre Dolomite and in the upper portion of the underlying Lamotte Sandstone, unusually Cu-(Ni-Co)-Zn-rich ores have recently been identified and exploited (Cavender, 2015; Cavender et al., 2016). Similar but smaller concentrations of these ores have been found throughout the Viburnum Trend, typically hosted

stratigraphically higher within the Bonneterre Dolomite (Hagni and Transcynger, 1977; Sweeney et al., 1977; Fennel et al., 1996). These ores are similar to those mined historically in the Indian Creek and Fredericktown-Mine La Motte subdistricts to the north and east of the Viburnum Trend in southeast Missouri (Figs. 3.1 and 3.2).

Epigenetic dolomite cement associated with the atypical lower section ores in the Viburnum Trend exhibit cathodoluminescent (CL) patterns that are distinct from the pervasive CL cement stratigraphy observed in the upper Bonneterre Dolomite throughout southern Missouri and northern Arkansas, indicating the presence of multiple, chemically distinct fluids. This investigation expands dolomite CL studies to ore deposits in several mining districts throughout southeast Missouri in order to document the continuity/variability in CL cement stratigraphy on a broader scale with the aim of understanding of the influence of localized, potentially fault-related fluids on mineralization within the Viburnum Trend and elsewhere in southeast Missouri.

This chapter reports the results of cathodoluminescence petrography and stable isotope studies of samples from the Old Lead Belt, Mine La Motte, and Annapolis subdistricts (which were collected by W. A. Tarr in the 1930s and are reposited in the University of Missouri's research collection) and samples from the West Fork and Fletcher mines in the Viburnum Trend (which were used for the research of Adelstein et al., 2016) (Fig. 3.2). These studies aim to address the following questions:

1. Do Cu-(Ni-Co)-Zn-rich mineralization and associated carbonate cements in the lower Bonneterre Dolomite fit into the known mineral paragenesis of Pb-Zn-Cu ores of the Viburnum Trend or might they represent a previously unrecognized ore-forming event(s)?

2. Are the ores in the southeast Missouri MVT district products of a regional fluid flow system that has been previously hypothesized for the Viburnum Trend (Appold and Garven, 1999, 2000) or could they have formed from more localized, structurally controlled flow systems (Horrall et al., 1993; Shelton et al., 1995), or some combination of both (Clendenin et al., 1994; Shelton et al., 2009)?
3. Are there particular geochemical signatures of the ore-forming processes that can assist geologists in exploring for Cu-(Ni-Co)-Zn-rich ores in the lower Bonneterre Dolomite throughout southeast Missouri?

Geological Setting

Mississippi Valley-type mineral deposits typically are carbonate hosted (and less commonly sandstone hosted), stratabound base-metal sulfide bodies that occur as both open-space fillings and replacements of host rocks (Anderson and Macqueen, 1988). Principal sulfide minerals in MVT deposits include sphalerite, galena, pyrite, marcasite, and less frequently minor chalcopyrite.

The southeastern Missouri lead district is part of the Ozark MVT region located in the stable interior platform of the North American continent (Fig. 3.1). Mineralization in the Ozark MVT region is thought to be associated genetically with the Alleghanian-Ouachita orogeny (Pennsylvanian – Permian) (Wu and Beals, 1981; Symons et al., 1998). The Ozark Uplift (or Ozark Dome) is bounded on the northwest by the Forest City Basin, on the northeast by the Illinois Basin, on the south by the Arkoma Basin and the Ouachita Mountains, and on the southeast by the Reelfoot Rift (Keller et al., 2000; Palmer et al., 2012) (Fig. 3.1). The Proterozoic St. Francois Mountain complex represents the summit

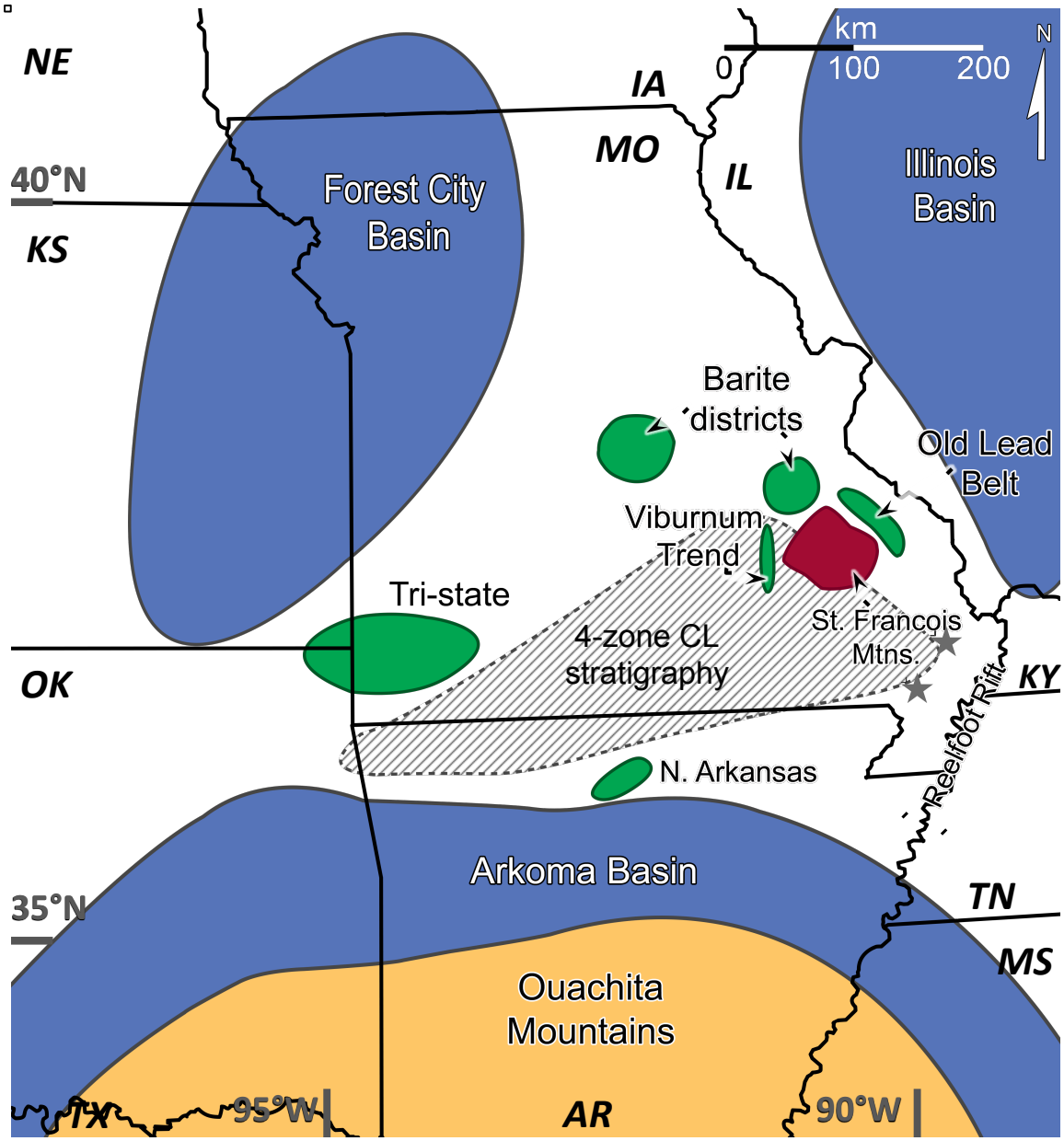

Figure 3.1. Regional geologic setting of the Ozark MVT ore districts (green) relative to major sedimentary basins (blue), the Reelfoot Rift and the igneous St. Francois Mountains (red) (after Gregg and Shelton, 1989; Shelton et al., 2009). The shaded portion of southern Missouri and northern Arkansas represents sample localities documented to contain gangue dolomite cements that exhibit the characteristic four-zone CL stratigraphy (discussed in text) that is found in the upper Bonneterre Dolomite in the Viburnum Trend (Voss and Hagni, 1985; Rowan, 1986; Frank and Lohmann, 1986). Grey stars indicate locations of deep drill holes of "Western Platform" carbonates analyzed by Keller et al. (2000).

Figure 3.2. A) Map showing locations of major ore districts, mines and faults (blue) relative to Precambrian igneous outcrop and the trend of the reef-grainstone facies of the Bonneterre Dolomite (after Snyder and Gerdemann, 1968). Mine abbreviations: CS = Casteel, MG = Magmont, BK = Buick, BC = Brushy Creek, WF = West Fork, FL = Fletcher, SW = Sweetwater, BT = Bonne Terre. B) Cross-section A-A' (after Gregg and Shelton, 1989b). Mineralization discussed in the present study is hosted in and above the reef-grainstone facies and in sandy/shaly dolomite of the lower Bonneterre Dolomite and the underlying upper Lamotte Sandstone.

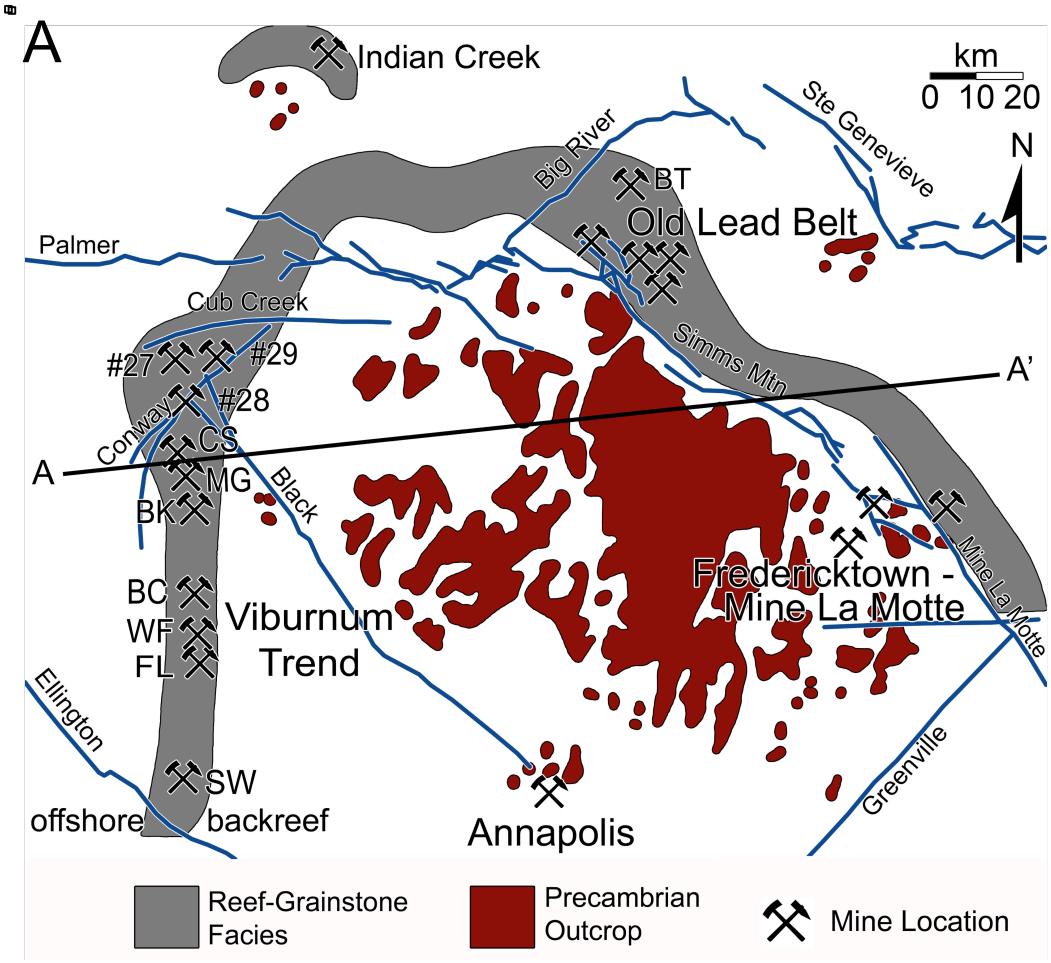
A
Indian Creek
km
0 10 20
N
Ste Genevieve
Big River
BT
Old Lead Belt
Palmer
Cub Creek
#27
#29
#28
Conway
CS
MG
BK
Black
Simms Mtn
A'
A
BC
WF
FL
Viburnum
Trend
Fredericktown -
Mine La Motte
Mine La Motte
Ellington
SW
offshore
backreef
Annapolis
Greenville
Reef-Grainstone
Facies
Precambrian
Outcrop
Mine Location

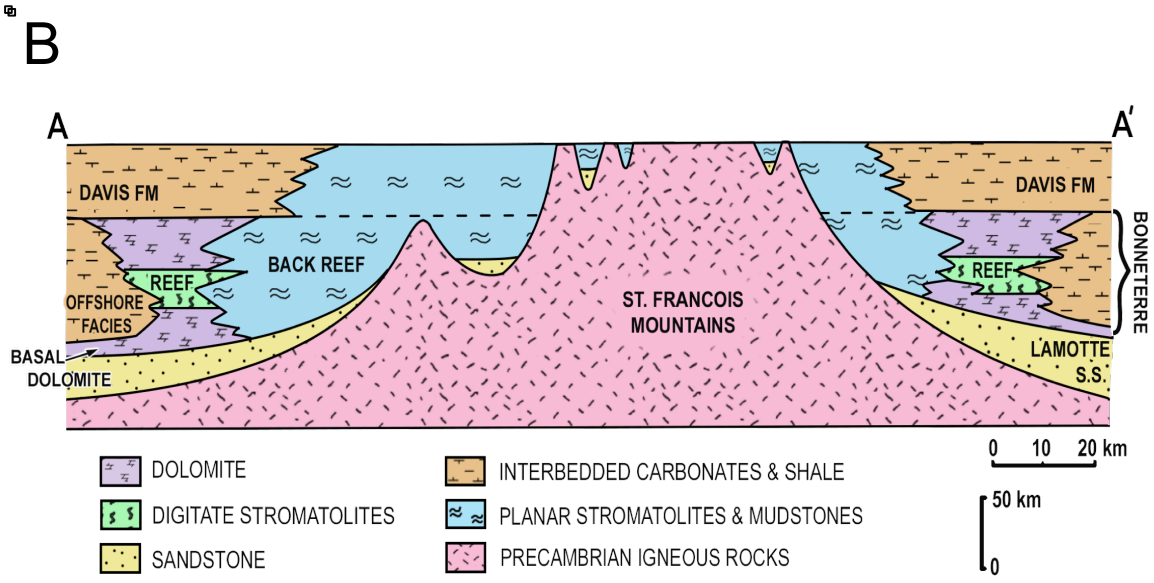
B
A
A'
DAVIS FM
DAVIS FM
BACK REEF
REEF
REEF
OFFSHORE
FACIES
ST. FRANCOIS
MOUNTAINS
BONNETERRE
BASAL
DOLOMITE
LAMOTTE
S.S.
0 10 20 km
DOLOMITE
INTERBEDDED CARBONATES & SHALE
DIGITATE STROMATOLITES
PLANAR STROMATOLITES & MUDSTONES
SANDSTONE
PRECAMBRIAN IGNEOUS ROCKS
50 km
0

of the dome and is surrounded partially by the southeast Missouri mining district. A number of northwest-striking transform faults and northeast-striking normal faults comprise the major fault zones of the southeast Missouri region (Clendenin et al., 1994) (Fig. 3.2).

The approximately 1.5-billion-year-old crystalline basement rocks beneath southeast Missouri were emplaced as multiple intrusions of stocks and batholiths and are regionally domed, faulted, and tilted. The igneous rocks are predominantly rhyolitic ignimbrites/flows and anorogenic granites crosscut by minor intermediate to mafic intrusive rocks (Kisvarsanyi, 1977; Sides et al., 1981; Lowell, 1991). The surface of the basement is undulatory and contains numerous topographic highs (knobs) created by weathering and erosion. These structural features act as a control on the distribution and thickness of sedimentary facies in the overlying units, in particular, pinch-outs of the Lamotte Sandstone (Cambrian) and the locations of the development of stromatolitic reef-grainstone facies of the Bonneterre Dolomite (Cambrian), both of which control the distribution of MVT orebodies in the southeast Missouri region (Gerdemann and Myers, 1972; Kisvarsanyi, 1977) (Figs. 3.2 and 3.3). The igneous basement also rocks represent a potential local source(s) (in addition to more distal basinal sources) for metals and sulfur for MVT mineralization in southeast Missouri, as fluids may have leached and transported ore constituents to overlying ore-hosting carbonate rocks (Kisvarsanyi, 1977; Burstein et al., 1993; Shelton et al., 1995).

Cambrian-Ordovician siliciclastic and carbonate units lap onto the topographic highs of the buried crystalline basement and exposed St. Francois Mountains. Cambrian sedimentary rocks are nearly horizontal or dip gently away from igneous knobs and

domes, except locally, where faulted. The lowermost unit is the Lamotte Sandstone (upper Cambrian), a fine-grained quartz arenite that becomes arkosic and/or conglomeritic near its base and on the flanks of igneous knobs. The Lamotte Sandstone is generally regarded as the main aquifer for ore fluid migration in the region (Sverjensky, 1984; Kyle and Gutierrez, 1988; Goldhaber et al., 1995). This formation is overlain conformably by the Bonneterre Dolomite, which forms the lower part of an Upper Cambrian platform-carbonate sequence in southeastern Missouri (He et al., 1997) (Fig. 3.3). The Bonneterre Dolomite contains a stromatolitic reef complex that partially surrounds the St. Francois Mountains. The reef and associated back-reef facies (often referred to locally as "white rock" by mining geologists due to its bleached gray appearance) of the formation are dolomitized extensively from the reef toward the St. Francois Mountains; toward the west, the formation grades into limestone and green shales of the offshore facies. An extensive basal dolomite (avg. 6 meters thick) occurs above the contact between the Bonneterre Dolomite and Lamotte Sandstone throughout the region and has been shown to have formed by reaction with warm brines from the Arkoma basin (Fig. 1) that were moving through the Lamotte Sandstone (Gregg, 1985; Gregg and Shelton, 1989b).

Within the Viburnum Trend, the lower Bonneterre Dolomite consists of carbonate mudstones, greywackes, and wackestones, whereas the upper Bonneterre Dolomite contains oolitic grainstones and stromatolitic reefstones that are the main host rocks of Pb-Zn MVT ores in this district. A transgressive sequence of interbedded basinal limestones, dolomites, shales, and glauconitic siltstones and sandstones of the Davis Formation and Derby-Doerun Dolomite overlies the Bonneterre Dolomite (Fig. 3.3).

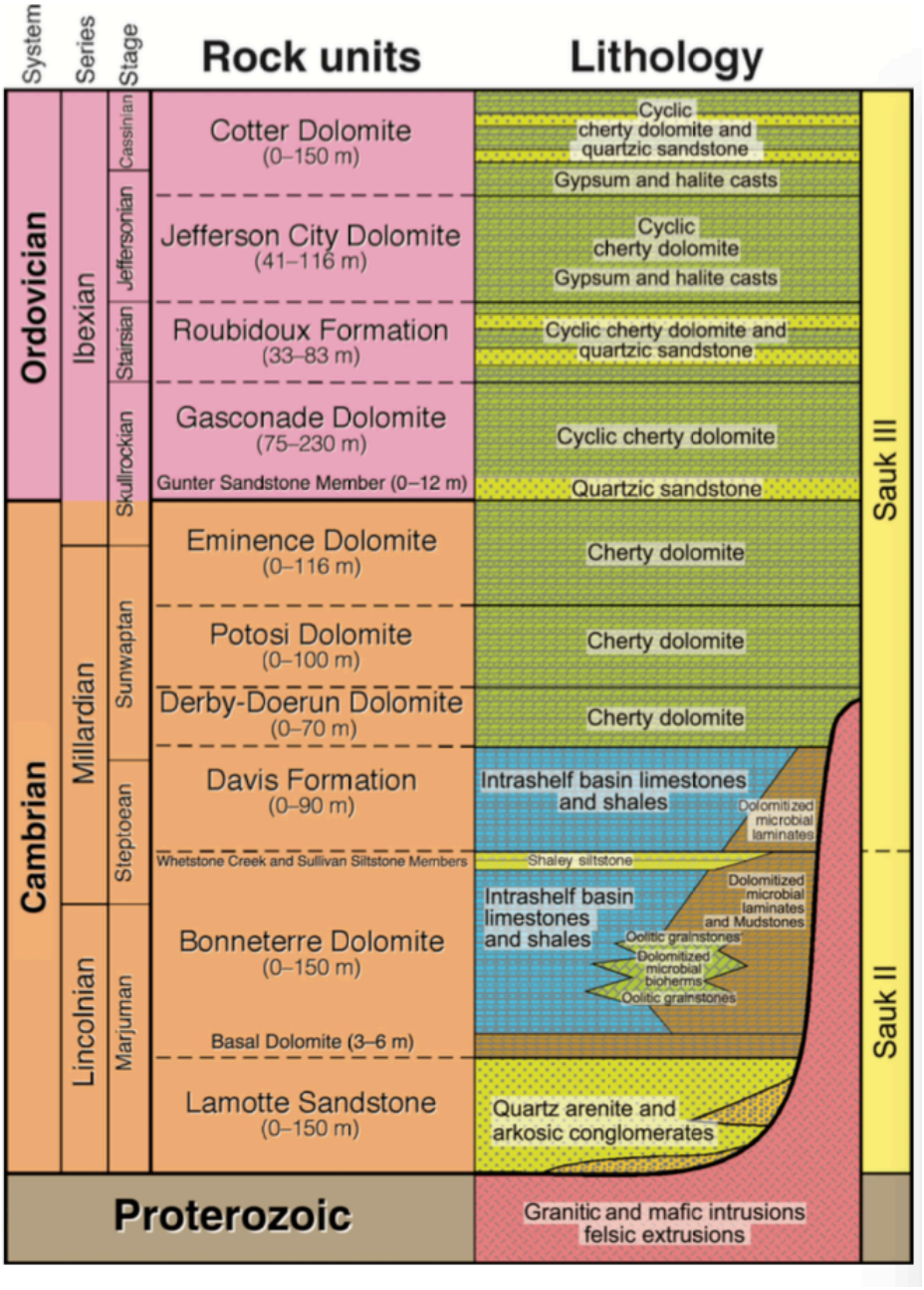

Figure 3.3. Stratigraphic column showing Cambrian – Ordovician strata and facies relationships in southeast Missouri (after Palmer et al., 2012). The St. Francois aquifer (Cambrian) is host to MVT ore deposits in southeast Missouri and is comprised of the Lamotte Sandstone and the Bonneterre Dolomite. The Davis and Derby-Doerun Formations form the St. Francois Confining Unit, which underlies the Ozark aquifer (Upper Cambrian – Ordovician), which hosts MVT ore deposits of Central Missouri and Northern Arkansas (Imes, 1990; He et al., 1997; Appold and Garven, 1999).

These relatively impermeable strata likely act as an effective aquitard separating the Lamotte Sandstone and the Bonneterre Dolomite, through which MVT fluids traveled, from overlying Upper Cambrian and Lower Ordovician platform dolomites (Imes, 1990; He et al., 1997).

MVT Ore Deposits in Southeast Missouri

The majority of Pb-Zn-Cu MVT mineralization in the southeastern Missouri lead district occurs in the Viburnum Trend (currently mined), Old Lead Belt, and Fredericktown-Mine La Motte subdistricts, but minor deposits have also been mined from Indian Creek and Annapolis (Fig. 3.2). Most ore mineralization in southeast Missouri occurs as disseminated deposits in dolomite pore systems or as bedded or replacement deposits in grainstone host dolomite above the reef-grainstone facies (Gregg and Shelton, 2012). Dissolution brecciation, stratigraphic pinch-outs of the Lamotte Sandstone against Precambrian knobs, and fault/fracture systems have been identified as locally important geologic controls on ore mineralization (Kisvarsanyi, 1977; Paarlberg and Evans, 1977; Rogers and Davis, 1977; Sweeney et al., 1977; Mavrogenes et al., 1992; Clendenin et al., 1994; Leach, 1994).

The Viburnum Trend

The Viburnum Trend is a world-class, Pb-Zn-Cu MVT district that extends north-south for ~ 64 km on the western flank of the St. Francois Mountains. Mineralization within the Viburnum Trend typically conforms to a general paragenetic sequence that can be traced throughout most of the district with relatively minor variations (Hagni, 1986) (Fig. 3.4). Sulfide ore mineralization in the district is generally lead-dominant (Pb:Zn > 5) and is hosted primarily in the middle and upper portions of the Bonneterre Dolomite.

Several instances of lateral metal/mineral zoning in the ore deposits of the Viburnum Trend have been reported (Dunn and Grundmann, 1989; Mavrogenes et al., 1992; Childers et al., 1995), but significant vertical zoning is less common and has been reported mostly in the Magmont mine (Grundmann, 1977; Hagni and Transcynger, 1977; Fennel et al., 1996).

Typical ore mineral paragenesis of the Viburnum Trend

Early, meter-scale, podiform bodies of massive bornite-chalcopyrite replacing disseminated Fe-sulfides are rare. They have been found in several mines and were interpreted to be as the earliest ore mineralization in the Viburnum Trend (Hagni, 1986). This mineralization occurs typically as the replacement of disseminated iron sulfides lower within the Bonneterre Dolomite's ore horizon (i.e. closer to the Lamotte Sandstone) and is crosscut and replaced by later mineralization. Massive and disseminated sphalerite and massive and euhedral, cuboctahedral galena constitute the main stage Pb-Zn ores in the district. Massive chalcopyrite occurs before, during, and after deposition of main stage cuboctahedral galena (Heyl, 1983; Hagni, 1986). Cuboctaheral galena is affected by a major dissolution event that is followed typically by the deposition of colloform iron sulfides. The last lead-mineralizing event in the district is characterized by vug-filling, cubic galena and is followed by deposition of vug-filling sphalerite, chalcopyrite, and iron sulfides. Early Ni-Co-sulfide (e.g. siegenite) was deposited in minor amounts before and during the early portions of octahedral galena deposition, and commonly occurs intergrown with or replaced by chalcopyrite; later siegenite crystals occur commonly in vugs (Snyder and Gerdemann, 1968; Hagni, 1986) (Fig. 3.4).

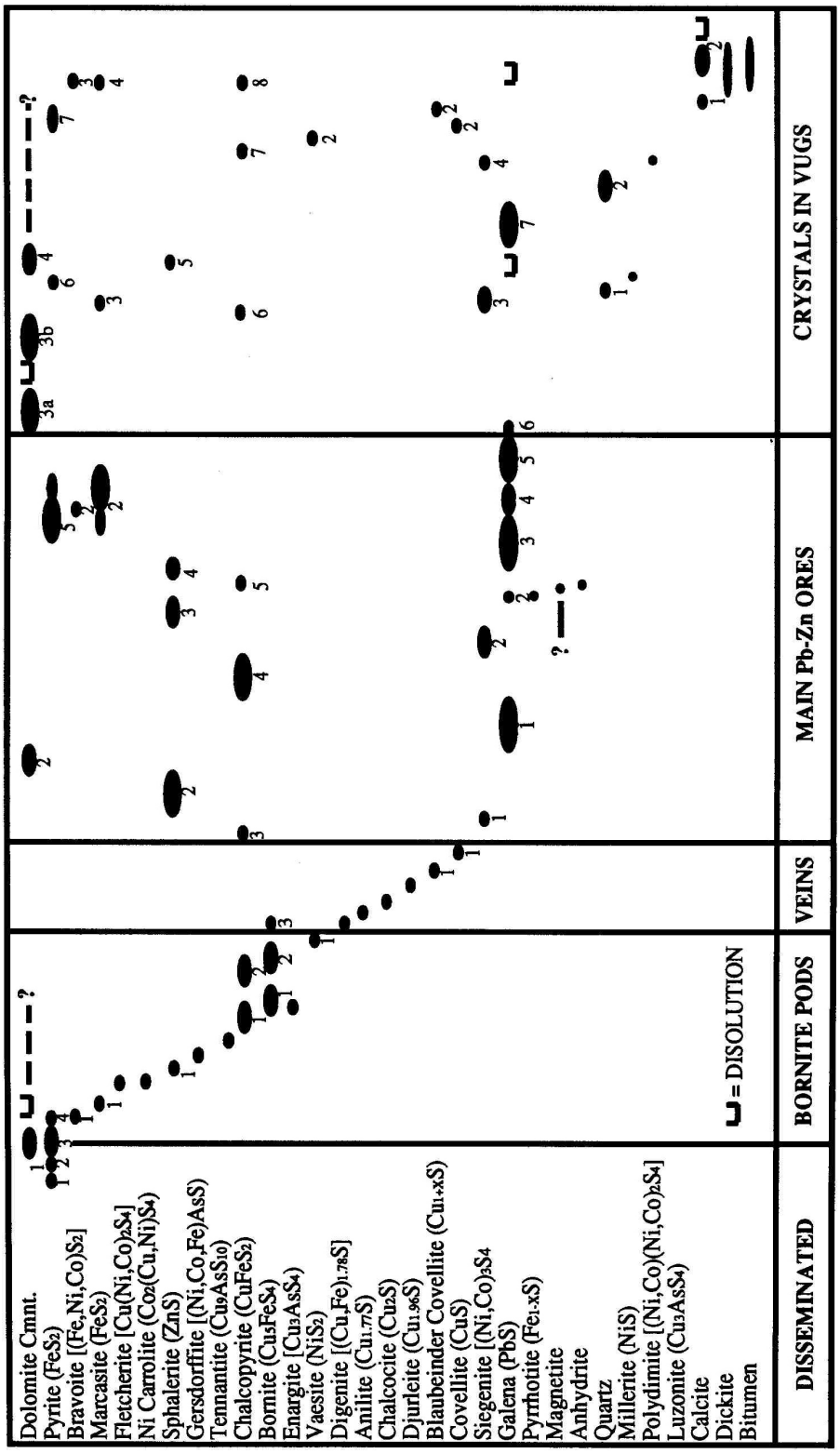

Figure 3.4. A generalized paragenetic sequence for MVT sulfide mineralization in the southeast Missouri lead district (modified from Hagni, 1986). Numbers refer to consecutive generations of respective minerals.

Ore-associated dolomite cements

Pore-filling epigenetic dolomite cement with a distinctive four-zone cathodoluminescent (CL) stratigraphy has been shown to be associated closely with main and late stage sulfide mineralization in the Bonneterre Dolomite (Voss et al., 1989). The distinct CL zonation is found in gangue dolomite cements in the Viburnum Trend and throughout southern Missouri and northern Arkansas (Gregg, 1985; Rowan, 1986; Farr, 1989) (Fig. 3.1). The regional scale of this dolomite CL stratigraphy is a chief tenet for the idea that ore formation in the Viburnum Trend resulted from a large-scale fluid flow system (Leach and Rowan, 1986; Appold and Garven, 1999, 2000).

West Fork mineralization

The West Fork mine and equivalent mineralization in the northern portion of the Fletcher mine (Fig. 3.2) is abnormally Zn-rich and represents a different sequence of mineral deposition compared to the rest of the Viburnum Trend Pb-Zn-Cu district (Fig. 3.5). This "West Fork-type" mineralization (Burstein, 1993) exhibits distinct lateral mineral zoning and is characterized by zoned deposition of early, fine-grained Zn-sulfides, followed by deposition of massive and colloform marcasite/pyrite which is then followed by deposition of main stage cuboctahedral galena. Lateral metal/mineral zoning in the main ore horizon (M bed) consists of an inner zone of colloform Fe- and Zn-sulfides that become disseminated moving outward, with Pb- and Pb-Cu-rich mineralization in the outermost zones (Mavrogenes et al., 1992; Burstein, 1993) (Fig. 3.5). The variations in mineral parageneses and sulfur isotope signatures between West Fork-type mineralization and the rest of the Viburnum Trend suggest the presence of multiple ore fluids whose relative influence on ore deposition varied temporally and

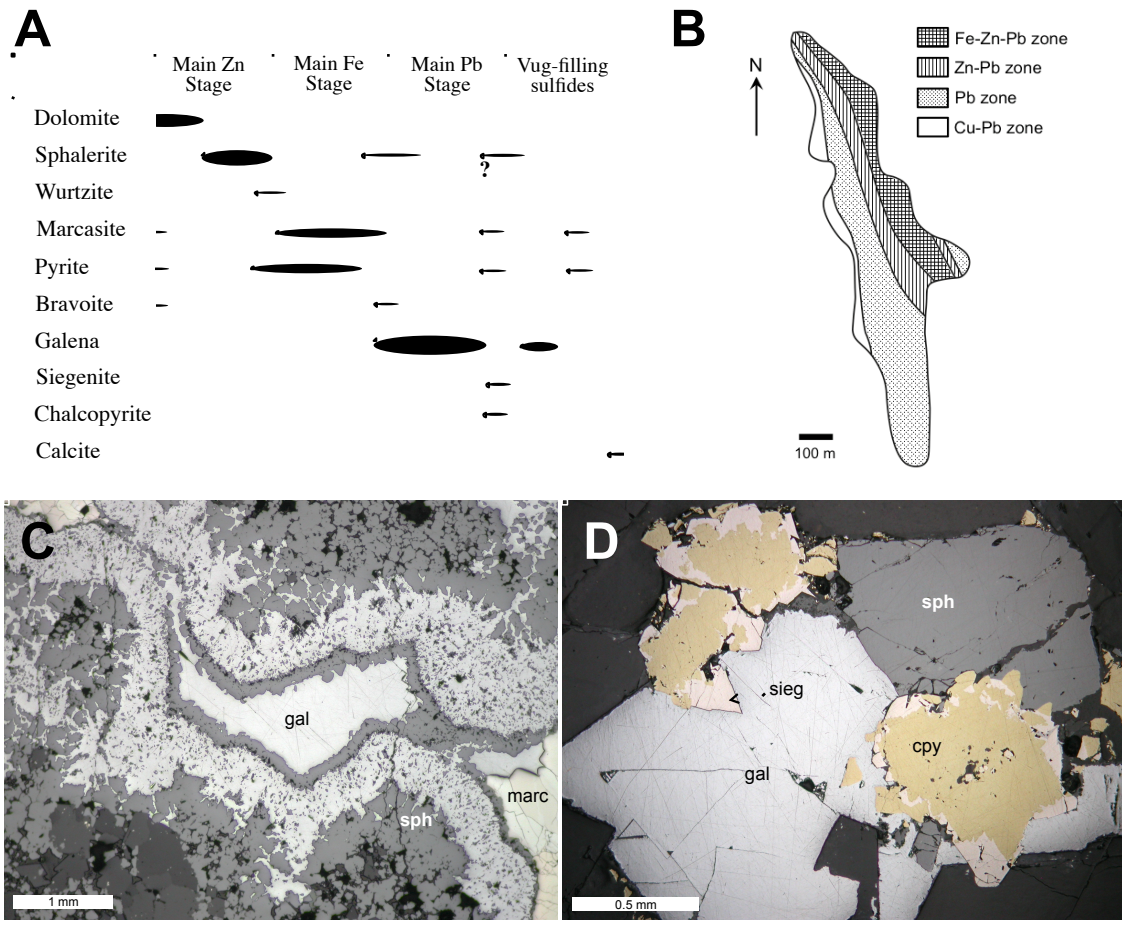

Figure 3.5. A) Generalized paragenetic sequence of mineral deposition in the West Fork mine (modified from Mavrogenes et al., 1992). Note the reversal in the paragenetic position of marcasite and galena relative to other mines of the Viburnum Trend (see Fig. 3.4). B) Map showing the lateral mineral/metal zoning at the West Fork mine (modified from Shelton et al., 1993). The easternmost portion of the mine is dominated by Fe- and Pb-rich mineralization. C) Reflected light (RL) photomicrograph representative of mineralization in Zn-Pb- to Zn-Fe-Pb-rich areas of the West Fork mine. Early sphalerite (sph) is replaced by galena (gal), which is overgrown by a subsequent generation of sphalerite. Pore space is filled by marcasite (marc) and later galena. D) Representative RL photomicrograph of the Cu-Pb-rich area of the West Fork mine. Early sphalerite is accompanied by chalcopyrite (cpy) associated with siegenite (sieg), followed by galena.

spatially throughout the district (Burstein et al., 1993; Shelton et al., 1993).

Lower Ore Zone (LOZ) mineralization

High-grade, unusually Zn-Cu-rich mineralization has been recently identified and exploited more than 30 m below the typical ore horizon in the Viburnum Trend. The LOZ orebody of the Brushy Creek mine has been documented by Cavender (2015). Its deposits have assays in the ranges of 11 to 29% Zn, < 1 to 8% Cu and 6 to 15% Pb with notable enrichments of Ni, Co, and Ag (Cavender et al., 2016). This orebody is hosted dominantly within sandy and shaley dolomite in the lower third of the Bonneterre Dolomite, but may occur stratigraphically up to the contact with the bottom of the reef facies (Fig. 3.3). Ore mineralization extends into the overlying reef facies along fractures and dissolution breccias. Mineralization also extends locally several meters into underlying quartz arenite of the Lamotte Sandstone (Fig. 3.3).

The LOZ deposits contain multiple generations of chalcopyrite and sphalerite that display frequent breccia textures composed dominantly of Zn-Cu-rich sulfides that have been brecciated and subsequently cemented by later generations of sulfides (and minor carbonate) resulting in a massive ore (Fig. 3.6). These textures are distinct from typical Viburnum Trend breccias that are composed of large carbonate clasts cemented by sulfides. LOZ ores at Brushy Creek display pronounced vertical zoning of Fe and Cu-Ni-Co transitioning upward to Zn and Pb mineralization, which may indicate multiple entry points of ore-metal-specific fluids (Cavender et al., 2016;) (Fig. 3.7).

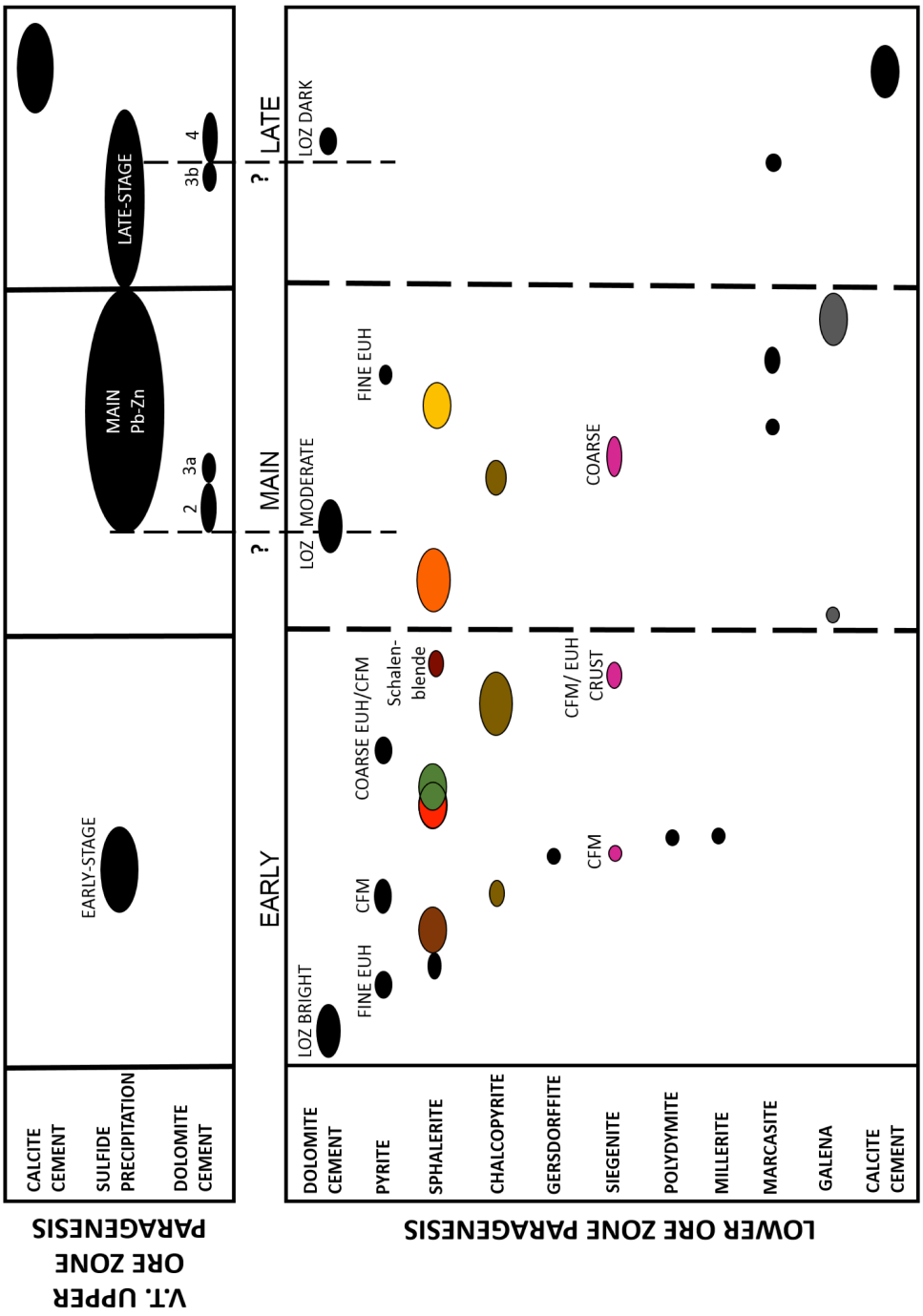

Figure 3.6. Generalized paragenesis of ore minerals from the lower ore zone (LOZ) mineralization at the Brushy Creek mine in the Viburnum Trend (after Cavender, 2015). Also included is a simplified paragenesis of sulfide and carbonate cement precipitation associated with more typical mineralization of the Viburnum Trend hosted stratigraphically higher within the Bonneterre Dolomite (modified from Shelton et al., 2009). Numbers refer to CL zones of the regional four-zone dolomite cement. Abbreviations: CFM = colloform; EUH = euhedral; VT = Viburnum Trend.

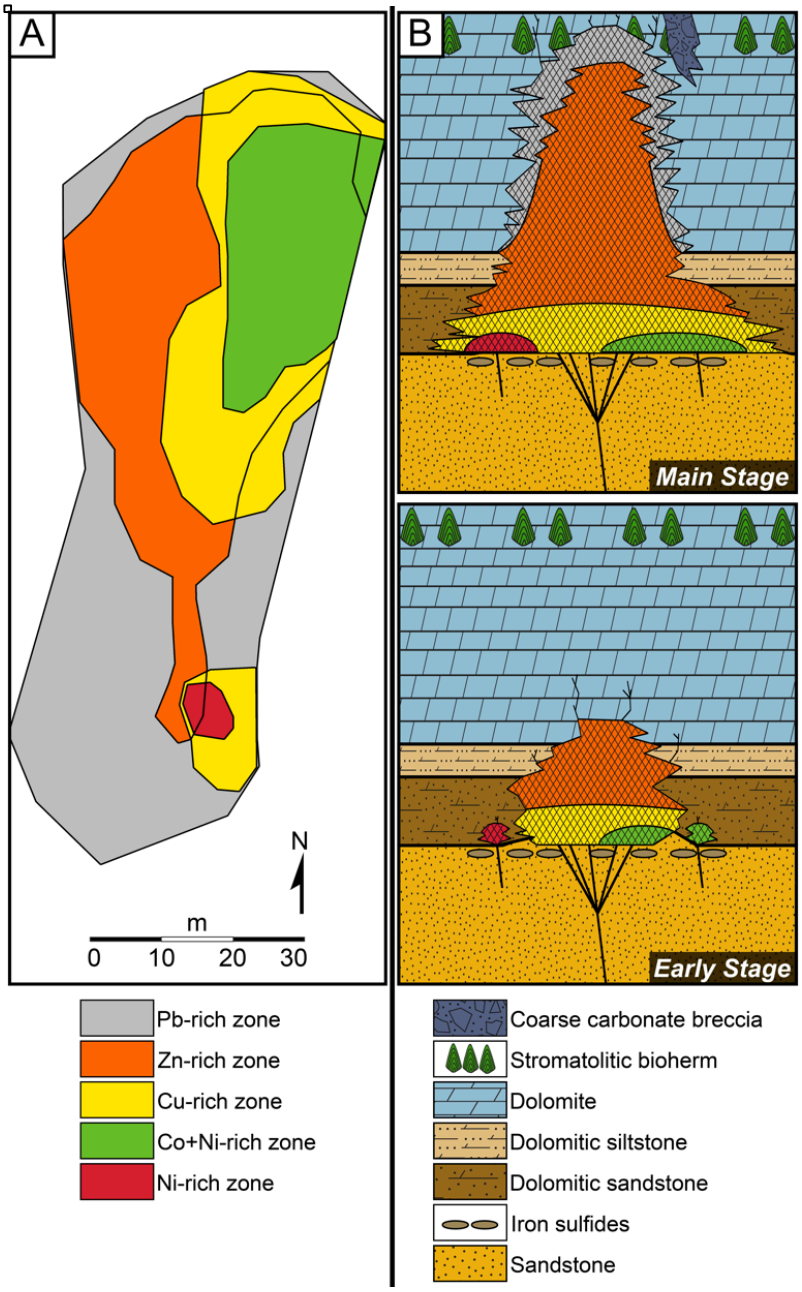

Figure 3.7. A) Idealized map of metal zoning within the lower ore zone (LOZ) mineralization at the Brushy Creek mine (after Cavender et al., 2015). Ni-rich mineralization at the southern end and Co-Ni-rich mineralization at the northern end are hosted within the lowermost ~ 0.5 m of the orebody. Chalcopyrite-rich mineralization may extend upward from Ni-rich and Co-Ni-rich areas up to 6 m, above which is ≤ 20 m of sphalerite-rich ore and an additional 5 m of galena-rich ore encasing the orebody. B) Schematic illustration of progressive vertical development of LOZ ores as early mineralizing fluids moved through fault/fracture systems (after Cavender et al., 2016). This lower ore system may have breached less permeable units in the lower Bonneterre Dolomite, allowing interaction with fluids and host rocks present higher in the stratigraphic section.

Other subdistricts in southeast Missouri

The Old Lead Belt

The Old Lead Belt subdistrict, mined from 1720 to 1972, is located about 50 km east-northeast of the northern end of the Viburnum Trend (Fig. 3.2). Sulfide ore mineralization is lead dominant (Pb:Zn ~ 16), and occurs typically as bedded replacement ores but is also found filling fractures (Snyder and Gerdemann, 1968). The primary sulfide minerals include galena, sphalerite, chalcopyrite, pyrite and marcasite, with minor bornite, millerite, and siegenite (Fig. 3.8). Most ores are hosted in the lower third of the Bonneterre Dolomite and extend locally into the underlying Lamotte Sandstone, but mineralization can occur stratigraphically higher in the formation, as is the case in the Bonne Terre mine (Tarr, 1936; Ohle and Brown, 1954; Snyder and Gerdemann, 1968; Hagni, 1995) (Fig. 3.2). Orebodies in the Old Lead Belt are influenced primarily by domal structures and stratigraphic pinch-outs related to Precambrian knobs and ridges, sedimentary arch structures such as sand ridges or bar-reef structures, and fracture zones (Ohle and Brown, 1954; Snyder and Emery, 1956). Although ore distribution often follows sedimentary structures, ore grade is controlled primarily by northwest-trending strike-slip fault complexes in the subdistrict (Snyder and Gerdemann, 1968). Typical metal/mineral zoning occurs as Cu-Co-Ni-sulfides at the base of ore deposits, Pb-sulfides in main orebodies, and Zn- and Fe-sulfides fringing upward and outward at the margins of the lead deposits. Copper-bearing ores are more abundant along the northern and eastern edges of the subdistrict, whereas zinc is more abundant in the central-southern portion of the subdistrict (Davis, 1960; Hagni, 1995).

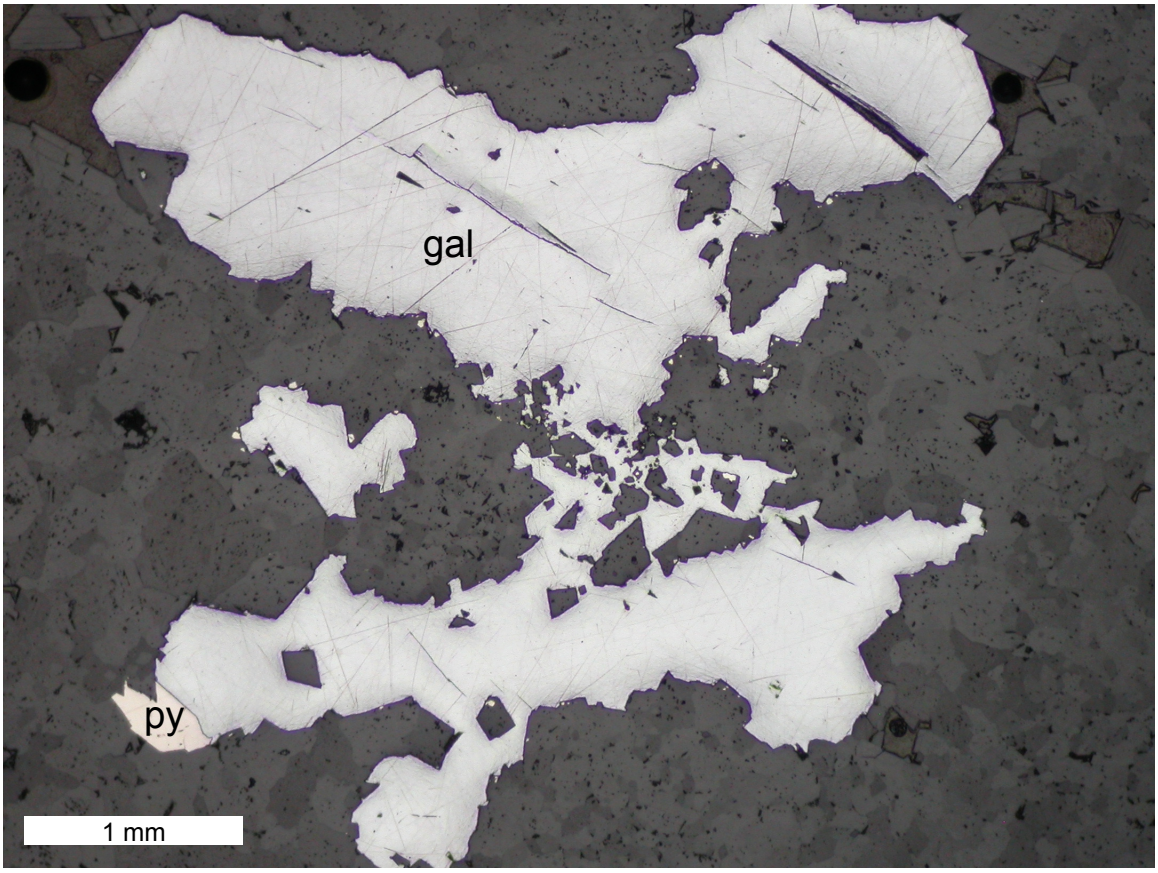

Figure 3.8. Representative RL photomicrograph of Pb-rich ores from the Old Lead Belt in which pyrite (py) deposition is followed by galena (gal).

Fredericktown-Mine La Motte

Ore mineralization in the Cu-Co-Ni-rich Fredericktown-Mine La Motte subdistrict (Fig. 3.2) generally occurs within the lower ~ 15 m of the Bonneterre Dolomite and within the underlying Lamotte Sandstone; a shaly unit in the lower Bonneterre Dolomite marks the upper limit of ore (Snyder and Gerdemann, 1968). Most deposits in this subdistrict are controlled largely by pinch-outs of the sandstone against Precambrian knobs, but some deposits are associated with solution collapse breccias (Tarr, 1936; Snyder and Gerdemann, 1968; Horrall et al., 1983, 1993; Pignolet and Hagni, 1983). Early ores consisted typically of siegenite and chalcopyrite, followed paragenetically by sphalerite, galena, and trace amounts of covellite (Fig. 3.9), with apparent vertical and lateral zoning of Pb and/or Zn mineralization occurring above Cu-Co-Ni sulfides (Pignolet and Hagni, 1983).

One orebody in this subdistrict consisted of Zn-rich ore mineralization concentrated in an anticlinal structure proximal to the Mine La Motte fault (Fig. 3.2), which likely served as a conduit for ore fluids. These ores are presumed to reflect early fault- and fracture-related systems, which involved ore fluids that interacted with mafic and felsic basement metal source-rocks prior to the onset of the regional flow system thought to be responsible for main stage Pb-Zn ores in the Viburnum Trend (Horrall et al., 1993).

Annapolis

The historic Annapolis subdistrict is a small concentration of dominantly lead sulfide located about 35-40 km east of the southern end of the Viburnum Trend and was

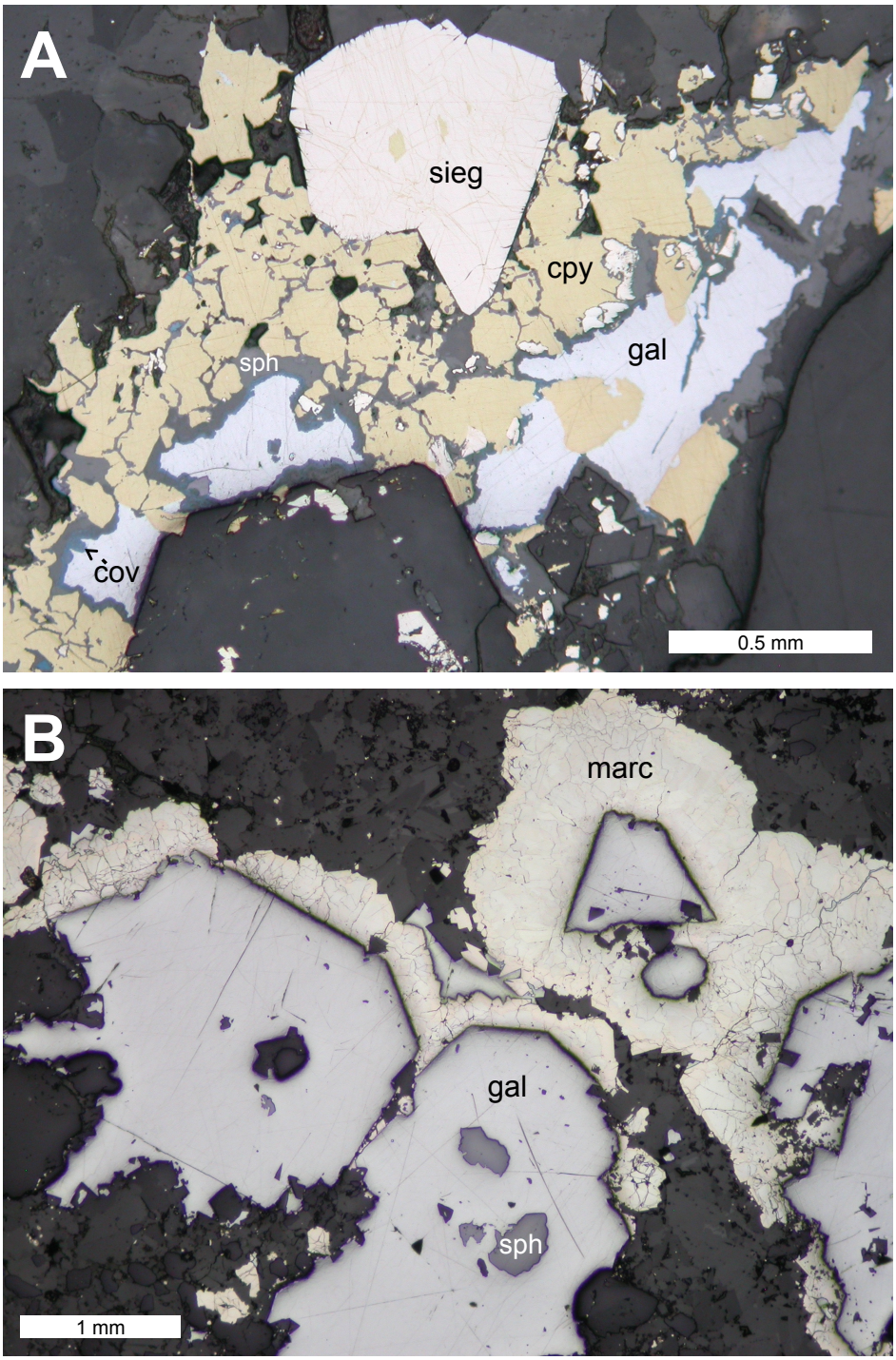

Figure 3.9. RL photomicrographs representative of Cu-(Ni-Co)-Zn and Pb-Zn-rich mineralization, respectively, in the Mine La Motte subdistrict. A) Chalcopyrite (cpy) is intergrown with and fills microfractures within siegenite (sieg). Chalcopyrite is replaced by sphalerite (sph) followed by minor covellite (cov) and galena (gal). B) Euhedral galena containing remnants of earlier sphalerite is overgrown by colloform marcasite (marc), followed by galena that fills minor pore space.

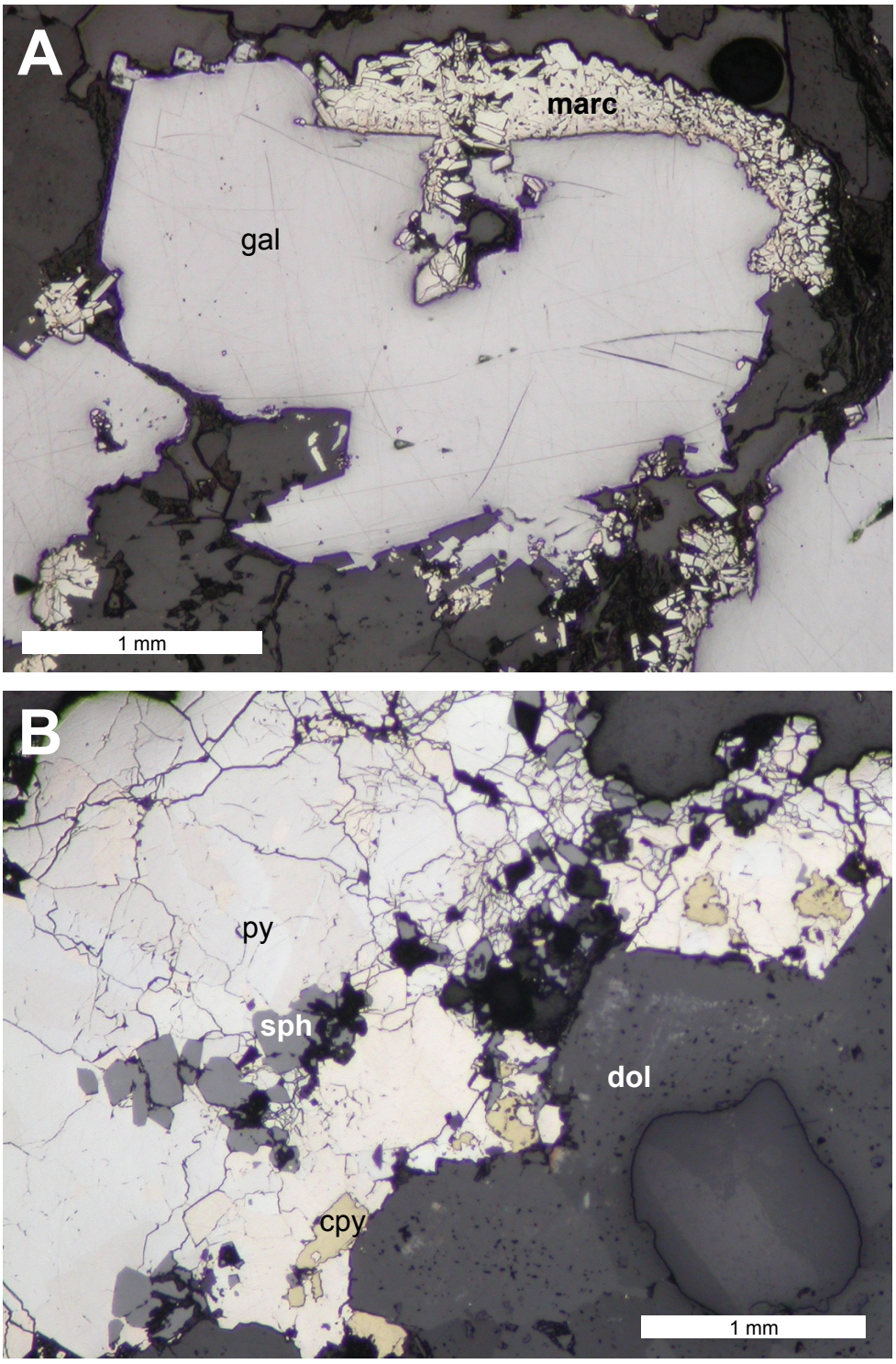

Figure 3.10. RL photomicrographs representative of the Pb-dominant Annapolis subdistrict. A) Galena (gal) overgrown by fine marcasite (marc) crystals. B) Pyrite (py) associated with earlier sphalerite and chalcopyrite. Note the inclusions of sulfides in some dolomite (dol) cement crystals.

mined until 1931 (Fig. 3.2). Mineralization was localized around igneous knobs and occurred primarily in the lower third of the Bonneterre Dolomite (Snyder and Gerdemann, 1968; Hagni, 1995). Annapolis ores are unique in that they are hosted exclusively in the vuggy, porous backreef (lagoonal) facies ("white rock") of the Bonneterre Dolomite. Primary sulfide minerals are galena, sphalerite, pyrite and marcasite, and minor chalcopyrite (Fig. 3.10).

CATHODOLUMINESCENCE (CL) PETROGRAPHY

Cathodoluminescence (CL) microscopy was used to document growth zoning patterns (proxies for compositional variations) in dolomite cements (Fairchild, 1983; Machel, 1985) and to assess the similarity and relationship of gangue dolomite cements associated with Zn- and Cu-(Ni-Co)-rich ores in the lower Bonneterre Dolomite to the well-documented CL responses of dolomite cements in the Viburnum Trend orebodies hosted stratigraphically higher within the Bonneterre Dolomite (Voss et al., 1989). Petrographic correlation of CL stratigraphy in epigenetic dolomite cements in MVT deposits across the region has been used, particularly in the Viburnum Trend district, to evaluate the areal and stratigraphic extent of regional diagenetic events, to determine relative time frameworks within which ore stages can be placed, and to understand the relationship among aquifers, fluid flow, and metal/sulfur sources (Gregg, 1985; Rowan, 1986; Gregg and Hagni, 1987; Farr, 1989; Voss et al., 1989; Gregg and Shelton, 1989a; Keller et al., 2000; Perry et al., 2015a, 2015b). Generally, Mn^{2+} and Fe^{2+} are the major trace elements that control the luminescence of dolomite cements, where Mn^{2+} is an activator of luminescence and Fe^{2+} inhibits luminescence (Machel, 1985).

Viburnum Trend Dolomite Cements

Main Ore Zone (Middle to Upper Bonneterre Dolomite)

A characteristic CL stratigraphy in ore-associated dolomite cements with four distinctive zones (zones 1-4) is pervasive throughout the Viburnum Trend Pb-Zn deposits in the upper Bonneterre Dolomite and regionally throughout the southeastern Missouri region (Voss and Hagni, 1985; Gregg, 1985; Rowan, 1986; Farr, 1989) (Figs. 3.1 and 3.11). Each of the four zones is recognized on the basis of texture, color, presence or absence of banding, and intensity of CL response.

Zone 1 is pre-ore in occurrence and is characterized by a moderate to bright luminescence, mottled texture, absence of well-defined banding, and a gradational contact with host dolomite. The zone has a strong variability in luminescence compared to the other zones, which may reflect variability of the original host rock lithology/chemistry and/or effects of interaction with later fluids. Zone 2 consists of a thin, dull to non-luminescent band that may show faint alternating light and dark bands. A single, bright marker band within zone 2 is found from the Fletcher mine north to the Magmont mine, whereas zone 2 is generally absent altogether in dolomite cements north of the Casteel mine or east of the Viburnum Trend in the backreef facies of the Bonneterre Dolomite (Fig. 3.2). Zone 3 is characterized by numerous, alternating bright and non-luminescent bands, and is commonly divided into two subzones (3a and 3b) by a dissolution surface. The thickness of zone 3 and the frequency of occurrence of a dissolution surface between its inner and outer portions decrease westward from the Viburnum Trend (Voss et al., 1989). Zone 4 is post-main stage ore in occurrence and is characterized by a thick, dull to non-luminescent band.

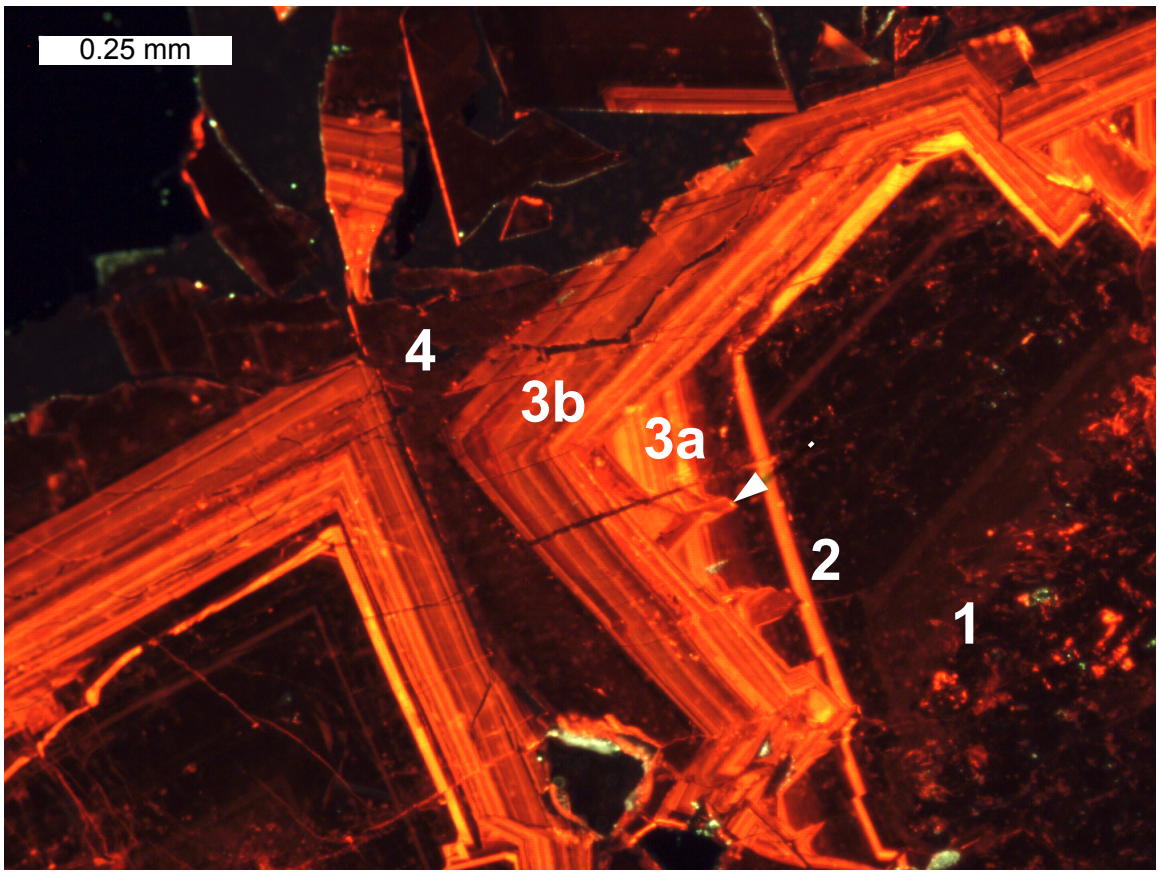

Figure 3.11. Representative image of dolomite cement displaying the characteristic regional four-zone CL stratigraphy recognized throughout southern Missouri, associated typically with Pb-Zn ores hosted in the upper Bonneterre Dolomite of the Viburnum Trend. The arrow indicates the dissolution surface between subzones 3a and 3b, which penetrates frequently into zone 2 (as seen in image) and less frequently into zone 1.

Minor element variations and the presence of dissolution surfaces within dolomite cements are consistent with the characteristic CL patterns forming from multiple pulses of fluids being introduced into the mineralizing system. The number of observable growth bands and the proportion of non-luminescent bands within the entire CL stratigraphy generally decrease westward from the northwest margin of the Reelfoot Rift and northward from south-central Missouri (Buelter and Guillemette, 1988; Farr, 1989; Gregg and Shelton, 1989b) (Fig. 3.1).

Lower Ore Zone (Lower Bonneterre Dolomite and Lamotte Sandstone)

CL microscopy performed by Cavender (2015) on samples from the LOZ of the Brushy Creek mine indicates that two generations of dolomite cement are associated with LOZ ore deposition (Fig. 3.12). The first of the two generations ("LOZ Bright") formed pre-ore as fine-grained, euhedral dolomite crystals and is characterized by bright, multi-banded CL. A second generation of medium- to coarse-grained cements with moderately bright to moderately dull bands ("LOZ Moderate") formed paragenetically between episodes of orange and yellow sphalerite deposition (Fig. 3.6). A paragenetically later, thick, dull to non-luminescent zone of dolomite cement ("LOZ Dark", resembling zone 4 of the regional four-zone CL stratigraphy) occurs in infrequent late pore spaces.

Minor occurrences of LOZ Bright and Moderate dolomite cements were observed filling fractures that extend above the LOZ orebody to within 4 meters of an overlying, more typical Viburnum Trend Pb-Zn breccia orebody in the Brushy Creek mine. Cavender (2015) described these occurrences as remnants of earlier cement overgrown by more typical four-zone regional cement and interpreted them to reflect early, fault-related ore fluid pathways that remained active during main stage Pb-Zn mineralization. The disparity between CL patterns of LOZ dolomite cements and those in the upper Bonneterre Dolomite may reflect the influence of temporally and chemically distinct fluid reservoirs during the history of ore deposition in the Viburnum Trend, or alternatively may represent chemically distinct fluids that existed contemporaneously in different portions of the stratigraphic section. The LOZ Bright and Moderate cements are similar to those described from the "Western Platform" by Keller et al. (2000; see locations of stars in Fig. 3.1). The latter cements were interpreted by Keller et al. (2000)

to reflect distinct fault-bounded fluid reservoirs that had little communication with regional fluid flow in adjacent carbonate platform rocks. A similar fault-related source for LOZ cement-depositing fluids was proposed by Cavender (2015).

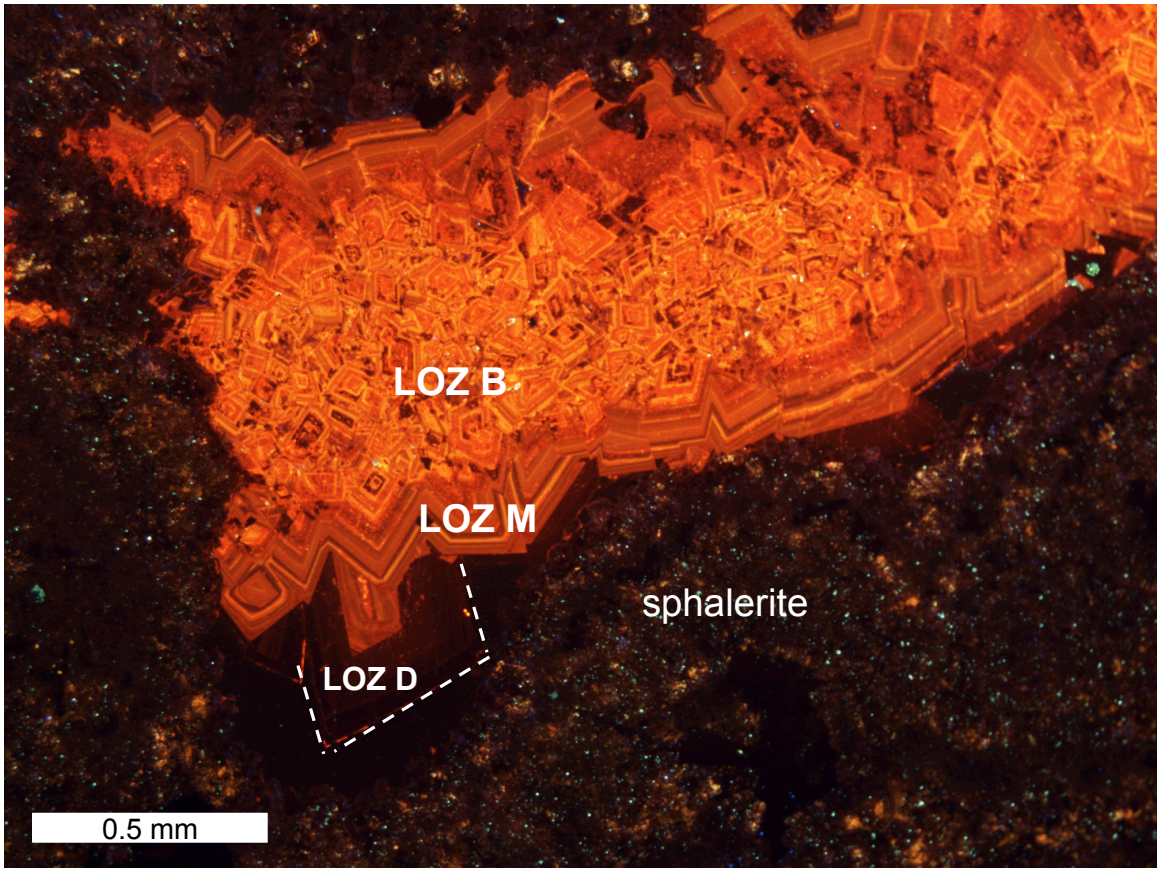

Figure 3.12. Representative images of the atypical CL stratigraphy in dolomite cements from the Cu-(Ni-Co)-Zn-rich lower ore zone (LOZ) of the Brushy Creek mine in the Viburnum Trend (Cavender, 2015). Earlier LOZ Bright (LOZ B) occurs as finer euhedra, overgrown by coarser LOZ Moderate (LOZ M) cement. Infrequently, LOZ Dark (LOZ D) occurs as an outer non-luminescent zone overgrowing the two earlier cements.

New CL Studies

Samples collected by W. A. Tarr in the 1930s from the historic Old Lead Belt, Mine La Motte, and Annapolis subdistricts have been archived in the University of Missouri's research collection, providing a unique opportunity to study the CL stratigraphy of ore-related dolomite cements throughout southeast Missouri that would otherwise be inaccessible. Samples from the West Fork and Fletcher mines studied by Adelstein et al. (2016) were also included in the present study to investigate the distinct lateral mineral/metal zoning, paragenetic reversal between iron sulfides and octahedral galena, and unusually Zn-rich character of "West Fork-type mineralization". If CL cement stratigraphies are distinct from the regional four-zone stratigraphy of the Viburnum Trend, we may develop a better understanding of the history of mineralization in southeast Missouri and the relationship between fault-related mineralization in the lower Bonneterre Dolomite and regional fluid flow responsible for upper Bonneterre Dolomite-hosted mineralization in the Viburnum Trend.

The Old Lead Belt and Mine La Motte subdistricts (Lower Bonneterre Dolomite and Lamotte Sandstone)

Dolomite cements from the lower Bonneterre Dolomite and Lamotte Sandstone in both the Old Lead Belt and Mine La Motte subdistricts (n = 21) commonly exhibit a distinctive CL stratigraphy that consists of repeated sequences of alternating bright and non-luminescent bands (Fig. 3.13). The first zone in this CL cement stratigraphy is a dull to non-luminescent zone that frequently displays very faint zoning and nearly always contains a thin, bright marker band (similar in appearance to zone 2 of the regional four-zone cement). This is followed by a second zone characterized by 2 to 3 discrete

sequences of banding that vary outwardly in the cement from bright toward moderately luminescent. Each of these sequences is separated typically by a discernible non-luminescent band and, in some samples, a dissolution surface. Geographically, the individual bands in these sequences of alternating dark and bright bands – including the bright marker band in the early cement – appear to increase in thickness from south (Mine La Motte) to north (Old Lead Belt). Early portions of these cements appear texturally to be more resorbed in samples that are hosted in the Lamotte Sandstone (Fig. 3.13c) than those hosted in the lower Bonneterre Dolomite. A third, final CL cement zone is observed in dolomite cement crystals that extend into open space. This cement zone is thicker (up to ~ 0.25 mm) and dull to non-luminescent, and can exhibit faint banding. This outer zone resembles zone 4 of the regional four-zone cements.

The distinctive, oscillatory CL stratigraphy is present typically in samples from the Old Lead Belt and Mine La Motte that contain at least minor galena ± sphalerite. However, the CL stratigraphy of dolomite cement in samples of chalcopyrite-rich mineralization from Mine La Motte (Fig. 3.13d) appears similar to zone 3 of the regional four-zone cement stratigraphy and to the LOZ Moderate cement of Cavender (2015). This cement contains remnants of earlier cement zones that are similar to the CL stratigraphy more commonly found at Mine La Motte.

The Annapolis subdistrict (Backreef facies of the Bonneterre Dolomite)

The CL stratigraphy of gangue dolomite cement in the Annapolis subdistrict (n = 4), hosted in the backreef facies of the Bonneterre Dolomite, is distinct from that of cement from the lower Bonneterre Dolomite in the Old Lead Belt and Mine La Motte and from the regional four-zone cement in the Viburnum Trend area (Fig. 3.14).

Replacement and recrystallized host dolomite from the Annapolis district has a mottled texture and is typically moderate to bright in luminescence, but also can display dark, iron-rich CL characteristics. The earliest CL zone in this dolomite cement can range from dull to moderately bright in luminescence and exhibits a mottled texture with its original growth banding frequently still intact. This early zone exhibits greater variability in its CL character than the rest of the cement stratigraphy.

A period of dissolution produced a corroded surface on the first zone of cement, upon which a second zone was precipitated. The second zone is consists of three discrete sequences of finely banded dolomite that progress from sequences characterized by (a) bright banding to (b) moderately luminescent banding to (c) alternating dull and non-luminescent bands. The brightly banded sequence (a) is commonly absent. When present, it is thin and frequently has a resorbed texture. This sequence of bands (a) experienced a subsequent period of dissolution followed by the precipitation of a third zone of cement that consists of two discernible, very bright bands (up to ~ 35 μm each). These bands are succeeded frequently by a continuation of dull to non-luminescent, finely banded cement. A third period of dissolution frequently removes this dull CL cement zone and penetrates the set of two bright bands beneath. In cements where dissolution is not as extensive (where the dull banding remains intact) the rim of the third zone of cement is marked by a very thin (~ 10 μm), discontinuous, bright CL line (Fig. 3.14a). This CL line may represent a later, bright CL cement that has been removed by dissolution or could be a product of the leaching of iron (or the addition of manganese) from the crystal surface. A final, fourth CL zone is a thick (up to ~ 0.3 mm), uniform cement with a dull to non-luminescent CL character (Fig 3.14).

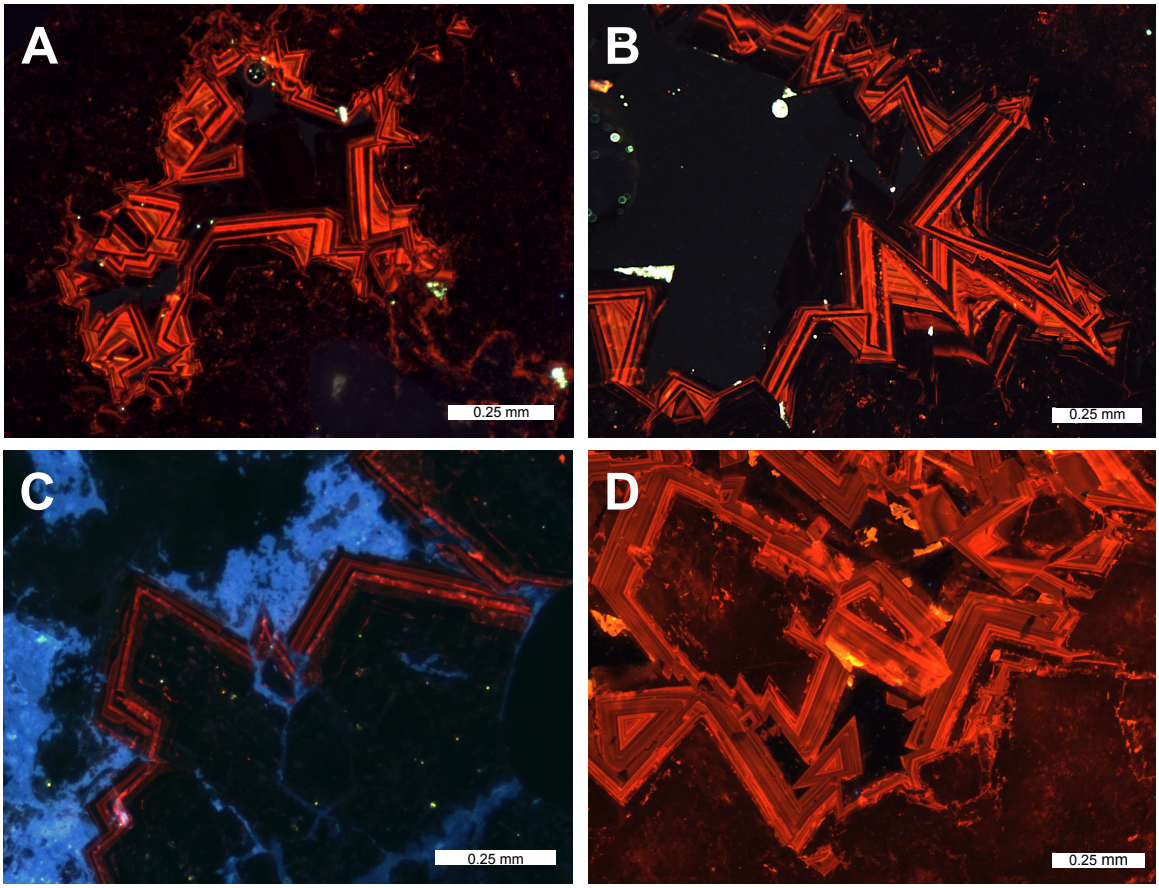

Figure 3.13. Representative images of the CL stratigraphy in dolomite cements from subdistricts to the east of the Viburnum Trend hosted in the lower Bonneterre Dolomite and the underlying upper Lamotte Sandstone. The cements display a distinctive CL stratigraphy that is characterized typically by repeating sequences of very bright banding alternating with dull to non-luminescent bands and are found in the A) Old Lead Belt and B) Mine La Motte subdistricts. C) Ores hosted in sandy carbonates within the Lamotte Sandstone at Mine La Motte are associated with cement that displays a similar, but typically more resorbed, CL stratigraphy. Blue luminescence indicates quartz grains of initial igneous origin (Marshall, 1988). D) The CL patterns in dolomite cement associated with samples of chalcopyrite-rich ores from the Mine La Motte subdistrict, however, frequently appear similar to zone 3 of the regional four-zone CL stratigraphy found in the upper Bonneterre in the Viburnum Trend and southern Missouri.

Only a limited number of samples from the Annapolis subdistrict were available for this study and few of their dolomite cements exhibit the CL stratigraphy in its entirety; those that did contain the entire CL stratigraphy were typically from samples containing very little sulfide. The presence of all three sequences of the second zone of cement (bright, moderate, and dull/non-luminescent banding) is associated typically with the partial or complete removal of the two distinctive bright bands of the third zone (Fig. 3.14b). However, the second zone of cement frequently contains only its final sequence of alternating dull and non-luminescent bands and, in these cases, the two distinctive bright bands of the third zone are typically continuous and relatively undisturbed by dissolution (Fig. 3.14c).

The West Fork mine, Viburnum Trend (Middle to Upper Bonneterre Dolomite)

CL microscopy of gangue dolomite cements from the West Fork mine and the northern portion of the Fletcher mine (n = 24) was employed to determine if cement stratigraphies in these anomalously Zn-rich areas show similar geochemical and temporal variations in ore fluids as cements associated with more typical Pb-rich ores of the Viburnum Trend. CL studies document that the dolomite cement CL stratigraphies are variations on the regional four-zone cement stratigraphy that is prevalent throughout the Viburnum Trend district. However, dolomite cements from the West Fork and northern Fletcher mines exhibit differences in CL patterns that appear to be associated spatially with the distinct lateral metal zoning present in the mine area (Figs. 3.5a and 3.15).

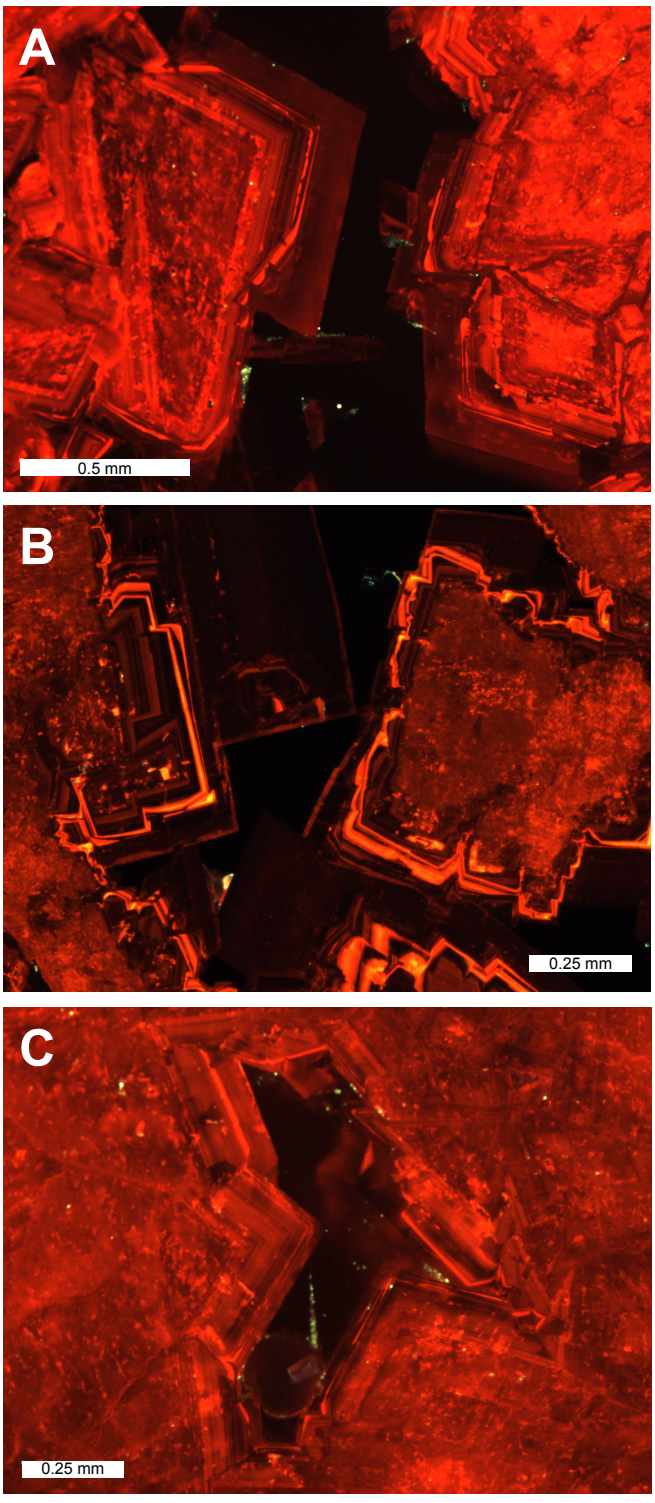

Figure 3.14. Representative images of the CL stratigraphy in dolomite cement from the Annapolis subdistrict hosted in the backreef (lagoonal) facies of the Bonneterre Dolomite. A) Dolomite cement containing the entire CL stratigraphy is characterized by three discrete sequences of banding progressing from (a) bright to (b) moderately luminescent to (c) dull to non-luminescent. This is followed by a zone that consists of two distinctive, bright marker bands, that may be partially removed by a later period of dissolution. B) The two bright marker bands remain intact/undissolved, whereas the bright (a) to moderate (b) sequences of banding in the previous CL zone are absent. C) The two bright marker bands are nearly removed completely, whereas all three sequences of bright (a), moderate (b), and dull (c) banding in the previous CL zone are present.

Dolomite cements in Pb- and Cu-Pb dominated areas at West Fork display all four zones of the regional four-zone CL stratigraphy of the upper Bonneterre Dolomite ores in the Viburnum Trend. However, dark to non-luminescent CL zone 4 is not abundant and is found typically filling minor pore space. In the western portion of the Pb-rich area and in the Cu-Pb-rich area of the mine, CL zones 2 and 3a become thinner and more discontinuous or may be absent altogether as a result of the dissolution event prior to the precipitation of zone 3b. Consequently, zone 3b penetrates frequently into zones 1 and 2 and the occurrence of zone 3a is uncommon. Similar CL patterns to the Pb- and Cu-rich areas are found in cements from the northern portion of the Fletcher Mine, where "West Fork-type" mineralization transitions laterally into more typical Viburnum Trend ores. To the east of the Pb-rich area, mineralization eventually becomes Fe-Zn-Pb-dominant and the dissolution surface separating CL subzones 3a and 3b in dolomite cements is subtle. Zone 3b in these Fe-Zn-Pb-rich areas generally decreases in thickness (in contrast to the increased thickness in zone 3b that is commonly observed in samples from areas dominated by later, Pb-rich mineralization). CL zone 2 and its characteristic, bright marker band become more prevalent in the Zn-rich ore samples from the Zn-Pb-rich area toward the Fe-Zn-Pb-rich area. Dolomite cements in the Fe-Zn-Pb area also commonly display highly resorbed textures and brighter luminescence, which may be the product of CL zone 3-depositing fluids locally invading host dolomite.

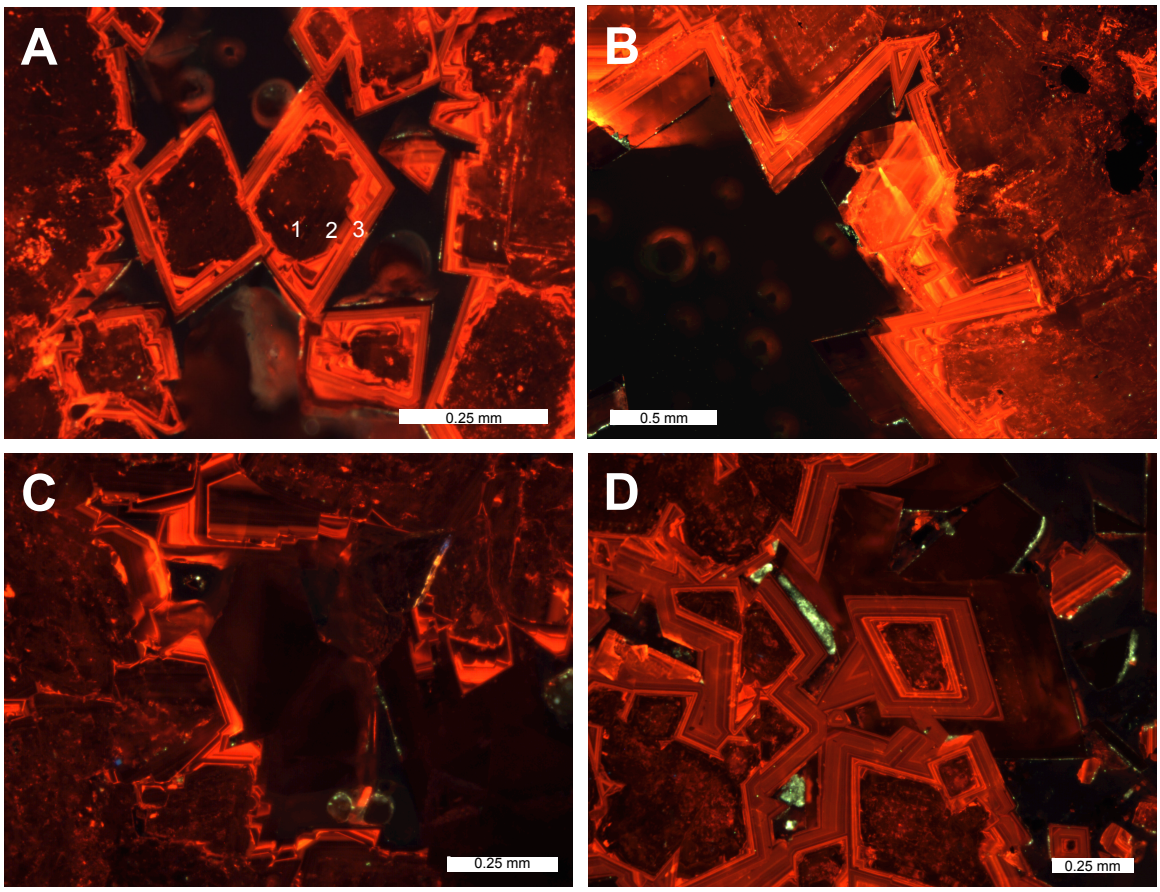

Figure 3.15. Representative images of the CL stratigraphy in dolomite cements hosted in the middle to upper Bonneterre Dolomite that are associated with "West-Fork type" mineralization and display variations on the regional four-zone CL stratigraphy. Zone 4 is commonly absent but may occur in cements projecting into open space. A) Dolomite cement from areas of Pb-dominated mineralization in the West Fork mine exhibits the typical, regional four-zone CL stratigraphy. B) CL zone 2 is thin and discontinuous or absent in cement from the Cu-Pb-rich area on the western fringes of the West Fork mine. C) CL zones 2 (with a pervasive, bright marker band) and 3 in cements from Zn-Pb to Fe-Zn-Pb-rich areas. CL subzone 3b (separated from the earlier 3a by a dissolution surface) in these cements is commonly very thin. D) Dolomite cement from the northern portion of the Fletcher mine exhibits a similar CL stratigraphy to the Cu-Pb- to Pb-rich zones of the West Fork mine, in which zone 2 is frequently absent.

Summary of CL Studies – Relationship to Stratigraphic Position

Lower Bonneterre Dolomite and Lamotte Sandstone

A distinctive CL stratigraphy in dolomite cements from the Old Lead Belt and Mine La Motte subdistricts (Fig. 3.2) is characterized by dark to non-luminescent, mottled host rock overgrown by repeating sequences of moderate to bright banding alternating with non-luminescent bands. These sequences are followed frequently by a final dark zone that resembles zone 4 of the regional four-zone CL stratigraphy. The repetitive nature of the CL zoning in these cements suggests deposition by multiple pulses of dolomitizing fluids and/or oscillatory variations in fluid chemistry caused by partitioning of iron or manganese associated with the deposition of other minerals (e.g. Fe-sulfides). In two chalcopyrite-rich samples from Mine La Motte, this dolomite CL stratigraphy is overgrown by dolomite cement that appears similar to late zone 3 of the regional four-zone cement (Fig. 3.13d), which may indicate that the distinctive dolomite CL cement stratigraphy and its associated ore mineralization in the Old Lead Belt and Mine La Motte is younger paragenetically than main stage Pb-Zn mineralization (associated with CL zone 3) in the Viburnum Trend.

Backreef facies of the Bonneterre Dolomite

Dolomite cements from the backreef facies (not associated typically with ore mineralization) of the Bonneterre Dolomite to the east of the Viburnum Trend have been reported to display CL stratigraphies that are correlative to the regional four-zone stratigraphy (Voss et al., 1989; Gregg and Shelton, 1990). The CL patterns in some samples of these dolomite cements were characterized by an absence of CL zone 2 and an increased thickness of zone 3 (Voss et al., 1989).

However, gangue dolomite cement in ore samples analyzed in the current study from the Pb-rich Annapolis subdistrict (Fig. 3.2) display CL patterns unlike the regional four-zone CL stratigraphy found in the upper Bonneterre Dolomite elsewhere in southeast Missouri. Their unusual CL stratigraphy is characterized by an early, mottled cement that frequently contains preserved growth banding, in contrast to zone 1 of the regional four-zone CL stratigraphy that is characterized by a distinct absence of well-defined banding. The first, mottled zone of cement is followed by a second zone of finely banded cement that transitions outwardly from bright banding toward dull and non-luminescent banding. The third zone of cement, whose surface can be corroded to variable degrees, consists of two very bright bands followed frequently by dull to non-luminescent banding and likely resulted from fluids that differed chemically from those of the regional flow system in the upper Bonneterre Dolomite in the Viburnum Trend and southern Missouri. The frequency of occurrence of this third zone appears to coincide with the absence of the early, bright and moderate CL banding of the second zone of cement. The final, fourth zone of dull to non-luminescent dolomite is deposited upon another dissolution surface and resembles zone 4 of the regional four-zone CL stratigraphy (Fig. 3.14).

The disparity in CL patterns between dolomite cements from the Pb-rich Annapolis subdistrict and the rest of the backreef facies of the Bonneterre Dolomite indicates that the fluids responsible for Pb-rich ore deposition at Annapolis were likely associated closely with the unique CL stratigraphy observed in dolomite cement from the subdistrict. The resemblance between the fourth, dark zone in Annapolis dolomite cement and zone 4 of the regional four-zone CL stratigraphy may suggest that an earlier,

chemically distinct system in the backreef facies in the Annapolis subdistrict was inundated by later, post-ore fluids from the regional flow system present higher in the Bonneterre Dolomite in the Viburnum Trend.

Middle to upper Bonneterre Dolomite

CL zoning in gangue dolomite cements in the middle to upper Bonneterre Dolomite typically appear to exhibit variations on the regional four-zone CL cement stratigraphy characteristic of the rest of the Viburnum Trend, even in the unusually Zn-rich areas of the West Fork mine and the northern portion of the Fletcher mine (Fig. 3.15). The occurrence and thickness of CL zones 2 and 3 appear to be related spatially to the dominance of Pb- and Zn-rich mineralization (Fig. 3.5c). Zone 2 is most prevalent in portions of the West Fork mine where early, Zn-rich mineralization is dominant, whereas an increased thickness of zone 3b appears to correspond to later, Pb-rich mineralization. Dissolution of dolomite cement and host rock associated with iron sulfide deposition that followed early sphalerite precipitation and the later, Pb-rich mineralizing event may have both contributed locally to the development of resorbed textures and the partial or complete removal of CL zones 2 and 3a. The survival and textural appearance of specific CL cement zones appear to depend on the dominant type of metal sulfide (i.e. Zn-rich areas are associated with a thick zone 2 and resorbed textures, whereas Pb-rich areas are associated with a thinner zone 2 and thicker zone 3b) in the West Fork mine and may indicate that dolomite CL cement stratigraphy in this mine is a product of multiple, metal-specific mineralizing fluids whose influence varied spatially and temporally.

CARBON AND OXYGEN ISOTOPE GEOCHEMISTRY

Stable isotope studies of ore-associated carbonates can provide valuable information about the source and chemical evolution of mineralizing fluids, and the temperature and extent of fluid-rock interaction along flow pathways (Frank and Lohmann, 1986; Shelton et al., 1986; Gregg and Shelton, 1989a; Shelton et al., 2011). Carbon and oxygen studies of gangue dolomite cements and host replacement dolomites from several subdistricts in the southeast Missouri lead district were undertaken to investigate these processes.

Viburnum Trend Dolomite Cements

Main Ore Zone (Middle to Upper Bonneterre Dolomite)

Dolomite cements associated with typical Pb-Zn-Cu ores of the Viburnum Trend have $\delta^{13}C$ values of ~ -3.0 to -1.0‰ and $\delta^{18}O$ values of ~ -10.0 to -7.5‰ VPDB (Fig. 3.16a) (Braunsdorf, 1983; Frank and Lohmann, 1986; Shelton et al., 1986; Gregg and Shelton, 1990). Frank and Lohmann (1986) delineated an isotopic trend for the regional four-zone CL stratigraphy in which zones 2 and 3 progressively have higher values with time ($\delta^{13}C$ = -2‰ and $\delta^{18}O$ = -9‰ toward $\delta^{13}C$ = 0‰ and $\delta^{18}O$ = -3‰). Zone 4 cement displays a return to lower $\delta^{13}C$ and $\delta^{18}O$ values of ~ -2‰ and -9‰ VDPB, respectively. This temporal evolution in isotopic composition has been modeled to represent a single, evolving basinal brine (zones 1-3), punctuated by the appearance of a later, distinct basinal fluid (zone 4) (Gregg, 1985; Gregg and Shelton, 1989a).

Lower Ore Zone (Lower Bonneterre Dolomite and Lamotte Sandstone)

Carbon and oxygen isotope studies by Cavender (2015) show that host dolomite of the LOZ orebody displays wide variability in both $\delta^{13}C$ and $\delta^{18}O$ values (Fig. 3.16b).

Dolomite cements from the lower orebody at the Brushy Creek mine show a paragenetic decrease in $\delta^{18}O$ values with paragenesis while $\delta^{13}C$ values remain relatively constant. Both generations of LOZ cement share similar $\delta^{13}C$ values, but the early, LOZ Bright cement has higher $\delta^{18}O$ values (-3.3 to -4.4‰) than LOZ Moderate cement (-6.2 to -8.2‰) (Fig. 3.16b). Fluid inclusion studies indicate that the LOZ Bright dolomite cement was formed at a higher temperature ($T_h \sim 180$ºC) than the LOZ moderate cement ($T_h \sim$ 130 to 150ºC) (Cavender, 2015). The relative $\delta^{18}O$ values of these two cement types ($\delta^{18}O_{LOZ\ B} > \delta^{18}O_{LOZ\ M}$) is opposite to what would be expected if they had been deposited from a single fluid with progressively decreasing temperature. Thus, the decrease in $\delta^{18}O$ values from the earlier LOZ Bright cement to the LOZ Moderate cement is not a simple temperature effect and must be the result of multiple, isotopically distinct fluids.

Many LOZ samples analyzed for oxygen isotope composition had accompanying drill hole information documenting their distance above the Lamotte Sandstone-Bonneterre Dolomite contact. The lower-$\delta^{18}O$ LOZ Bright cements are restricted typically to the lower portion of the stratigraphic section; together with the LOZ Moderate cements and their associated wall rock dolomites, they show a progressive decrease in $\delta^{18}O$ values with increasing distance above the Lamotte-Bonneterre contact (Fig. 3.17). This isotopic relationship to stratigraphic position could reflect that that deep, likely fault-related fluids moved up the stratigraphic section into overlying host rock (Fig. 3.7b) and reacted progressively with previously dolomitized host rock of the stratigraphically higher lead-rich ore system.

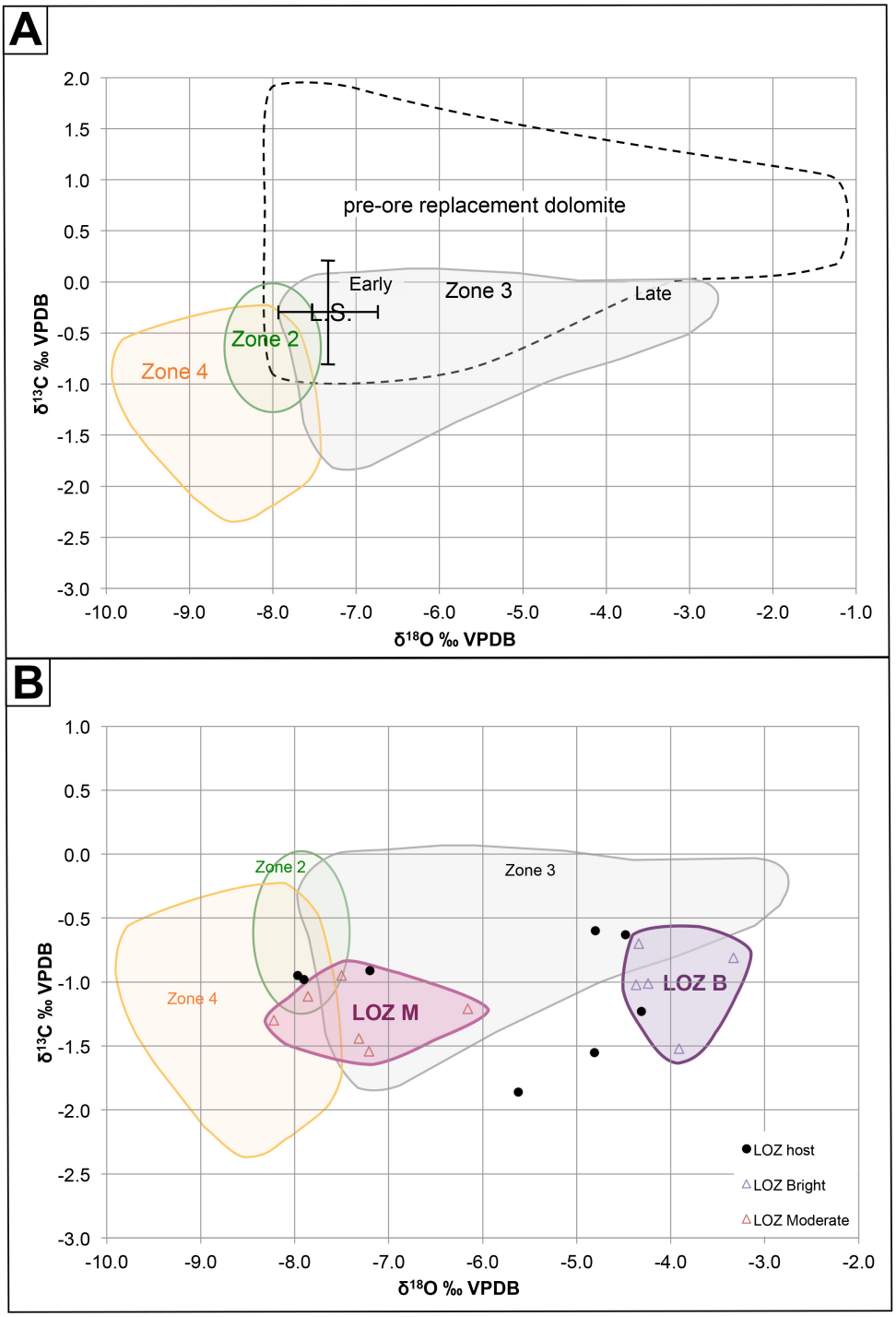

Figure 3.16. A) Carbon and oxygen isotopic ranges of pre-ore replacement dolomite, ore-associated dolomite cements, and Cambrian limestone (L.S.) in the Viburnum Trend (after Frank and Lohmann, 1986; Gregg and Shelton, 1989a). Zones 2, 3 and 4 refer to CL zones in the regional four-zone dolomite cement. B) Carbon and oxygen isotopic ranges of dolomite cement associated with LOZ ores of the Viburnum Trend (after Cavender, 2015). Isotopic compositions for zones 2, 3 and 4 of regional four-zone dolomite cement are also plotted for reference (after Frank and Lohmann, 1986; Gregg and Shelton, 1989a).

The L-shaped curve on Figure 3.17 has been modeled in the present study as a progressive equilibrium isotope exchange pattern (with increasing water/rock ratios) in which a deep LOZ fluid reacts with overlying dolomitized host rock. Water/rock ratios of this progressive reaction were evaluated using the following equation (Taylor, 1979):

$$W/R_o = ln\left(\frac{\delta^f_{dolomite} - \delta^i_{dolomite}}{\delta^i_{water} - \left(\delta^f_{dolomite} - \Delta_{water\text{-}dolomite}\right)}\right) = ln\left(W/R_c + 1\right),$$

where W/R_o refers to the water/rock (dolomite) ratio in an open system, W/R_c refers to the water/rock ratio in a closed system, δ^i is the initial $\delta^{18}O$ value of the rock or water in the system, δ^f is the final $\delta^{18}O$ value of the rock or water in system after equilibration, and $\Delta_{water\text{-}dolomite}$ is determined by the dolomite-water oxygen isotope fractionation curve (Friedman and O'Neil, 1977) based on temperature. The calculations assumed a temperature of 145ºC (average T_h value of fluid inclusions in LOZ M cements), an initial $\delta^{18}O^i_{dolomite}$ value of -3.0‰ VPDB (27.8‰ VSMOW, an approximated maximum value for LOZ host dolomite), and a final $\delta^{18}O^f_{dolomite}$ value of -9.0‰ VPDB (21.6‰ VSMOW), which corresponds roughly to the minimum $\delta^{18}O$ values of LOZ M cements and those of typical ore-hosting dolomite host rock in the Viburnum Trend (Braunsdorf, 1983; Frank and Lohmann, 1986; Shelton et al., 1986; Cavender, 2015) (see "Simulation 1" in Table 3.1).

The dashed line in Figure 3.17 traces the change in $d^{18}O$ values of LOZ dolomite relative to paragenetic time and distance above the Bonneterre Dolomite-Lamotte Sandstone contact. An initial $d^{18}O^i_{water}$ value (10.8‰ VSMOW) was chosen to be in equilibrium with an initial $\delta^{18}O^i_{dolomite}$ value of -3‰ VPDB at 145ºC in order to include water/rock ratios corresponding to nearly the entire range of $\delta^{18}O$ values

Figure 3.17. Variation of $\delta^{18}O$ values of host dolomite and dolomite cement associated with LOZ ores in the Viburnum Trend versus distance above Lamotte Sandstone-Bonneterre Dolomite contact (after Cavender, 2015). The dashed curve traces the change in $\delta^{18}O$ values and water/rock (W/R) ratios (in open and closed systems) relative to paragenetic time as deep, fault-related fluids ($\delta^{18}O_{water}$ = 10.8‰ VSMOW, T = 145ºC) react progressively with stratigraphically higher host rock ($\delta^{18}O_{dolomite}$ = -9‰ VPDB) produced by an overlying dolomitizing system. Note that water-rock isotopic exchange becomes progressively more host rock-dominated (i.e. water/rock ratios decrease) as fluids move up through overlying host rock.

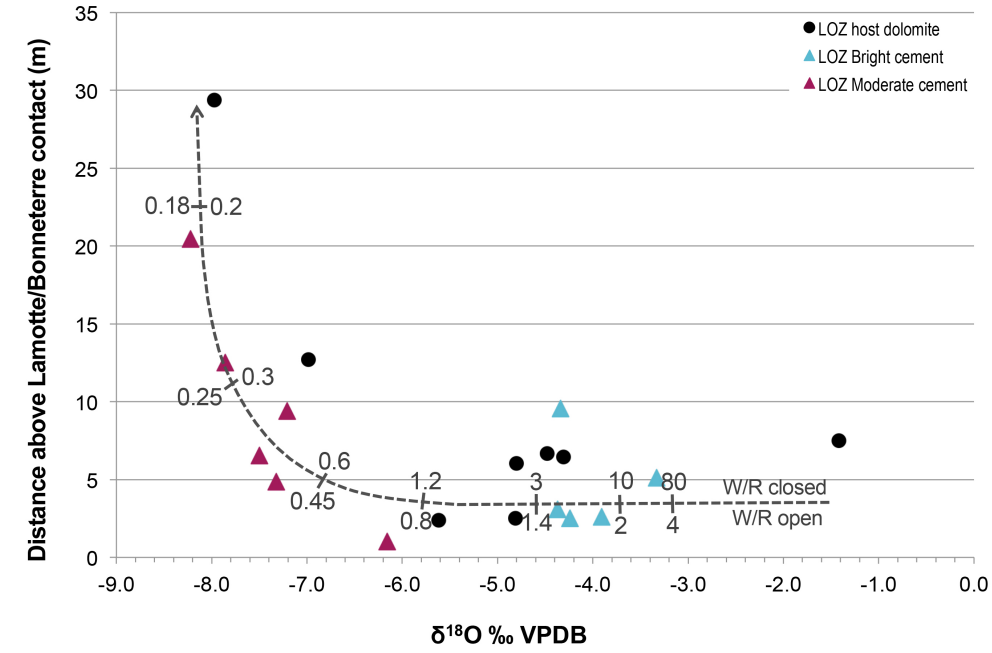

Table 3.1. Values used for parameters in calculations of water/rock ratios (Fig. 3.17) during the progressive equilibration of LOZ dolomite with stratigraphically higher host rock produced by an overlying dolomitizing system.

Constant Parameters	
T	145ºC
$\Delta_{water\text{-}dolomite}$	17‰ VSMOW (Friedman and O'Neil, 1977)
$\delta^{18}O^{f}_{dolomite}$	-9‰ VPDB
Simulation 1	
$\delta^{18}O^{i}_{water}$	10.8‰ VSMOW
$\delta^{18}O^{i}_{dolomite}$	-3‰ VPDB (27.8‰ VSMOW)
Simulation 2	
$\delta^{18}O^{i}_{water}$	7.7‰ VSMOW
$\delta^{18}O^{i}_{dolomite}$	-6‰ VPDB (24.7‰ VSMOW)

measured for LOZ host dolomite. This model shows that water/rock ratios decrease (closed system = from 80.0 toward 0.2, open system = from 4.00 toward 0.18) as isotopic exchange continues between the LOZ water and host dolomite as the system gradually becomes more rock-dominated higher in the stratigraphic section.

If the initial $\delta^{18}O^{i}_{dolomite}$ value had been -6‰ VPDB (corresponding to measured LOZ M cement values, Cavender, 2015; see "Simulation 2" in Table 3.1), water/rock ratios could only be calculated for $\delta^{18}O$ values > -6‰ and would effectively represent only half of the measured LOZ dolomite data shown on Figure 3.17. However, calculations in this scenario would still produce the same trend of decreasing water/rock values with decreasing $\delta^{18}O$.

New Stable Isotope Studies

Dolomite cements and host dolomite from orebodies in the Old Lead Belt, Mine La Motte, and Annapolis subdistricts were sampled in order to compare their isotopic compositions to their CL patterns and to the typical isotopic trends and CL patterns of the upper Bonneterre ores in the Viburnum Trend. Individual CL zones could not be sampled due to the small size (< 2 mm) of the cements being analyzed. The relative abundance of individual CL zones was known in many of the cements that were sampled, however, which may permit us to evaluate the relationship between CL zones and stable isotope values in some cases. Data are shown in Table 3.2 and plotted in Figure 3.18.

The Old Lead Belt (Lower Bonneterre Dolomite)

All but one of the host dolomite samples from the Old Lead Belt have $\delta^{13}C$ values of -0.90 to -0.49‰ and $\delta^{18}O$ values of -7.78 to -6.78‰ VPDB (n = 8). An outlier with $\delta^{13}C$ and $\delta^{18}O$ values of -1.85‰ and -3.66‰, respectively, may reflect differences in

Table 3.2. Carbon and oxygen isotope data from powdered samples. Data are presented in standard δ notation as per mil (‰) deviations from VPDB. Abbreviations: dol = dolomite.

SAMPLE ID	DESCRIPTION	$\delta^{13}C$ ‰ (VPDB)	$\delta^{18}O$ ‰ (VPDB)
The Old Lead Belt			
BT1632 C1	cement in vug	**-6.08**	**-0.73**
BT1632 HR1	recrystallized white host dol	**-7.41**	**-0.61**
BT1632 HR2	brown host dol	**-7.27**	**-0.49**
FR1591 C1	cement core	**-7.08**	**-0.53**
FR1591 HR1	brown host dol	**-7.25**	**-0.46**
FR1666 C1	cement with galena	**-7.89**	**-2.01**
FR1666 C2	cement core	**-7.20**	**-1.04**
FR1666 HR1	brown host dol	**-3.66**	**-1.85**
FR1666 HR2	coarse recrystallized host dol	**-6.87**	**-0.72**
FR1677 C1	cement in vug with sulfide	**-7.66**	**-1.42**
FR1677 HR1	host	**-7.31**	**-0.56**
FR1683 C1	cement in open vug	**-7.32**	**-1.17**
FR1683 C2	cement in open vug	**-7.26**	**-1.18**
FR1683 HR1	host	**-7.78**	**-0.90**
RM1608 C1	cement filling vug	**-6.72**	**-0.69**
RM1608 HR1	host	**-6.83**	**-0.73**
Mine La Motte			
1795 C1	cement in vug	**-6.47**	**-1.40**
1795 HR1	host	**-7.36**	**-0.92**
LM1623 C1	cement in vug	**-7.37**	**-1.15**
LM1623 dol	recrystallized host	**-7.79**	**-0.76**
LM1623 HR1	brown host dol	**-7.79**	**-1.04**
LM1775 C1	cement filling vug, post-galena	**-7.03**	**-1.71**
LM1775 C2	cement, pre-galena	**-6.91**	**-1.50**
LM1775 HR1	host	**-7.19**	**-1.40**
LM1919 C1	cement	**-7.55**	**-1.46**
LM1919 C3	cement core	**-6.95**	**-1.26**
LM1919 HR1	brown host dol	**-7.26**	**-0.71**
LM1925 C1	cement core	**-7.41**	**-1.34**
LM1925 C2	cement edge	**-7.22**	**-1.42**
LM1925 HR1	host adjacent to cement	**-7.81**	**-1.17**
LM1925 HR2	host away from cement	**-7.73**	**-1.33**
LM8279 C1	cement with chalcopyrite	**-6.46**	**-1.96**
LM8279 C2	cement filling vug	**-5.48**	**-2.08**
LMCPY C1	cement filling vug	**-6.86**	**-1.07**
LMSIEG C1	cement in vug, edge	**-6.99**	**-1.46**
LMSIEG C2	cement in vug, core	**-7.32**	**-0.94**
LMSIEG C3	cement	**-7.31**	**-1.60**
LMSIEG HR1	brown host dol	**-7.10**	**-0.81**
LMSIEG HR2	white recrystallized host dol	**-7.06**	**-0.76**
LMSIEG HR3	gray recrystallized host dol	**-7.18**	**-0.57**

SAMPLE ID	DESCRIPTION	$\delta^{13}C$ ‰ (VPDB)	$\delta^{18}O$ ‰ (VPDB)
Annapolis			
ANP1820 C1	cement	**-7.21**	**-0.98**
ANP1820 C2	cement	**-7.40**	**-1.52**
ANP1820 C3	cement	**-7.13**	**-1.32**
ANP1820 HR1	host	**-7.53**	**-0.65**
ANP1820.4 C1	cement	**-7.48**	**-1.36**
ANP1820.4 HR1	white recrystallized host dol	**-7.45**	**-0.70**
ANP1820.4 HR2	brown host dol	**-7.56**	**-0.73**
West Fork (Adelstein et al., 2016)			
WF 1025/203 C1	cement	**-7.73**	**-0.92**
WF 1025/203 R1	recrystallized host	**-7.37**	**-0.33**
WF 204/988 C1	cement	**-7.36**	**-0.56**
WF 204/988 R1	recrystallized host	**-7.33**	**-0.51**
WF 21 R1	recrystallized host	**-7.35**	**-0.38**
WF 211/978 C1	cement	**-6.84**	**-0.58**
WF 211/978 R	recrystallized host	**-7.63**	**-0.21**
WF 214/1000 HR	host	**-7.82**	**-0.06**
WF 214/995 C1	cement	**-7.32**	**-0.17**
WF 214/995 C2	cement	**-7.64**	**0.01**
WF 214/995 R1	recrystallized host	**-7.63**	**0.16**
WF 214/999 C1	cement	**-7.00**	**-0.02**
WF 214/999 R1	recrystallized host	**-7.75**	**-0.26**
WF 217S C1	cement	**-6.75**	**-0.62**
WF 217S R1	recrystallized host	**-7.80**	**-0.25**
WF 217S R2	recrystallized host	**-7.98**	**-0.42**
WF 38A-R	recrystallized host	**-7.69**	**-0.29**
WF 42 R1	recrystallized host	**-7.29**	**-0.42**
WF 44 C1	cement	**-7.51**	**-0.35**
WF 44 R1	recrystallized host	**-7.86**	**-0.49**
WF 974/210 C	cement	**-5.89**	**-0.47**
WF 974/210 R1	recrystallized host	**-7.54**	**-0.32**
WF 974/210 R2	recrystallized host	**-7.63**	**-0.33**
WF 974/210 R3	recrystallized host	**-7.69**	**-0.22**
WF 988/217 C1	cement	**-7.38**	**-0.71**
WF 988/217 R1	recrystallized host	**-7.32**	**-0.44**
WF 993 C1	cement	**-6.74**	**-0.56**
WF 993 R1	recrystallized host	**-7.24**	**-0.55**
WF 994 R	recrystallized host	**-7.43**	**0.04**
WF2 C1	cement	**-7.84**	**-1.39**
WF2 H1	host	**-7.56**	**-0.25**
WFL C1	cement	**-7.65**	**-1.76**
WFL H1	host	**-7.93**	**-0.23**

original host rock lithology and the extent of dolomite replacement that has taken place. Dolomite cements have $\delta^{13}C$ values of -2.01 to -0.53‰ and $\delta^{18}O$ values of -7.89 to -6.08‰ (n = 8). Cements from the Old Lead Belt have ranges of $\delta^{13}C$ and $\delta^{18}O$ values that overlap early zone 3 and zone 4 of the regional four-zone dolomite cement from the upper Bonneterre Dolomite of the Viburnum Trend (Fig. 3.18a), despite the majority of Old Lead Belt ores occurring in a lower portion of the stratigraphic section and having a different CL character than those of the Viburnum Trend.

Mine La Motte (Lower Bonneterre Dolomite and Lamotte Sandstone)

Host dolomite from Mine La Motte has $\delta^{13}C$ values of -1.40 to -0.57‰ and $\delta^{18}O$ values of -7.81 to -7.10‰ (n = 9). Dolomite cements have $\delta^{13}C$ values of -2.08 to -1.32‰ and $\delta^{18}O$ values of -7.55 to -5.48‰ (n = 14). The isotopic composition of most dolomite cement at Mine La Motte falls within the typical ranges for zone 3 of the regional four-zone cement and LOZ Moderate cement. However, two cement samples extend to lower $\delta^{13}C$ (-2.08‰) and higher $\delta^{18}O$ (-5.48‰) values than those measured from any other subdistrict in southeast Missouri (Fig. 3.18b). The fact that these values vary in opposite directions (as opposed to both $\delta^{13}C$ and $\delta^{18}O$ values decreasing or increasing concurrently) precludes them from forming as a function of temperature alone, and indicates the presence of fluid(s) at Mine La Motte that is isotopically distinct from those associated with typical mineralization in the Viburnum Trend.

Annapolis (Backreef facies of the Bonneterre Dolomite)

Host dolomite and dolomite cements from the Annapolis subdistrict have relatively narrow ranges of both $\delta^{13}C$ and $\delta^{18}O$ values, which may reflect of the limited number of samples that were measured. Host dolomite has $\delta^{13}C$ values of -0.73 to -

0.65‰ and $\delta^{18}O$ values of -7.56 to -7.45‰ (n = 3). Cements have $\delta^{13}C$ values of -1.52 to -1.32‰ and $\delta^{18}O$ values of -7.48 to -7.13‰ (n = 4). Although dolomite from the backreef facies is not associated typically with ore mineralization and displays a large range in $\delta^{13}C$ and $\delta^{18}O$ values (from -2.6 to -0.1‰ and -8.6 to -5.1‰, respectively, which are unpublished data that formed the basis of diagrams produced in Gregg and Shelton, 1989a), the ore-hosting "white rock" from the Annapolis subdistrict form a narrow range of values that are similar isotopically to LOZ Moderate cement from the Brushy Creek mine and early zone 3 of the regional four-zone cement throughout the Viburnum Trend (Fig. 3.18c).

The West Fork mine, Viburnum Trend (Middle to Upper Bonneterre Dolomite)

In order to investigate the relationship between ore fluid source(s), flow pathways, and depositional processes between the anomalously Zn-rich ores of the West Fork mine and mineralization elsewhere in the Viburnum Trend, stable isotope analysis of dolomite cement with atypical CL patterns from West Fork was employed. Data for dolomite from the West Fork mine are from Adelstein et al. (2016). Host dolomite has $\delta^{13}C$ values of -0.55 to 0.16‰ and $\delta^{18}O$ values of -7.98 to -7.24‰ (n = 20). Dolomite cements containing mostly bright CL zones 2 and 3 have $\delta^{13}C$ values of -0.92 to -0.02‰ and $\delta^{18}O$ values of -7.73 to -5.89‰ (n = 11), which correspond to the typical ranges for zones 2 and 3 of the regional four-zone cement in the Viburnum Trend; dolomite cements in which dull CL zone 4 is most abundant and bright CL zones 2 and 3 are thin have $\delta^{13}C$ values of -1.76 to -1.39‰ and $\delta^{18}O$ values of -7.84 to -7.65‰ (n = 2), which is consistent with the typical range of values for zone 4 in regional four-zone cements (Fig. 3.18d).

Figure 3.18. Carbon and oxygen isotopic ranges of dolomite cements analyzed in the present study are plotted relative to zones 2, 3 and 4 of the regional four-zone CL stratigraphy found in dolomite cement in the upper Bonneterre Dolomite in the Viburnum Trend and southern Missouri. A) Dolomite cement from the Old Lead Belt (OLB) subdistrict, hosted predominantly within the lower Bonneterre Dolomite. B) Dolomite cement from the Mine La Motte (MLM) subdistrict, hosted in the lower Bonneterre Dolomite and the upper portion of the underlying Lamotte Sandstone. C) Dolomite cement from the Annapolis (ANP) subdistrict, hosted in the backreef (lagoonal) facies ("white rock") of the Bonneterre Dolomite. Also shown for reference are the measured isotopic ranges of "white rock" that formed the basis of the studies documented by Shelton et al. (1986). D) Dolomite cement from the West Fork (WF) mine in the Viburnum Trend, hosted in the middle to upper Bonneterre Dolomite.

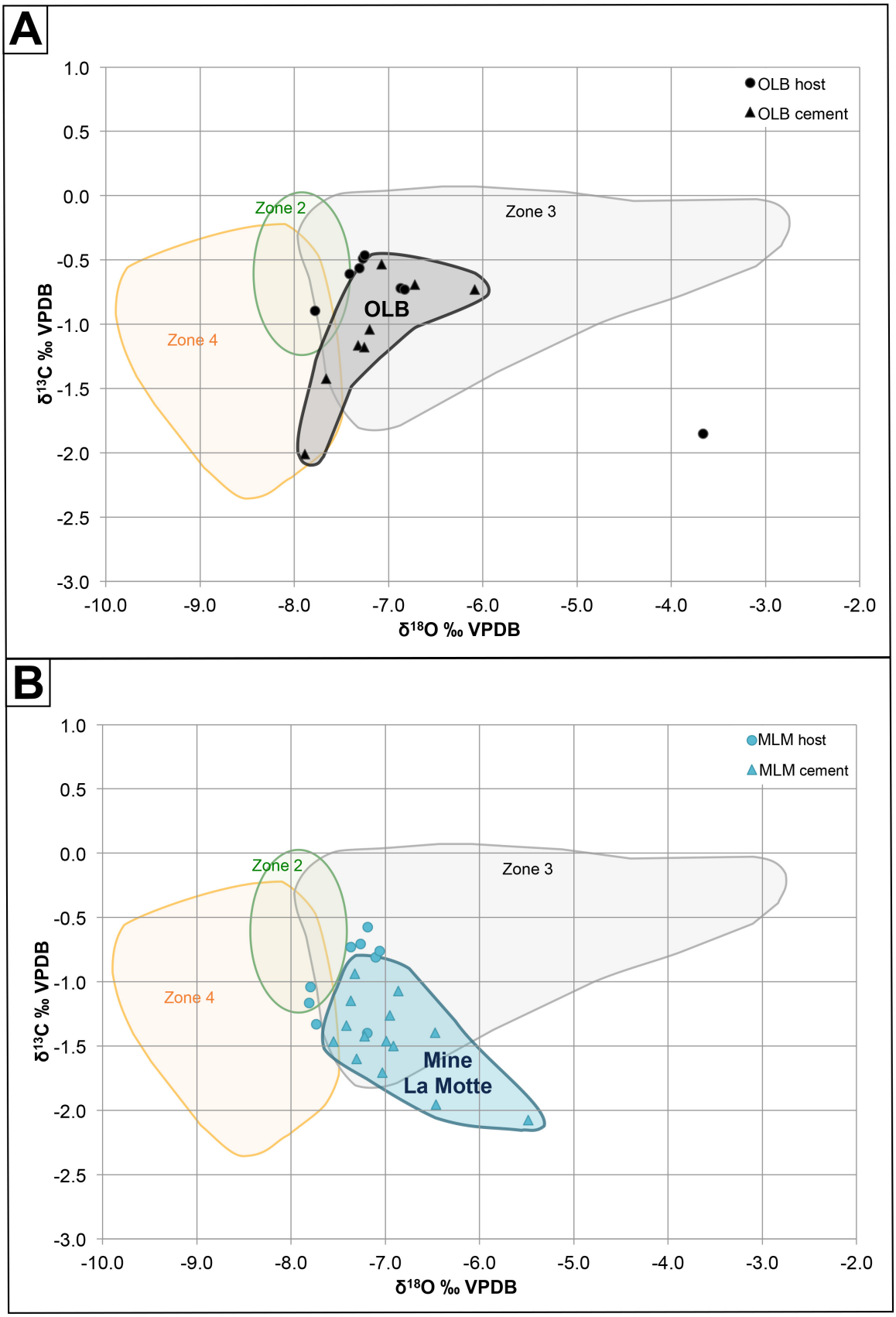
A
OLB host
OLB cement
Zone 2
Zone 3
Zone 4
OLB
δ13C ‰ VPDB
δ18O ‰ VPDB
B
MLM host
MLM cement
Zone 2
Zone 3
Zone 4
Mine
La Motte
δ13C ‰ VPDB
δ18O ‰ VPDB

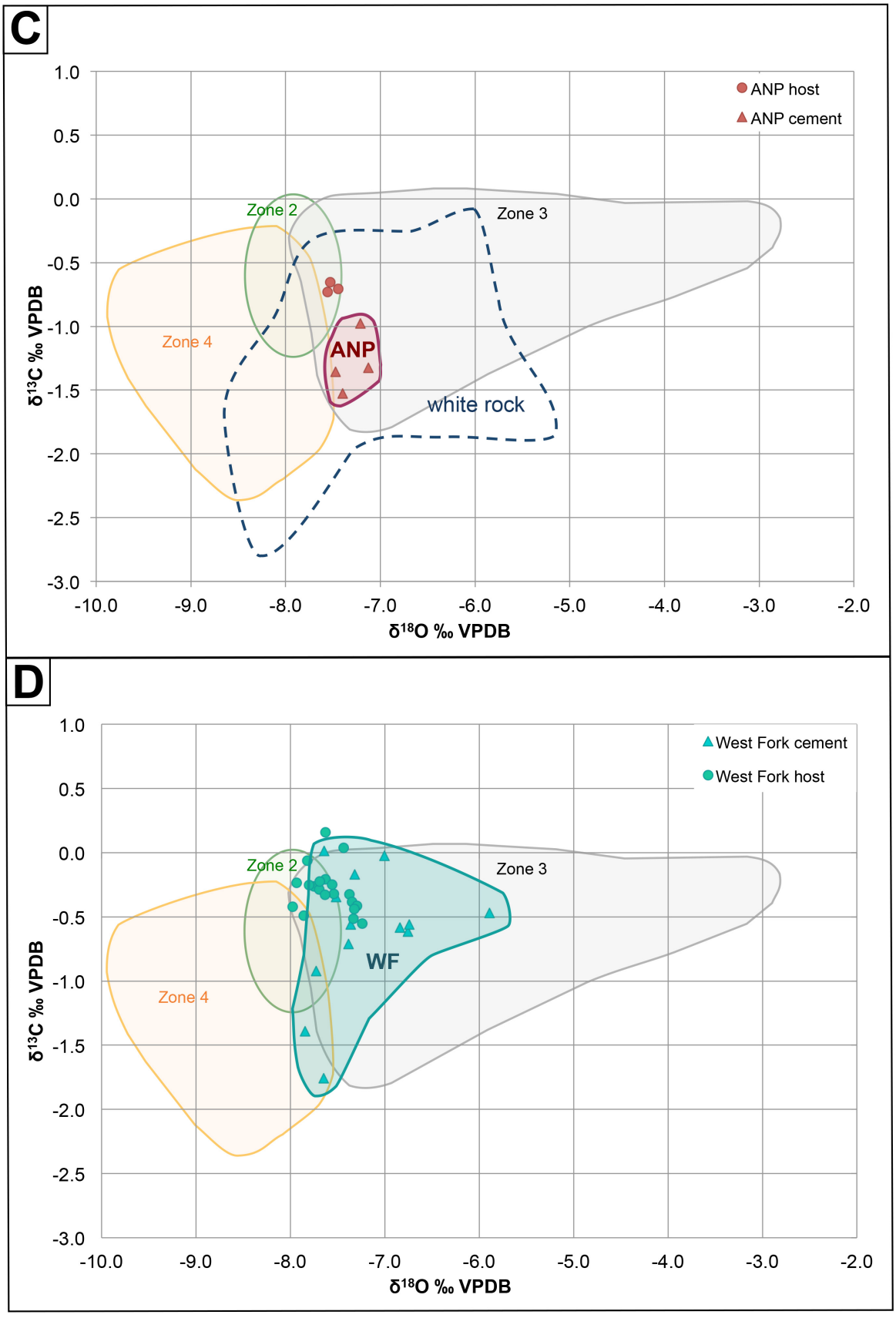
C
ANP host
ANP cement
Zone 2
Zone 3
Zone 4
ANP
white rock
δ13C ‰ VPDB
δ18O ‰ VPDB
D
West Fork cement
West Fork host
Zone 2
Zone 3
Zone 4
WF
δ13C ‰ VPDB
δ18O ‰ VPDB

These isotopic values support the initial assumption that the unusual CL patterns in West Fork dolomite represent a variation on the four-zone stratigraphy typical of the Viburnum Trend. Dolomite cement from the Pb-rich areas in the West Fork mine (with a CL stratigraphy in which zone 1 and host dolomite has undergone extensive dissolution, zone 2 is thin/absent, and zone 3 is thick) is associated with higher $\delta^{18}O$ values than those from the Zn-Pb and Fe-Zn-Pb-rich areas of the West Fork mine (where CL zone 2 is prevalent and zone 3b is thinner) (Adelstein et al., 2016).

Summary of Stable Isotope Studies

Host rock dolomite in the lower Bonneterre Dolomite ores of southeast Missouri is restricted to a relatively narrow range of $\delta^{13}C$ and $\delta^{18}O$ values compared to gangue dolomite cements, except in lower ore zone (LOZ) dolomite at the Brushy Creek mine within the Viburnum Trend. Host dolomite in the subdistricts east of the Viburnum Trend generally has lower $\delta^{13}C$ values than those of the stratigraphically higher mines in the Viburnum Trend (e.g. West Fork and Fletcher mines; Adelstein et al., 2016). Spatial and stratigraphic variations in $\delta^{13}C$ values of host dolomite in the southeast Missouri subdistricts may reflect differences in original host rock lithologies or multiple sources and/or flow paths of dolomitizing fluids prior to the onset of ore mineralization in the region.

Dolomite cement from all subdistricts analyzed in this study overlap at least partially in $\delta^{18}O$ values with LOZ Moderate cement (associated with Zn-rich mineralization in the lower Bonneterre Dolomite of the Viburnum Trend) and early zone 3 of regional four-zone cements (associated with main stage Pb-Zn mineralization in the middle to upper Bonneterre Dolomite) (Figs. 3.16 and 3.18). This may reflect a single

fluid reservoir tapped by multiple fault systems through the history of ore deposition in southeast Missouri or may reflect mineralizing systems with similar water/rock ratios in which distinct fluids interacted with isotopically similar host rocks at similar water/rock ratios. Some isotopic compositions of dolomite cement from Mine La Motte extend toward $\delta^{13}C$ values of -2.08‰ and $\delta^{18}O$ values of -5.48‰ (Fig. 3.18b), however, which may reflect the presence of a distinct fluid in the fault-related mineralizing system of Mine La Motte that did not equilibrate isotopically with host carbonates.

DISCUSSION

By comparing the CL and stable isotope signatures of gangue dolomite cements from several subdistricts in the southeast Missouri MVT district, whose ores are hosted in the upper and lower Bonneterre Dolomite and the Lamotte Sandstone, the present study aims to address the following questions: Why do dolomite cements from some subdistricts display similar CL patterns, but differ in isotopic composition (e.g. the Old Lead Belt and Mine La Motte)? Why do subdistricts with distinct dolomite CL cement patterns have similar $\delta^{13}C$ and $\delta^{18}O$ values? What influence does stratigraphic position appear to have on the CL behavior and stable isotope composition of ore-associated dolomite cement? Did the ores in these subdistricts form as a product of a chemically and isotopically evolving fluid in a regional flow system or did they instead result from multiple, structurally controlled fluids, or some combination of both?

Lower Bonneterre Dolomite and Lamotte Sandstone

Distinctive CL stratigraphy in dolomite cement from the Mine La Motte subdistrict is likely a product of local fault and fracture networks, with which Cu-Ni-Co-

rich mineralization is related spatially. The CL stratigraphy is also present in the Old Lead Belt that lies ~ 65 km northwest of Mine La Motte (Fig. 3.2), which suggests that fault-related fluid flow also played a crucial role in mineralization in the Old Lead Belt. This is supported by the research of Brown (1967), which documented multiple periods of fluid flow along faults and stressed the influence of faults on lead isotope patterns in the Old Lead Belt. The oscillatory nature of the distinctive dolomite CL cement stratigraphy in these subdistricts may reflect multiple pulses of dolomite-depositing fluids and/or fluctuations in iron and manganese concentrations as a result of the mineral precipitation (e.g. Fe-sulfides) elsewhere in the mineralizing system (Fig. 3.13). The presence of what appears to be CL zone 3 of the regional four-zone CL stratigraphy in chalcopyrite-rich samples from Mine La Motte (Fig. 3.13d) suggests that the regional fluid system hypothesized for ore mineralization in the Viburnum Trend may have been able to reach areas in the lower Bonneterre Dolomite as far east as the Mine La Motte subdistrict.

Dolomite cement from the Old Lead Belt has similar ranges in $\delta^{13}C$ and $\delta^{18}O$ values to those of LOZ Moderate cement and early zone 3 and zone 4 of the regional four-zone cement (Figs. 3.16 and 3.18a). Mine La Motte cement, however, ranges from isotopic values that overlap with LOZ Moderate and early zone 3 toward unusually low $\delta^{13}C$ and high $\delta^{18}O$ values that define a distinct isotopic signature outside the published range of values of LOZ and regional four-zone cements (Figs. 3.16 and 3.18b). The low $\delta^{13}C$ values could be the effect of fluid interactions with different host rock lithologies (e.g. the Bonneterre Dolomite and the Lamotte Sandstone) or incorporation of an oxidized, organic carbon component into the dolomite-depositing fluids. The $\delta^{18}O$

values, however, suggest that Mine La Motte dolomite cement likely precipitated from a distinct fluid, perhaps from a more local, structurally-controlled reservoir.

The vertical and lateral mineral/metal zoning of Cu-(Ni-Co)-Zn mineralization in LOZ ores and dolomite cement CL patterns that are distinct from the regional four-zone cement have been shown to represent a complex system of multiple fluids introduced to the site of ore deposition along faults and fractures (Cavender, 2015). Mineralogically similar ores in the Mine La Motte subdistrict, which are also hosted in the lower Bonneterre Dolomite and underlying Lamotte Sandstone, have been interpreted to reflect fluids entering southeast Missouri through north-northwest trending faults associated with the Reelfoot rift (Horrall et al., 1993) (Figs. 3.1 and 3.2). Inferred mafic and ultramafic intrusions near the rift complex were proposed by Horrall et al. (1993) as a potential metal source for early Cu-Co-Ni-rich ores commonly hosted in the lower Bonneterre Dolomite and Lamotte Sandstone in southeast Missouri.

If early, Cu-Co-Ni-rich LOZ and Mine La Motte ores were the result of fault-related fluid flow, it is possible that ore fluids in other subdistricts of southeast Missouri also utilized such faults, such as the Old Lead Belt. The distinctive, oscillatory CL stratigraphy in dolomite cements from both Mine La Motte and the Old Lead Belt suggest that regional north-northwest trending fault/fracture networks may have focused fluid flow within Mine La Motte and the Old Lead Belt.

Backreef facies of the Bonneterre Dolomite

Dolomite cement in the Annapolis subdistrict (Fig. 3.2) hosted in the backreef facies of the Bonneterre Dolomite displays a CL stratigraphy that is distinct from the CL patterns of dolomite cements from any other subdistrict in southeast Missouri (Fig. 3.14).

All four zones that make up this CL stratigraphy do not occur typically within a single dolomite crystal. In some cases, one or more CL zones may not have been precipitated or may have been partially or completely dissolved, which could reflect dolomite-depositing fluid(s) moving through different portions of the stratigraphic section or sporadic acid generation associated with sulfide precipitation. Specific CL zones in the cement stratigraphy could be associated with chemically distinct fluids, in which case the occurrence of the entire CL stratigraphy may represent areas where stratigraphic barriers restricting these fluids were breached or absent.

The $\delta^{13}C$ and $\delta^{18}O$ values of dolomite cement from Annapolis overlap with those from LOZ Moderate, the Old Lead Belt, Mine La Motte, and early zone 3 of the regional four-zone cement (Fig. 3.18), indicating that the unique CL patterns in dolomite cement from the Annapolis subdistrict resulted from isotopically similar fluids. This may suggest a similar fluid source for Annapolis and other subdistricts in southeast Missouri whereas the unique CL patterns in dolomite cements from Annapolis may reflect more local chemical variations in iron and manganese contents.

Middle to upper Bonneterre Dolomite

The regional extent of the distinctive four-zone dolomite CL stratigraphy found in the middle to upper Bonneterre Dolomite points to a large-scale fluid flow system being responsible for the formation of the Viburnum Trend's ores (Rowan, 1986; Frank and Lohmann, 1986; Appold and Garven, 1999, 2000). In contrast to elsewhere in the Viburnum Trend, ore-associated dolomite cement from the West Fork mine (Fig. 3.2) displays CL variations on the regional four-zone CL stratigraphy that appear to be related spatially to the dominance of Zn- and Pb-rich mineralization. Dolomite cements from

Zn-rich and Fe-Zn-rich areas of the mine frequently contain a thicker CL zone 2 than those from Pb-rich areas; dolomite cements from Pb-rich areas of the mine exhibit zone 3 accompanied frequently by the partial or complete removal of CL zone 2 (Fig. 3.15). Bright CL and resorbed textures that occur commonly in samples from the Zn- and Fe-Zn-rich areas may be the product of sulfide-depositing fluids leaching iron from earlier cement zones and host dolomite and incorporating it into massive marcasite, which pre-dates octahedral galena deposition in the West Fork mine (unlike elsewhere in the Viburnum Trend where main stage iron sulfide deposition is typically post-octahedral galena) (Fig. 3.5a).

Sulfur isotope studies have shown that late octahedral galena-depositing fluids within the West Fork mine incorporated sulfur from earlier iron and zinc sulfide minerals, the earliest of which was a ^{32}S-enriched source/fluid present locally in the West Fork area (Burstein et al., 1993; Shelton et al., 1993). The overprinting of early Zn-Fe-rich mineralization by these Pb-rich fluids was likely associated with dolomite dissolution (i.e. the removal of CL zone 3a and/or zone 2) followed by the precipitation of zone 3b dolomite cement.

The $\delta^{13}C$ and $\delta^{18}O$ values of dolomite cement from the West Fork mine (Adelstein et al., 2016) are within the typical ranges for the Viburnum Trend (Fig. 3.18d), which suggests that isotopically similar ore fluids experienced more localized control on their chemistry and the resultant CL signatures. The abnormally Zn-rich, laterally zoned "West Fork-type" mineralization may indicate that the regional flow system hypothesized for Pb-Zn mineralization in the Viburnum Trend was interrupted by a more localized, likely fault-related system that tapped fluids from distinct reservoirs (Shelton et al., 1993;

Adelstein et al., 2016). The CL behavior and stable isotope compositions of ore-associated dolomite cement in the West Fork mine suggest further that the influence of isotopically similar, ore-metal-specific fluids (associated with specific CL zones of dolomite cements) varied spatially and temporally within the Viburnum Trend, and that these fluids may have experienced local control on their chemistry along distinct flow paths (e.g. the Lamotte Sandstone and/or the underlying igneous basement).

CONCLUSIONS

The primary goal of the present study was to better understand the spatial relationship between regional fluid flow and more localized fault-related ore systems in southeast Missouri by comparing the CL and stable isotope signatures of ore-associated dolomite cements from several subdistricts in the southeast Missouri MVT Pb-Zn-Cu district. Understanding the key similarities and differences in ore processes throughout the district will help geologists interpret the significance of locally distinct, fault-related mineralization commonly hosted in the lower Bonneterre Dolomite and Lamotte Sandstone and potentially develop exploration strategies to search for more lower section ores.

Studies on CL stratigraphy and stable isotope geochemistry of ore-associated dolomite cements from the Viburnum Trend, Old Lead Belt, Mine La Motte, and Annapolis subdistricts in the southeastern Missouri MVT Pb-Zn-Cu district have determined the following:

1. Epigenetic dolomite cements from ores in the Old Lead Belt, Mine La Motte, and Annapolis subdistricts to the east of the Viburnum Trend do not display the typical

four-zone regional CL stratigraphy found throughout southeast Missouri and northern Arkansas in dolomite cements hosted in the upper Bonneterre Dolomite. A distinctive, oscillatory CL stratigraphy consisting of sequences of bright banding alternating with dark bands is present in dolomite cements from the lower Bonneterre Dolomite and Lamotte Sandstone in both the Old Lead Belt and Mine La Motte subdistricts. Dolomite cement from the Annapolis subdistrict, hosted in the backreef facies of the lower Bonneterre Dolomite, is characterized by the presence of two very bright bands overgrowing a finely banded zone of cement ranging from bright to dull luminescence.

2. The variations in CL behavior of dolomite cements throughout southeast Missouri indicate the introduction of multiple mineralizing fluids whose compositions and flow pathways were influenced by local- and regional-scale fault and fracture systems. The Old Lead Belt and Mine La Motte show that these fault/fracture systems may have facilitated fluid flow within the two subdistricts, resulting in the similar CL stratigraphy in their associated dolomite cements. Such faults and fractures could also allow for deeper, chemically distinct fluids to access and equilibrate with host dolomite formed in overlying fluid system(s), as is the case in the vertically zoned LOZ ores in the Brushy Creek mine of the Viburnum Trend.
3. Subdistricts with distinct dolomite cement CL patterns that share similar $\delta^{18}O$ values could be the result of isotopically similar fluids migrating through separate, stratigraphically defined pathways. Isotopically similar fluids moving through different portions of the stratigraphic section may have reacted with host carbonate with different concentrations in Fe^{2+} and Mn^{2+}, resulting in the precipitation of

dolomite cements with distinct CL signatures. However, these chemical differences in host rocks would not greatly affect the $\delta^{18}O$ values of each fluid, as the isotopic composition of the host limestone/dolomitized limestone is fairly constant throughout the Bonneterre Dolomite.

4. The four-zone CL stratigraphy found in dolomite cements from the Viburnum Trend and throughout southeast Missouri dolomite that are hosted in the upper Bonneterre Dolomite resulted from a basinal fluid flow system that overprinted mostly earlier, fault-related flow systems' isotopic and CL signatures. However, this interpretation does not preclude that the two types of flow systems were, in part, contemporaneous, but existed in separate portions of the stratigraphic sections.
5. Unusual CL patterns in dolomite cement from the laterally zoned, abnormally Zn-rich West Fork mine of the Viburnum Trend are associated with multiple, ore-metal-specific fluids. Early CL zones of dolomite cements, associated with Zn- and Zn-Fe-rich mineralization, are partially removed and overprinted by a later CL zone that is associated with main stage Pb-rich mineralization.

REFERENCES

Adelstein, T. A., Shelton, K. L., Perry, L. E., and Gregg, J. M., 2016, Stable isotope and CL studies of the zinc-rich West Fork mine: Multiple-fluid involvement in the southeast Missouri MVT mining district: Geological Society of America Abstracts with Programs [submitted].

Anderson, G. M., 1975, Precipitation of Mississippi Valley-type ores: Economic Geology, v. 70, p. 937-942.

------ 2008, The mixing hypothesis and the origin of Mississippi Valley-type ore deposits: Economic Geology, v. 103, no. 8, p. 1683-1690.

Anderson, G. M., and Macqueen, R. W., 1988, Mississippi Valley-type lead-zinc deposits, *in* Roberts, R. G., and Sheahan, P. A., eds., Ore deposit models: Geoscience Canada, Reprint Series 3, p. 79-90.

Appold, M. S., and Garven, G., 1999, The hydrology of ore formation in the southeast Missouri district: Numerical models of topography-driven fluid flow during the Ouachita Orogeny: Economic Geology, v. 94, p. 913-936.

------ 2000, Reactive flow models of ore formation in the southeast Missouri district: Economic Geology, v. 95, p. 1605-1626.

Bethke, C. M., and Marshak, S., 1990, Brine migrations across North America – The plate tectonics of groundwater: Annual Reviews of Earth and Planetary Science, v. 18, p. 287-315.

Braunsdorf, N. R., 1983, Isotopic trends in gangue carbonates from the Viburnum Trend: Implications for Mississippi Valley-type mineralization [M.S. thesis]: Ann Arbor, University of Michigan.

Brown, J. S., 1967, Isotopic zoning of lead and sulfur in southeast Missouri, *in* Brown, J. S., ed., Genesis of stratiform lead-zinc-barite-fluorite deposits (Mississippi Valley-type deposits)—A symposium: Economic Geology Monograph, v. 3, p. 410-426.

Buelter, D. P., and Guillemette, R. N., 1988, Geochemistry of epigenetic dolomite associated with lead-zinc mineralization of the Viburnum Trend, southeast Missouri, *in* Shukla, V., Baker, P. A., eds., Sedimentology and Geochemistry of

Dolostones: Society of Economic Paleontologists Special Publication, no. 43, p. 85-93.

Burstein, I. B., 1993, Sulfur isotope studies of the Viburnum Trend Pb-Zn-Cu district, southeast Missouri: Implications for ore genesis [M.S. thesis]: Columbia, University of Missouri, 164 p.

Burstein, I. B., Shelton, K. L., Gregg, J. M., and Hagni, R. D., 1993, Complex, multiple ore fluids in the world class southeast Missouri Pb-Zn-Cu MVT deposits: Sulfur isotope evidence, *in* Shelton, K. L., and Hagni, R. D, eds., Geology and geochemistry of Mississippi Valley-type ore deposits: Rolla, MO, University of Missouri-Rolla Press, p. 1-16.

Cavender, B. D., 2015, Atypical MVT, Zn-Cu-rich mineralization in the lower portion of the Bonneterre Dolomite, Viburnum Trend, Southeast Missouri, U.S.A. [M.S. thesis]: Columbia, University of Missouri, 167 p.

Cavender, B. D., Shelton, K. L., and Husman, J., 2013, Unusual MVT, Zn-Pb-Cu mineralization in the lower portion of the Bonneterre Dolomite, Viburnum Trend, southeast Missouri: Geological Society of America Abstracts with Programs, v. 45, no. 7, p. 424.

Cavender, B. D., Shelton, K. L., and Schiffbauer, J. D., 2016, An atypical orebody in the Brushy Creek mine, Viburnum Trend, Missouri: Early Cu-(Ni-Co)-Zn-rich ores at the Lamotte Sandstone/Bonneterre Dolomite contact: Economic Geology, v. 111, no. 1, p. 259-269.

Childers, G. A., Paarlberg, N. L, and Evans, L. L., 1995, Geology of the Fletcher Mine, Viburnum Trend, Southeast Missouri: Society of Economic Geologists Guidebook Series, v. 22, p. 99-111.

Clendenin, C. W., Niewendorp, C. A., Duane, M. J., and Lowell, G. R., 1994, The paleohydrology of Southeast Missouri Mississippi Valley-type deposits: Interplay of faults, fluids, and adjoining lithologies: Economic Geology, v. 89, p. 322-33.

Craig, H., 1961, Standard for reporting concentrations of deuterium and oxygen-18 in natural waters: Science, v. 133, no. 3467, p. 1833-1834.

Davis, J. H., 1960, Mineralization in the southeast Missouri lead district: Unpublished Ph.D. dissertation, University of Wisconsin, 140 p.

Dunn, R. G., Jr., and Grundmann, W. H., Jr., 1989, Geology of the Casteel mine: Copper-rich ore in a MVT setting, *in* Hagni, R. D., and Coveney, R. M., Jr., eds., Mississippi Valley-type Mineralization of the Viburnum Trend, Missouri: Economic Geology Guidebook Series, v. 5, p. 58-83.

Fairchild, I. J., 1983, Chemical controls of cathodoluminescence of natural dolomite and calcites: Sedimentology, v. 30, p. 579-583.

Farr, M. R., 1989, Compositional zoning characteristics of late dolomite cements in the Cambrian Bonneterre Formation, Missouri: Implications for parent fluid migration pathways: Carbonates and Evaporites, v. 4.2, p. 177-194.

Fennel, M. J., Hagni, R. D., and Bradley, M. F., 1996, Mineralogy, paragenetic sequence, mineral zoning, and genesis at the Magmont-West mine, southeast Missouri lead district, *in* Sangster, D. F., ed., Carbonate hosted lead-zinc deposits: Society of Economic Geologists Special Publication, v. 4, p. 597-610.

Frank, M. H., and Lohmann, K. C., 1986, Textural and chemical alteration of dolomite: Interaction of mineralizing fluids and host rock I a Mississippi Valley-type deposit, Bonneterre Formation, Viburnum Trend, *in* Hagni, R. D., ed., Process Mineralogy VI: Warrendale, PA, The Metallurgical Society, p. 103-116.

Friedman, I., and O'Neil, J. R., 1977, Compilation of stable isotope fractionation factors of geochemical interest: U.S. Geological Survey Professional Paper 440-KK, 116 p.

Gerdemann, P. E., and Myers, H. E., 1972, Relationships of carbonate facies patterns to ore distribution and to ore genesis in the southeast Missouri lead district: Economic Geology, v. 67, p. 426-433.

Goldhaber, M. B., Church, S. E., Doe, B. R., Aleinikoff, J. N., Brannon, J. C., Podosek, F. A., Mosier, E. L., Taylor, C. D., and Gent, C. A., 1995, Lead and sulfur isotope investigation of Paleozoic sedimentary rocks from the southern midcontinent of the United States: Implications for paleohydrology and ore genesis of the southeast Missouri lead belts: Economic Geology, v. 90, p. 1875-1910.

Gregg, J. M., 1985, Regional epigenetic dolomitization in the Bonneterre Dolomite (Cambrian), southeast Missouri: Geology, v. 13, p. 503-506.

Gregg, J. M., and Hagni, R. D., 1987, Irregular cathodoluminescent banding in late dolomite cements: Evidence for complex faceting and metalliferous brines: Geological Society of America Bulletin, v. 98, p. 86-91.

Gregg, J. M., and Shelton K. L., 1989a, Geochemical and petrographic evidence for fluid sources and pathways during dolomitization and lead-zinc mineralization in southeast Missouri: a review: Carbonates and Evaporites, v. 4.2, p. 153-175.

------ 1989b, Minor- and trace-element distributions in the Bonneterre Dolomite Cambrian), southeast Missouri: Evidence for possible multiple-basin fluid sources and pathways during lead-zinc mineralization: Geological Society of America Bulletin, v. 101, p. 221-230.

------ 1990, Dolomitization and dolomite neomorphism in the back reef facies of the Bonneterre and Davis Formations (Cambrian), southeastern Missouri: Journal of Sedimentary Petrology, v. 60, no. 4, p. 549-562.

------2012, Mississippi Valley-type mineralization and ore deposits in the Cambrian-Ordovician great American carbonate bank, *in* Derby, J.R., Fritz, R.D., Longacre, S.A., Morgan, W.A., and Sternbach, C.A., eds., The great American carbonate bank: The geology and economic resources of the Cambrian-Ordovician Sauk megasequence of Laurentia: American Association of Petroleum Geologists Memoir 98, p. 1013-1030.

Grundmann, W. H., Jr., 1977, Geology of the Viburnum Number 27 mine, Viburnum Trend, Southeast Missouri: Economic Geology, v. 72, p. 249-263.

Hagni, R. D., 1986, Paragenetic sequence of the lead-zinc-copper-cobalt-nickel ores of the southeast Missouri lead district, U.S.A., *in* Craig, J. R., Hagni, R. D., Kiedl, W., Lange, I. M., Petrovskaya, N. V., Shadlun, T. N., Udubasa, G., Augustithis, S. S., eds., Mineral paragenesis: Athens, Greece, Theophrastus, p. 90-132.

------ 1995, The southeast Missouri lead district: Society of Economic Geologists Guidebook Series, v. 22, p. 44-78.

Hagni, R. D., and Transcynger, T. C., 1977, Sequence of deposition of the ore minerals at the Magmont Mine, Viburnum Trend, southeast Missouri: Economic Geology, v. 72, p. 451-464.

He, Z., Gregg, J. M., Shelton, K. L., and Palmer, J. R., 1997, Sedimentary facies control of fluid flow and mineralization in Cambro-Ordovician strata, southern Missouri, *in* Montañez, I. P., Gregg, J. M., and Shelton, K. L., eds., Basin-wide diagenetic patterns: Integrated petrologic, geochemical, and hydrologic considerations: Society of Economic Paleontologists and Mineralogists Special Publication, v. 57, p. 81-99.

Heyl, A.V., 1983, Geologic characteristics of three major Mississippi Valley districts, *in* Kisvarsanyi, G., Grant, S. K., Pratt, W. P., and Koenig, J. W., eds., International conference on Mississippi Valley type lead-zinc deposits: Rolla, MO, University of Missouri-Rolla, p. 27-60.

Horrall, K. B., Hagni, R. D., and Kisvarsanyi, G. A., 1981, The paragenesis of lead-zinc-copper ores from selected mines in the Southeast Missouri lead district and its possible relationship to ultramafic and mafic sources in the New Madrid rift: Geological Society of American Abstracts with Programs, v. 14, p. 476.

------ 1983, Mineralogical, textural and paragenetic studies of selected ore deposits of the southeast Missouri lead-zinc-copper district and their genetic implications, *in* Kisvarsanyi, G. A., Grant, S. K., Pratt, W. P., and Koenig, J. W., eds., International conference on Mississippi Valley type lead-zinc deposits: Rolla, MO, University of Missouri-Rolla, p. 289-316.

------ 1993, Mafic and ultramafic plutons associated with the New Madrid rift complex—a possible major source of the copper-cobalt-nickel mineralization of southeast Missouri: Economic Geology, v. 88, p. 328-343.

Imes, J. L., 1990, Major geohydrologic units in and adjacent to the Ozark Plateaus province, Missouri, Arkansas, Kansas, and Oklahoma—St. Francois confining unit: U.S. Geological Survey Hydrologic Investigation Atlas HA-711-D, scale 1:750,000.

Keller, T. J., Gregg, J. M., and Shelton, K. L., 2000, Fluid migration and associated diagenesis in the Greater Reelfoot Rift region, Midcontinent, United States: Geological Society of America Bulletin, v. 112, no. 11, p. 1680-93.

Kisvarsanyi, G. A., 1977, The role of the Precambrian igneous basement in the formation of the stratabound lead-zinc-copper deposits in Southeast Missouri: Economic Geology, v. 72, p. 435-442.

Kyle, J. R., and Gutierrez, G. N., 1988, Origin of the Indian Creek sandstone-hosted lead deposits, southeast Missouri, *in* Zachrisson, E., ed., Proceedings of the Seventh IAGOD Symposium, Lulea, Sweden 1986: E. Schweizerbart'sche Verlagsbuchhandlung, p. 669-684.

Leach, D. L., 1994, Genesis of the Ozark MVT metallogenic province, Missouri, Arkansas, and Oklahoma, USA, *in* Fonbonte, L. and Boni, M., eds., Sediment-hosted Zn-Pb ores: New York, Springer Berlin Heidelberg, p. 104–138.

Leach, D. L., and Rowan, E., 1986, Genetic link between Ouachita fold belt tectonism and the Mississippi Valley-type Pb-Zn deposits of the Ozarks: Geology, v. 14, p. 931-935.

Leach, D. L., and Sangster, D. F., 1994, Mississippi Valley-type (MVT) lead-zinc deposits: Geological Association of Canada Special Publication.

Lowell, G. R., 1991, The Butler Hill Caldera: A middle Proterozoic ignimbrite-granite complex: Precambrian Research, v. 51, p. 245-263.

Machel, H. G., 1985, Cathodoluminescence in calcite and dolomite and its chemical interpretation: Geoscience Canada, v. 12, p. 139-147.

Marshall, D. J., 1988, Cathodoluminescence of Geological Materials: London, U.K, Unwin Hyman Ltd., 146p.

Mavrogenes, J. A., Hagni, R. D., and Dingess, P. R., 1992, Geology, paragenesis and mineral zoning of the West Fork mine, Viburnum Trend, southeast Missouri: Economic Geology, v. 87, p. 113-124.

Ohle, E. L., and Brown, J. S., 1954, Geologic problems in the southeast Missouri lead district: Geological Society of America Bulletin, v. 65, no. 3, p. 201-222.

Paarlberg, N. L., and Evans, L. L., 1977, Geology of the Fletcher Mine, Viburnum Trend, southeast Missouri: Economic Geology, v. 72, p. 391-397.

Palmer, J. R., and Hayes, T. S., 1989, Late Cambrian lithofacies and their control on the Mississippi Valley-type mineralizing system in the Ozark region, *in* Schindler, K. S., ed., USGS Research on mineral resources, 1989 Program and Abstracts: U.S. Geological Survey Circular 1035, p. 51-53.

Palmer, J. R., Thompson, T. L., Seeger, C., Miller, J. F., and Gregg, J. M., 2012, The Sauk megasequence from the Reelfoot Rift to southwest Missouri, *in* Derby, J. R., Fritz, R. D., Longacre, S. A., Morgan, W. A., and Sternbach, C. A., eds., The great American carbonate bank: The geology and economic resources of the Cambrian-Ordovician Sauk megasequence of Laurentia: American Association of Petroleum Geologists Memoir 98, p. 1013-1030.

Perry, L. E., Shelton, K. L., Cavender, B. D., and Gregg, J. M., 2015a, A New Look at the CL Microstratigraphy of Dolomite Cements in the World-Class Southeast Missouri MVT Pb-Zn-Cu District: Interplay of Early Fault-Related Systems and Regional Fluid Flow: 15th Bathurst Meeting of Carbonate Sedimentologists, Edinburgh, Scotland, Abstracts, p. 90.

------ 2015b, Variations in CL microstratigraphy and isotope compositions of dolomite cements in the world-class Southeast Missouri MVT Pb-Zn-Cu district: Early fault-related systems versus regional fluid flow: Geological Society of America Abstracts with Programs, v. 47, p. 678.

Pignolet, S., and Hagni, R. D., 1983, Cobalt-nickel mineralization associated with lead-zinc-copper mineralization in the Mississippi Valley-type deposits at Fredericktown, Missouri, *in* Kisvarsanyi, G., Grant, S. K., Pratt, W. P., and Koenig, J. W., eds., International conference on Mississippi Valley type lead-zinc deposits: Rolla, MO, University of Missouri-Rolla, p. 187-194.

Plumlee, G. S., Leach, D. L., Hofstra, A. H., Landis, G. P., Rowan, E. L., and Viets, J. G., 1994, Chemical reaction path modeling of ore deposition in Mississippi Valley-type Pb-Zn deposits of the Ozark region, U. S. Midcontinent: Economic Geology, v. 89, p. 1361-1383.

Rogers, R. K., and Davis, J. H., 1977, Geology of the Buick Mine, Viburnum Trend, southeast Missouri: Economic Geology, v. 72, p. 372-380.

Rowan, E. L., 1986, Cathodoluminescent zonation in hydrothermal dolomite cements: Relationship to Mississippi Valley-type Pb-Zn mineralization in southeastern Missouri and northern Arkansas, *in* Hagni, R. D., ed., Process mineralogy – applications to precious metal deposits, industrial minerals, coal, liberation, mineral processing, agglomeration, metallurgical products, and refractories, with special emphasis on cathodoluminescent microscopy: Warrendale, PA, The Metallurgical Society, p. 69-87.

Rowan, E. L., and Leach, D. L., 1989, Constraints from fluid inclusions on sulfide precipitation mechanisms and ore fluid migration in the Viburnum Trend lead district, Missouri: Economic Geology, v. 84, p. 1948-1965.

Shelton, K. L., Reader, J. M., Ross, L. M., Viele, G. W., and Wasserman, M. D., 1986, Carbon and oxygen isotope systematics of the Bonneterre Formation, southeast Missouri: A dynamic basin-evolution model, *in* Gregg, J. M., Hagni, R. D., eds., Symposium on the Bonneterre Formation (Cambrian), southeastern Missouri, (Abstracts): Rolla, MO, University of Missouri-Rolla, p. 21.

Shelton, K. L., Burstein, I. B., Hagni, R. D., Mavrogenes, J. A., Dingess, P. R., and Childers, A. G., 1993, Comparison of sulfur isotope geochemistry of the West Fork and Fletcher mines, Viburnum Trend MVT Pb-Zn-Cu district, southeast Missouri, *in* Childers, A. G., ed., The Viburnum Trend, A Second Look: Salem, MO, Association of Missouri Geologists 40th Annual Meeting and Field Trip, Proceedings volume, p. 26-38.

Shelton, K. L., Burstein, I. B., Hagni, R. D., Vierrether, C. B., Grant, S. K., Hennigh, Q. T., Bradley, M. F., and Brandon, R. T., 1995, Sulfur isotope evidence for penetration of MVT fluids into igneous basement rocks, southeast Missouri, USA: Mineralium Deposita, v. 30, p. 339-350.

Shelton, K. L., Gregg, J. M., and Johnson, A. W., 2009, Replacement dolomites and ore sulfides as recorders of multiple fluids and fluid sources in the southeast Missouri MVT District, USA: Halogen-$^{87}Sr/^{86}Sr$-$\delta^{18}O$-$\delta^{34}S$ systematics in the Bonneterre Dolomite: Economic Geology, v.104, p. 733-748.

Shelton, K. L., Beasley, J. M., Gregg, J. M., Appold, M. S., Crowley, S. F., Hendry, J. P., and Somerville, I. D., 2011, Evolution of a Carboniferous carbonate-hosted sphalerite breccia deposit, Isle of Man: Mineralium Deposita, v. 46, no. 8, p. 859-880.

Sides, J. R., Brickford, M. E., Shuster, R. D., and Nusbaum, R. L., 1981, Calderas in the Precambrian terrane of the St. Francois mountains, southeastern Missouri: Journal of Geophysical Research, v. 86, p. 10349-10364.

Snyder, F. G., and Emery, J. A., 1956, Geology in development and mining, Southeast Missouri Lead Belt: Transactions of the American Institute of Mining, Metallurgical and Petroleum Engineers, v. 208, p. 1216-1224.

Snyder, F. G., and Gerdemann, P. E., 1968, Geology of the southeast Missouri lead district, *in* Ridge, J.D., ed., Ore deposits of the United States, 1933-1967, Graton-Sales Volume, Volume 1: New York, American Institute of Mining, Metallurgical and Petroleum Engineers, p. 326-358.

Sverjensky, D. S., 1984, Oil field brines as ore-forming solutions: Economic Geology, v. 79, p. 23-37.

Sweeney, P. H., Harrison, E. D., and Bradley, M., 1977, Geology of the Magmont mine, Viburnum Trend, southeast Missouri: Economic Geology, v. 72, p. 365-371.

Symons, D. T. A., Lewchuk, M., and Leach, D. L., 1998, Age and duration of the Mississippi Valley-type mineralizing fluid flow events in the Viburnum Trend, southeast Missouri, U.S.A., from paleomagnetism: Geological Society (London) Special Publication 144, p. 27–39.

Tarr, W. A., 1936, Origin of the southeastern Missouri lead deposits. Part I: Economic Geology, v. 31, p. 712-754.

Taylor, H. P, 1979, Oxygen and hydrogen isotope relationships in hydrothermal ore deposits, in Barnes, H. L., ed., Geochemistry of hydrothermal ore deposits: New York, John Wiley, p. 236-277.

Voss, R. L., and Hagni, R. D., 1985, The application of cathodoluminescence microscopy to the study of sparry dolomite from the Viburnum Trend, Southeast Missouri, *in* Hausen, D. M., and Kopp, O. C., eds., Mineralogy—Applications to Mineral Industry: New York, American Institude of Mining, Metallurgy, and Petroleum Engineering, Inc., p. 51-68.

Voss, R. L., Hagni, R. D., and Gregg, J.M., 1989, Sequential deposition of zoned dolomite and its relationship to sulfide mineral paragenetic sequence in the Viburnum Trend, southeast Missouri: Carbonates and Evaporites, v. 4, p. 195-210.

Wu, Y., and F. W. Beals, 1981, A reconnaissance study by paleomagnetic methods of the age of mineralization along the Viburnum Trend, southeast Missouri: Economic Geology, v. 76, p. 1879–1894.

CHAPTER IV: REACTION PATH MODELING OF Cu-(Ni-Co)-Zn-RICH MINERALIZATION IN THE LOWER BONNETERRE DOLOMITE IN THE VIBURNUM TREND, SOUTHEAST MISSOURI, U.S.A.

ABSTRACT

MVT deposits of the Viburnum Trend are typically lead-dominant (Pb/Zn > 5) and occur mainly in the reef-grainstone facies of the upper Bonneterre Dolomite (Cambrian). Unusually Cu-(Ni-Co)-Zn-rich ores have recently been discovered in economic concentrations within the lower Bonneterre Dolomite and underlying Lamotte Sandstone of the Brushy Creek mine, more than 30 m below the main ore-bearing horizon of the Viburnum Trend.

Pronounced vertical zoning of Ni-Co-, Cu-, Zn-, and Pb-rich mineralization with increasing distance about the Lamotte Sandstone has been interpreted to reflect multiple entry sites for ore fluid introduction (Cavender et al., 2016). A trend of increasing $\delta^{34}S$ values of ore sulfides (from -5 toward +17‰ VCDT; Cavender, 2015) with vertical distance above the Lamotte/Bonneterre contact suggests that as ore fluids migrated upward, likely through faults and fractures, sulfide from a ^{32}S-enriched source was displaced progressively by pulses of ^{34}S-enriched sulfur from an overlying system (Shelton et al., 2016).

Reaction path modeling was undertaken to determine if the multiple generations and sporadic $\delta^{34}S$ values of ore sulfide minerals in the lower section orebody resulted from the chemical evolution of a single metal-bearing fluid or if they instead are the product of mixing of multiple, metal-rich fluids, or some combination of both. Reaction

path calculations for single fluid models are generally inconsistent with the sequence and abundance of ore minerals in the deposit and could have contributed only to minor ore formation on a local scale. Modeling shows that mixing between a sulfide-rich fluid and a metal-rich fluid is the most suitable depositional mechanism for these ores, and that multiple pulses of ore-metal-specific fluids are required to reproduce the sequence and relative concentrations of base metal sulfides in the orebody.

INTRODUCTION

Mississippi Valley-type (MVT) deposits of the Viburnum Trend in southeast Missouri (Fig. 4.1) are typically lead dominant (Pb/Zn > 5) and occur mainly in the reef-grainstone facies of the middle to upper Bonneterre Dolomite (Cambrian) (Figs. 4.2 and 4.3). Atypically Cu-(Ni-Co)-Zn-rich ores have been discovered recently in the lower Bonneterre Dolomite and the underlying Lamotte Sandstone in the Brushy Creek mine (Fig. 4.2), more than 30 m below the main ore-bearing horizon of the district. Early stage mineralization in the lower Bonneterre Dolomite is characterized by a complex paragenetic sequence that consists of multiple generations of Fe-, Zn-, Cu-, and Ni-Co-sulfides and exhibits distinct vertical metal/mineral zoning from Cu-(Ni-Co)- to Zn- to Pb-rich mineralization with increasing distance above the Lamotte Sandstone-Bonneterre Dolomite contact (Cavender, 2015; Cavender et al., 2016). Sulfur isotope compositions of sulfide minerals in the lower section ores vary paragenetically and may reflect fluids from multiple sources that entered the system in pulses (Shelton et al., 2016). The lower section ores have been interpreted to reflect distinct, fault-related mineralization that

predates the main stage Pb-Zn ores hosted in the upper Bonneterre Dolomite elsewhere in the Viburnum Trend (Cavender et al., 2016).

The multiple generations of sulfide deposition and the sporadic nature of early ore sulfide introduction in the lower section orebody points to a system that required mixing of multiple distinct, likely fault-related fluids whose influence varied both temporally and spatially during ore deposition (Cavender, 2015). Based on geochemical data from these lower ores (Cavender, 2015) and on previous investigations of ore deposition in the Viburnum Trend (e.g. Plumlee et al., 1994; Appold and Garven, 2000; Wenz et al., 2012), the current study will use reaction path calculations to model potential ore fluid compositions and depositional processes in order to address the following questions:

1. Are the atypical Cu-(Ni-Co)-Zn-rich ores in the lower Bonneterre Dolomite in the Viburnum Trend products of a single, regional ore fluid that evolved chemically along different flow paths or do they reflect the presence of multiple fluids that involved more localized, structurally controlled flow systems (Horrall et al., 1993; Clendenin et al., 1994; Shelton et al., 1995, 2009), or both?
2. What depositional processes and chemical conditions are required in order to produce the observed paragenetic sequence and relative proportions of ore minerals in the lower Bonneterre Dolomite?

The Southeast Missouri Pb-Zn-Cu MVT District

Southeast Missouri hosts world-class, Pb-Zn-Cu Mississippi Valley-type (MVT) deposits of the Viburnum Trend and represents the world's known concentration of lead (Ohle and Gerdemann, 1989; Hagni, 1989, 1995). The district is also an important

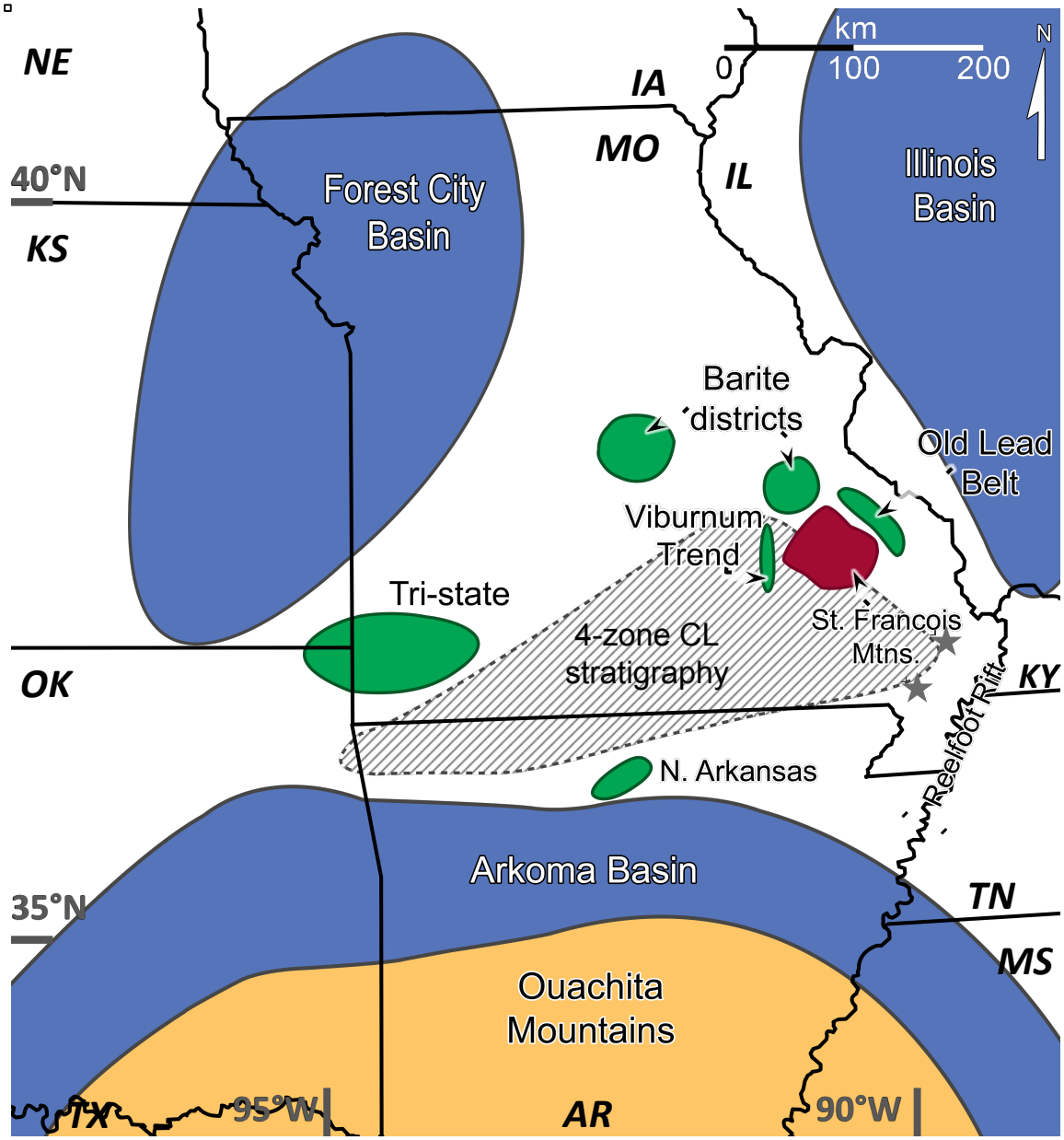

Figure 4.1. Regional geologic setting of the Ozark MVT ore districts (green) relative to major sedimentary basins (blue), the Reelfoot Rift and the igneous St. Francois Mountains (red) (after Gregg and Shelton, 1989; Shelton et al., 2009). The shaded portion of southern Missouri and northern Arkansas represents sample localities documented to contain gangue dolomite cements that exhibit the characteristic four-zone CL stratigraphy (discussed in text) that is found in the upper Bonneterre Dolomite in the Viburnum Trend (Voss and Hagni, 1985; Rowan, 1986; Frank and Lohmann, 1986).

producer of zinc, copper, and silver. Sulfide ore mineralization in the Viburnum Trend is generally lead-dominant (Pb:Zn > 5) and occurs almost exclusively in the middle to upper portion of the Bonneterre Dolomite as bedded or replacement deposits, associated typically with the reef-grainstone facies of the formation. Mineralogically, the ores are dominated by galena and lesser sphalerite, chalcopyrite, pyrite, and marcasite, and they contain minor but economically recoverable Cu- and Co-Ni-bearing sulfides. A more detailed review of the paragenesis, textures, and host rocks for these ores is given in the introduction of the previous chapter.

Lower Ore Zone (LOZ) Mineralization

High-grade, unusually Zn-Cu-rich mineralization has been identified recently and exploited more than 30 m below the typical ore horizon in the Brushy Creek mine in the Viburnum Trend (Fig. 4.2), hosted in the lower Bonneterre Dolomite and underlying Lamotte Sandstone (Fig. 4.3). These lower ore zone (LOZ) ores are distinct from more "typical" Viburnum Trend ores hosted stratigraphically higher in the Bonneterre Dolomite and are characterized by a unique ore mineral paragenesis (Fig. 4.4), pronounced vertical zoning of Fe, Cu-Ni-Co, Zn, and Pb mineralization, and distinct CL and stable isotope signatures of gangue dolomite cement (Cavender, 2015; Cavender et al., 2016) (refer to Figs. 3.7, 3.12, and 3.16b from the previous chapter). LOZ mineralization has been interpreted to reflect the involvement of multiple, ore-metal-specific fluids that likely utilized faults and fractures as conduits (Cavender et al., 2016). Textural, paragenetic, and geochemical characteristics of LOZ ores and their associated dolomite cement are discussed in more detail in the previous chapter.

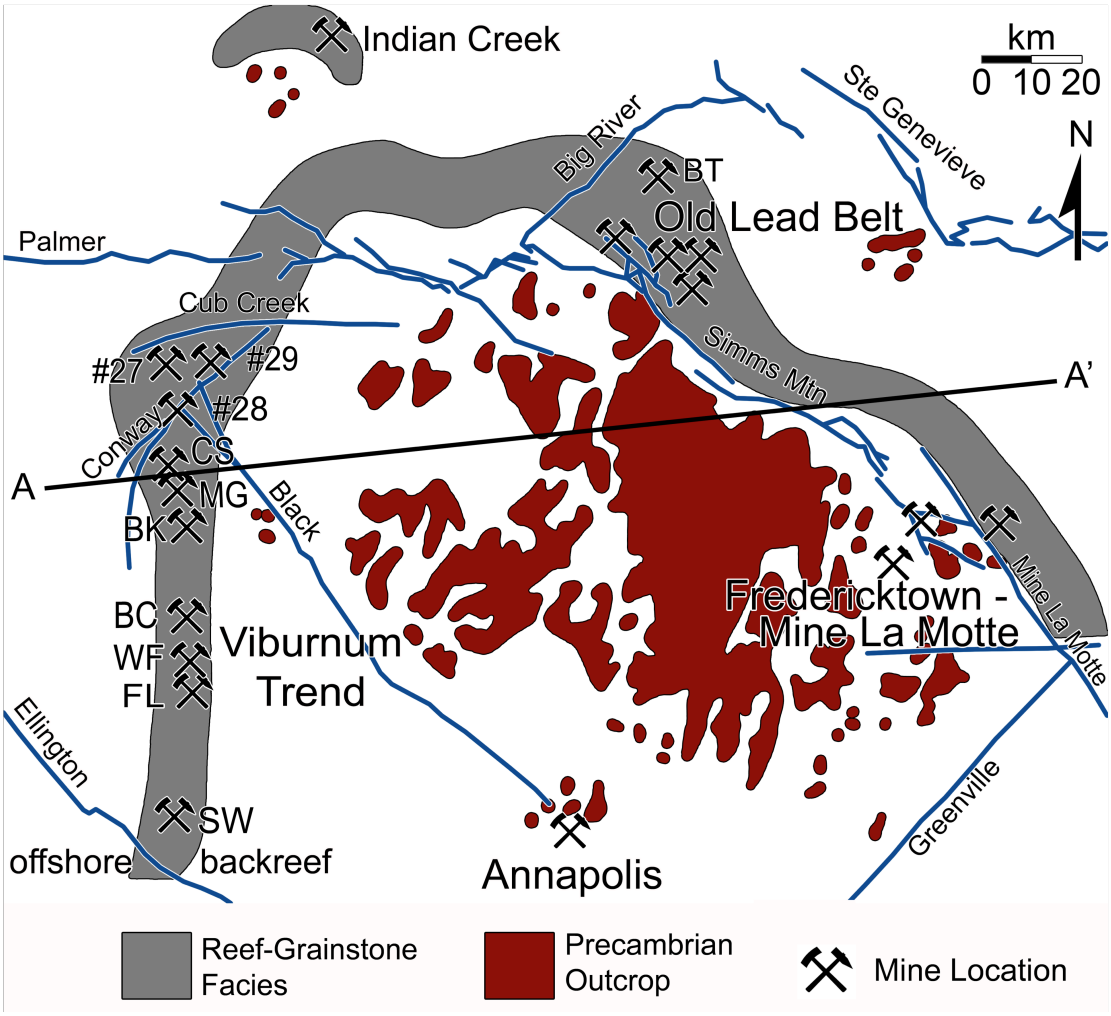

Figure 4.2. Map showing locations of major ore districts, mines and faults (blue) relative to Precambrian igneous outcrop and the trend of the reef-grainstone facies of the Bonneterre Dolomite (after Snyder and Gerdemann, 1968). Mine abbreviations: CS = Casteel, MG = Magmont, BK = Buick, BC = Brushy Creek, WF = West Fork, FL = Fletcher, SW = Sweetwater, BT = Bonne Terre.

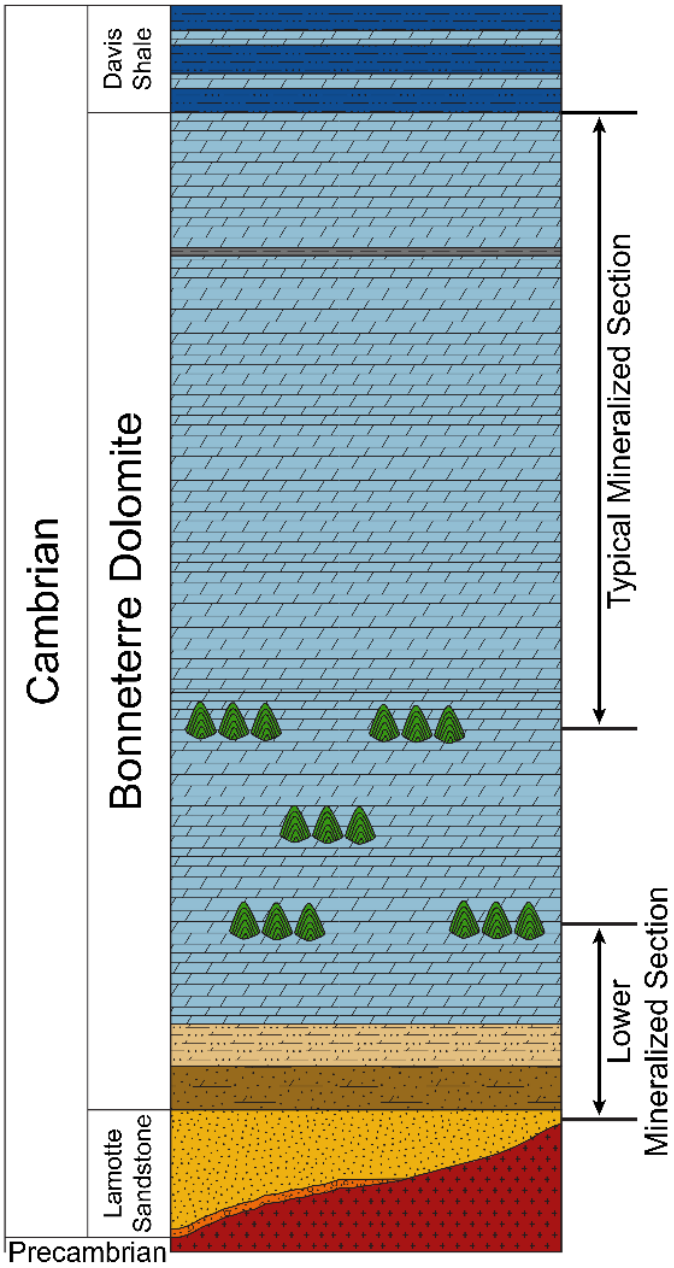

Figure 4.3. Idealized geologic column for the Viburnum Trend (after Cavender et al., 2016). The reef-grainstone facies of the upper Bonneterre Dolomite hosts typical Pb-Zn MVT deposits of the Viburnum Trend. Cu-Zn-rich deposits of the present study are hosted principally in shaly dolomite of the lower Bonneterre Dolomite and in quartz arenite of the upper Lamotte Sandstone. Legend: blue = dolomite, brown/tan = sandy/shaly dolomite, dark blue = shale, gray = siltstone, green = stromatolite-bearing, orange = conglomerate, red = Precambrian granitic rocks, yellow = sandstone.

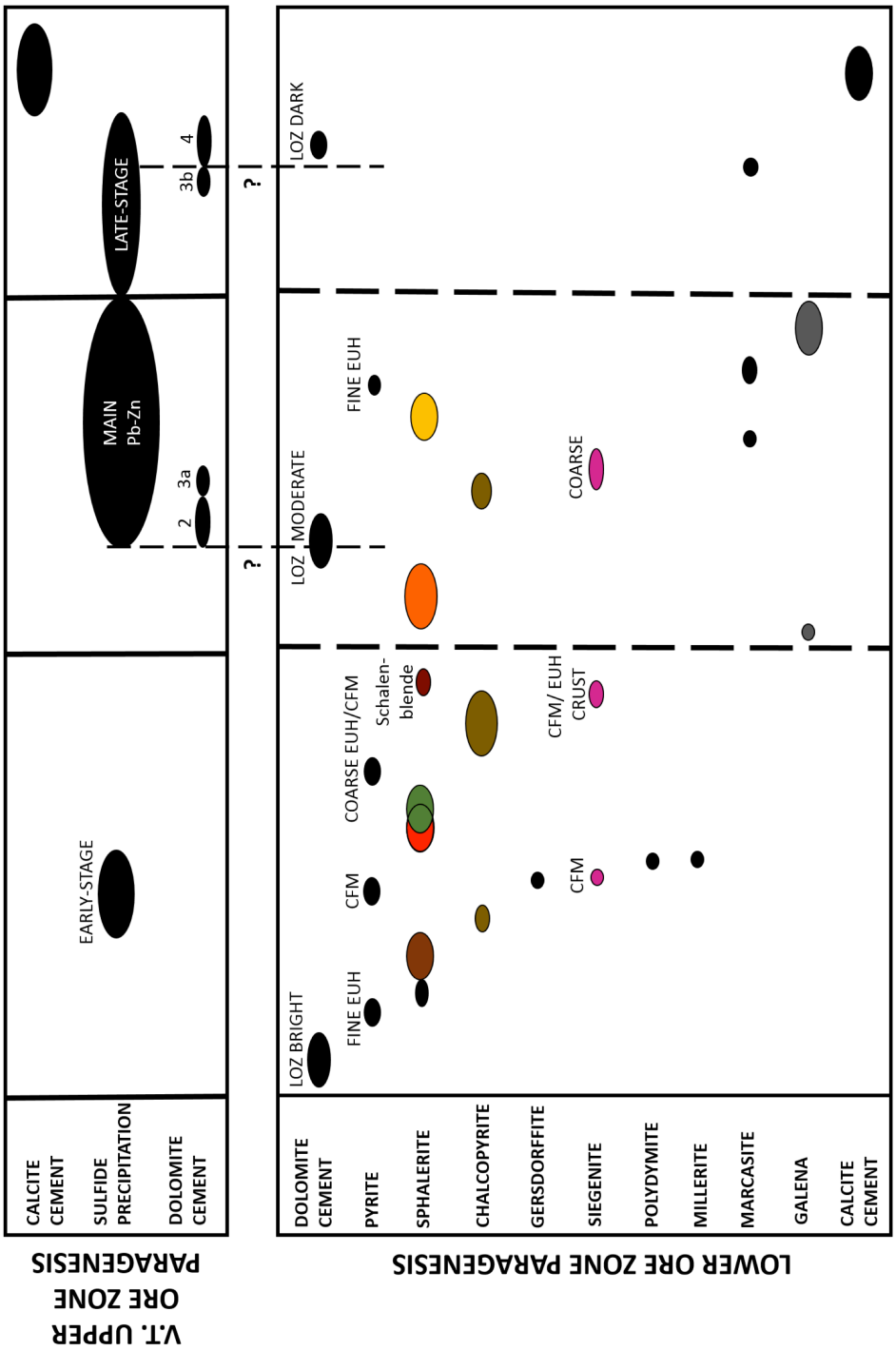

Figure 4.4. Generalized paragenesis of ore minerals from the lower ore zone (LOZ) mineralization at the Brushy Creek mine in the Viburnum Trend (after Cavender, 2015). Also included is a simplified paragenesis of sulfide and carbonate cement precipitation associated with more typical mineralization of the Viburnum Trend hosted stratigraphically higher within the Bonneterre Dolomite (modified from Shelton et al., 2009). Numbers refer to CL zones of the regional four-zone dolomite cement. Abbreviations: CFM = colloform; EUH = euhedral; VT = Viburnum Trend.

Fluid inclusion studies

Cavender (2015) compared homogenization temperatures (T_h), salinities, and fluid chemistries of two-phase (liquid and vapor) fluid inclusions from LOZ ores in the Brushy Creek mine to those of fluid inclusions from more typical orebodies elsewhere in the Viburnum Trend. Several inclusions hosted in LOZ sphalerites and dolomite cements (particularly the LOZ Bright cement) indicated the presence of a hotter fluid (e.g. schalenblende avg. T_h = 191ºC, LOZ Bright avg. T_h = 177ºC) that has not been detected in the Viburnum Trend's upper ore horizon. Salinities of sphalerite-hosted fluid inclusions vary in salinity from 8.4 to 26.3 wt% equiv. NaCl (avg. = 20.1 wt% equiv. NaCl), which overlap the average salinities but extend to significantly lower salinities than fluid inclusions from upper orebodies of the Viburnum Trend (22 to 26 wt% equiv. NaCl) (Roedder, 1977; Hagni, 1983; Rowan and Leach, 1989; Shelton et al., 1992; Appold et al., 2004; Wenz et al., 2012; Cavender, 2015).

LOZ fluid inclusions have elevated Mg/Na, Sr/Na, and Ba/Na ratios and particularly higher K/Na ratios than those of fluid inclusions from more typical Viburnum Trend ores (Wenz et al., 2012; Cavender, 2015). The LOZ ore fluids may have acquired such high K/Na ratios locally by reaction with potassic feldspar and mica within the Lamotte Sandstone and/or the granitic basement rocks, or they may reflect basinal potassium sources in distal sedimentary basins, such as the Arkoma basin (Rothbar, 1983; Hanor, 1994; Diehl and Goldhaber, 1995; Appold and Garven, 1999). Large variations in major element ratios support the existence of geochemically distinct fluids in the LOZ mineralizing system that may have migrated along different pathways than those utilized by the regional, Pb-rich MVT fluids (Shelton et al., 2016).

Sulfur isotope studies

Sulfur isotope compositions of sulfides can provide information about sulfur sources, temperatures of coprecipitated minerals, and variations in fluid redox chemistry. Isotope thermometry of coprecipitated minerals is not applicable to the LOZ orebody because sulfides were deposited sequentially. Mineralogical and fluid inclusion studies have determined previously that the ore fluids are likely reducing and acidic (Wenz et al., 2012), so redox variations are thought to be insignificant. Thus, sulfur isotope studies (Cavender, 2015) are most useful to determine potential sulfur sources that may have contributed to the formation of the LOZ ores and to compare their sulfur isotope sources with those responsible for the more typical Viburnum Trend sulfide ores hosted in the upper Bonneterre Dolomite (Burstein, 1993). In general, higher $\delta^{34}S$ values suggest derivation of sulfide from sulfate sources (sedimentary brines or evaporites, Claypool et al., 1980), whereas lower $\delta^{34}S$ values may reflect sulfide derived from underlying granitic basement or diagenetic pyrite and/or organic material in sedimentary rocks (Orr, 1974; Goldhaber and Mosier, 1989; Shelton et al., 1995).

The $\delta^{34}S$ values of ore sulfides hosted in the upper Bonneterre Dolomite in the Viburnum Trend generally conform to a paragenetic pattern that applies throughout most of the district (Burstein et al., 1993; Shelton et al., 1995) (Fig. 4.5). Many sulfides of the LOZ orebody have comparable sulfur isotope compositions to those of the main stage Pb-Zn-rich ores mined higher in the Bonneterre Dolomite (approximately +12 to +17‰) (Fig. 4.6a). However, sulfides from the LOZ orebody appear to have overall lower $\delta^{34}S$ values and show a trend of increasing $\delta^{34}S$ values with increasing distance above the Lamotte Sandstone-Bonneterre Dolomite contact (Fig. 4.6). Early stage LOZ

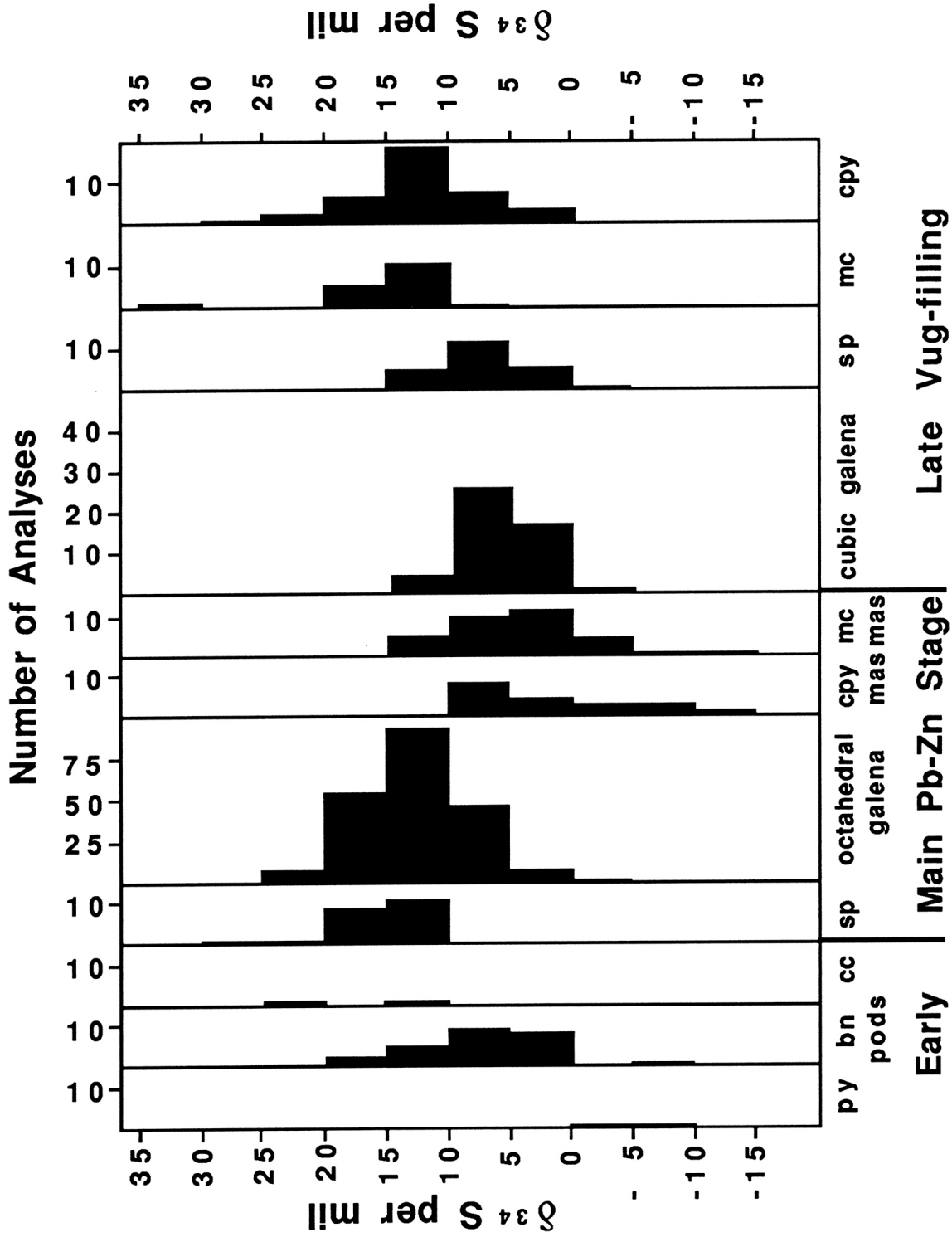

Figure 4.5. Frequency diagram of $\delta^{34}S$ values (VDCT) of sulfides throughout the mineral paragenesis in the Viburnum Trend district (after Burstein, 1993).

mineralization shows greater variability in $\delta^{34}S$ values than main stage LOZ mineralization (Cavender, 2015). Some early stage LOZ sphalerites show abrupt decreases in $\delta^{34}S$ values, the lowest of which (-14.1‰) is lower than any value for a sphalerite from the entire Viburnum Trend (Burstein, 1993; Shelton et al., 1995), which reflect significant influence from a distinct, ^{32}S-enriched sulfur source (Shelton et al., 2016). Since redox conditions are thought to be reducing and acidic throughout the paragenesis, this variation in $\delta^{34}S$ values with time is not the effect of varying redox conditions of a single source, and instead likely reflects multiple sulfur sources whose influence varied with time.

Detailed Secondary Ionic Mass Spectrometry (SIMS) analysis of banded schalenblende and sphalerite (Cavender, 2015) showed repetitive patterns in their $\delta^{34}S$ values (from +14 toward -8.2‰) (Fig. 4.6b). The rhythmicity of these patterns was interpreted to indicate pulses of metal-rich fluids that utilized two distinct sources of sulfur, one more enriched in ^{32}S (lower $\delta^{34}S$ values) and one more enriched in ^{34}S (higher $\delta^{34}S$ values). The trend from highly variable $\delta^{34}S$ values in schalenblende to more steady, higher $\delta^{34}S$ values in coarse sphalerite overgrowths illustrates that with time (from early to main stage mineralization), a lower-$\delta^{34}S$ sulfide source was supplanted by a higher-$\delta^{34}S$ sulfide source, more typical of the Pb-Zn orebodies present higher in the stratigraphy (Cavender, 2015; Shelton et al., 2016) (Fig. 4.6).

The temperature, salinity, and major element ratio variations of fluid inclusions and the sulfur isotope compositions of LOZ ores are most consistent with a model that involves mixing of multiple, geochemically distinct fluids whose influence varied in time

Figure 4.6. A) Variation of $\delta^{34}S$ values of LOZ sulfides in order of increasing paragenetic time from left to right. Note the greater variability in $\delta^{34}S$ values during early stage mineralization (left) compared to main stage mineralization (right) (after Cavender, 2015). The black bars in the left diagram indicate the ranges in $\delta^{34}S$ values of early pyrite and banded ZnS as determined by SIMS. Abbreviations: sph = sphalerite, py = pyrite, ccp = chalcopyrite, schl = schalendblende (including its associated coarse sphalerite overgrowths). B) The $\delta^{34}S$ values from SIMS analysis along the detailed traverse of schalenblende and coarse sphalerite overgrowth bands (after Cavender, 2015). Note that the boundary between the two ZnS phases (schalenblende vs. coarse sphalerite) is marked by an abrupt decrease in $\delta^{34}S$ value. C) Variation of $\delta^{34}S$ values of sulfides versus distance above and below the Lamotte Sandstone-Bonneterre Dolomite contact (indicated by a thin, black line) (after Cavender, 2015).

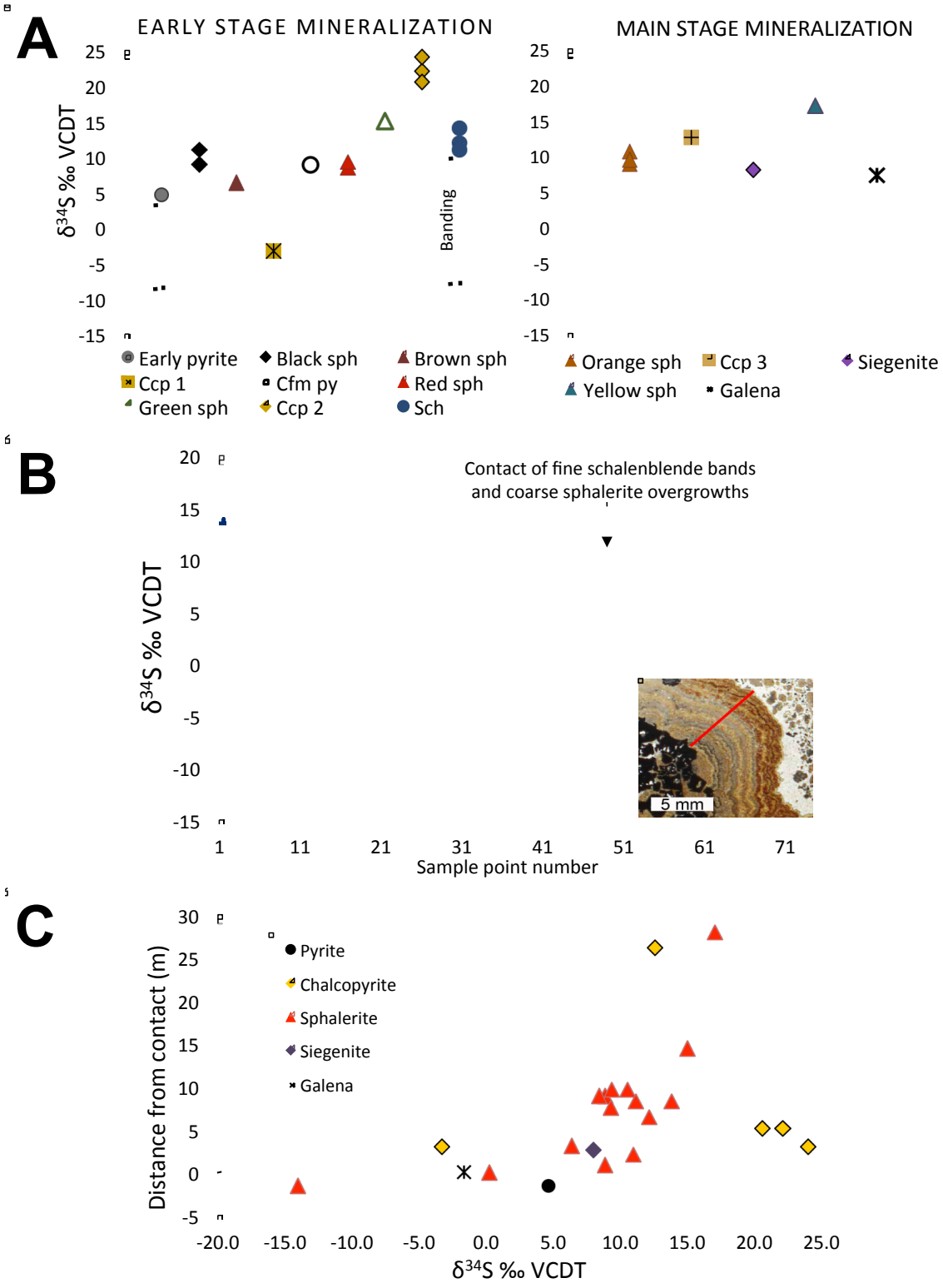
A
EARLY STAGE MINERALIZATION
MAIN STAGE MINERALIZATION
δ34S ‰ VCDT
Banding
Early pyrite
Black sph
Brown sph
Orange sph
Ccp 3
Siegenite
Ccp 1
Cfm py
Red sph
Yellow sph
Galena
Green sph
Ccp 2
Sch
B
Contact of fine schalenblende bands
and coarse sphalerite overgrowths
δ34S ‰ VCDT
5 mm
Sample point number
C
Pyrite
Chalcopyrite
Sphalerite
Siegenite
Galena
Distance from contact (m)
δ34S ‰ VCDT

and space. Reaction path calculations carried out in the present study aim to test this hypothesis by modeling multiple depositional mechanisms that may be responsible for LOZ ore formation, such as cooling of a sulfide-bearing ore fluid, reduction of a sulfate-bearing ore fluid, and mixing between sulfide-rich fluids and metal-rich fluids.

Genesis of Southeast Missouri MVT Deposits

Extensive research on the MVT ore deposits of southeast Missouri has resulted in agreement regarding several features of their origin. The Pb-rich deposits are likely the result of a regional-scale hydrothermal mineralizing system (Rowan, 1986; Buelter and Guillemette, 1988; Farr, 1989; Gregg and Shelton, 1989b; Viets and Leach, 1990; Appold and Garven, 1999, 2000) whose saline fluids resemble modern sedimentary brines (Roedder, 1977; Hagni, 1983; Rowan and Leach, 1989; Shelton et al., 1992; Hanor, 1994, 1996; Wenz et al., 2012). The most likely driving force for fluid flow in this system was gravitational head gradients associated with topographic relief that was generated during the Late Paleozoic uplift of the Arkoma basin (Leach and Rowan, 1986; Bethke and Marshak, 1990; Garven et al., 1993; Appold and Garven, 1999) (Fig. 4.1).

An important aquifer for ore fluids in the southeast Missouri MVT district is widely recognized as the Lamotte Sandstone (e.g. Brown, 1967; Gregg, 1985). More recent studies suggest another important component of fluid flow was through the overlying Bonneterre Dolomite (e.g. Viets and Leach, 1990). Sulfur isotope compositions of copper sulfides in the Viburnum Trend also provide evidence for MVT ore fluid penetration into underlying Precambrian igneous basement rocks along fault/fracture networks (Shelton et al., 1995).

Mechanisms of ore transport and deposition

A general problem for MVT ore formation is that the solubility of metals necessary to form the ores is very low over the temperature ranges associated with sulfide deposition and in the presence of reduced sulfur. Three general end-member models of possible ore transportation and deposition have been used to explain the origin of MVT mineralization in southeast Missouri: reduced-sulfur, sulfate-reduction, and mixing models (Sverjensky et al., 1979; Sverjensky, 1986; Plumlee et al., 1994; Appold and Garven, 2000).

Reduced-sulfur model

In the reduced-sulfur model, metals and reduced sulfur (H_2S) are transported together in the same fluid and ore deposition is triggered by cooling, dilution, or changing fluid conditions (e.g. increase in pH) (Anderson, 1975; Sverjensky, 1986; Spirakis and Heyl, 1995). Supporting evidence for this model has been cited in ore textures and in the covariance of lead and sulfur isotope compositions of galena (Brown, 1967; Sverjensky et al., 1979; Sverjensky, 1981; Crocetti and Holland, 1989; Goldhaber et al., 1995). However, due to the relatively low solubility of metals in the presence of reduced sulfur, the model requires more fluid and more time to form the metal-rich orebodies than the other two models described below. A reduced-sulfur model is inconsistent with the volume of ore sulfide mineralization observed in the district (Plumlee et al., 1994; Appold and Garven, 2000).

Sulfate-reduction model

In the sulfate-reduction model, metals are transported together with sulfate in the ore fluid. This model eliminates the issue of low solubilities of metals in the presence of

sulfide, but requires a sulfate reduction mechanism, such as bacterial or thermochemical sulfate reduction, in order to precipitate ore sulfides (Machel, 2001; Appold et al., 2004). Anderson (1991) suggested that the reduction of sulfate occurred through reaction with methane or other organic compounds in the brown rock facies of the Bonneterre Dolomite. Locally, organic matter has been documented as a potential genetic trigger for some ore precipitation in the Sweetwater and Magmont West mines (Niewendorp and Clendenin, 1993; Marikos et al., 1986). However, previous reaction path models (Plumlee et al., 1994) have shown that sulfate reduction at the site of ore deposition generally produces either a dolomite- or a sulfide-dominant mineral assemblage with limited dissolution of the host carbonate rocks, which is inconsistent with the pervasive replacement ores that are observed in the Viburnum Trend.

Mixing model

In fluid mixing models, sulfur (typically as sulfide) is carried in one fluid and metals in another fluid, and ore precipitation occurs where the two fluids meet and mix (Anderson, 1983; Goldhaber and Mosier, 1989; Leach, 1994). Other mixing models involve metalliferous brines that encounter a reduced sulfur source (e.g. sour gas, diagenetic pyrite, or sulfur-rich organic matter or its thermal degradation products) at the site of deposition (Davis, 1960; Jackson and Beales, 1967; Beales, 1975; Anderson, 1975, 1991; Sverjensky, 1986).

The mixing model has been postulated as a likely deposition mechanism for the Viburnum Trend ores (e.g. Sverjensky, 1981, 1986; Goldhaber and Mosier, 1989; Gregg and Shelton, 1989a, 1989b; Rowan and Leach, 1989; Viets and Leach, 1990; Brannon et al., 1991; Plumlee et al., 1994). Viets and Leach (1990) identified two distinct brine

compositions in the ion ratios of Na, Ca, Mg, K, and Cl in fluid inclusions, one of which was responsible for the deposition of early octahedral galena in the Viburnum Trend and the other that was responsible for later cubic galena. Temperature-salinity relationships in fluid inclusions in the Viburnum Trend also indicate the presence of more than one distinct fluid during mineralization in the Viburnum Trend (Rowan and Leach, 1989; Shelton et al., 1992) and that fluid mixing incorporated at least two end-member fluid components: a warmer, less saline fluid (120 to 187ºC; 5 wt% equiv. NaCl) and a cooler, more saline fluid (60 to 80ºC; > 30 wt% equiv. NaCl) (Shelton et al., 1992). Variations in mineral parageneses and sulfur isotope signatures within the Viburnum Trend (e.g. early bornite ores in several mines and the Zn-rich mineralization of the West Fork mine) also suggest the presence of multiple ore fluids and sulfur sources (Burstein et al., 1993; Shelton et al., 1993).

In an extensive reaction path modeling study (Plumlee et al., 1994), the main stage Pb-Zn ores of the Viburnum Trend ores were shown to best represent a mixing model in which a dolomite-saturated, lead-rich and H_2S-poor brine mixed with a less saline, H_2S-rich brine (Fig. 4.7). In this scenario, mixing between fluids from different aquifers would be controlled by pinchouts of the Lamotte Sandstone and Bonneterre Dolomite against Precambrian knobs, and fluid flow may have been focused by faults and abrupt facies changes. Reactive transport models produced by Appold and Garven (2000) show that although fluid mixing is a viable ore-forming mechanism from a purely geochemical standpoint, the efficiency of mixing as a depositional process likely requires very high dispersivities, dissolved metal concentrations, and/or fluid velocities.

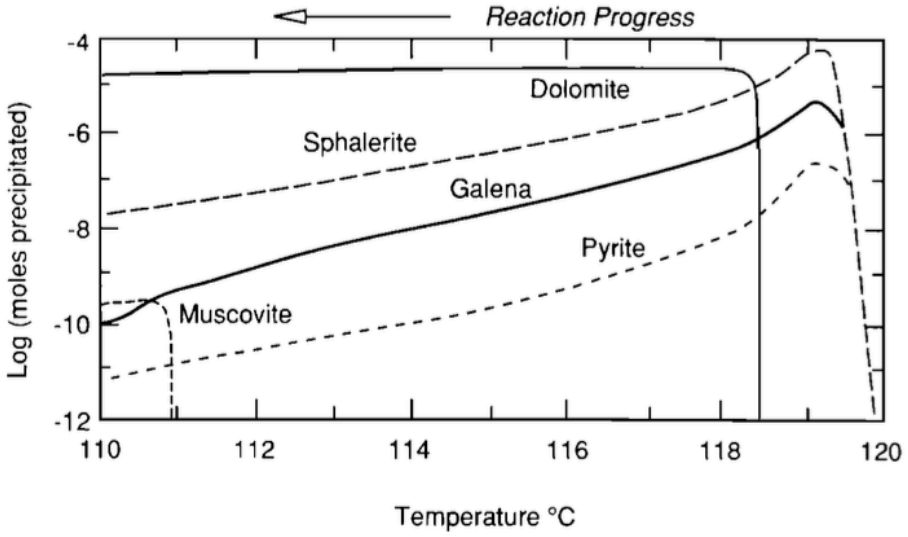

Figure 4.7. Reaction path diagram produced by Plumlee et al. (1994, Fig. 14) showing minerals precipitated during mixing of a 120ºC, saline, low-H_2S brine with a 100ºC, dilute, high-H_2S brine. The mixing of two brines with different total salinities, temperatures, H_2S content and metal content was interpreted as the reaction path that best reproduces the ores of the Viburnum Trend.

LOZ ore deposition

Cu-(Ni-Co)-Zn-rich ores of the lower Bonneterre Dolomite/upper Lamotte Sandstone in the Brushy Creek mine (Fig. 4.3) are mostly earlier paragenetically than main stage Pb-Zn ores hosted in the upper Bonneterre Dolomite that comprise the majority of the Viburnum Trend and are interpreted to reflect fault-related fluid flow (Cavender et al., 2016). Aerial and vertical zoning of LOZ sulfide mineralization suggest that ore fluids utilized multiple entry points provided by fault/fracture systems. The measured ranges of salinities, temperatures and chemical compositions of fluid inclusions and abrupt changes in sulfur isotope compositions of minerals in LOZ ores suggest that these fault-related fluids did not originate from a single evolving fluid source and are

instead the result of complex mixing of multiple, ore-metal-specific fluids and sulfur-bearing fluids from distinct sources (Cavender, 2015; Shelton et al., 2016).

REACTION PATH MODELING

Chemical speciation and reaction path calculations were evaluated in order to determine possible ore-forming fluid compositions and precipitation mechanisms that are consistent with the mineral assemblages and zoning observed in ores hosted in the lower Bonneterre Dolomite and upper Lamotte Sandstone in the Viburnum Trend. Reaction path models aim to investigate whether the multiple generations of LOZ chalcopyrite, sphalerite, and later galena might reflect a single fluid evolving chemically along different flow paths, or if they instead represent the introduction and interaction of multiple ore fluids (Cavender et al., 2016; Shelton et al., 2016), or some combination of both.

Methodology

Using the Geochemist's Workbench® (GWB) software package (Bethke, 2005, 2006, 2008), initial fluid compositions and temperatures were estimated with the GWB chemical speciation program, SpecE8©, based generally on the geology, mineralogy, and quantitative fluid inclusion data for the LOZ ores (Cavender, 2015) and ores elsewhere in the Viburnum Trend (e.g. Roedder, 1977; Hagni, 1983; Rowan and Leach, 1989; Shelton et al., 1992; Appold et al., 2004; Wenz et al., 2012). These initial fluid compositions were then used as input for the GWB reaction path program, React©, to simulate water-rock reactions and fluid mixing. Thermodynamic data used in the speciation and reaction

path calculations are from the Lawrence Livermore National Laboratory (LLNL) dataset (Delany and Lundeen, 1989) that is included in the GWB software package.

Tables 4.1 and 4.2 list the starting fluid compositions and thermochemical conditions that were used as initial basis compositions in reaction path calculations. During most iterations of reaction path calculations, these initial fluid conditions were modified in order to yield mineral assemblages that corresponded most closely to LOZ ore mineralogy. Such modifications included variations in temperature, dissolved solids (i.e. salinity), and sulfur and metal contents. Details of the fluid compositions used for each reaction path model are listed in Appendix 4.

Reaction paths in which ore fluid(s) reacted with host rocks assumed a host rock mineralogy consisting of dolomite and/or pyrite as a gross representation of the Bonneterre Dolomite and the underlying sandy carbonates of the upper Lamotte Sandstone. The primary depositional mechanisms simulated in reaction paths of a single, chemically evolving fluid included cooling, reaction with host rock, and/or the addition of methane (as a thermochemical sulfate reductant).

Mixing models simulated ore deposition from fluid mixing with or without cooling and/or reaction with host rock. These reaction paths represent depositional processes at sites where brines migrating in separate aquifers (i.e. the Lamotte Sandstone and Bonneterre Dolomite) converge, such as in breccia and fault zones. Fluid compositions used in mixing models were estimated on the basis of a metal-poor, H_2S-rich fluid reacting with a metal-rich, H_2S-poor fluid (Plumlee et al., 1994). Dilution and cooling during mixing (both of which encourage sulfide precipitation) were simulated by assuming lower total dissolved solids (i.e. salinity) and/or temperature in H_2S-rich end-

member fluids, and higher total dissolved solids and/or temperature in metal-rich end-member fluids.

Although cobalt and nickel are important components of the LOZ ore paragenesis, they could not be included in these calculations due to insufficient thermodynamic data for the formation of siegenite ($(Ni,Co)_3S_4$). Thus, the primary focus of reaction path models will concern the formation of Fe-, Cu-, Zn-, and Pb-sulfides. In order to identify (or reject) possible depositional mechanism(s) capable of producing LOZ ores, reaction path models will be assessed primarily according to the relative proportions of precipitated minerals (i.e. in order of decreasing abundance, LOZ mineralization consists

Table 4.1. Chemical composition of ore fluids used in reaction path calculations for simulations of ore deposition according to the reduced-sulfur and sulfate-reduction models.

Aqueous parameter	**Values**	
	Reduced-sulfur	**Sulfate-reduction**
Temperature (°C)	140	140
pH	4.4	4.4
$\log fO_2$	-57	-55
CH_4^+ (ppm)	300	300
TDS (%)	22	25
SiO_2 (*m*)	1.87×10^{-3}	1.87×10^{-3}
Cl^- (*m*)	4.81	5.13
H_2S (*m*)	2.0×10^{-3}	---
SO_4^{2-} (*m*)	---	1.0×10^{-3}
Ca^{2+}(*m*)	0.468	0.499
Mg^{2+} (*m*)	0.118	0.126
K^+ (*m*)	0.102	0.109
Na^+ (*m*)	3.53	3.77
Al^{3+} (*m*)	2.0×10^{-8}	2.0×10^{-8}
Fe^{2+} (ppm)	30	45
Cu^{2+} (ppm)	1	1
Zn^{2+} (ppm)	1	2.5
Pb^{2+} (ppm)	0.3	0.5

Table 4.2. Chemical composition of ore and non-ore fluids used in reaction path calculations for ore deposition by mixing. Fluid mixing models simulated the mixture of a metal-rich end-member fluid and a H_2S-rich end-member fluid. Mixing between a metal-bearing fluid and pyrite in the host rock was also tested in the calculations.

Aqueous parameter	**Values**		
	Metal-fluid + pyrite	**Metal-fluid**	**H_2S-fluid**
Temperature (°C)	140	150	120
pH	4.4	4.4	4.4
log fO_2	-57	-57	-57
CH_4^+ (ppm)	200	200	300
TDS (%)	25	25	19
SiO_2 (*m*)	1.91×10^{-3}	1.91×10^{-3}	1.52×10^{-3}
Cl^- (*m*)	5.14	5.1	4.75
H_2S (*m*)	1.0×10^{-10}	1.0×10^{-10}	0.02
SO_4^{2-} (*m*)	---	---	---
Ca^{2+}(*m*)	0.499	0.499	0.462
Mg^{2+} (*m*)	0.126	0.126	0.117
K^+ (*m*)	0.109	0.133	0.101
Na^+ (*m*)	3.77	3.67	3.49
Al^{3+} (*m*)	2.0×10^{-8}	2.0×10^{-8}	2.0×10^{-8}
Fe^{2+} (ppm)	300	300	1.0×10^{-5}
Cu^{2+} (ppm)	200	200	---
Zn^{2+} (ppm)	250	250	---
Pb^{2+} (ppm)	150	200	---

mainly of sphalerite, chalcopyrite, and galena) and, when applicable, the sequences in which they precipitate (i.e. early stage chalcopyrite and sphalerite followed by main stage sphalerite and galena).

Results

Figures 4.8 through 4.11 show reaction path diagrams produced in the current study that model ore deposition (a) by the chemical evolution of a single fluid and (b) from the mixing of two fluids. Reaction progress in each model is from left to right. The x-axis shows the reaction step, where 0 represents the equilibrium state of the original

basis fluid (pre-reaction) and 1 represents the equilibrium state of the fluid after titration of the reactant(s) is complete (post-reaction). The y-axis indicates the abundance (in log moles) of minerals present in the system at each reaction step. Reaction path models that represent the mixing of fluids only are analogous to mineral paragenesis diagrams; models that represent host rock reactions with fluid are analogous to mineral zonation diagrams.

Reaction models presented in the current study allow fluids to back-react with minerals that have been precipitated, thus they best represent closed systems in which mineral precipitation occurs in open space, but can also be considered, to a lesser degree, reliable models of mineral dissolution and replacement during reaction. Reaction paths in which fluids reacted with host rock were limited generally to < 5 cm^3 (~ 14 g) of dolomite and < 0.2 cm^3 (~ 1 g) of pyrite (if included) per kg of solvent, as larger volumes of rock resulted frequently in dolomite- and clay-dominated or pyrite-dominated assemblages.

Reduced-sulfur model

Reaction path calculations for the reduced-sulfur model were used to evaluate the potential of a sulfide- and metal-bearing fluid for the formation of LOZ ores through cooling and/or reaction with host dolomite (Fig. 4.8). The low solubility of zinc, copper, and lead in the presence of sulfide limits metal concentrations to less than 1 to 2 ppm in fluids with H_2S concentrations on the order of 10^{-3} molal. As a result, sulfide mineral precipitation in reduced-sulfur reaction path models was minor. Reaction paths that simulated only a decrease in temperature of a metal- and H_2S-bearing fluid predict sphalerite, chalcopyrite, and galena precipitation, with galena and sphalerite always

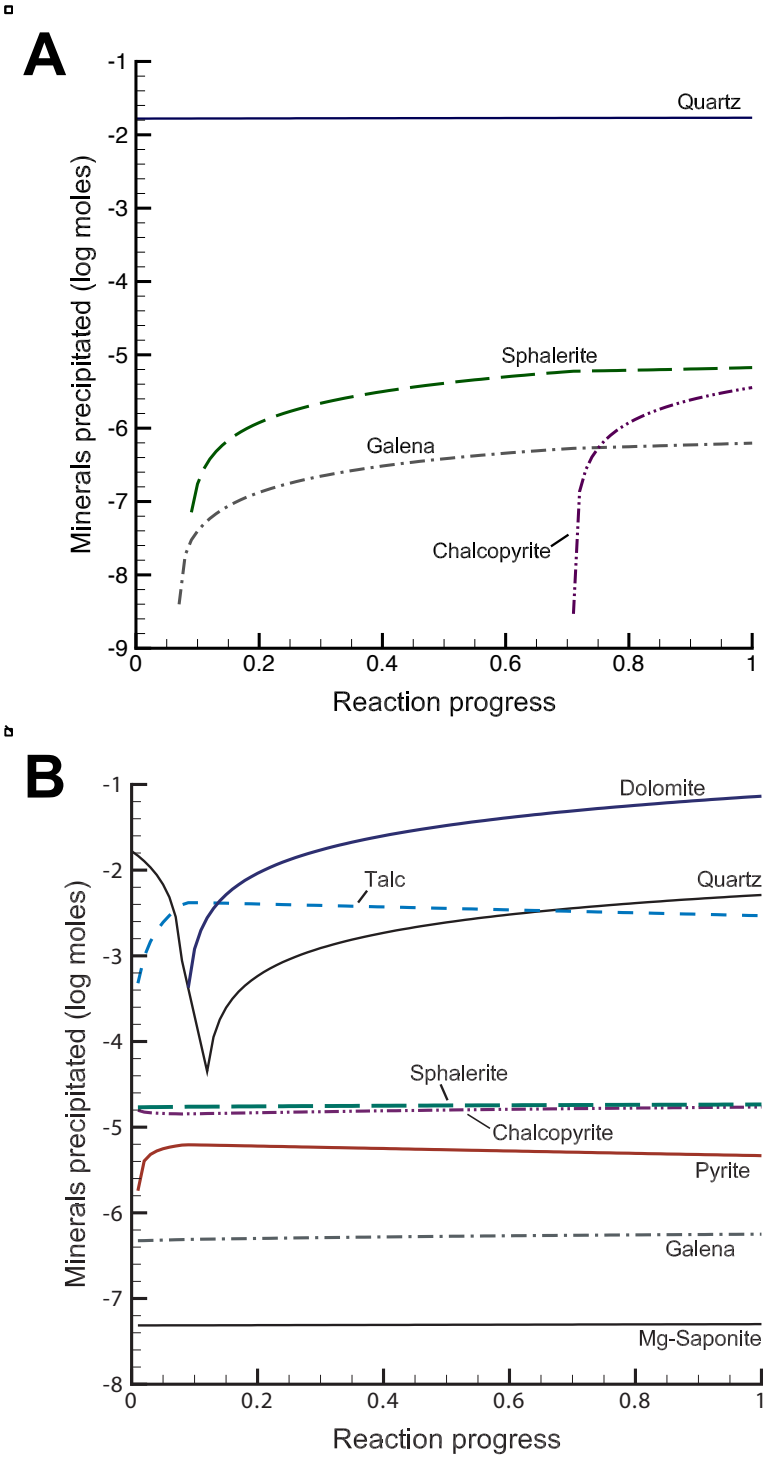

Figure 4.8. Reaction path diagrams showing minerals precipitated during simulations of the reduced-sulfur model. Copper, zinc, and lead concentrations in each reaction path were limited to ≤ 1 ppm. A) Cooling of a sulfide- and metal-bearing fluid from 145° to 130°C. B) Cooling of a sulfide- and metal-bearing fluid from 150° to 140°C that was reacted with 5 cm^3 dolomite.

occurring as the first precipitate(s) (Fig. 4.8a).

Reaction paths in which the ore fluid was allowed to react with dolomite host rock predict mineral assemblages dominated by dolomite, talc, and quartz (Fig. 4.8b) that appear to be unaffected by changes in temperature. Sulfide minerals in these paths quickly, if not instantaneously, became saturated and reached equilibrium with the fluid, after which only dolomite, talc, and quartz continued to react.

The low abundance of precipitated sulfides and the dolomite- and talc-dominated mineral assemblages that are produced by reduced-sulfur models indicate that a single, sulfide- and metal-bearing fluid would be incapable of producing the observed mineral paragenesis and the high ore grade in the LOZ orebody.

Sulfate-reduction model

Multiple reaction paths were evaluated to model sulfate reduction by the addition of methane into a metal- and sulfate-bearing fluid in addition to cooling and/or reaction with host rock (Fig. 4.9). Despite the absence of reduced sulfur in the initial fluid, sulfate concentrations on the order of 10^{-3} molal constrain ore metal concentrations to less than 10 ppm. Reaction path models show that cooling during sulfate reduction can produce mineral assemblages containing sphalerite, chalcopyrite, and galena in order of decreasing abundance (Fig. 4.9a). The Fe/Cu ratio that was necessary for chalcopyrite precipitation (instead of bornite) in this case greatly limited the copper content of the fluid (< 1 ppm Cu) and required iron concentrations at an order of magnitude greater than copper.

Sulfate-reduction models in which fluid was allowed to react with host rock predicted mineral assemblages dominated by dolomite, talc, and quartz, similar to those

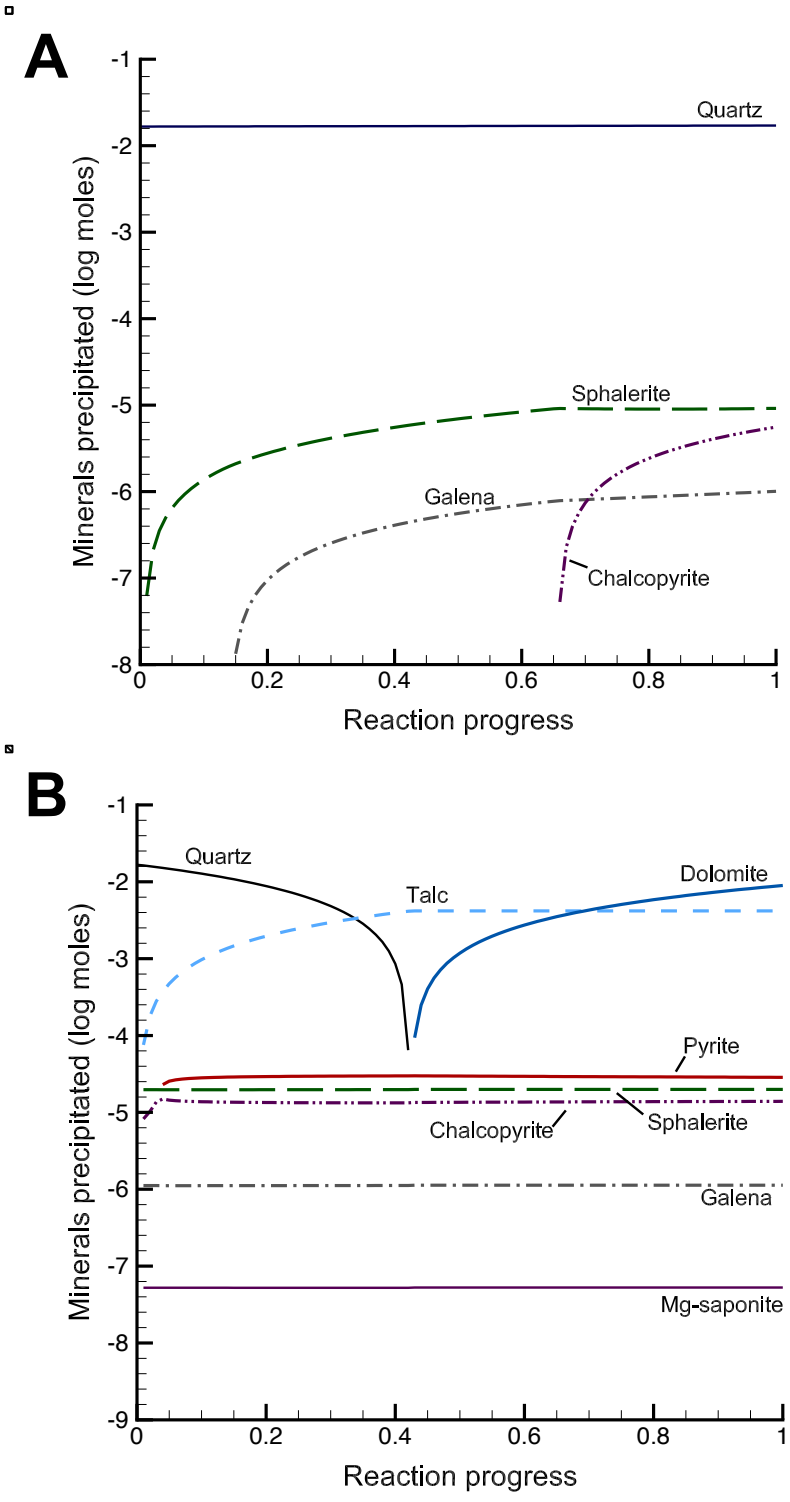

Figure 4.9. Reaction path diagrams showing minerals precipitated during simulations of the sulfate-reduction model. A) Cooling of a sulfate- and metal-bearing fluid (1 kg) from 145° to 130°C that was reacted with 5g of CH_4. B) Cooling of a sulfate- and metal-bearing fluid (1 kg) from 145° to 130°C that was reacted with 5g of CH_4 and 1 cm^3 of dolomite.

produced by fluid-host rock reaction in reduced-sulfur models (Fig. 4.9b). When host dolomite was included in sulfate-reduction reaction paths, temperature changes had very little effect on resultant mineral precipitation.

Although mineral assemblages similar to those seen in LOZ ores can be precipitated through sulfate reduction when reaction with host dolomite is not allowed, the limited metal concentrations (particularly copper) allowed in solution suggests that the sulfate-reduction model could not produce the abundance of ore sulfides or the paragenetic sequences that are observed in LOZ mineralization.

Mixing models

Mineral assemblages predicted to result from fluid mixing and from the mixing of a metal-bearing fluid with sulfide from diagenetic pyrite vary greatly depending on the initial chemistry and temperature of the end-member fluids involved. Slight adjustments to initial fluid compositions provided considerable control on resultant mineral precipitation, and reaction path calculations have shown that the mixing of a H_2S-rich fluid and a metal-rich fluid can result in sphalerite, chalcopyrite, and galena precipitation in similar proportions to the LOZ ores (Figs. 4.10 and 4.11). However, the sequential precipitation of these ore sulfides that is observed in LOZ mineralization, however, would likely require multiple, ore-metal-specific fluids to be introduced sequentially (e.g. alternating introduction of a Cu-rich fluid and Zn-rich fluid).

Compared to single fluid reaction paths, the phase transition between chalcopyrite and bornite ± pyrite was particularly sensitive to small modifications in fluid conditions and compositions along mixing reaction paths. The precipitation of chalcopyrite rather than bornite could be promoted by either decreasing the zinc content or increasing the

Fe/Cu ratio of the metal-rich fluid. Bornite precipitation could also be mitigated with other adjustments to reaction conditions, such as adding dolomite to the reactants, decreasing temperature, and increasing the H_2S content of the sulfide-rich fluid.

Reaction between metal-bearing fluid and pyrite

The reaction of a metal-rich, sulfur-poor (~ 10^{-5} molal S) fluid with pyrite can successfully precipitate sphalerite ± galena at zinc and lead concentrations in the hundreds to thousands of ppm and is not greatly affected by changes in temperature (Fig. 4.10a). However, the precipitation of bornite ± chalcocite together with chalcopyrite from a Cu-bearing fluid could not be avoided without the presence of zinc in solution at significantly higher concentrations (e.g. ~ 10 ppm Cu, 200 ppm Zn, and 1 ppm Fe precipitates sphalerite, pyrite, and chalcopyrite) (Fig. 4.10b). Conditions under which chalcopyrite could be precipitated as the only Cu-sulfide also always resulted in significant pyrite precipitation. Abundant pyrite precipitation also occurred when only one ore metal (i.e. copper, zinc, or lead) was present in the initial fluid. However, the low abundance of pyrite in the LOZ paragenesis suggests that diagenetic pyrite from the lower Bonneterre Dolomite or Lamotte Sandstone likely served only as a minor source of sulfide (or not at all) during LOZ ore formation.

Fluid mixing

Mixing reaction paths between a H_2S-rich fluid with a Fe-Cu-Zn-Pb-bearing fluid result in assemblages of sphalerite, chalcopyrite, and galena commonly at lower temperatures (toward 120ºC) or during cooling (Fig. 4.11a), whereas higher temperatures (toward 150ºC) promote the precipitation of bornite. However, changes in temperature had little effect on sulfide precipitation when the metal-rich fluid did not contain both

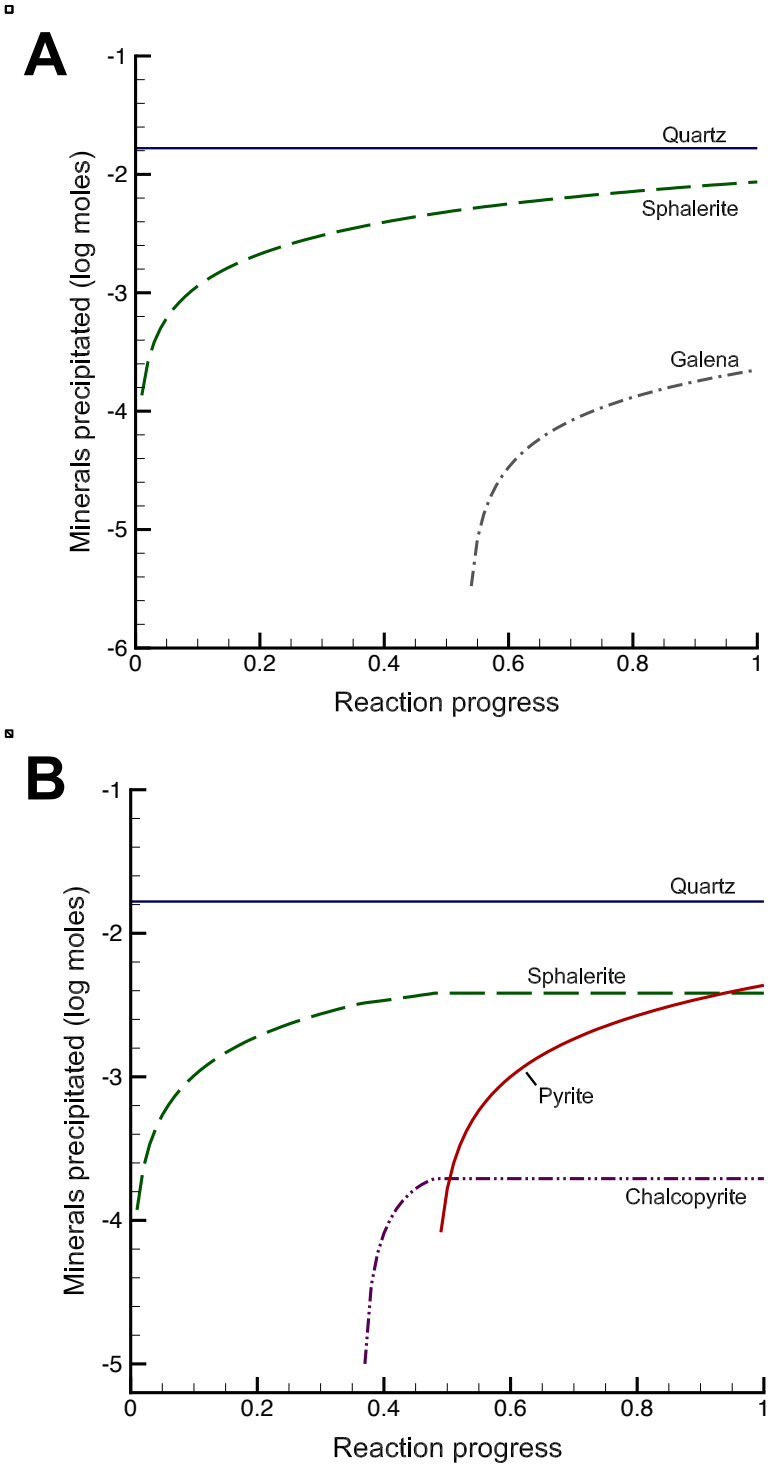

Figure 4.10. Reaction path diagrams showing minerals precipitated during the reaction of pyrite with a metal-rich fluid. Sulfide was assumed to be essentially absent from solution, allowing metals to reach concentrations in hundreds to thousands of ppm. A) A Zn-Pb-bearing fluid (1 kg) at 145ºC reacts with 0.2 cm^3 pyrite. B) A Zn-Cu-bearing fluid (1 kg) at 145ºC reacts with 0.2 cm^3 pyrite.

copper and zinc in comparable concentrations. Many reaction paths in which bornite originally precipitated with sphalerite became chalcopyrite-dominant when zinc was removed from the initial fluid composition (Figs. 4.11b,c).

The (a) simultaneous precipitation of chalcopyrite, sphalerite, and galena that results from a Cu-Zn-Pb-bearing fluid and (b) the frequent precipitation of bornite when both copper and zinc were present in solution demonstrate that the alternating generations of sulfide minerals observed in LOZ ores likely required the sequential introduction of ore-metal-specific fluids.

Fluid mixing and reaction with host rock

Mixing between two fluids together with reaction with dolomite host rock results frequently in mineral assemblages similar to those produced by mixing fluids alone (Fig. 4.11d). Reaction paths with slightly larger amounts of dolomite involved in reaction appear more favorable for the coprecipitation of sphalerite and chalcopyrite, which may be related to fO_2 and pH changes (due to increased CO_2 production) associated with dolomite dissolution. When sufficiently large amounts of dolomite are added to the system, such that acid production from sulfide precipitation is no longer the primary control on pH, dolomite eventually reaches saturation with continued mixing and becomes the dominant precipitate. These reaction path models, together with the lack of evidence for extensive carbonate replacement in the LOZ orebody, suggest that fluid mixing during LOZ ore formation must have occurred with very little or no interaction with host dolomite.

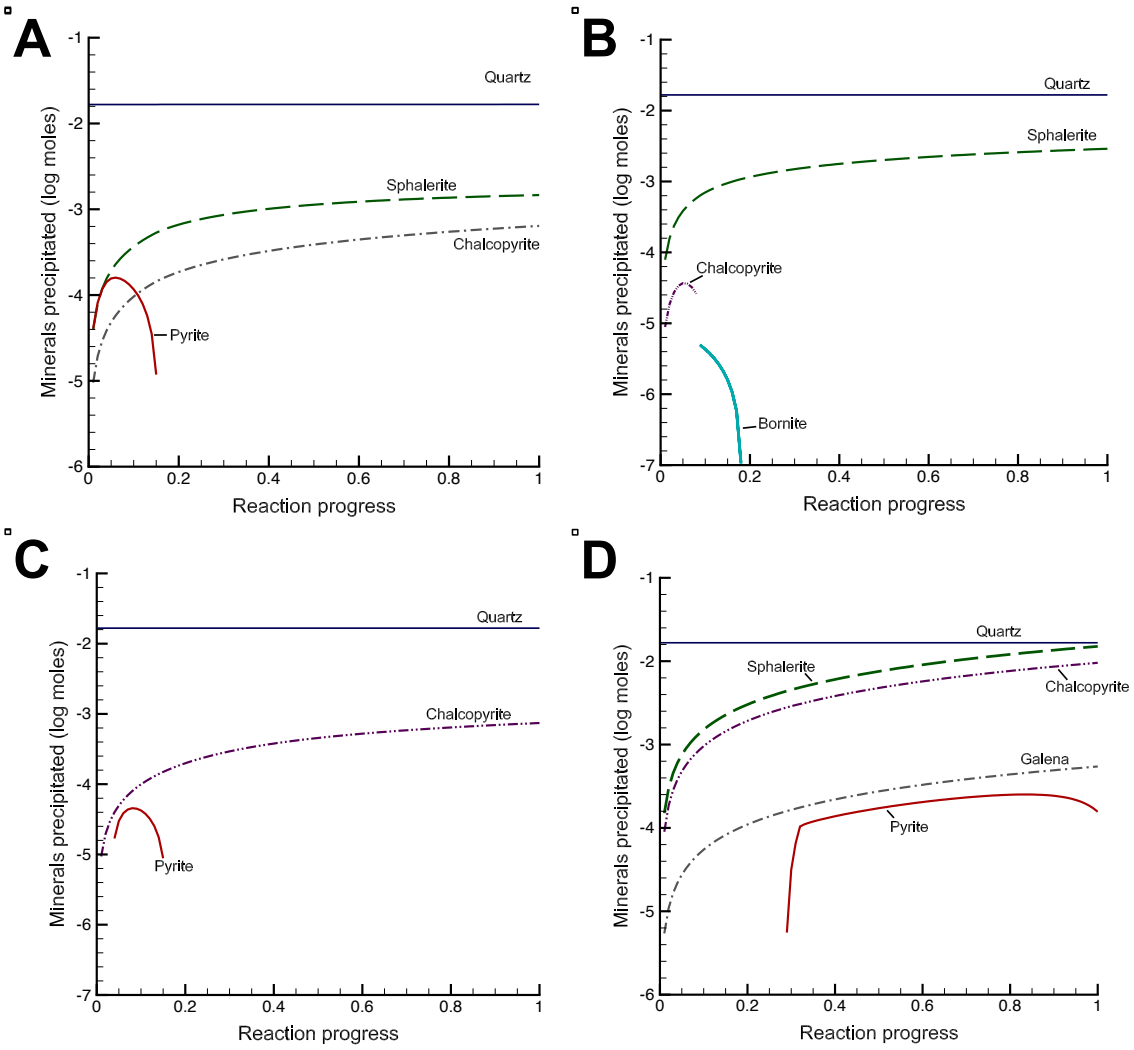

Figure 4.11. Reaction path diagrams showing minerals precipitated during the mixing of a metal-poor, H_2S-rich fluid with a metal-rich, H_2S-poor fluid. Sulfide concentrations in the H_2S-rich end-member were typically ~10^{-2} molal, and metal concentrations in the metal-rich end-member varied up to hundreds of ppm. A) Mixing of a 150ºC, Zn-Cu-bearing fluid and a 135ºC, H_2S-rich fluid. B) Isothermal mixing (150ºC) of a Zn-Cu-bearing fluid and a H_2S-rich fluid. C) Isothermal mixing (150ºC) of a Cu-bearing fluid and a H_2S-rich fluid. This reaction path uses the same initial fluid compositions as those in (B), but zinc has been removed from the metal-bearing end-member fluid. D) Reaction with 1 cm^3 dolomite during isothermal mixing (150ºC) of a Zn-Cu-Pb-bearing fluid with a H_2S-rich fluid. Note: in this reaction path, the mass of the metal-rich fluid (5 kg) is five times greater than the volume of the H_2S-rich fluid (1 kg).

DISCUSSION

Reaction path modeling shows multiple depositional mechanisms are capable of producing ore sulfide assemblages similar to those in the Zn-Cu-rich ores of the LOZ orebody. However, the reduced-sulfur and sulfate-reduction models produce only small amounts of ore sulfides that likely would be incapable of producing an ore deposit within the length of time (less than a few million years) and volumes of fluid that are feasible for the formation of the MVT deposits in the Viburnum Trend (Appold and Garven, 1999; Appold and Wenz, 2011). The relative proportions, paragenetic sequence, and temporal trend in $\delta^{34}S$ values of LOZ sulfide minerals are most consistent with the introduction of multiple metal-bearing fluids utilizing multiple sources of sulfide present in brines and, to a lesser degree, diagenetic pyrite.

Ore deposition by a single fluid

Reaction path modeling suggests that LOZ ore deposition likely was not a product of a single ore fluid transporting both reduced sulfur and metals due to the predicted dolomite- and clay-dominated mineral assemblages (during reaction with host dolomite) and the brief precipitation of minor sulfides resulting from the low solubility of metals in solution with H_2S (Fig. 4.8). Sulfate-reduction models produced similar results to reduced-sulfur models when host dolomite was allowed to react with the fluid; sulfate-reduction paths without reaction with host rock did not predict major gangue mineral precipitation and resulted in slightly larger amounts of sphalerite, chalcopyrite, and galena precipitation (Fig. 4.9). However, variations in $\delta^{34}S$ values of LOZ sulfides (-14‰ to +24‰ VCDT; Cavender, 2015) are inconsistent with sulfate reduction in the orebody since redox conditions remain reducing and acidic throughout the paragenesis

(assuming similar redox conditions to those calculated by Wenz et al., 2012 for the main ore zone of the Viburnum Trend apply to the LOZ ore system). Additionally, the abundance in sulfides that are precipitated from both the sulfate-reduction and reduced-sulfur models is likely too low to account for the size and grade of LOZ ores.

The low $\delta^{34}S$ values of early generations of pyrite, sphalerite, and chalcopyrite (-6.4 to +11.0‰; Cavender, 2015) and iron-sulfide replacement textures in ore samples suggest that early ore fluids may have incorporated sulfide locally from diagenetic pyrite in the base of the Bonneterre Dolomite and the Lamotte Sandstone (Shelton et al., 2016). Reaction path models that simulate this process predict that metals in a sulfide-poor fluid can precipitate ore sulfides when reacted with pyrite (Fig. 4.10), indicating a potential depositional mechanism for LOZ ores. However, the low abundance of sulfides that precipitate and the large amount of subsequent pyrite precipitation that occurs frequently in these paths (particularly when the fluid was not carrying copper, zinc, and lead together) may suggest that diagenetic pyrite served as a secondary source of sulfide during the history of LOZ ore deposition.

Ore deposition by fluid mixing

Reaction paths which best reproduce the Zn-Cu-rich LOZ ore mineralogy are those in which a fluid enriched in H_2S mixes with a more saline, metalliferous brine (Fig. 4.11). Ore metals being carried in a fluid without sulfide allows for high metal concentrations in solution (hundreds of ppm) and abundant sulfide precipitation in our simulations. However, elevated concentrations of ore metals were associated frequently with the precipitation of bornite rather than chalcopyrite. Precipitation of chalcopyrite is favored at lower temperatures or during cooling, at higher Fe/Cu ratios in solution, during

reaction with small amounts of host dolomite, and at lower zinc concentrations in solution (since lead concentrations in the simulations were very low relative to copper and zinc, the removal of lead had little effect on the precipitation of other ore sulfides).

Although lower temperatures promoted chalcopyrite and sphalerite coprecipitation, reaction paths that mixed ore-metal-specific fluids with H_2S-rich fluids resulted in consistent sulfide precipitation over wide ranges in temperature. The models suggest that sphalerite that was formed at higher temperatures (140 to 150ºC) was precipitated from fluid mixing in which zinc was the only ore metal involved; likewise, chalcopyrite precipitation at higher temperatures requires a fluid carrying only copper (and iron) in order to avoid significant bornite (and/or chalcocite) precipitation. Therefore the precipitation of sphalerite, chalcopyrite, and galena at higher temperature (without other Cu-sulfides) would likely require separate, ore-metal-specific end-member fluids, whereas a fluid at lower temperature that contains zinc, copper, and lead could result in the coprecipitation of sphalerite, chalcopyrite, and galena only.

The sequential deposition of LOZ sulfide ores implies that metal-bearing fluids mixed with sulfide-bearing fluids episodically through time. The specific conditions under which Cu- and Zn-sulfides can precipitate together also suggest that LOZ ore deposition resulted from the introduction of ore-metal-specific fluids. The coexistence of such metal-specific fluids would likely require faults in order to remain restricted from one another. Localized, fault-constrained fluids may have attained specific ore metals as they reacted with systems that were enriched locally in copper, zinc, or lead, such as igneous-hosted Fe-Cu deposits in the Precambrian basement rocks (e.g. the West and

Central Domes of Boss-Bixby, Shelton et al., 1995) or an overlying Pb-Zn-rich system in the upper Bonneterre Dolomite.

Conceptual model for LOZ mineralization

The high-grade, unusually Cu-(Ni-Co)-Zn-rich ores hosted in the lower Bonneterre Dolomite and upper Lamotte Sandstone of the Viburnum Trend have been interpreted to reflect multiple ore fluids that likely used faults and fractures as conduits (Cavender et al., 2016). The vertical metal zoning in the orebody and the sporadic nature of $\delta^{34}S$ values in sulfides suggest that complex mixing between multiple, metal-specific fluids from distinct sources was variable temporally and spatially (Cavender et al., 2016; Shelton et al., 2016). Sulfur isotope compositions of LOZ ores suggest that these metal-bearing fluids utilized distinct sulfur sources whose influence was variable through time. The low $\delta^{34}S$ values (< 10‰) in early stage ores may reflect a ^{32}S-enriched source for fluids in the Lamotte Sandstone, possibly derived from underlying igneous basement rocks, or could reflect from the assimilation of sulfur from ^{32}S-enriched diagenetic pyrite. Higher $\delta^{34}S$ values (~ 17‰) that are closer in value to those of more typical Pb-Zn ores higher in the Bonneterre Dolomite likely reflect sulfide derived from basinal or evaporitic sedimentary sources. Fluids containing ^{34}S-enriched sulfide appear to have entered the system in pulses, progressively becoming the dominant sulfur source during main stage mineralization (Cavender, 2015; Shelton et al., 2016).

Reaction path models show that the abundance of sulfide precipitation predicted from the chemical evolution of a single, Fe-Cu-Zn-Pb-S-bearing fluid is considerably smaller than what would be required to form an ore deposit over a reasonable length of time. Fluid mixing, as proposed previously for LOZ mineralization (Cavender et al.,

2016), is a better mechanism for ore deposit formation. Reaction paths suggest that early stage sphalerite that formed at lower temperatures (T_h = < 100ºC, Cavender, 2015) may have formed from a Cu-Zn-bearing fluid, although the alternating, sequential deposition of early chalcopyrite and sphalerite indicates that each of the sulfides formed from alternation of ore-metal-specific fluids.

It is most likely that higher temperature ZnS, such as schalenblende (T_h = ~ 175, Cavender, 2015), formed from a Cu-poor fluid, as reaction paths indicate that chalcopyrite does not precipitate readily with sphalerite at temperatures above ~ 140ºC and is often associated with abundant pyrite precipitation at such temperatures. Reaction path models typically predict the immediate precipitation of galena from any fluid with sufficient Pb-content (~ tens of ppm). This suggests that main stage Zn- and Pb-rich zones in the LOZ orebody (Fig. 4.12) resulted from metal-specific fluids as well.

Some mixing reaction path models that involve reaction with host dolomite are more compatible with the coprecipitation of chalcopyrite and sphalerite (Fig. 4.11d), but the absence of extensive carbonate replacement textures in the orebody and the sharp contacts between ore and wall rock belies the reaction of fluids with host dolomite during sulfide precipitation as a viable component of the LOZ mixing system. This suggests that ore-metal-specific fluids that mixed with H_2S-bearing brines in open space were required to form the Zn-Cu-rich mineralization.

Figure 4.12b shows a modified version of the conceptual genetic model for LOZ mineralization proposed by Cavender et al. (2016) according to the results of this study. In conjunction with previous geochemical studies on LOZ ore mineralization by Cavender (2015), reaction path models constructed in the current study support the

formation of LOZ ores by mixing. Multiple, ore-metal-specific fluids were introduced in pulses and mixed with H_2S-bearing brines that derived sulfide from multiple sources. Fluids carrying zinc, iron, or copper (potentially acquired through fluid interaction with igneous basement rocks) in the Lamotte Sandstone moved up the stratigraphic section into the Bonneterre Dolomite along fault and fracture networks, depositing ore sulfides where they encountered lower-$\delta^{34}S$ H_2S-bearing brines. As the lower ore system reached higher stratigraphic levels, it would have breached less permeable units in the lower Bonneterre Dolomite, allowing interaction with the Pb-Zn-rich fluid system associated with higher-$\delta^{34}S$ H_2S-bearing brines (Fig. 4.12b).

CONCLUSIONS

The primary goals of this study were to better understand the depositional mechanisms responsible for the unusually Cu-(Ni-Co)-Zn-rich ores in the lower Bonneterre Dolomite and upper Lamotte Sandstone and to address whether these ores formed from a single fluid evolving chemically along flow paths or if they instead reflect the interaction of multiple ore fluids through time, or some combination of both.

Using geochemical data for these Zn-Cu-rich lower ores (Cavender, 2015) and for more typical Pb-Zn ores of the Viburnum Trend (e.g. Plumlee et al., 1994; Appold and Garven, 2000; Wenz et al., 2012) as guides for initial fluid compositions, reaction path modeling of several depositional processes has determined the following:

Figure 4.12. A) Idealized map of metal zoning within the lower ore zone (LOZ) mineralization at the Brushy Creek mine (after Cavender et al., 2016). Areas of Ni-rich versus Ni-Co-rich mineralization indicate the presence of multiple entry points for ore-metal-specific, mineralizing fluids. B) Conceptual model for the progressive vertical development of LOZ ores (modified from Cavender et al., 2016). Metal-specific fluids introduced into the lower system sporadically utilized multiple, isotopically distinct sources of sulfide (i.e. diagenetic pyrite, H_2S-bearing brines) along fault-related flow paths. As the lower ore system reached higher stratigraphic levels, it would have breached less permeable units in the lower Bonneterre Dolomite, allowing interaction with an overlying Pb-Zn-rich, higher-$\delta^{34}S$ system.

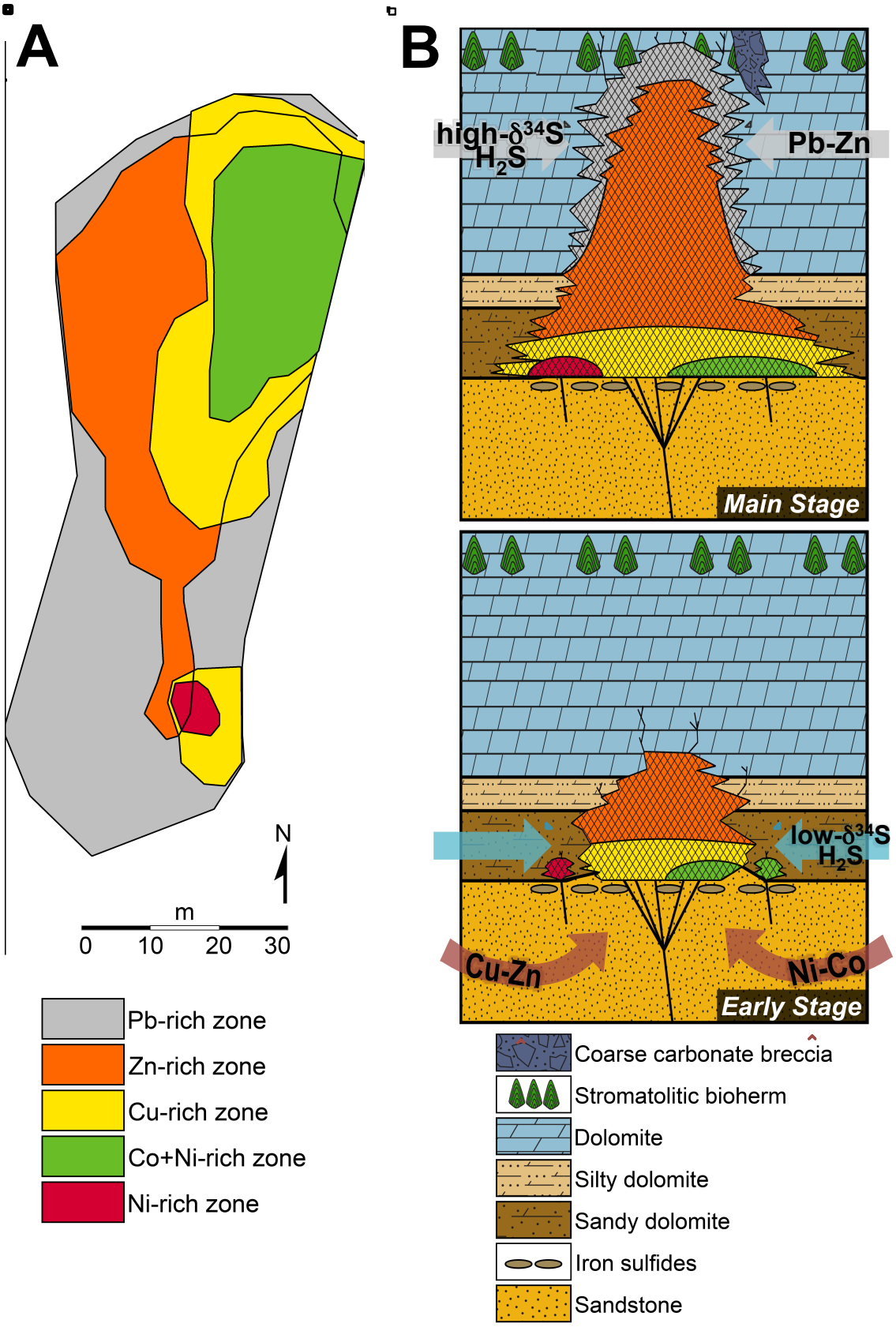
A
N
m
0
10
20
30
Pb-rich zone
Zn-rich zone
Cu-rich zone
Co+Ni-rich zone
Ni-rich zone
B
high-δ34S H2S
Pb-Zn
Main Stage
low-δ34S H2S
Cu-Zn
Ni-Co
Early Stage
Coarse carbonate breccia
Stromatolitic bioherm
Dolomite
Silty dolomite
Sandy dolomite
Iron sulfides
Sandstone

1. Diverse mineral assemblages can be produced from a Zn-Cu-Pb-bearing fluid under different geochemical conditions. The conditions under which sphalerite and galena are able to precipitate are much more flexible than for chalcopyrite precipitation, which is particularly sensitive to fluctuations in sulfur content, redox state, and the concentrations of other ore metals in solution.
2. LOZ ore formation likely did not result from the chemical evolution of a single metal-bearing brine. Cooling of a sulfide- and metal-bearing fluid and reduction of a sulfate- and metal-bearing fluid can each produce assemblages similar in mineralogy to the LOZ ores, and could potentially account for minor sulfide precipitation in the orebody. However, the capacity to carry sufficient metal concentrations necessary to form an ore deposit is not feasible for fluids with such high concentrations of sulfur and there is little evidence in sulfur isotope data of LOZ sulfide minerals for significant reduction of sulfate.
3. Ore replacement textures and low $\delta^{34}S$ values of early LOZ ores that suggest that ore fluids incorporated sulfide through the dissolution of pyrite are consistent with reaction path models to a small degree, but this process likely played a minor role in ore formation on local scales. Reaction of a metal-rich brine with pyrite is capable of producing LOZ ore minerals, but small changes in the volume of pyrite reacted with the fluid affected the resulting mineral assemblages greatly and frequently resulted in unrealistically large amounts of pyrite precipitation.
4. Fluid mixing was likely the dominant depositional mechanism responsible for the formation of LOZ ores. Conditions under which sphalerite, chalcopyrite, and galena could precipitate from mixing between a Zn-Cu-Pb-bearing fluid and a H_2S-bearing

fluid resulted typically in simultaneous precipitation of the minerals, which is not observed in the LOZ paragenesis. However, the multiple, alternating generations of sulfides (particularly sphalerite) indicate that ore fluids were ore-metal-specific and were introduced into the lower ore system sporadically. Their interaction with fluids containing H_2S from multiple, isotopically distinct sources was likely controlled by fault and fracture networks in the Bonneterre Dolomite and Lamotte Sandstone, through which fluid mixing would have been variable temporally and spatially. This complex series of discrete mixing events led to the formation of the massive, Zn-Cu-rich ores that are observed in the lower Bonneterre Dolomite and upper Lamotte Sandstone of the Brushy Creek mine in the Viburnum Trend. It is hoped that future studies can provide a more detailed hydrologic synthesis of how localized, chemically distinct fluids may have flowed and interacted physically within this system.

REFERENCES

Anderson, G. M., 1975, Precipitation of Mississippi Valley-type ores: Economic Geology, v. 70, p. 937-942.

------ 1983, Some geochemical aspects of sulfide precipitation in carbonate rocks, *in* Kisvarsanyi, G., Grant, S.K., Pratt, W.P., and Koenig, J.W., eds., International conference on Mississippi Valley Type lead-zinc deposits: Rolla, MO, University of Missouri-Rolla, p. 61–76.

------ 1991, Organic maturation and ore precipitation in southeast Missouri: Economic Geology, v. 86, p. 909-926.

------ 2008, The mixing hypothesis and the origin of Mississippi Valley-type ore deposits: Economic Geology, v. 103, no. 8, p. 1683-1690.

Anderson, G. M., and Thom, J., 2008, The role of thermochemical sulfate reduction in the origin of Mississippi Valley-type deposits. II. Carbonate-sulfide relationships: Geofluids, v. 8, no. 1, p. 27-34.

Appold, M. S., and Garven, G., 1999, The hydrology of ore formation in the southeast Missouri district: Numerical models of topography-driven fluid flow during the Ouachita Orogeny: Economic Geology, v. 94, p. 913-936.

------ 2000, Reactive flow models of ore formation in the southeast Missouri district: Economic Geology, v. 95, p. 1605-1626.

Appold, M. S., Numelin, T. J., Shepherd, T. J., and Chenery, S. R., 2004, Limits on the metal content of fluid inclusions in gangue minerals from the Viburnum Trend, southeast Missouri, determined by laser ablation ICP-MS: Economic Geology, v. 99, p. 185-198.

Appold, M. S., and Wenz, Z. J., 2011, Composition of ore fluid inclusions from the Viburnum Trend, southeast Missouri district, United States: Implications for transport and precipitation mechanisms: Economic Geology, v. 106, p. 55-78.

Beales, F. W., 1975, Precipitation mechanisms for Mississippi Valley-type ore deposits: Economic Geology, v. 70, p. 943-948.

Bethke, C.M., 2005, The Geochemist's Workbench Release 6.0 Reaction Modeling Guide: A user's guide to React and Gtplot: University of Illinois.

Bethke, C.M., 2006, The Geochemist's Workbench, version 6.0, a user's guide to Rxn, Act2, Tact, SpecE8, and Aqplot, hydrogeology program: Oxford University Press, Oxford, 397 p.

Bethke, C. M., 2008, Geochemical and Biogeochemical Reaction Modeling: Cambridge University Press, New York, 564 p.

Bethke, C. M., and Marshak, S., 1990, Brine migrations across North America—the plate tectonics of groundwater: Annual Reviews of Earth and Planetary Science, v. 18, p. 228-315.

Brannon, J. C., Podosek, F. A., Viets, J. G., Leach, D. L., Goldhaber, M. B., and Rowan, E. L., 1991, Strontium isotopic constraints on the origin of ore-forming fluids of the Viburnum Trend, southeast Missouri: Geochimica et Cosmochimica Acta, v. 55, no. 5, p. 1407-1419.

Brown, J. S., ed., 1967, Genesis of stratiform lead-zinc-barite-fluorite deposits (Mississippi Valley-type deposits): Economic Geology Monograph, v. 3, 443 p.

Buelter, D. P., and Guillemette, R. N., 1988, Geochemistry of epigenetic dolomite associated with lead-zinc mineralization of the Viburnum Trend, southeast Missouri, *in* Shukla, V., Baker, P. A., eds., Sedimentology and Geochemistry of Dolostones: Society of Economic Paleontologists Special Publication, no. 43, p. 85-93.

Burstein, I. B., Shelton, K. L., Gregg, J. M., and Hagni, R. D., 1993, Complex, multiple ore fluids in the world class southeast Missouri Pb-Zn-Cu MVT deposits: Sulfur isotope evidence, *in* Shelton, K.L., and Hagni, R.D, eds., Geology and geochemistry of Mississippi Valley-type ore deposits: Proceedings volume: Rolla, MO, University of Missouri-Rolla Press, p. 1-16.

Cavender, B. D., 2015, Atypical MVT, Zn-Cu-rich mineralization in the lower portion of the Bonneterre Dolomite, Viburnum Trend, Southeast Missouri, U.S.A. [M.S. thesis]: Columbia, University of Missouri, 167 p.

Cavender, B. D., Shelton, K. L., and Schiffbauer, J. D., 2016, An atypical orebody in the Brushy Creek mine, Viburnum Trend, Missouri: Early Cu-(Ni-Co)-Zn-rich ores at

the Lamotte Sandstone/Bonneterre Dolomite contact: Economic Geology, v. 111, no. 1, p. 259-269.

Claypool, G. E., Holser, W. T., Kaplan, I. R., Sakai, H., and Zak, I., 1980, The age curves of sulfur and oxygen isotopes in marine sulfate and their mutual interpretation: Chemical Geology, v. 28, p. 199-260.

Crocetti, C. A., and Holland, H. D., 1989, Sulfur-lead isotope systematics and the composition of fluid inclusions in galena from the Viburnum Trend, Missouri: Economic Geology, v. 84, p. 2196-2216.

Delany, J. M., and Lundeen, S. R., 1989, The LLNL Thermochemical Database: Lawrence Livermore National Laboratory Report UCRL-21658, 150 p.

Diehl, S. F., and Goldhaber, M. B., 1995, Feldspar diagenesis in Cambrian clastic rocks of the southern Ozark Mountains and Reelfoot rift, southeastern Missouri and northeastern Arkansas—implications for Mississisippi Valley-type ore genesis: U. S. Geological Survey Bulletin, no. 1989-F, p. F1-F17.

Farr, M. R., 1989, Compositional zoning characteristics of late dolomite cements in the Cambrian Bonneterre Formation, Missouri: Implications for parent fluid migration pathways: Carbonates and Evaporites, v. 4.2, p. 177-194.

Garven, G., Ge, S., Person, M. A., and Sverjensky, D. A., 1993, Genesis of stratabound ore deposits in the midcontinent basins of North America, 1, The role of regional groundwater flow: American Journal of Science, v. 293, p. 497-568.

Goldhaber, M. B., and Mosier, E. L., 1989, Sulfur sources for southeast Missouri MVT ores – Implications for ore genesis: U. S. Geological Survey Circular 1043, p. 8-9.

Goldhaber, M. B., Church, S. E., Doe, B. R., Aleinikoff, J. N., Brannon, J. C., Podosek, F. A., Mosier, E. L., Taylor, C. D., and Gent, C. A., 1995, Lead and sulfur isotope investigation of Paleozoic sedimentary rocks from the southern midcontinent of the United States: Implications for paleohydrology and ore genesis of the southeast Missouri lead belts: Economic Geology, v. 90, p. 1875-1910

Gregg, J. M., 1985, Regional epigenetic dolomitization in the Bonneterre Dolomite (Cambrian), southeast Missouri: Geology, v. 13, p. 503-506.

Gregg, J. M., and Shelton K. L., 1989a, Geochemical and petrographic evidence for fluid sources and pathways during dolomitization and lead-zinc mineralization in southeast Missouri: a review: Carbonates and Evaporites, v. 4.2, p. 153-175.

------ 1989b, Minor- and trace-element distributions in the Bonneterre Dolomite Cambrian), southeast Missouri: Evidence for possible multiple-basin fluid sources and pathways during lead-zinc mineralization: Geological Society of America Bulletin, v. 101, p. 221-230.

Hagni, R. D., 1983, Minor elements in Mississippi Valley-type ore deposits, *in* Shanks, W.C., ed., Cameron Volume on Unconventional Mineral Deposits: New York, Society of Economic Geology and Society of Mining Engineers, AIME, p. 44-88.

------ 1989, The Southeast Missouri lead district: Society of Economic Geologists Guidebook Series, v. 5, p. 12-57.

------ 1995, The southeast Missouri lead district: Society of Economic Geologists Guidebook Series, v. 22, p. 44-78.

Hanor, J. S., 1994, Origin of saline fluids in sedimentary basins, *in* Parnell, J., ed., Geofluids: Origin, migrations, and evolution of fluids in sedimentary basins: Geological Society Special Publications, v. 78, p. 151-174.

------ 1996, Variations in chloride as a driving force in siliciclastic diagenesis, *in* Crossey, L. J., Loucks, R., and Totten, M. W., eds., Siliciclastic Diagenesis and Fluid Flow; Concepts and Applications: Society of Economic Paleontology and Mineralogy Special Publication, v. 55, p. 3-12.

Jackson, S. A. and Beales, F. W., 1967, An aspect of sedimentary basin evolution: The concentration of Mississippi Valley-type ore during late stages of diagenesis: Bulletin of Canadian Petroleum Geology, v. 15, p. 353-433.

Leach, D. L., 1994, Genesis of the Ozark MVT metallogenic province, Missouri, Arkansas, and Oklahoma, USA, *in* Fonbonte, L. and Boni, M., eds., Sediment-hosted Zn-Pb ores: New York, Springer Berlin Heidelberg, p. 104–138.

Marikos, M. A., Laudon, R. C., and Leventhal, J. S., 1986, Solid, insoluble bitumen in the Magmont West orebody, southeast Missouri: Economic Geology, v. 81, p. 1983-1988.

Niewendorp, C. A., and Clendenin, C. W., 1993, Paragenetic link between organic matter and late-stage ore deposition in the Sweetwater Mine, Viburnum Trend, southeast Missouri: Geological Society of America Abstracts with Programs, v. 25, p. 70.

Ohle, E. L., and Gerdemann, P. E., 1989, Recent exploration history in southeast Missouri: Society of Economic Geologists Guidebook Series, v. 5, p. 1-11.

Orr, W. L., 1974, Changes in sulfur content and isotopic ratios of sulfur during petroleum maturation-study of Big Horn basin Paleozoic oils: American Association of Petroleum Geologists Bulletin, v. 58, p. 2295- 2318.

Plumlee, G. S., Leach, D. L., Hofstra, A. H., Landis, G. P., Rowan, E. L., and Viets, J. G., 1994, Chemical reaction path modeling of ore deposition in Mississippi Valley-type Pb-Zn deposits of the Ozark region, U.S. Midcontinent: Economic Geology, v. 89, no. 6, p. 1361-1383.

Roedder, E., 1977, Fluid inclusion studies of ore deposits in the Viburnum Trend, southeast Missouri: Economic Geology, v. 72, p. 391-397.

Rothbar, D. R., 1983, Diagenetic history of the Lamotte Sandstone, southeast Missouri, *in* Kisvarsanyi, G., Grant, S. K., Pratt, W. P., and Koenig, J. W, eds., International Conference on Mississippi Valley-type lead-zinc deposits: Rolla, MO, University of Missouri-Rolla, p. 385-395.

Rowan, E. L., 1986, Cathodoluminescent zonation in hydrothermal dolomite cements: Relationship to Mississippi Valley-type Pb-Zn mineralization in southeastern Missouri and northern Arkansas, *in* Hagni, R. D., ed., Process mineralogy – applications to precious metal deposits, industrial minerals, coal, liberation, mineral processing, agglomeration, metallurgical products, and refractories, with special emphasis on cathodoluminescent microscopy: Warrendale, PA, The Metallurgical Society, p. 69-87.

Rowan, E. L., and Leach, D. L., 1989, Constraints from fluid inclusions on sulfide precipitation mechanisms and ore fluid migration in the Viburnum Trend lead district, Missouri: Economic Geology, v. 84, p. 1948-1965.

Shelton, K. L., Bauer, R. M., Gregg, J. M., 1992, Fluid-inclusion studies of regionally extensive epigenetic dolomites, Bonneterre Dolomite (Cambrian), southeast Missouri: Evidence for multiple fluids during dolomitization and lead-zinc mineralization: Geological Society of America Bulletin, v. 104, p. 675-683.

Shelton, K. L., Burstein, I. B., Hagni, R. D., Vierrether, C. B., Grant, S. K., Hennigh, Q. T., Bradley, M. F., and Brandom, R. T., 1995, Sulfur isotope evidence for penetration of MVT fluids into igneous basement rocks, southeast Missouri, USA: Mineralium Deposita, v. 30, p. 339-350.

Shelton, K. L., Cavender, B. D., Perry, L. E., Appold, M. S., Schiffbauer, J. D., and Fike, D. A., 2016, Fluid inclusion and sulfur isotope studies of a new kind of Zn-Cu-rich MVT orebody at the Lamotte Sandstone/Bonneterre Dolomite contact, Viburnum Trend district, southeast Missouri: Evidence for multiple sulfur sources and metal-specific fluids: Pan-American Current Research on Fluid Inclusions (PACROFI-XIII) Abstract Volume, p. 106-107.

Spirakis, C. S., and Heyl, A. V., 1995, Evaluation of proposed precipitation mechansims for Mississippi Valley-type deposits: Ore Geology Reviews, v. 10, p. 1-17.

Sverjensky, D. A., 1981, The origin of a Mississippi valley-type deposit in the Viburnum Trend, southeast Missouri: Economic Geology, v. 76, p. 1848-1872.

------ 1986, Genesis of Mississippi Valley-type lead-zinc deposits: Annual Reviews of Earth and Planetary Science, v. 15, p. 177-199.

Sverjensky, D. A., Rye, D. M., and Doe, B. R., 1979, The lead and sulfur isotope compositions of galena from a Mississippi valley-type deposit in the New Lead Belt, southeast Missouri: Economic Geology, v. 74, p. 149-153.

Viets, J. G., and Leach, D. L., 1990, Genetic implications of regional and temporal trends in ore fluid geochemistry of Mississippi Valley-type deposits in the Ozark region: Economic Geology, v. 85, p. 842-861.

Wenz, Z. J., Appold, M. S., Shelton, K. L., and Tesfaye, S., 2012, Geochemistry of Mississippi Valley-type mineralizing fluids of the Ozark Plateau: A regional synthesis: American Journal of Science, v. 312, no. 1, p. 22-80, doi: 10.2475/01.2012.02.

CHAPTER V: CONCLUSIONS

Numerical analysis of alteration geochemistry of metavolcanic rocks in the Discovery-Ormsby and Clan Lake areas of the Yellowknife Greenstone Belt (Chapter 2)

The primary goal of this study was to better understand the spatial relationship between gold distribution and potassic alteration within metavolcanic host rocks of the Discovery-Ormsby and Clan Lake areas by calculating molar ratios among cations (i.e. K, Na, Ca, an Al) that correspond to minerals associated with potassic alteration and comparing the 3-D distribution of potassic alteration intensity to gold enrichment.

Previous studies that employed similar numerical methods (e.g. Warren et al., 2007; Booden et al., 2011) have shown that the calculated intensity of potassic alteration can serve effectively as a vector to sites of mineralization within volcanic host rocks. The current study demonstrates that the same techniques can be applied to metamorphosed volcanic host rocks and may be a valuable tool in targeting future exploration efforts. These methods may also assist geologists in determining major factors controlling the formation of metavolcanic-hosted gold deposits in the northern YGB, such as local and regional structural features influencing hydrothermal fluid flow (e.g. fault systems).

In addition to evaluating the applicability of 3-D modeling of potassic alteration as an exploration tool for gold hosted in metavolcanic rocks, numerical analysis and 3-D models have led to the following conclusions for the Discovery-Ormsby and Clan Lake areas:

1. Although lithogeochemical data for the mafic metavolcanic rocks in the Ormsby Member are limited, the lack of spatial correlation between potassic alteration and gold enrichment may suggest that gold distribution was influenced strongly by physical properties of host rocks, such as enhanced porosity and permeability.
2. Irregular, patchy occurrences of strong potassic alteration in the central portion of Clan Lake appear to be associated with similarly patchy gold distribution and likely reflect areas of dominantly quartz vein-hosted gold. These strongly altered rocks also exhibit a south-dipping, linear trend that may indicate significant influence of faults on hydrothermal fluid flow. In contrast, the southwestern portion of Clan Lake is characterized by a uniform distribution in moderate potassic alteration, high gold anomalies, and high $\delta^{18}O$ values (Hansen, 2013), which may represent a zone in which hydrothermal fluids were controlled principally by enhanced porosity and permeability in wall rocks, resulting in extensive reaction with wall rocks and formation of refractory ± vein-hosted gold.
3. The spatial distribution of potassic alteration at Clan Lake may reflect a hydrothermal event subsequent to the main gold mineralizing event. The later hydrothermal fluids would have overprinted previous alteration patterns and may have remobilized gold to produce the irregular, patchy distribution of potassic alteration and gold enrichment that is observed in the central portion of 3-D models for Clan Lake.

Geochemical studies and reaction path modeling of MVT ores in the southeastern Missouri Pb-Zn-Cu ore field, U.S.A. (Chapters 3 and 4)

The primary goals of geochemical studies on ores in the southeastern Missouri MVT Pb-Zn-Cu district were to better understand the formation of ores hosted in the lower Bonneterre Dolomite, to determine their genetic relationship to the stratigraphically higher, more typical Pb-Zn mineralization that is currently mined in the Viburnum Trend, and to determine whether the lower section ores resulted from a single fluid evolving chemically along different flow paths or if they were instead products of the interactions between multiple, distinct fluids. Understanding key similarities and differences in ore processes throughout the district will help geologists interpret the significance of locally distinct, fault-related mineralization commonly hosted in the lower Bonneterre Dolomite and Lamotte Sandstone and may help to develop exploration strategies to search for more lower section ores.

Reaction path modeling of potential depositional processes responsible for LOZ ore formation in the Viburnum Trend as well as studies on CL stratigraphy and stable isotope geochemistry of ore-associated dolomite cements from the Viburnum Trend, Old Lead Belt, Mine La Motte, and Annapolis subdistricts in the southeastern Missouri MVT Pb-Zn-Cu district have determined the following:

1. Variations in CL behavior of dolomite cements throughout southeast Missouri indicate the introduction of multiple mineralizing fluids whose compositions and flow pathways were influenced by local- and regional-scale fault and fracture systems. The similar CL stratigraphy among gangue dolomite cements from the Old Lead Belt and Mine La Motte show that these fault/fracture systems may have facilitated fluid

flow within the two subdistricts. Other subdistricts with distinct dolomite cement CL patterns that share similar $\delta^{18}O$ values could be the result of isotopically similar fluids migrating through separate, stratigraphically defined pathways.

2. Unusual CL patterns in dolomite cement from the laterally zoned, abnormally Zn-rich West Fork mine of the Viburnum Trend suggest that individual CL zones within the four-zone stratigraphy found regionally in the upper Bonneterre Dolomite are associated with ore-metal-specific (i.e. Zn-rich, Fe-rich, or Pb-rich) fluids. This regional four-zone CL stratigraphy likely resulted from a basinal fluid flow system that overprinted mostly earlier, fault-related flow systems' isotopic and CL signatures. However, this interpretation does not preclude that the two types of flow systems were, in part, contemporaneous, but existed in separate portions of the stratigraphic sections.
3. Reaction path models indicate that fluid mixing was likely the dominant depositional mechanism responsible for the formation of LOZ ores. The multiple, alternating generations of sulfides (particularly sphalerite) indicate that ore fluids were ore-metal-specific and were introduced into the lower ore system sporadically. Their interaction with fluids containing H_2S from multiple, isotopically distinct sources was likely controlled by fault and fracture networks in the Bonneterre Dolomite and Lamotte Sandstone, through which fluid mixing would have been variable temporally and spatially. This complex series of discrete mixing events led to the formation of the massive, Zn-Cu-rich ores that are observed in the lower Bonneterre Dolomite and upper Lamotte Sandstone of the Brushy Creek mine in the Viburnum Trend.

APPENDIX I: GEOLOGICAL MAP OF THE SLAVE PROVINCE, NORTHWEST TERRITORIES, CANADA (CH. 2)

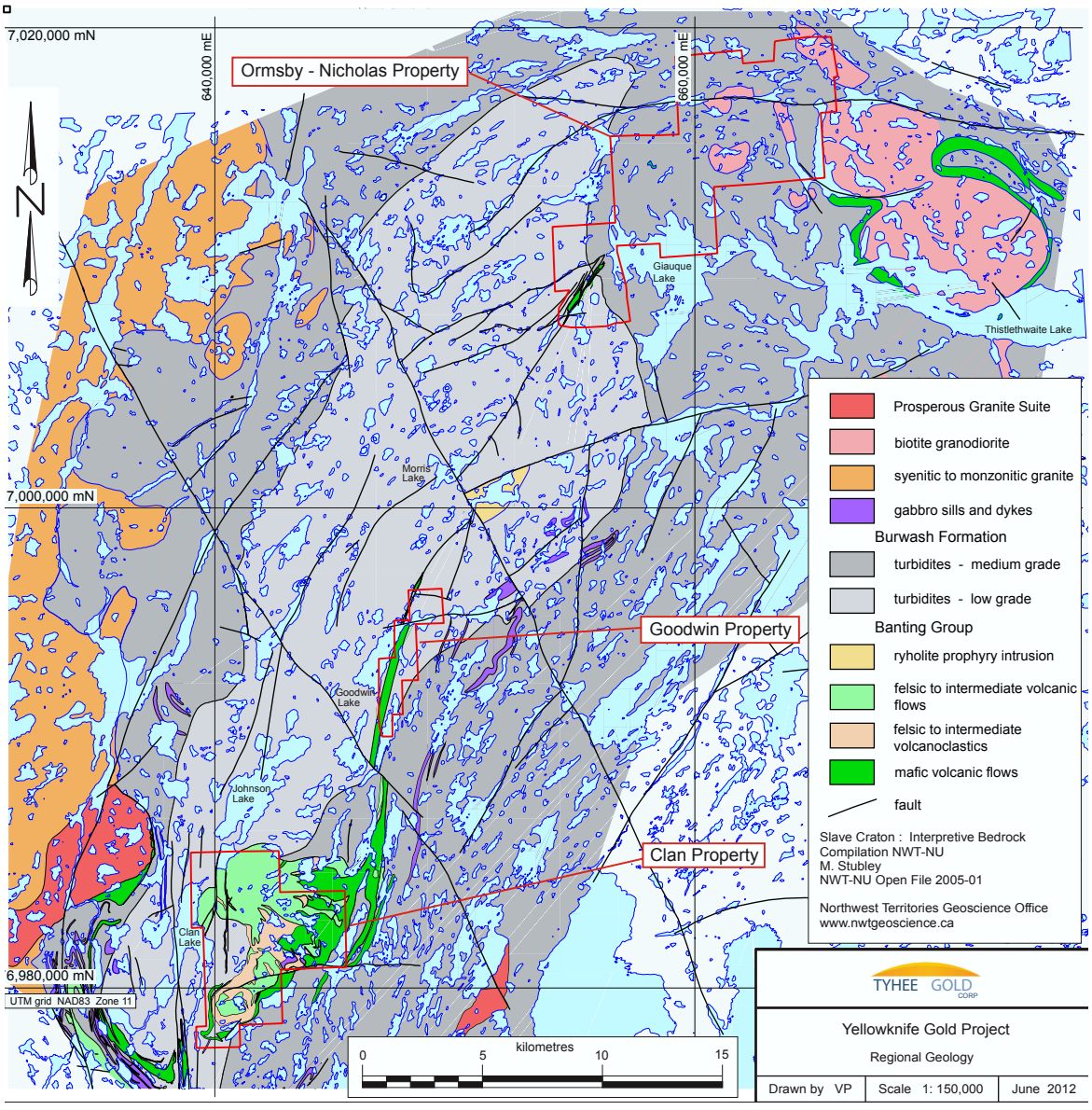

APPENDIX II: ADDITIONAL 3-D BLOCK MODELS FOR THE NORTHERN YGB (CH. 2)

Below are the 3-D models discussed in the text in addition to numerous models that were not included in chapter 2. For Clan Lake models, potassic alteration and gold distribution models are placed in adjacent columns for comparison. Plan view models are listed according to the elevation in meters above sea level. N-S and E-W transect models are listed according to their northing or easting coordinates.

Discovery-Ormsby area

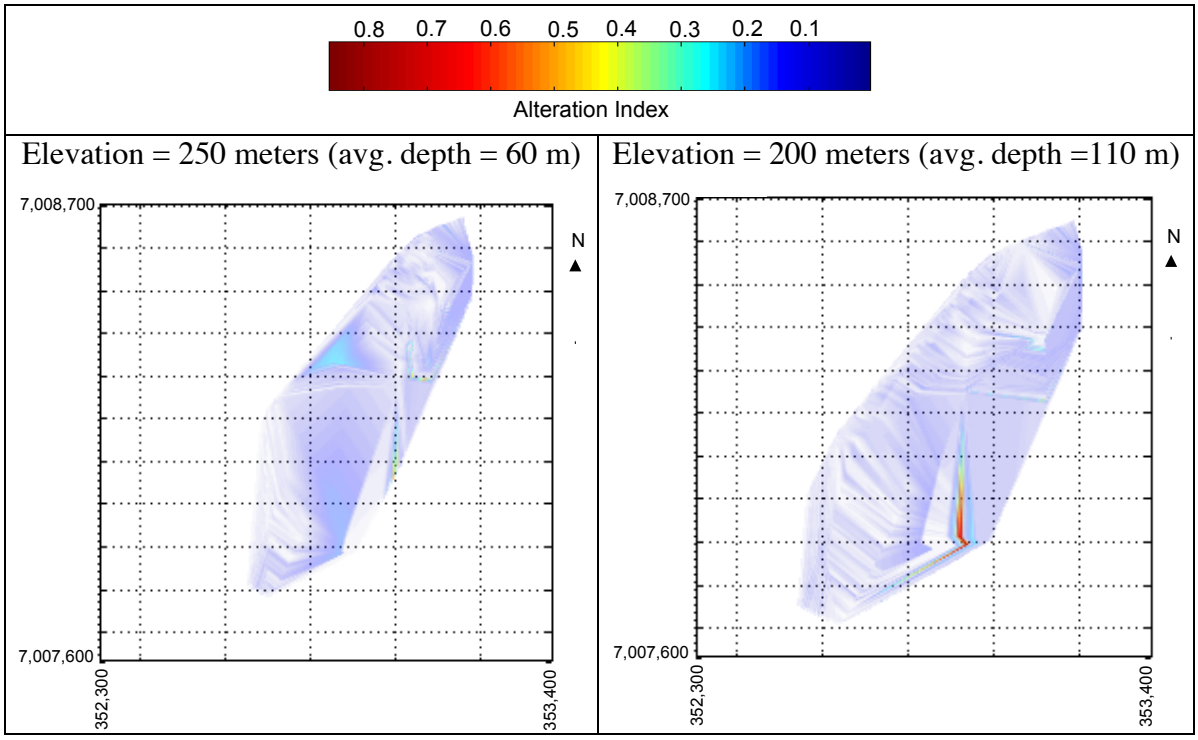

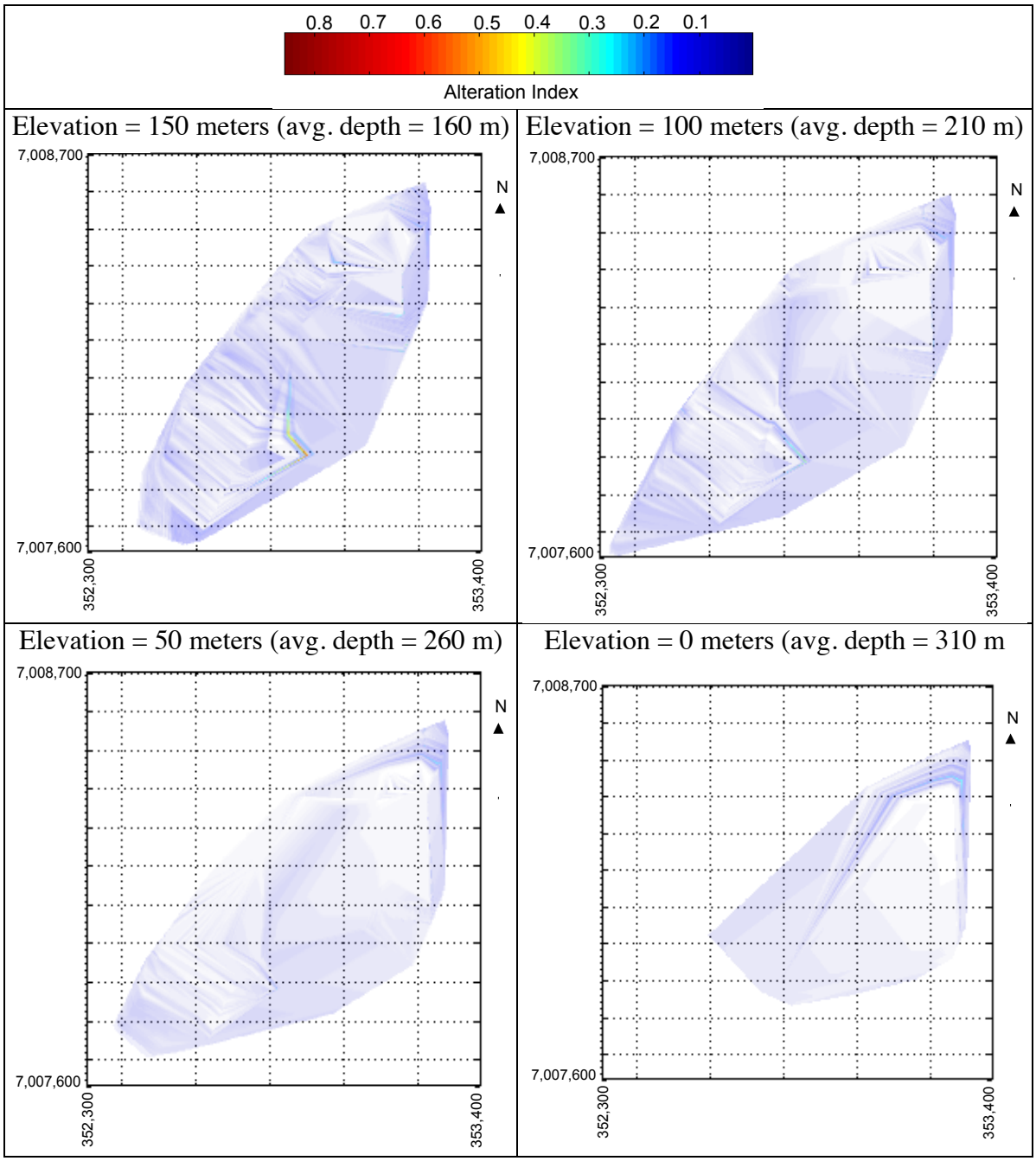
0.8 0.7 0.6 0.5 0.4 0.3 0.2 0.1
Alteration Index
Elevation = 150 meters (avg. depth = 160 m)
Elevation = 100 meters (avg. depth = 210 m)
Elevation = 50 meters (avg. depth = 260 m)
Elevation = 0 meters (avg. depth = 310 m
7,008,700
7,007,600
352,300
353,400
N

Clan Lake area

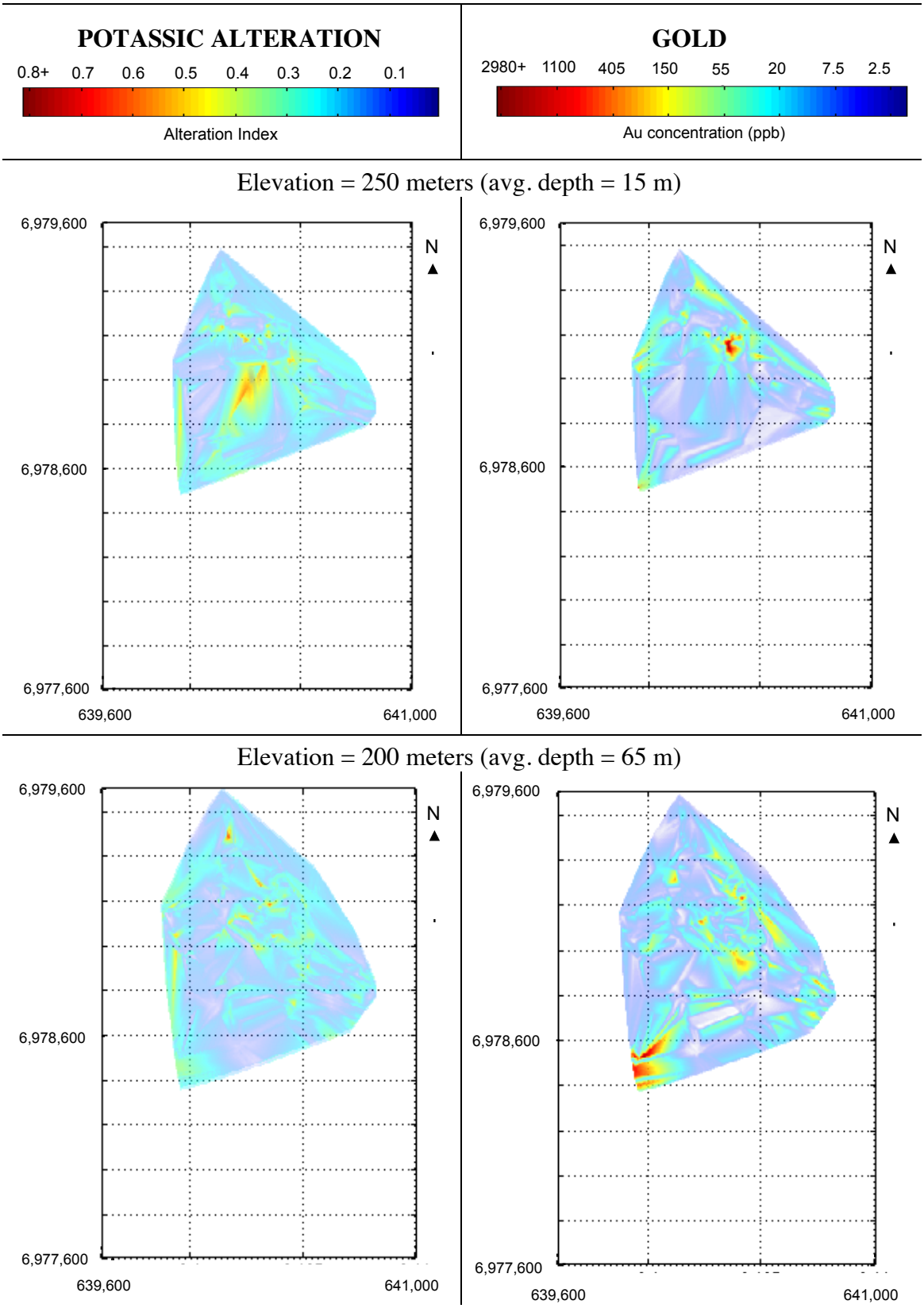

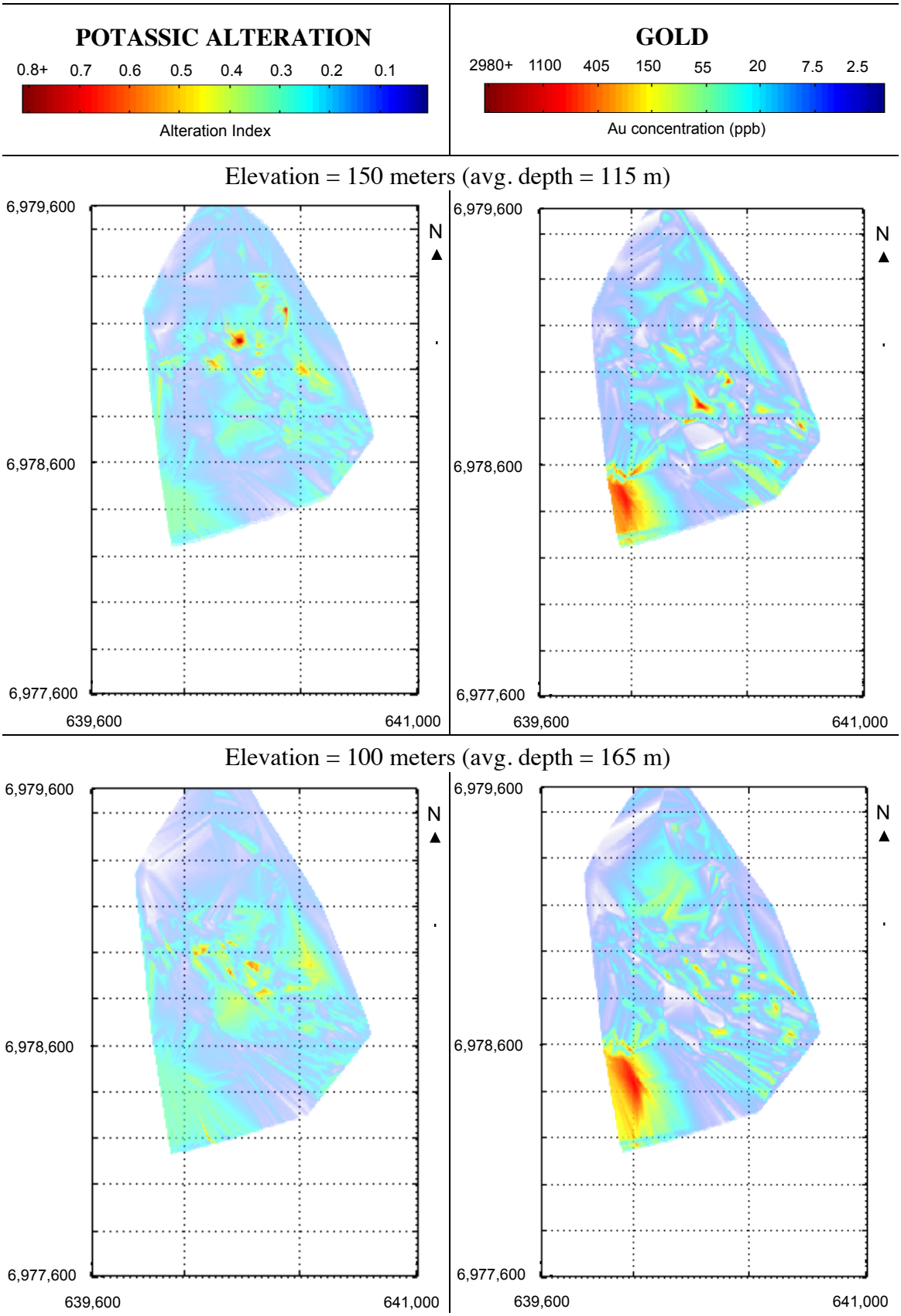
POTASSIC ALTERATION
0.8+ 0.7 0.6 0.5 0.4 0.3 0.2 0.1
Alteration Index
GOLD
2980+ 1100 405 150 55 20 7.5 2.5
Au concentration (ppb)
Elevation = 150 meters (avg. depth = 115 m)
6,979,600
6,978,600
6,977,600
639,600
641,000
N
Elevation = 100 meters (avg. depth = 165 m)

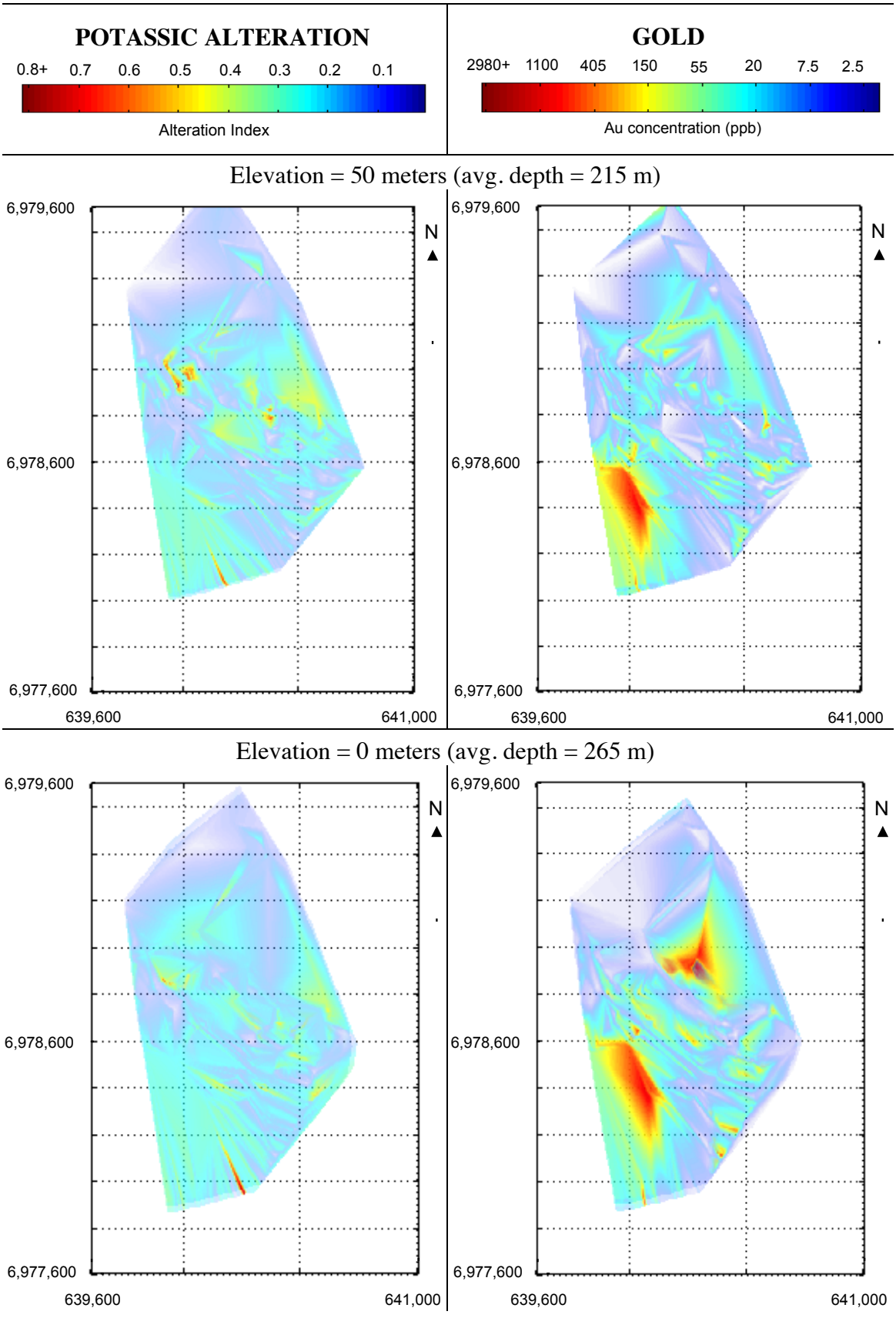
POTASSIC ALTERATION
0.8+ 0.7 0.6 0.5 0.4 0.3 0.2 0.1
Alteration Index
GOLD
2980+ 1100 405 150 55 20 7.5 2.5
Au concentration (ppb)
Elevation = 50 meters (avg. depth = 215 m)
6,979,600
6,978,600
6,977,600
639,600
641,000
N
Elevation = 0 meters (avg. depth = 265 m)

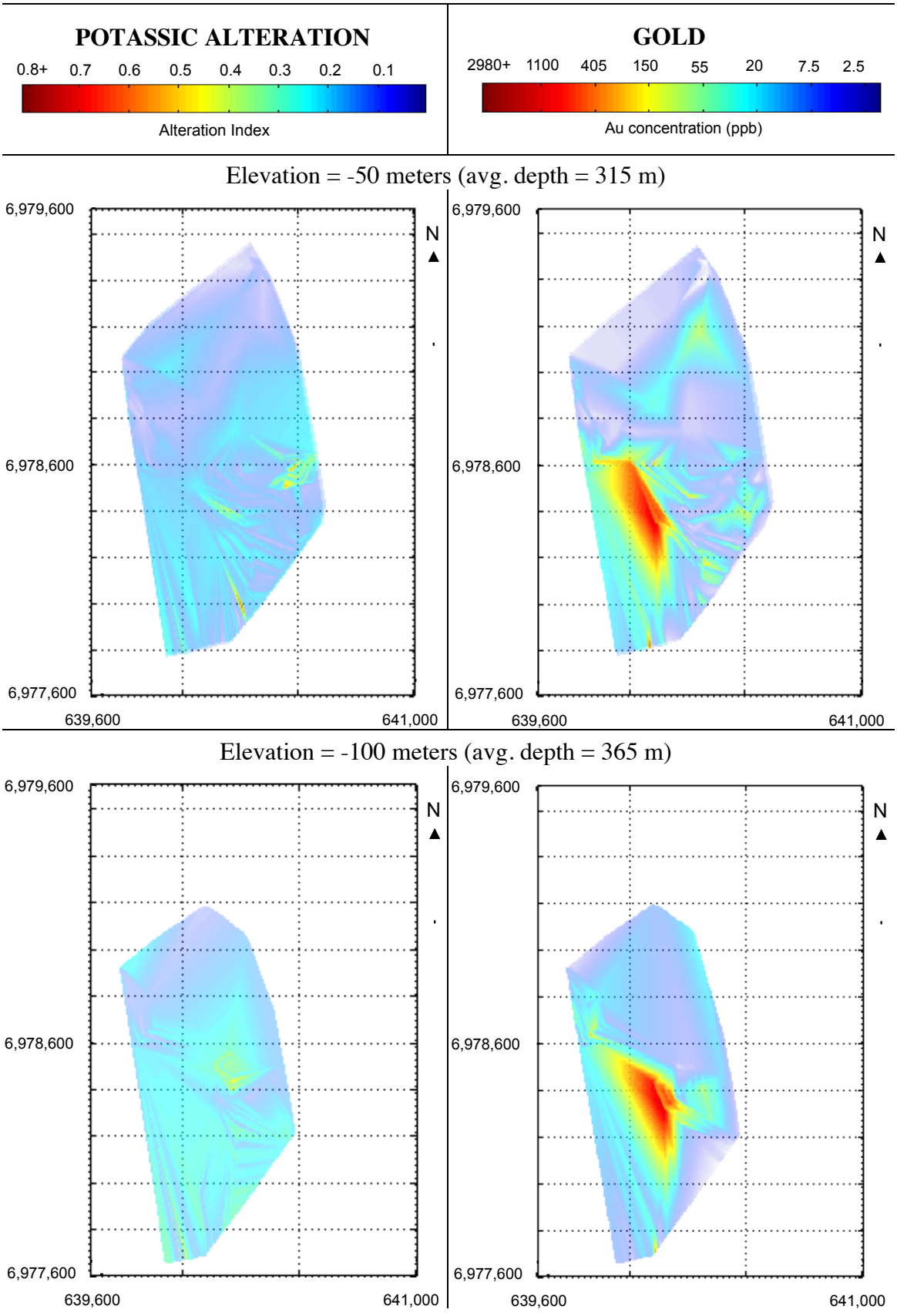
POTASSIC ALTERATION
0.8+ 0.7 0.6 0.5 0.4 0.3 0.2 0.1
Alteration Index
GOLD
2980+ 1100 405 150 55 20 7.5 2.5
Au concentration (ppb)
Elevation = -50 meters (avg. depth = 315 m)
6,979,600
6,978,600
6,977,600
639,600
641,000
N
Elevation = -100 meters (avg. depth = 365 m)

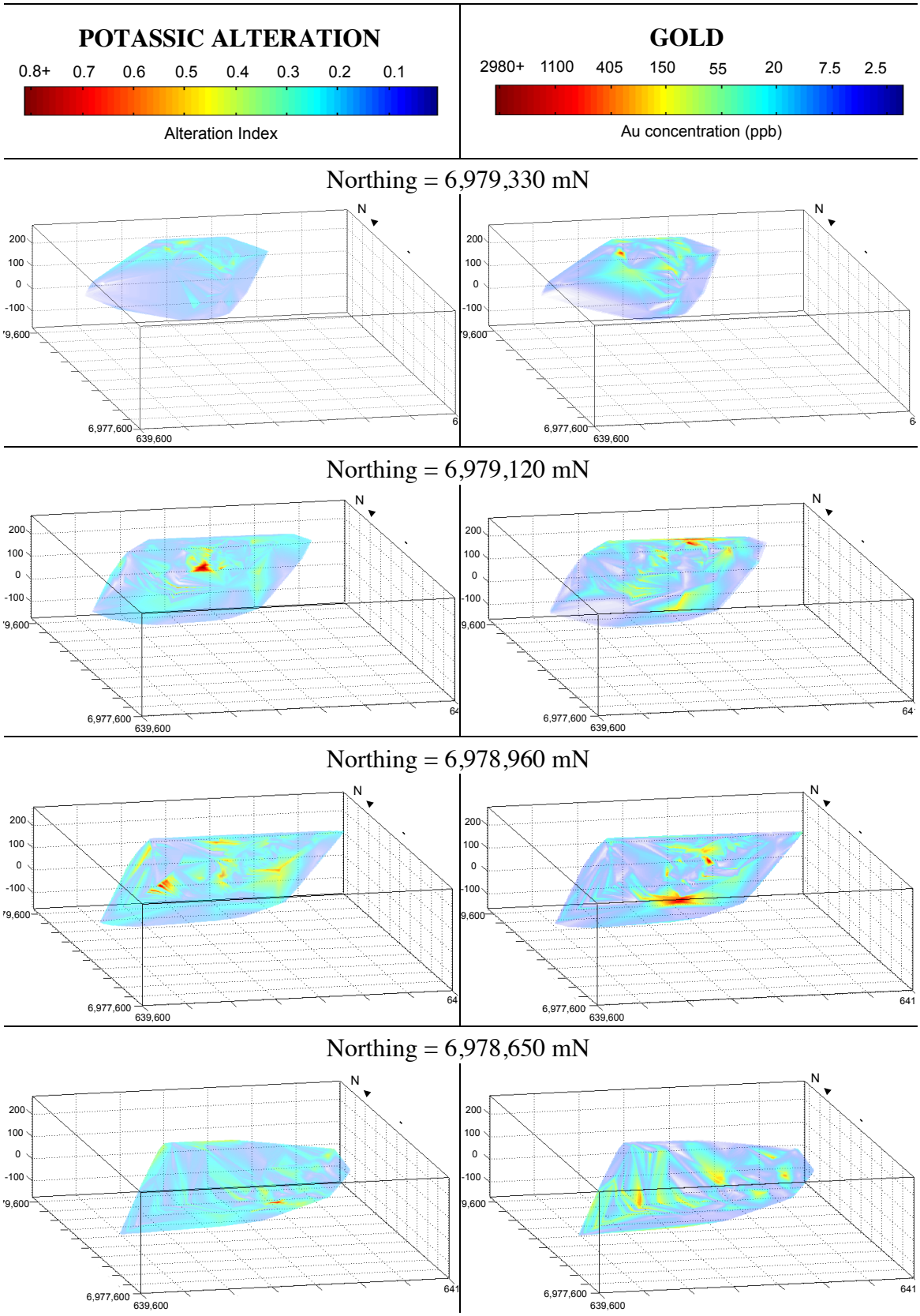
POTASSIC ALTERATION
0.8+ 0.7 0.6 0.5 0.4 0.3 0.2 0.1
Alteration Index
GOLD
2980+ 1100 405 150 55 20 7.5 2.5
Au concentration (ppb)
Northing = 6,979,330 mN
Northing = 6,979,120 mN
Northing = 6,978,960 mN
Northing = 6,978,650 mN
N
200
100
0
-100
6,977,600
639,600

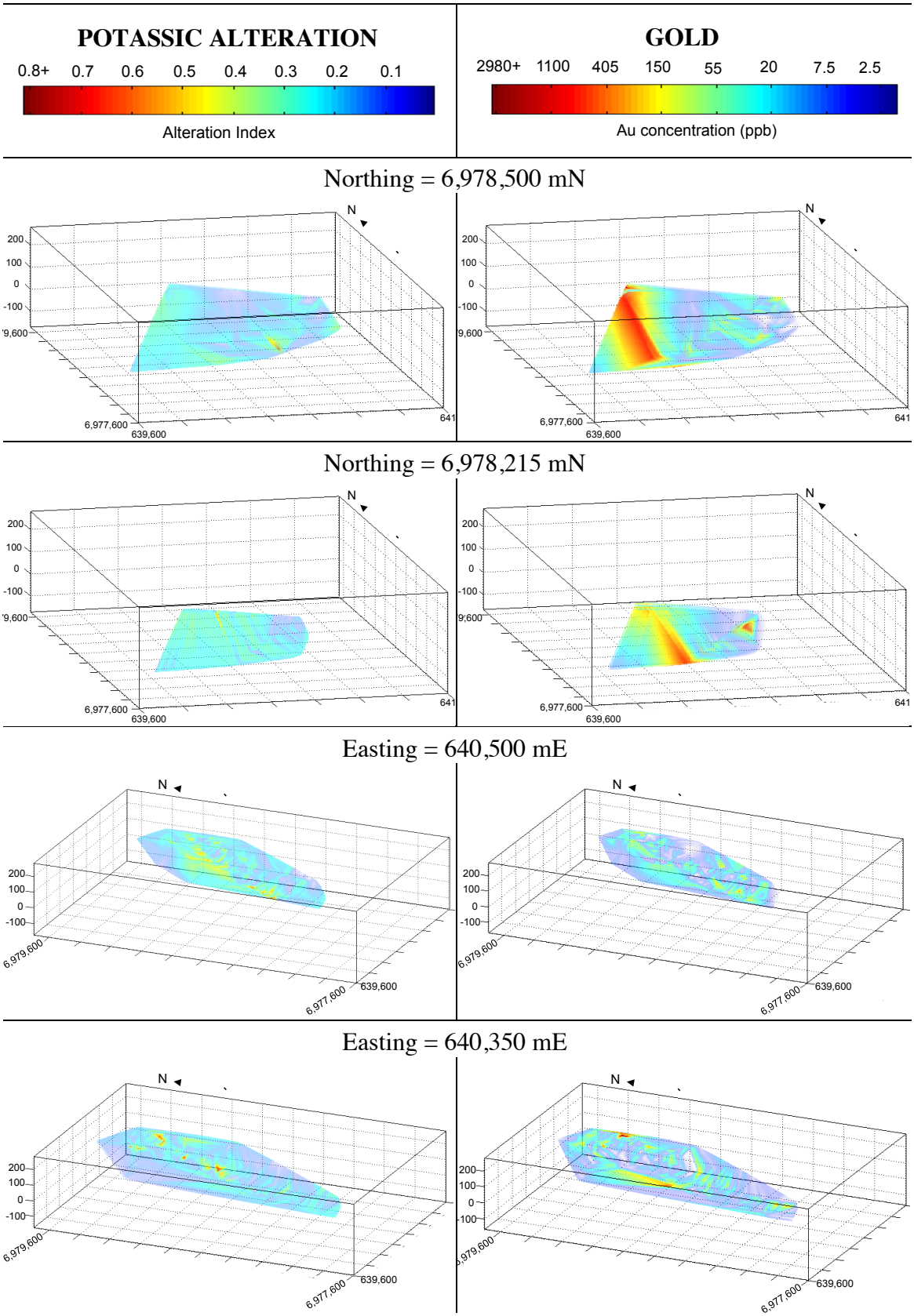
POTASSIC ALTERATION
0.8+ 0.7 0.6 0.5 0.4 0.3 0.2 0.1
Alteration Index
GOLD
2980+ 1100 405 150 55 20 7.5 2.5
Au concentration (ppb)
Northing = 6,978,500 mN
Northing = 6,978,215 mN
Easting = 640,500 mE
Easting = 640,350 mE
N
200
100
0
-100
6,977,600
639,600
6,979,600

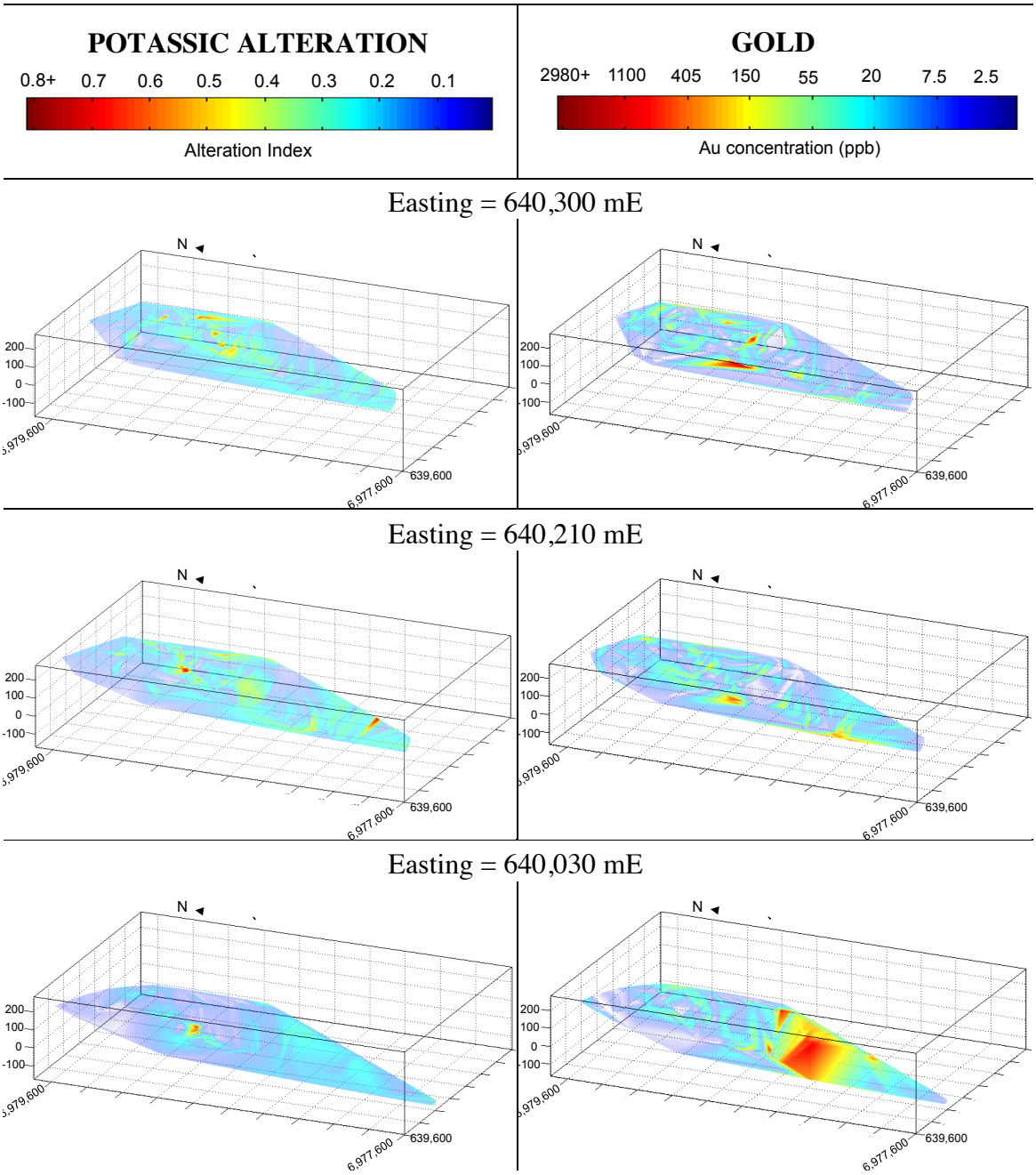
POTASSIC ALTERATION
0.8+ 0.7 0.6 0.5 0.4 0.3 0.2 0.1
Alteration Index
GOLD
2980+ 1100 405 150 55 20 7.5 2.5
Au concentration (ppb)
Easting = 640,300 mE
Easting = 640,210 mE
Easting = 640,030 mE
N
200
100
0
-100
6,979,600
6,977,600
639,600

APPENDIX III: METHODOLOGY OF GEOCHEMICAL RESEARCH (CH. 3)

Sampling

Samples from the Old Lead Belt, Fredericktown-Mine La Motte, and Annapolis subdistricts were collected by W. A. Tarr in the 1930s and are reposited in the University of Missouri's research collection. Samples examined from West Fork, most of which were originally collected for the research of Burstein (1993), were recently used for CL studies and stable isotope analysis by Adelstein et al. (2016).

Microscopy

Optical Microscopy

Polished sections, thin sections, and doubly polished fluid inclusion sections of ore sulfides and gangue dolomite cements from the Bonneterre Dolomite and Lamotte Sandstone were examined using an Olympus BX51 petrographic microscope with reflected light capabilities. Images were taken using a Nikon Coolpix MDC Lens digital camera.

Cathodoluminescence (CL) Petrography

Polished sections of dolomite cement samples were examined using a cold cathode, CITL cathodoluminescence system (model CL8200 MK5-2) mounted on an Olympus BX51 optical microscope equipped with a 5-megapixel Olympus Q-Color camera. The device operated at between 13-15 keV and a current of 150 to 250 μA for dolomite and quartz, respectively. Images were taken using "Q-imaging" software. The average exposure time of the camera when using plane polarized light was ~ 100 milliseconds; the average exposure time when using CL was varied from ~ 5-7 seconds depending on the luminescence of the sample.

Carbon and Oxygen Isotope Geochemistry

Powdered samples of host dolomite and dolomite cements were acquired by micro-drilling of thin section billets and hand samples using a Dremel microdrill equipped with diamond-bonded dental burrs. Carbon and oxygen isotopic compositions of carbonates were determined using a Thermo-Finnigan Delta Plus gas-source mass spectrometer with an automated Kiel device. Carbon and oxygen isotopic compositions are reported in standard δ notation as per mil (‰) deviations from VPDB (Vienna Pee Dee Belemnite; $^{13}C/^{12}C = 0.0112372$; $^{18}O/^{16}O = 0.0020672$). The $\delta^{13}C$ and $\delta^{18}O$ values have standard errors of less than ± 0.05‰, based on replicate measurements of the NBS-19 calcite reference standard, and have been corrected for reaction with 103% phosphoric acid at 70°C (Rosenbaum and Sheppard, 1986).

Sample List for CL & Ore Microscopy

Abbreviations: diss. = disseminated, dol = dolomite, cc = calcite, gal = galena, qtz = quartz.

SAMPLE ID	DESCRIPTION
The Old Lead Belt	
BT 1	diss. galena, vuggy host dol.
BT 2	diss. galena
FR1591	iron sulfides & cc vein
FR1677	white dolomite, minor gal
FR1677.5	galena, sandy & glauconitic host dol
FR1683	galena w/ dolomite host and glauconite
FR1689	diss. chalcopyrite, minor galena in fractures

SAMPLE ID	DESCRIPTION
Mine La Motte	
1795	galena, white host dol w/ qtz & glauconite
LM1620	massive chalcopyrite w/ siegenite
LM1775	chalcopyrite and galena
LM1925	galena w/ vuggy, sandy dolomite
LM1927	chalcopyrite & calcite in sandstone
LM2884	chalcopyrite
LM3370	diss. chalcopyrite and galena
LM8279-M12	chalcopyrite breccia
LM8279-M24	chalcopyrite breccia
LMCU-A	massive & bedded chalcopyrite
LMCU-B	massive & bedded chalcopyrite
LMCPY	sandy dolomite
LMSIEG	siegenite, iron sulfides, white host dol
LM-TARR-M3F	sandy dolomite w/ minor gal & chalcopyrite
LM-TARR-M26	sandy dolomite w/ minor gal & chalcopyrite
LM-WV	galena in sandstone
MLM9	chalcopyrite and siegenite
MLM-BIG	bedded galena
Annapolis	
ANP1820	galena w/ trace chalcopyrite in white rock
ANP1820-C2F	galena w/ trace chalcopyrite in white rock
ANP1820.4	trace chalcopyrite
ANP1820.5	diss. galena in dol net rock fabric

APPENDIX IV: REACTION PATH MODELS

Models discussed in Chapter 4

Figure 4.8a

Aqueous species	H_2S-fluid
Temperature (°C)	145
pH	4.4
log fO_2	-57
CH_4^+ (ppm)	300
TDS (%)	22
SiO_2 (*m*)	1.87×10^{-3}
Cl^- (*m*)	4.81
H_2S (*m*)	2.0×10^{-3}
SO_4^{2-} (*m*)	---
Ca^{2+}(*m*)	0.468
Mg^{2+} (*m*)	0.118
K^+ (*m*)	0.102
Na^+ (*m*)	3.53
Al^{3+} (*m*)	2.0×10^{-8}
Fe^{2+} (ppm)	30
Cu^{2+} (ppm)	0.6
Zn^{2+} (ppm)	1
Pb^{2+} (ppm)	0.2

Figure 4.8b

Aqueous species	H_2S-fluid
Temperature (°C)	150
pH	4.4
log fO_2	-57
CH_4^+ (ppm)	300
TDS (%)	21
SiO_2 (*m*)	1.87×10^{-3}
Cl^- (*m*)	4.81
H_2S (*m*)	2.0×10^{-3}
SO_4^{2-} (*m*)	---
Ca^{2+}(*m*)	0.468
Mg^{2+} (*m*)	0.118
K^+ (*m*)	0.102
Na^+ (*m*)	3.53
Al^{3+} (*m*)	2.0×10^{-8}
Fe^{2+} (ppm)	0.1
Cu^{2+} (ppm)	0.1
Zn^{2+} (ppm)	0.1
Pb^{2+} (ppm)	0.01

Figure 4.9a

Aqueous species	Sulfate-fluid
Temperature (°C)	145
pH	4.4
log fO_2	-57
CH_4^+ (ppm)	300
TDS (%)	25
SiO_2 (*m*)	1.87×10^{-3}
Cl^- (*m*)	5.13
H_2S (*m*)	---
SO_4^{2-} (*m*)	1.0×10^{-3}
Ca^{2+}(*m*)	0.499
Mg^{2+} (*m*)	0.126
K^+ (*m*)	0.109
Na^+ (*m*)	3.77
Al^{3+} (*m*)	2.0×10^{-8}
Fe^{2+} (ppm)	46
Cu^{2+} (ppm)	1
Zn^{2+} (ppm)	2.5
Pb^{2+} (ppm)	0.5

Figure 4.9b

Aqueous species	Sulfate-fluid
Temperature (°C)	145
pH	4.4
log fO_2	-57
CH_4^+ (ppm)	300
TDS (%)	25
SiO_2 (*m*)	1.87×10^{-3}
Cl^- (*m*)	5.13
H_2S (*m*)	---
SO_4^{2-} (*m*)	2.0×10^{-3}
Ca^{2+}(*m*)	0.499
Mg^{2+} (*m*)	0.126
K^+ (*m*)	0.109
Na^+ (*m*)	3.77
Al^{3+} (*m*)	2.0×10^{-8}
Fe^{2+} (ppm)	2.1
Cu^{2+} (ppm)	0.9
Zn^{2+} (ppm)	1.1
Pb^{2+} (ppm)	0.2

Figure 4.10a

Aqueous species	Metal-fluid
Temperature (°C)	145
pH	4.4
log fO_2	-57
CH_4^+ (ppm)	300
TDS (%)	25
SiO_2 (*m*)	1.91×10^{-3}
Cl^- (*m*)	5.15
H_2S (*m*)	1.0×10^{-10}
SO_4^{2-} (*m*)	---
Ca^{2+}(*m*)	0.499
Mg^{2+} (*m*)	0.126
K^+ (*m*)	0.109
Na^+ (*m*)	3.77
Al^{3+} (*m*)	2.0×10^{-8}
Fe^{2+} (ppm)	10
Cu^{2+} (ppm)	---
Zn^{2+} (ppm)	514
Pb^{2+} (ppm)	51

Figure 4.10b

Aqueous species	Metal-fluid
Temperature (°C)	145
pH	4.4
log fO_2	-57
CH_4^+ (ppm)	300
TDS (%)	25
SiO_2 (*m*)	1.91×10^{-3}
Cl^- (*m*)	5.15
H_2S (*m*)	1.0×10^{-10}
SO_4^{2-} (*m*)	---
Ca^{2+}(*m*)	0.499
Mg^{2+} (*m*)	0.126
K^+ (*m*)	0.109
Na^+ (*m*)	3.77
Al^{3+} (*m*)	2.0×10^{-8}
Fe^{2+} (ppm)	100
Cu^{2+} (ppm)	10
Zn^{2+} (ppm)	205
Pb^{2+} (ppm)	---

Figure 4.11a

Aqueous species	Metal-fluid	H_2S-fluid
Temperature (°C)	150	135
pH	4.4	4.4
log fO_2	-57	-57
CH_4^+ (ppm)	300	300
TDS (%)	25	19
SiO_2 (*m*)	1.91×10^{-3}	1.52×10^{-3}
Cl^- (*m*)	5.0	4.75
H_2S (*m*)	1.0×10^{-15}	0.06
SO_4^{2-} (*m*)	---	---
Ca^{2+}(*m*)	0.486	0.462
Mg^{2+} (*m*)	0.123	0.117
K^+ (*m*)	0.133	0.101
Na^+ (*m*)	3.67	3.49
Al^{3+} (*m*)	2.4×10^{-8}	2.0×10^{-8}
Fe^{2+} (ppm)	307	1.0×10^{-5}
Cu^{2+} (ppm)	64	---
Zn^{2+} (ppm)	262	---
Pb^{2+} (ppm)	---	---

Figure 4.11b

Aqueous species	Metal-fluid	H_2S-fluid
Temperature (°C)	150	150
pH	4.4	4.4
log fO_2	-57	-57
CH_4^+ (ppm)	300	300
TDS (%)	25	19
SiO_2 (*m*)	1.91×10^{-3}	1.91×10^{-3}
Cl^- (*m*)	5.0	4.75
H_2S (*m*)	1.0×10^{-15}	0.06
SO_4^{2-} (*m*)	---	---
Ca^{2+}(*m*)	0.486	0.462
Mg^{2+} (*m*)	0.123	0.117
K^+ (*m*)	0.133	0.101
Na^+ (*m*)	3.67	3.49
Al^{3+} (*m*)	2.4×10^{-8}	2.0×10^{-8}
Fe^{2+} (ppm)	391	1.0×10^{-5}
Cu^{2+} (ppm)	64	---
Zn^{2+} (ppm)	523	---
Pb^{2+} (ppm)	---	---

Figure 4.11c

Aqueous species	Metal-fluid	H_2S-fluid
Temperature (°C)	150	150
pH	4.4	4.4
log fO_2	-57	-57
CH_4^+ (ppm)	300	300
TDS (%)	25	19
SiO_2 (*m*)	1.91×10^{-3}	1.52×10^{-3}
Cl^- (*m*)	5.0	4.75
H_2S (*m*)	1.0×10^{-15}	0.06
SO_4^{2-} (*m*)	---	---
Ca^{2+}(*m*)	0.486	0.462
Mg^{2+} (*m*)	0.123	0.117
K^+ (*m*)	0.132	0.101
Na^+ (*m*)	3.67	3.49
Al^{3+} (*m*)	2.4×10^{-8}	2.0×10^{-8}
Fe^{2+} (ppm)	391	1.0×10^{-5}
Cu^{2+} (ppm)	64	---
Zn^{2+} (ppm)	---	---
Pb^{2+} (ppm)	---	---

Figure 4.11d

Aqueous species	Metal-fluid	H_2S-fluid
Temperature (°C)	150	150
pH	4.4	4.4
log fO_2	-57	-57
CH_4^+ (ppm)	300	300
TDS (%)	25	19
SiO_2 (*m*)	1.91×10^{-3}	1.52×10^{-3}
Cl^- (*m*)	5.0	4.71
H_2S (*m*)	1.0×10^{-15}	0.04
SO_4^{2-} (*m*)	---	---
Ca^{2+}(*m*)	0.486	0.462
Mg^{2+} (*m*)	0.123	0.102
K^+ (*m*)	0.132	0.095
Na^+ (*m*)	3.67	3.49
Al^{3+} (*m*)	2.4×10^{-8}	1.8×10^{-8}
Fe^{2+} (ppm)	101	---
Cu^{2+} (ppm)	111	---
Zn^{2+} (ppm)	180	---
Pb^{2+} (ppm)	21	---

Additional Reaction Path Models

Reduced-sulfur models

Simulation 1: Cooling from 150º to 130ºC.

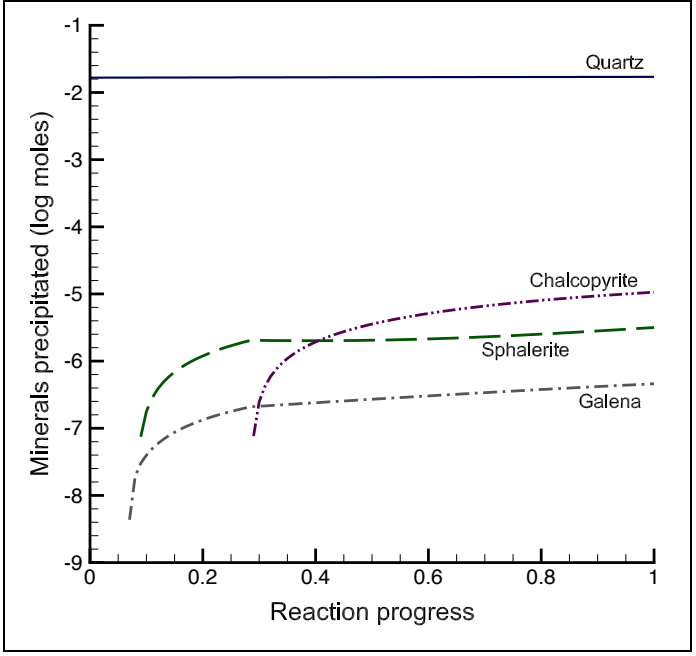

Aqueous species	H_2S-fluid
Temperature (°C)	150
pH	4.4
log fO_2	-57
CH_4^+ (ppm)	300
TDS (%)	26
SiO_2 (*m*)	1.87×10^{-3}
Cl^- (*m*)	5.2
H_2S (*m*)	1.0×10^{-3}
SO_4^{2-} (*m*)	---
Ca^{2+}(*m*)	0.513
Mg^{2+} (*m*)	0.13
K^+ (*m*)	0.112
Na^+ (*m*)	3.87
Al^{3+} (*m*)	2.0×10^{-8}
Fe^{2+} (ppm)	0.1
Cu^{2+} (ppm)	1.8
Zn^{2+} (ppm)	1.1
Pb^{2+} (ppm)	0.2

Simulation 2: Cooling (1 kg of fluid) from 150º to 140ºC while reacting with 2 cm^3 of host dolomite and 0.1 cm^3 of host pyrite.

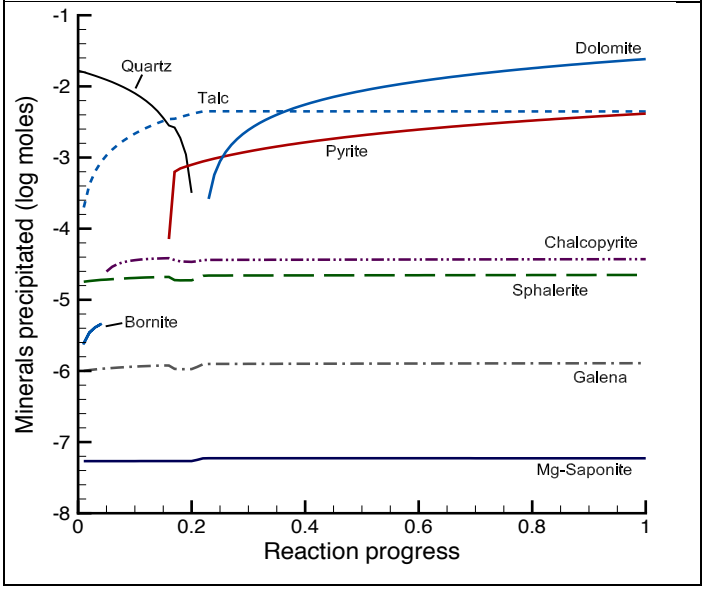

Aqueous species	H_2S-fluid
Temperature (°C)	150
pH	4.4
log fO_2	-57
CH_4^+ (ppm)	300
TDS (%)	21
SiO_2 (*m*)	1.87×10^{-3}
Cl^- (*m*)	4.81
H_2S (*m*)	2.0×10^{-3}
SO_4^{2-} (*m*)	---
Ca^{2+}(*m*)	0.468
Mg^{2+} (*m*)	0.118
K^+ (*m*)	0.102
Na^+ (*m*)	3.53
Al^{3+} (*m*)	2.0×10^{-8}
Fe^{2+} (ppm)	40
Cu^{2+} (ppm)	1
Zn^{2+} (ppm)	1
Pb^{2+} (ppm)	0.2

Sulfate-reduction model

Simulation 1: Cooling (1 kg of fluid) from 150° to 130°C, reacting with 5g CH_4 and 1 cm^3 dolomite.

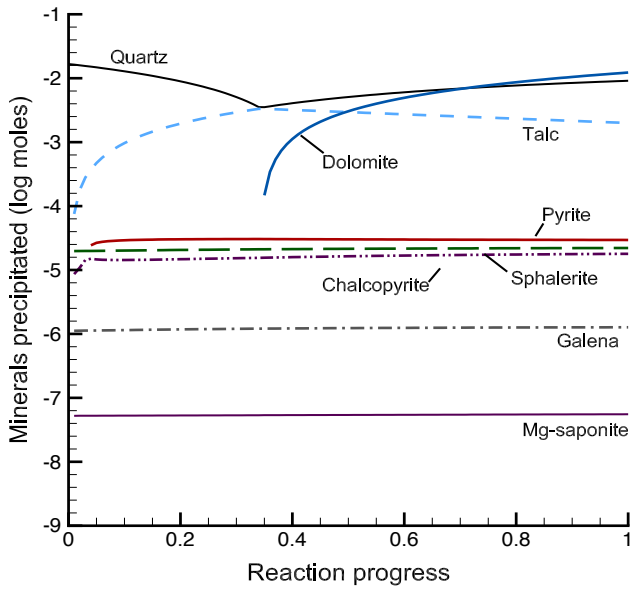

Aqueous species	Sulfate-fluid
Temperature (°C)	150
pH	4.4
log fO_2	-55
CH_4^+ (ppm)	300
TDS (%)	25
SiO_2 (*m*)	1.87×10^{-3}
Cl^- (*m*)	5.13
H_2S (*m*)	---
SO_4^{2-} (*m*)	2.0×10^{-3}
Ca^{2+}(*m*)	0.499
Mg^{2+} (*m*)	0.126
K^+ (*m*)	0.109
Na^+ (*m*)	3.77
Al^{3+} (*m*)	2.0×10^{-8}
Fe^{2+} (ppm)	2
Cu^{2+} (ppm)	0.9
Zn^{2+} (ppm)	1.1
Pb^{2+} (ppm)	0.2

Mixing models

Metal-bearing fluid reacting with host pyrite

Simulation 1: Metal-rich fluid (1 kg) reacts with 0.2 cm^3 pyrite.

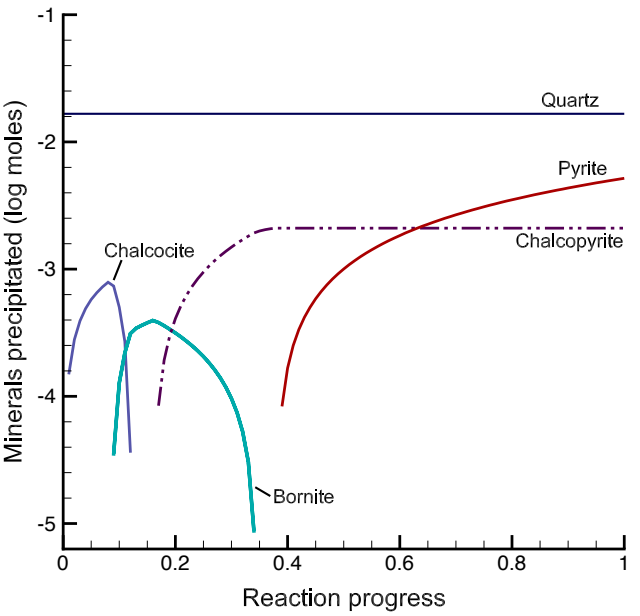

Aqueous species	Metal-fluid
Temperature (°C)	150
pH	4.4
log fO_2	-55
CH_4^+ (ppm)	300
TDS (%)	25
SiO_2 (*m*)	1.91×10^{-3}
Cl^- (*m*)	5.14
H_2S (*m*)	1.0×10^{-10}
SO_4^{2-} (*m*)	---
Ca^{2+}(*m*)	0.499
Mg^{2+} (*m*)	0.126
K^+ (*m*)	0.109
Na^+ (*m*)	3.77
Al^{3+} (*m*)	2.0×10^{-8}
Fe^{2+} (ppm)	100
Cu^{2+} (ppm)	100
Zn^{2+} (ppm)	1.0×10^{-4}
Pb^{2+} (ppm)	---

Fluid mixing: The table below lists initial fluid compositions used for the following reaction paths (simulations 1-5) during which temperature was the only parameter that was varied. Also see Figs. 4.11a,b,c for other reaction paths using the same initial fluid compositions, but with variable zinc and lead (in addition to temperature). Unless stated otherwise, the mass of each end-member fluid in all of the following mixing paths is 1 kg.

Aqueous species	**Metal-fluid**	**H_2S-fluid**
Temperature (°C)	120-150	120-150
pH	4.4	4.4
log fO_2	-57	-57
CH_4^+ (ppm)	200	300
TDS (%)	25	19
SiO_2 (m)	1.91×10^{-3}	1.63×10^{-3}
Cl^- (m)	5.0	4.75
H_2S (m)	2.0×10^{-15}	0.06
SO_4^{2-} (m)	---	---
Ca^{2+}(m)	0.486	0.462
Mg^{2+} (m)	0.123	0.117
K^+ (m)	0.133	0.101
Na^+ (m)	3.67	3.49
Al^{3+} (m)	2.4×10^{-8}	2.0×10^{-6}
Fe^{2+} (ppm)	391	2.0×10^{-5}
Cu^{2+} (ppm)	64	---
Zn^{2+} (ppm)	589	---
Pb^{2+} (ppm)	41	---

Simulation 1: T = 120ºC

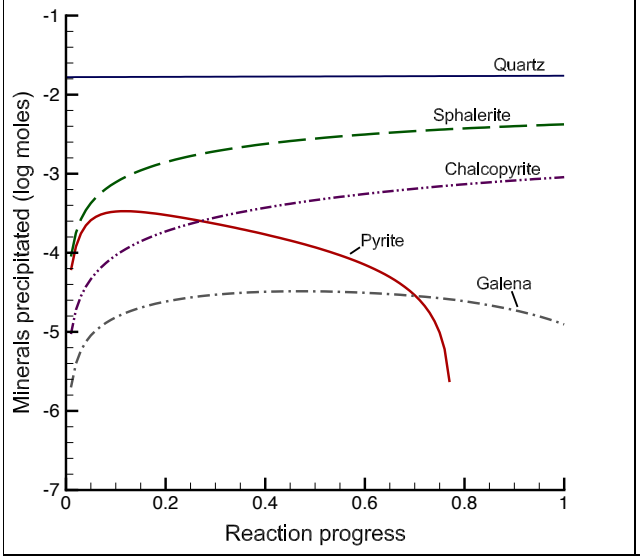

Simulation 2: T = 130ºC

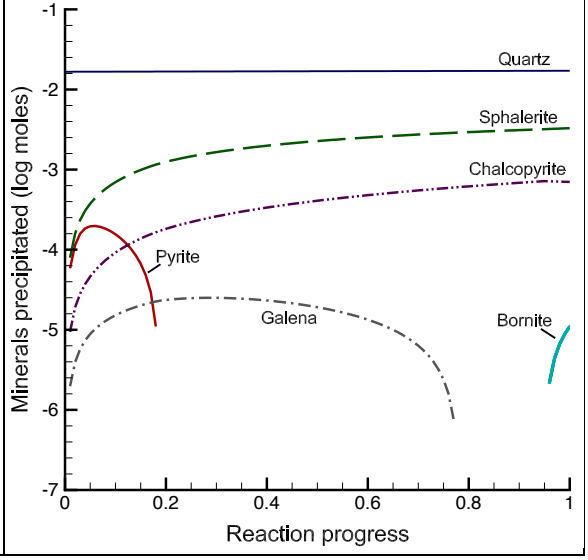

Simulation 3: T = 140 ºC

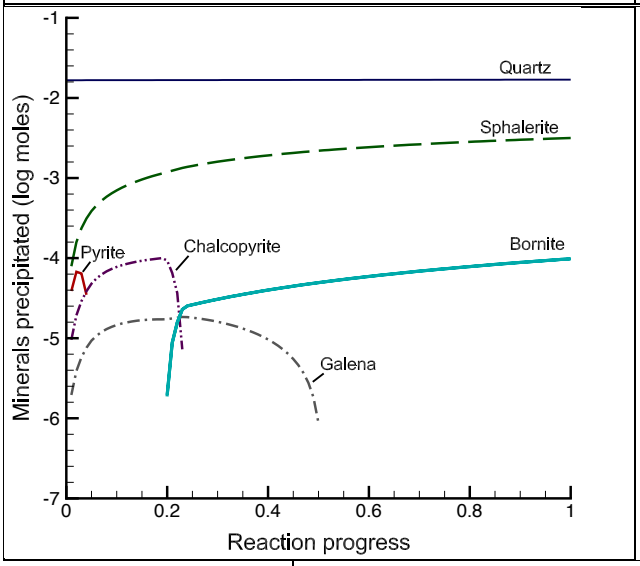

Simulation 4: T = 150ºC

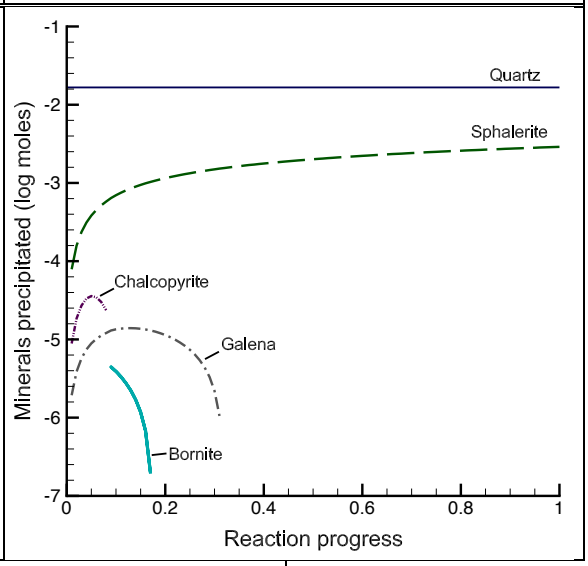

Simulation 5: Metal-fluid T = 150ºC
H_2S-fluid T = 120ºC

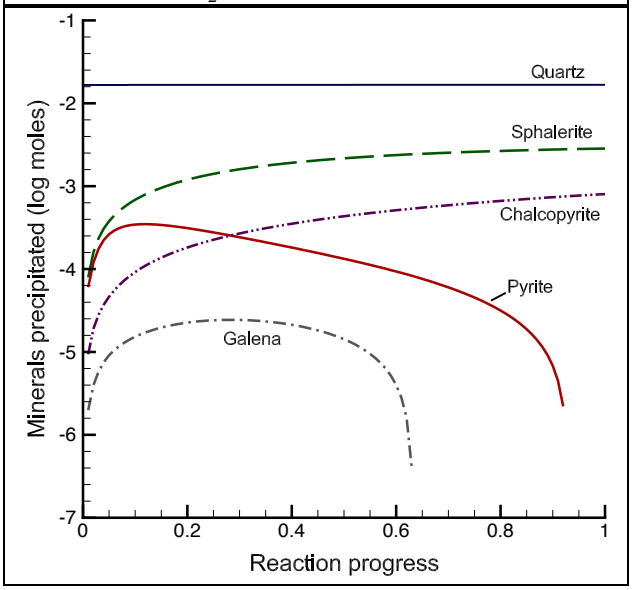

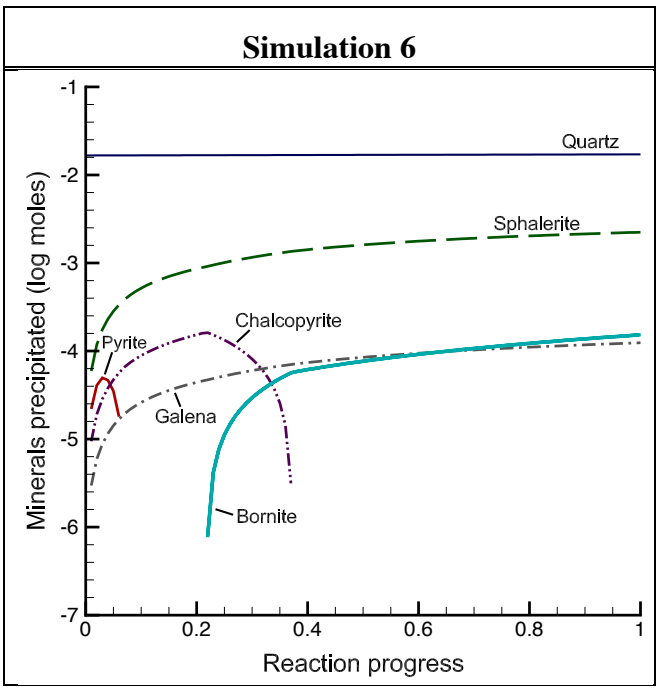

Aqueous species	Metal-fluid	H_2S-fluid
Temperature (°C)	130	130
pH	4.4	4.4
log fO_2	-57	-57
CH_4^+ (ppm)	200	300
TDS (%)	25	19
SiO_2 (m)	1.91×10^{-3}	1.42×10^{-3}
Cl^- (m)	5.0	4.71
H_2S (m)	1.0×10^{-15}	0.04
SO_4^{2-} (m)	---	---
Ca^{2+}(m)	0.486	0.462
Mg^{2+} (m)	0.123	0.102
K^+ (m)	0.133	0.095
Na^+ (m)	3.67	3.49
Al^{3+} (m)	2.4×10^{-8}	2.0×10^{-8}
Fe^{2+} (ppm)	196	1.0×10^{-3}
Cu^{2+} (ppm)	64	---
Zn^{2+} (ppm)	392	---
Pb^{2+} (ppm)	62	---

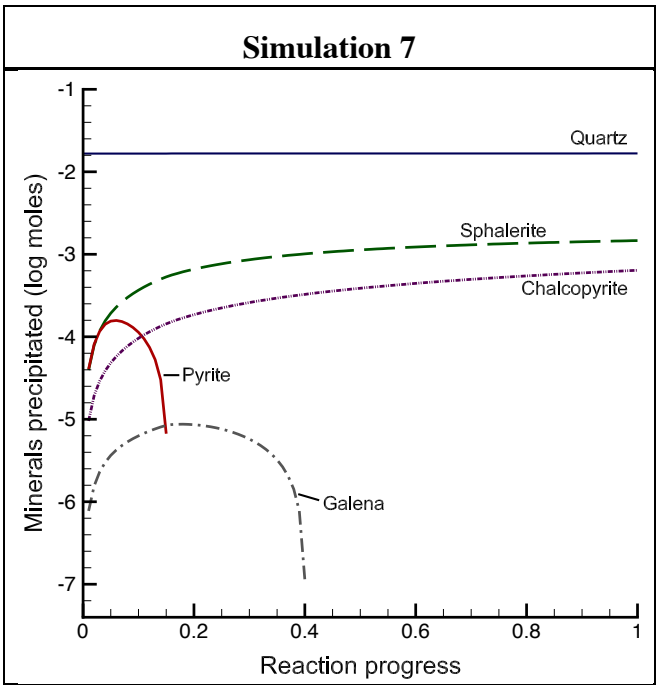

Aqueous species	Metal-fluid	H_2S-fluid
Temperature (°C)	150	135
pH	4.4	4.4
log fO_2	-57	-57
CH_4^+ (ppm)	200	300
TDS (%)	25	19
SiO_2 (m)	1.91×10^{-3}	1.42×10^{-3}
Cl^- (m)	5.0	4.71
H_2S (m)	1.0×10^{-15}	0.04
SO_4^{2-} (m)	---	---
Ca^{2+}(m)	0.486	0.462
Mg^{2+} (m)	0.123	0.102
K^+ (m)	0.133	0.095
Na^+ (m)	3.67	3.49
Al^{3+} (m)	2.4×10^{-8}	2.0×10^{-8}
Fe^{2+} (ppm)	196	1.0×10^{-3}
Cu^{2+} (ppm)	64	---
Zn^{2+} (ppm)	392	---
Pb^{2+} (ppm)	62	---

Fluid mixing plus reaction with host dolomite: also see Fig. 4.11d. Unless stated otherwise, the mass of each end-member fluid used in mixing calculations is 1 kg.

Simulation 1: reaction with 2.5 cm^3 dolomite; mass of metal-fluid = 5 times the mass of H_2S-fluid (total 6 kg of fluid)

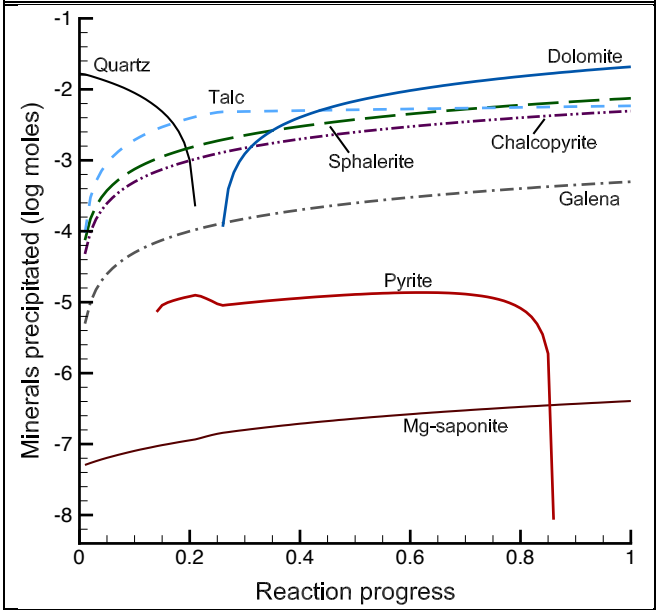

Aqueous species	Metal-fluid	H_2S-fluid
Temperature (°C)	145	145
pH	4.4	4.4
log fO_2	-57	-57
CH_4^+ (ppm)	200	300
TDS (%)	25	19
SiO_2 (m)	1.91×10^{-3}	1.91×10^{-3}
Cl^- (m)	5.0	4.71
H_2S (m)	1.0×10^{-15}	0.02
SO_4^{2-} (m)	---	---
Ca^{2+}(m)	0.486	0.462
Mg^{2+} (m)	0.123	0.117
K^+ (m)	0.133	0.101
Na^+ (m)	3.67	3.49
Al^{3+} (m)	2.4×10^{-8}	2.0×10^{-8}
Fe^{2+} (ppm)	56	0.1
Cu^{2+} (ppm)	64	---
Zn^{2+} (ppm)	98	---
Pb^{2+} (ppm)	21	---

Simulation 2: reaction with 0.01 cm^3 dolomite and 0.001 cm^3 pyrite (same fluid compositions as **Simulation 6** in previous *Fluid mixing* section)

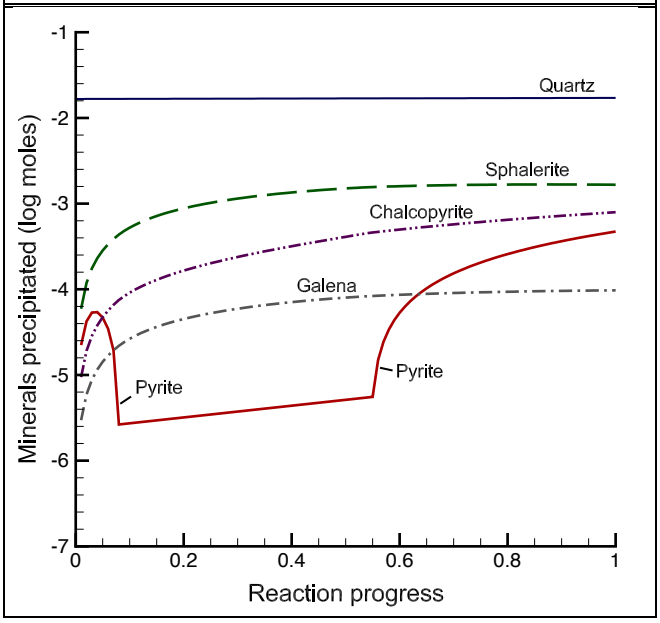

Aqueous species	Metal-fluid	H_2S-fluid
Temperature (°C)	130	130
pH	4.4	4.4
log fO_2	-57	-57
CH_4^+ (ppm)	200	300
TDS (%)	25	19
SiO_2 (m)	1.91×10^{-3}	1.42×10^{-3}
Cl^- (m)	5.0	4.71
H_2S (m)	1.0×10^{-15}	0.04
SO_4^{2-} (m)	---	---
Ca^{2+}(m)	0.486	0.462
Mg^{2+} (m)	0.123	0.102
K^+ (m)	0.133	0.095
Na^+ (m)	3.67	3.49
Al^{3+} (m)	2.4×10^{-8}	2.0×10^{-8}
Fe^{2+} (ppm)	196	1.0×10^{-3}
Cu^{2+} (ppm)	64	---
Zn^{2+} (ppm)	392	---
Pb^{2+} (ppm)	62	---

Simulation 3: reaction with 0.04 cm^3 dolomite and 0.004 cm^3 pyrite; mass of metal-fluid = 4 times the mass of H_2S-fluid (total 5 kg of fluid)

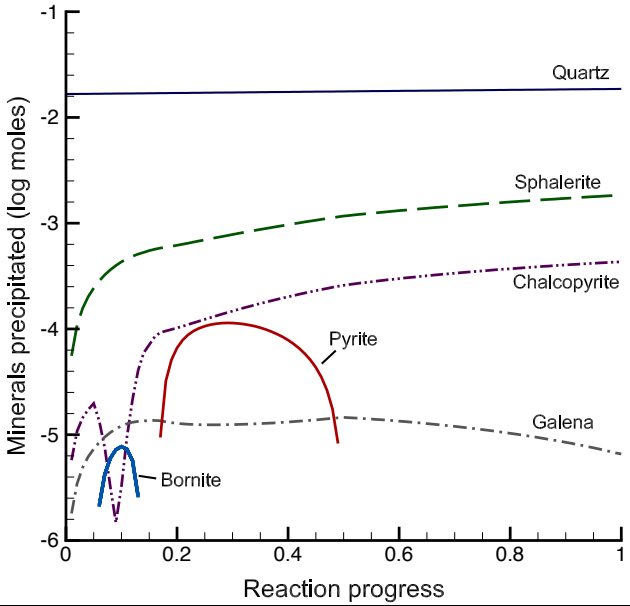

Aqueous species	Metal-fluid	H_2S-fluid
Temperature (°C)	130	130
pH	4.4	4.4
log fO_2	-57	-57
CH_4^+ (ppm)	200	300
TDS (%)	25	19
SiO_2 (m)	1.91×10^{-3}	1.42×10^{-3}
Cl^- (m)	5.0	4.71
H_2S (m)	1.0×10^{-15}	0.04
SO_4^{2-} (m)	---	---
Ca^{2+}(m)	0.486	0.462
Mg^{2+} (m)	0.123	0.102
K^+ (m)	0.133	0.095
Na^+ (m)	3.67	3.49
Al^{3+} (m)	2.4×10^{-8}	2.0×10^{-8}
Fe^{2+} (ppm)	32	1.0×10^{-3}
Cu^{2+} (ppm)	13	---
Zn^{2+} (ppm)	98	---
Pb^{2+} (ppm)	10	---

Simulation 4: reaction with 0.25 cm^3 dolomite; mass of metal-fluid = 3 times the mass of H_2S-fluid (total 4 kg fluid)

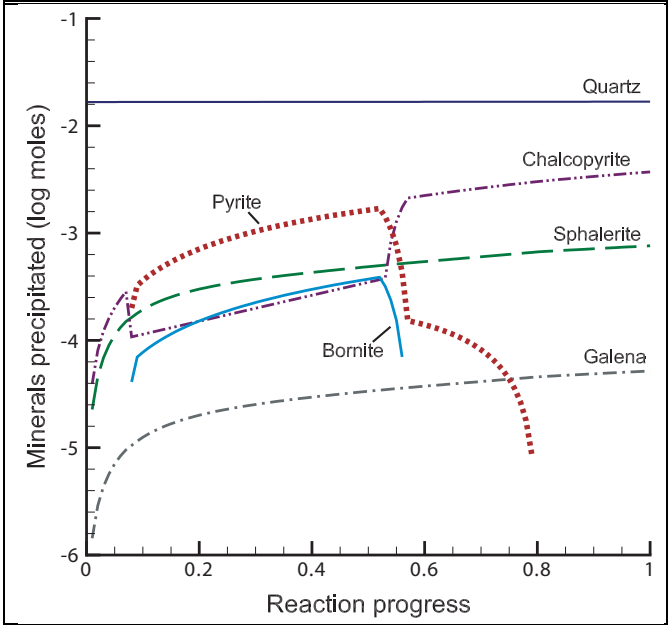

Aqueous species	Metal-fluid	H_2S-fluid
Temperature (°C)	150	135
pH	4.4	4.4
log fO_2	-57	-57
CH_4^+ (ppm)	200	300
TDS (%)	25	19
SiO_2 (m)	1.91×10^{-3}	1.91×10^{-3}
Cl^- (m)	5.0	4.71
H_2S (m)	1.0×10^{-15}	0.02
SO_4^{2-} (m)	---	---
Ca^{2+}(m)	0.486	0.462
Mg^{2+} (m)	0.123	0.117
K^+ (m)	0.133	0.101
Na^+ (m)	3.67	3.49
Al^{3+} (m)	2.4×10^{-8}	2.0×10^{-8}
Fe^{2+} (ppm)	83.8	1.0×10^{-5}
Cu^{2+} (ppm)	114.4	---
Zn^{2+} (ppm)	52.3	---
Pb^{2+} (ppm)	10.4	---